



**32nd Summer School and
International Symposium on
the Physics of Ionized Gases**

Belgrade, Serbia,
August 26 - 30, 2024

CONTRIBUTED PAPERS
&
**ABSTRACTS of INVITED LECTURES,
TOPICAL INVITED LECTURES and PROGRESS REPORTS**

Editors:
**Bratislav Obradović, Jovan Cvetić,
Miroslav Kuzmanović and Nikola Cvetanović**



**БЕОГРАД
2024**

**32nd Summer School and
International Symposium on
the Physics of Ionized Gases**



August 26 – 30, 2024, Belgrade, Serbia

S P I G 2024

CONTRIBUTED PAPERS

&

ABSTRACTS OF INVITED LECTURES,
TOPICAL INVITED LECTURES AND
PROGRESS REPORTS

Editors

Bratislav Obradović, Jovan Cvetic,
Miroslav Kuzmanović and Nikola Cvetanović

University of Belgrade –
Faculty of Physical
Chemistry

Serbian Academy of
Sciences and Arts

Belgrade, 2024

PUBLICATIONS OF THE ASTRONOMICAL OBSERVATORY OF BELGRADE

FOUNDED IN 1947

EDITORIAL BOARD:

Dr. Srdjan SAMUROVIĆ, Editor-in-Chief (Astronomical Observatory, Belgrade)

Dr. Rade PAVLOVIĆ (Institute of Physics, Belgrade)

Dr. Miroslav MIĆIĆ (Astronomical Observatory, Belgrade)

Dr. Branislav VUKOTIĆ (Astronomical Observatory, Belgrade)

All papers in this Publication are peer reviewed.

Published and copyright © by Astronomical Observatory, Volgina 7, 11060 Belgrade 38, Serbia

Director of the Astronomical Observatory: Dr. Luka Č. Popović

Typesetting: Tatjana Milovanov

Internet address <https://publications.aob.rs>

ISSN 0373-3742

ISBN 978-86-82296-08-9

Financially supported by the Ministry of Science, Technological Development and Innovation of the Republic of Serbia

CIP - Каталогизacija у публикацији - Народна библиотека Србије, Београд

537.56(082)

539.186.2(082)

539.121.7(082)

533.9(082)

SUMMER School and International Symposium on the Physics of Ionized Gases (32 ; 2024 ; Beograd)

Contributed papers & abstracts of invited lectures, topical invited lectures and progress reports / 32nd Summer School and International Symposium on the Physics of Ionized Gases - SPIG 2024, August 26 – 30, 2024, Belgrade, Serbia ; editors Bratislav Obradović ... [et al.]. - Belgrade : Astronomical Observatory, 2024 (Beograd : Skripta Internacional). - 215 str. : ilustr. ; 24 cm. - (Publications of the Astronomical Observatory of Belgrade, ISSN 0373-3742)

Na nasl. str.: University of Belgrade, Faculty of Physical Chemistry; Serbian Academy of Sciences and Arts. - Tiraž 200. - Str. 17-18: Preface / editors Bratislav Obradović ... [et al.]. - Bibliografija uz svaki rad. - Registar.

ISBN 978-86-82296-08-9

1. Kuzmanović, Miroslav, 1967- [urednik] [autor dodatnog teksta]

a) Јонизовани гасови - Зборници b) Атоми - Интеракција - Зборници

v) Плазма - Зборници

COBISS.SR-ID 150439689

SPIG 2024

SCIENTIFIC COMMITTEE

J. Cvetić (Co-chair), Serbia
B. Obradović (Co-chair), Serbia

A. Antoniou, Greece
J. Burgdörfer, Austria
M. Čosić, Serbia
V. Guerra, Portugal
M. Ivković, Serbia
J. Kovačević-Dojčinović, Serbia
K. Kutasi, Hungary
I. Mančev, Serbia
D. Marić, Serbia
N. J. Mason, UK
A. Milosavljević, France
V. Milosavljević, Serbia
D. Milošević, BH
K. Mima, Japan
L. Nahon, France
G. Poparić, Serbia
I. Radović, Serbia
P. Ranitovic, Serbia
P. Rousseau, France
I. Savić, Serbia
Y. Serruys, France
N. Simonović, Serbia
V. Srečković, Serbia
M. Škorić, Japan
S. Tošić, Serbia
M. Trtica, Serbia
R. White, Australia

ADVISORY COMMITTEE

D. Belić
N. Bibić
M. S. Dimitrijević
S. Đurović
D. Ilić
N. Konjević
M. M. Kuraica
J. Labat
G. Malović
B. P. Marinković
M. Milosavljević
Z. Mišković
Z. Lj. Petrović
L. Č. Popović
B. Stanić

ORGANIZING COMMITTEE

M. Kuzmanović (Chair)
M. Ristić (Co-secretary)
B. Stankov (Co-secretary)
N. Konjević
N. Cvetanović
D. Ranković
M. Milovanović
M. Marković
A. Šajić
I. Traparić

Reviewers for the Book of SPIG 2024

Jovan Cvetić, Full Professor, University of Belgrade, School of Electrical Engineering, Belgrade, Serbia

Marko Čosić, Associate research professor, Vinča Institute of Nuclear Sciences, Belgrade, Serbia

Milivoje Ivković, Principal Research Fellow, Institute of Physics, Belgrade, Serbia

Jelena Kovačević-Dojčinović, Associate research professor, Astronomical Observatory Belgrade, Serbia

Ivan Mančev, Full Professor, University of Niš, Faculty of Sciences and Mathematics, Niš, Serbia

Dragana Marić, Principal Research Fellow, Institute of Physics, Belgrade, Serbia

Aleksandar R. Milosavljević, Principal Research Fellow, Synchrotron SOLEIL, Saint-Aubin, France

Vladimir Milosavljevic, Full Professor, University of Belgrade - Faculty of Physics, Belgrade, Serbia

Dejan Milošević, Full Professor, University of Sarajevo – Faculty of Science, Sarajevo, Bosnia and Herzegovina

Bratislav Obradović, Full Professor, University of Belgrade - Faculty of Physics, Belgrade, Serbia

Goran Poparić, Full Professor, University of Belgrade - Faculty of Physics, Belgrade, Serbia

Ivan Radović, Principal Research Fellow, Vinča Institute of Nuclear Sciences, Belgrade, Serbia

Predrag Ranitović, Principal Research Fellow, University of Belgrade - Faculty of Physics, Belgrade, Serbia

Igor Savić, Full Professor, University of Novi Sad, Faculty of Sciences and Mathematics, Novi Sad, Serbia

Nenad Simonović, Principal Research Fellow, Institute of Physics, Belgrade, Serbia

Vladimir Srećković, Principal Research Fellow, Institute of Physics, Belgrade, Serbia

Miloš Škorić, Principal Research Fellow, Vinča Institute of Nuclear Sciences, Belgrade, Serbia

Sanja Tošić, Research Associate Assistant, Institute of Physics, Belgrade, Serbia

Milan Trtica, Principal Research Fellow, Vinča Institute of Nuclear Sciences, Belgrade, Serbia

CONTENTS

Bratislav Obradović, Jovan Cvetić, Miroslav Kuzmanović and Nikola Cvetanović <i>Preface</i>	17
Section 1. ATOMIC COLLISION PROCESSES	
Invited Lectures	
O. Asvany, P.C. Schmid, S. Thorwirth and S. Schlemmer <i>Missing Ions in Laboratory and Space</i>	21
Himadri Chakraborty <i>Impact Spectroscopy and Chronoscopy of Gas Phase Atoms, Molecules and Fullene</i>	22
Alicja Domaracka <i>Ion Processing of Molecular Systems: A Way to Form Complex Systems in Space</i>	23
Carla Figueira de Morisson Faria <i>Exploring Quantum Effects in the Attosecond Domain</i>	24
G. G. Paulus <i>Extreme UV Imaging with High Harmonics</i>	25
Xiao-Min Tong <i>Theory on Dynamics of Atoms in Strong Laser Field</i>	26
Topical Invited Lectures	
N. Pinhão <i>Description of Electron Swarms in an Electric Field: A Finite Elements Computation Including Third-order Transport Parameters</i>	27
Helgi Rafn Hrodmarsson <i>VUV Photionization of Interstellar Molecules: Making Sense of Our Beautifully Mysterious Universe, Molecule by Molecule</i>	28
Progress Reports	
Jasmina Atić and Saša Dujko <i>Electron Transport and Negative Ionization Fronts in Strongly Attaching Gases</i>	29

Daan Boer and Jan Van Dijk <i>LOKI-B C++: An Open-Source Boltzmann Solver for Reproducible Electron Boltzmann Calculations</i>	30
Danijela Danilović, Dušan K. Božanić, Aleksandar R. Milosavljević, Radovan Dojčilović and Vladimir Djoković <i>Synchrotron Radiation Photoelectron Spectroscopy Study of the Electronic Structure of Ag-Bi-I Rudorffite Nanoparticles</i>	31
M. Fournier, J. Palaudoux, R. Dupuy, F. Penent and C. Nicolas <i>Photoelectron Spectroscopy of Solvated Biological Interest Molecules in Liquid Jet Configuration</i>	32
D. Habibović and D. B. Milošević <i>Strong-field Processes Induced by Tailored Laser Fields</i>	33
Emilia Heikura, Christina Zindell, Denis Kargin, Aleksandar Milosavljevic, Andreas Hans, Rudolf Pietschnig and Arno Ehresmann <i>Towards Distant Dependent Inner-shell Photoelectron Circular Dichroism</i>	34
Laura Pille, Bart Oostenrijk, Juliette Leroux, Carlos Ortiz Mahecha, Robert Meißner, Debora Scuderi, Sadia Bari and Lucas Schwob <i>Exploring Biomolecular Properties in the Gas Phase by Using Advanced Light Sources</i>	35
M. Werl, T. Koller, P. Haidegger, S. Wrathall, L. Esletzbichler, A. Niggas, F. Aumayr, K. Tókési and R.A. Wilhelm <i>De-excitation Cascade Calculation for Highly Excited Hollow Atoms</i>	36
Posters	
Danko Bošnjaković, Ilija Simonović and Saša Dujko <i>Studies on Streamer Discharges in Ultra-low GWP Gases</i>	37
G. J. Boyle, N. A. Garland, R. P. Mceachran and R. D. White <i>Electron Transport in Simple Liquid Mixtures</i>	38
Saša Dujko, Ilija Simonović, Danko Bošnjaković, Jasmina Atić and Zoran Lj. Petrović <i>Electron Transport in Radio-Frequency Electric and Magnetic Fields in Ultra-low GWP Gases</i>	39
Saša Dujko, Ilija Simonović, Danko Bošnjaković, Zoran LJ. Petrović and J. De Urquijo <i>Studies on Electron Swarms and Streamer Discharges in Eco-friendly RPC Gases</i>	40

N. A. Garland, R. D. White, R. E. Robson and M. Hildebrandt <i>An Aliasing Method for Determination of Transport Data for Exotic Charged Particles in Crossed Electric and Magnetic Fields</i>	41
Mai Hao, Gerjan Hagelaar, Boya Zhang and Xingwen Li <i>Monte Carlo Simulation of Electron Swarms in Pulsed Townsend Experiment and Validation of the Swarm Data Derived from Waveform Analysis</i>	45
Jelena B. Maljković, Jelena Vukalović, Francisco Blanco, Gustavo Garcia and Bratislav P. Marinković <i>Investigation of Elastic Electron Scattering by Anaesthetic Molecules in Gaseous Phase</i>	46
Bratislav P. Marinković and Stefan Đ. Ivanović <i>Electron Scattering Cross Sections Represented in Belgrade Electron-atom/molecule Database (BEAM)</i>	47
Bratislav P. Marinković, Jozo J. Jureta and Lorenzo Avaldi <i>Ejected Electron Spectra of Krypton Studied by High and Low Energy Electrons</i>	48
Nenad Milojević, Ivan Mančev, Danilo Delibašić and Miloš Milenković <i>Post-prior Discrepancy in the CBI-4B Method for Single-electron Capture in Fast $\text{Li}^{3+} + \text{He}$ Collisions</i>	49
D. L. Muccignat, D. B. Jones, J. R. Gascooke, G. J. Boyle, N. A. Garland and R. D. White <i>Direct Electron-liquid Energy Loss Spectra Measurements Using a Liquid Micro-jet</i>	53
Željka Nikitović and Zoran Raspopović <i>Diffusion Coefficients of H_2^+ Ions in H_2 Gas</i>	57
T. Rook, L. Cruz Rodriguez and C. Figueira de Morisson Faria <i>Influence of Catastrophes and Hidden Dynamical Symmetries on Ultrafast Backscattered Photoelectrons</i>	61
Ilija Simonović, Danko Bošnjaković and Saša Dujko <i>Three-dimensional Streamer Model in the AMReX Environment</i>	62
Barbora Stachová, Juraj Országh and Štefan Matejčík <i>Excitation of Acetone Induced by Electron Impact</i>	63
Sanja Tošić, Vladimir Srećković and Veljko Vujčić <i>Small Molecules Essential to Astrophysics: Collisional and Radiative Processes</i>	64

Mirjana M. Vojnović, Miroslav M. Ristić, Violeta V. Stanković-Mališ and Goran B. Poparić <i>Dissociative Electron Attachment to CO₂ in Electric and Magnetic Fields</i>	65
Jelena Vukalović, Jelena B. Maljković, Francisco Blanco, Gustavo Garcia and Bratislav P. Marinković <i>Investigation of Elastic Electron Scattering from Desflurane Molecule at Intermediate Electron Energy</i>	66
Guanyu Wang, Boya Zhang and Xingwen Li <i>Transport Properties of Two-temperature SF₆ and Its Alternative Gases</i>	67
Section 2. PARTICLE AND LASER BEAM INTERACTIONS WITH SOLIDS	
Topical Invited Lectures	
Marija Gorjanc <i>Plasma Modification of Natural Fibres to Improve Adhesion in Bio-composites</i>	71
Milan Radović <i>Integrating Pulse Laser Deposition and Advanced Spectroscopy: Unveiling Hidden Phenomena in Transition Metal Oxides</i>	72
Progress Reports	
Hristina Delibašić-Marković <i>Characterizing Ionization and Electron Dynamics in Biological Materials: Theoretical and Numerical Insights into Pulsed Laser-induced Breakdown Processes</i>	73
Ana Kalinić, Ivan Radović, V. Despoja, Lazar Karbunar and Z. L. Mišković <i>Interaction of Ions with Graphene-insulator-graphene Composite Systems</i>	74
Violeta V. Stanković Mališ and Goran B. Poparić <i>Modeling the Surface Interaction of Cellulosic Materials with CO₂ Plasmas</i>	75
Posters	
Milivoje Hadžijojić and Marko Ćosić <i>Low Energy Heavy Ion Rainbow Scattering by Graphene</i>	76
Ana Kalinić, Ivan Radović, Lazar Karbunar and Z. L. Mišković <i>Interaction of Ions with Drift-current Biased Supported Graphene</i>	80

F. Komarov, O. Milchanin, M.V. Puzyrev and I.S. Rahavaya <i>Forming Nanocrystalline SnO₂ Films on Silicon and Silicon Dioxide by Laser-Plasma Deposition Method</i>	81
Dragan Ranković, Biljana Stankov, Ivan Traparić, Miroslav Kuzmanović and Milivoje Ivković <i>Target Selection for LIBS Studies of Hydrogen Isotope Retention</i>	85
Miroslav Ristić, Aleksandra Šajić, Jovana Babić and Miroslav Kuzmanović <i>Equilibrium Composition of Plasma Obtained by Laser Ablation of Glass</i>	86
Violeta V. Stanković Mališ and Goran B. Poparić <i>Semiquantum Simulation of Cellulosic Materials Interaction with CO₂ Plasmas</i>	87
Nikola Starčević and Srdjan Petrović <i>Rainbows in Transmission of Proton Through Thin Silicon Carbide Crystal</i>	88
N. Tarasenko, V. Kornev, M. Nedelko, A. Radomtsev, N. Tarasenska, Jovan Ciganovic, Sanja Zivkovic and Miloš Momcilovic <i>Properties of Cu/Zn Oxide Nanostructures Formed by Plasma-activated Electrolysis</i>	92

Section 3. LOW TEMPERATURE PLASMAS

Invited Lectures

Satoshi Hamaguchi <i>Opportunities and Challenges in Low-temperature Plasma Science for Atomic-layer Processing</i>	99
Jan van Dijk and Daan Boer <i>LXCat 3 and Beyond – Fostering Reproducibility in Low-temperature Plasma Science</i>	100

Topical Invited Lectures

Peter Hartmann <i>Using Dust Particles as Probes in Low Pressure Gas Discharges</i>	101
Mirjana Kostic, Ana Kramar, Bratislav Obradovic and Milorad Kuraica <i>Atmospheric Pressure Plasma in Processing of Cellulose Fibers: From Surface Cleaning to Tailored Properties</i>	102
Violeta Lazic <i>LIBS Spectroscopy: What We Can Measure, and How?</i>	103

C. Lazzaroni, A. Remigy, M. Jacquemin, H. Kabbara, S. Kasri, B. Menacer, K. Gazeli, V. Mille and G. Lombardi <i>Micro Hollow Cathode Discharges in Argon/Nitrogen Used for Boron Nitride PECVD</i>	104
P. Maguire, N. Hendaway, H. Mcquaid and D. Mariotti <i>Liquid Microdroplets in a Microplasma: Phenomena and Technological Applications</i>	105
Peter Papp, Samuel Peter Kovár, Ladislav Moravský and Štefan Matejčík <i>Ion Induced Reactions in IMS Studied by DFT</i>	106
G. Primc, M. Zver, R. Zaplotnik, A. Filipič, D. Dobnik and M. Mozetič <i>Inactivation of Viruses in Water by Plasma Treatment</i>	107
Nevena Puač, Nikola Škoro, Sergej Tomić, Andjelija Marković, Neda Babucić, Olivera Jovanović, A. Morina, Gordana Malović, Miodrag Čolić and Zoran Lj. Petrović <i>Diagnostics and Applications of Atmospheric Pressure Plasmas for Triggering of Cell Mechanisms</i>	108
Progress Reports	
A. P. Jovanović, H. Höft, D. Loffhagen, T. Gerling and M. M. Becker <i>Fluid Modelling of Single-filament DBD and Self-pulsing Discharges at Atmospheric Pressure Using FEDM</i>	109
Sanja Pavlovic and Goran Poparić <i>Thermal and Acoustic Properties of Cellulose Fibrous Materials</i>	110
M. Stankov, M. M. Becker, L. Bröcker, C.-P. Klages and D. Loffhagen <i>Analysis of Dielectric Barrier Discharges in Ar-monomer Mixtures Using a Standardized Fluid Modelling Approach</i>	111
Olga Stepanova, Vadim Snetov, Oleg Grushko, Dmitry Subbotin, Ilya Ruchkin and Mikhail Pinchuk <i>“Air-plasma-water” Electrophysical System Based on DBD Plasma Jet: Prospects and Problems</i>	112
Ivan Traparić <i>Application of Machine Learning and Artificial Intelligence in Plasma Spectroscopy</i>	113

Posters

- E.N. Bocharnikova, O.N. Tchaikovskaya, S.A. Chaykovsky,
V.I. Solomonov, A.S. Makarova and I.V. Sokolova
*Luminescent Analysis of E-beam Induced Transformation of Phenol in
the Presence of Humic Substances*..... 114
- N.N. Bogachev, A.S. Bakshaev, L.V. Kolik, E.M. Konchekov and
A.S. Kon'kova
*Compact Piezotransformer Source of the Cold Atmospheric Plasma
with Three Types of Discharges*..... 118
- N.N. Bogachev, I.L. Bogdankevich, V.I. Zhukov, D.M. Karfidov,
V.P. Stepin and N.G. Gusein-Zade
*Ionization of a Plasma Antenna Channel in a Dielectric
Gas-discharge Tube*..... 119
- Nikola Cvetanović, Saša S. Ivković and Bratislav M. Obradović
*Estimation of Nitrogen Impurity Level in Helium Atmospheric
Discharge via Emission Spectroscopy*..... 120
- Lazar Gavanski, Nataša Simić and Stevica Djurović
*Measurement of the Velocity of the Plasma Jet Appearing from a Wall
Stabilized Arc*..... 121
- Jovica Jovović
*The Measurement of Pulsed Gas Discharge Parameters by Means of
Fe I Lines in Argon and Argon-hydrogen Mixture*..... 125
- E.M. Konchekov, N.G. Gusein-Zade, D.V. Yanykin, L.V. Kolik,
Yu.K. Danileiko, V.I. Lukanin, K.F. Sergeichev, I.V. Moryakov,
V.D. Borzosekov, V.V. Gudkova, M.E. Astashev and S.V. Gudkov
*Low-temperature Plasma and Plasma-activated Liquids in Solving
Agricultural Problems: Experimental Technique*..... 129
- A. Kropotkin, A. Chukalovsky, A. Kurnosov, T. Rakhimova and
A. Palov
*Modelling of an ICP Discharge in Oxygen with Full Kinetics Scheme
with Newly Calculated VV/VT Rate Constants*..... 130
- Vitaly Kuzmenko, Andrey Miakonkikh and Konstantin Rudenko
*The Formation of Microneedles Structures from Silicon Using Plasma
Etching in SF_6/O_2 Mixture in Inductively Coupled Plasma*..... 134
- James Lalor and Vladimir Milosavljević
*Investigating the Thermal Profile of an Atmospheric Pressure Argon
Plasma Jet on a Conductive and Insulating Mesh Surface*..... 135

Zlatko Majlinger <i>Stark Width Estimates for the Most Prominent Ce II Spectral Lines Important for Astrophysical Investigations.....</i>	136
Zlatko Majlinger, Milan S. Dimitrijević and Vladimir A. Srećković <i>Stark Widths of Several Te II Spectral Lines for Investigation of Astrophysical Spectra.....</i>	137
Jelena Marjanović, Dragana Marić, Marija Puač, Antonije Đorđević and Zoran Lj. Petrović <i>RF Breakdown in Argon at Low-pressures: Experiment and Modelling.....</i>	138
Milica Marković, Dragan Ranković and Miroslav Kuzmanović <i>The Effect of Acids on Pig Bone Estimated by LIBS.....</i>	142
A. Miakonkikh, V. Kuzmenko and K. Rudenko <i>Fluorocarbon Polymerizing Plasmas Etching Processes for Structures of Microelectronics.....</i>	143
Nikodin V. Nedić, Nikola V. Ivanović, Ivan R. Videnović, Djordje Spasojević and Nikola Konjević <i>Cathode Sheath Diagnostics by Integral End-on Optical Emission Spectroscopy in an Analytical Glow Discharge Source in Argon.....</i>	144
S.A. Poniaev, P.A. Popov, N.A. Monakhov, T.A. Lapushkina and M.A. Kotov <i>The Use of Thermoelectric Radiation Detectors for Heat Flux Measurements in Shock-tubes with Gas Ionization.....</i>	145
Aleksandra Šajić, Dragan Ranković, Miroslav Ristić and Miroslav Kuzmanović <i>Determination of Unknow Analyte Concentration in Glass Samples Using the LIBS Method.....</i>	146
Biljana Stankov, Marijana R. Gavrilović Božović, Dragan Ranković, Jelena Savović and Milivoje Ivković <i>Fast Photography in the Service of Spatially and Temporally Resolved LIBS Diagnostics of Doped Tungsten.....</i>	147
Desanka Topalović, Neda Babucić, Nikola Škoro and Nevena Puač <i>Measurements of Reactive Oxygen and Nitrogen Species in Plasma Activated Water by Microwave Discharge.....</i>	148
Ivan Traparić, Biljana Stankov and Milivoje Ivković <i>Detection of Rhenium in Tungsten Using LIBS with Additional Fast Pulse Discharge.....</i>	152

Ivan Traparić, Biljana Stankov, Nikola Vujadinović, Milica Vinić and Milivoje Ivković <i>Influence of the Ablation Angle Change on Spectral Line Intensities in LIBS Experiments.....</i>	153
V.V. Voevodin, O.I. Korzhova, V.Yu. Khomich, V.A. Yamschikov, N. Yu. Lysov and A.V. Klubkov <i>Influence of Interelectrode Distance on the Characteristics of Three-electrode Pulsed SDBD.....</i>	154
Veljko Vujčić, Vladimir A. Srećković, Ognjan Kounchev and Felix Jacob <i>A&M Datasets for LTP Treatment of Plants.....</i>	158
Section 4. GENERAL PLASMAS	
Invited Lecture	
Andreja Gomboc <i>How Stars Get Thorn Apart by Supermassive Black Holes.....</i>	161
Paola Marziani <i>Super-Eddington Quasars: From Atomic Physics to Cosmology.....</i>	162
Luca Volpe <i>Current Situation and Future Prospectives of the European IFE Program, Technology Development, Science and Related Applications.....</i>	163
Topical Invited Lectures	
M. D. Christova, Milan S. Dimitrijević and S. Sahal-Bréchet <i>Astrophysical Applications of Stark Broadening of Spectral Lines.....</i>	164
A. Cinins, Milan S. Dimitrijević, Vladimir A. Srećković, K. Miculis, I. I. Beterov and N. N. Bezuglov <i>Penning and Photo Ionizations of Cold Rydberg Alkali-metal Atoms Under Föster Resonance Conditions.....</i>	165
Ugo Jacovella <i>Exploring the Importance of Interstellar Ions in the Enigma of Diffuse Interstellar Bands.....</i>	166
G. La Mura, G. Mulas, M. A. Iati, C. Cecchi-Pestellini, S. Rezaei and R. Saija <i>Interstellar Dust as a Dynamic Environment.....</i>	167
S.V. Ryzhkov <i>Magneto-inertial Fusion and Powerful Installations.....</i>	168

C. Suzuki, F. Koike, N. Tamura, T. Oishi, Y. Kawamoto, T. Kawate, M. Goto, N. Nakamura and I. Murakami <i>Comprehensive Z-dependence Analysis of Soft X-ray Spectra from Highly Charged Heavy Ions Using Magnetically Confined High-temperature Plasmas</i>	169
Miroslava Vukcevic <i>On the Conditions for Soliton Formation in the Galactic Environment</i>	170
Progress Reports	
B. Z. Djordjević, D. J. Strozzi, C. A. Walsh, J. D. Moody, C. R. Weber, S. A. Maclaren and G. B. Zimmerman <i>Integrated Radiation-magneto-hydrodynamic Simulations of Magnetized Burning Plasmas</i>	171
M. Drissi, G.A. Garcia, L. Nahon, S. Boye-Peronne, B. Gans, H.R. Hrodmarsson, H.L. Le, M.-X. Jiang and J.-C. Loison <i>Photoelectron Spectroscopy of Radicals of Astrochemical Interest</i>	172
Felix Iacob <i>Electron NS^+ Collisions in Cold Plasma</i>	173
Aleksandra Kolarski <i>Properties of Earth's Lower Ionospheric Plasma Perturbed by Solar Flares</i>	174
Petar Kostić <i>Supernova Remnants in Clumpy Medium: Hydrodynamic and Radio Synchrotron Evolution</i>	175
Nikola Veselinović, Mihailo Savić, Aleksandar Dragić, Dimitrije Maletić, Dejan Joković, Radomir Banjanac, Miloš Travar and Vladimir Udovičić <i>Fluctuations in the Flux of Energetic Protons in Heliosphere Before and During Sudden Decreases in Galactic Cosmic Ray Intensity</i>	176
Vladimir Zeković <i>SLAMS-enhanced Particle Acceleration at High-Mach Number Astrophysical Shocks: TeV in a Blink of Supernova</i>	177
Posters	
Edi Bon, Paola Marziani and Nataša Bon <i>Variability Along the Main Sequence of Quasars</i>	178
Andjelka B. Kovačević, Dragana Ilić, Luka Č. Popović, Marina Pavlović, Aman Raju, Momčilo Tošić and Iva Čvorović-Hajdinjak <i>Advanced Nonlinear Analysis for Detecting Binary Quasars and Transient Events in the LSST Era</i>	182

Jelena Kovačević-Dojčinović, Ivan Dojčinović and Luka Č. Popović <i>Two-component Model of Fe II Lines in Spectra of Active Galactic Nuclei</i>	183
Nenad M. Sakan, Zoran Simić, Vladimir A. Srećković and Momchil Dechev <i>The Complex Emmitter Inside Dense Plasma, Continuation of a Coulomb Cut-off Approach, Argon Case</i>	184
Vladimir A. Srećković, Nicolina Pop, Milan Dimitrijević and Magdalena Christova <i>Investigation of Chemistry of Hydrogen, Helium and Lithium Molecular Ions in the Early Universe</i>	185
Vladimir A. Srećković, Nicolina Pop, Milan S. Dimitrijević, Magdalena D. Christova and Veljko Vujčić <i>Dataset for Photodissociation of Small Molecular Ions</i>	186
Vladimir A. Srećković, Nicolina Pop and Veljko Vujčić <i>New Molecular Data for Confined Molecular Systems and Astrochemical Modelling</i>	187
 2nd Workshop on Swarm Physics and Gaseous Dielectrics (2nd SPGD)	
G. J. Boyle, D. L. Muccignat, M. J. E. Casey, R. D. White, H. Vemulapilli, M. M. van Rijn and C. M. Franck <i>Analysis of Current Waveforms in the Pulsed-Townsend Experiment</i>	191
N. A. Garland, D. L. Muccignat, G. J. Boyle and R. D. White <i>Rapidly Exploring and Designing Electron Transport Quantities in Dielectric Gas Insulator Mixtures with Approximation Theories</i>	192
Satoru Kawaguchi, Kazuhiro Takahashi and Kohki Satoh <i>Physics-informed Neural Networks for Studies on Electron Swarms in Gases</i>	193
Marnik Metting van Rijn, Stephen F. Biagi and Christian M. Franck <i>Electron Scattering Cross Sections of 1,1,1,2-Tetrafluoroethane (R134a)</i>	194
D. L. Muccignat, G. J. Boyle, N. A. Garland and R. D. White <i>Advances in Machine Learning Methods for the Determination of Electron Scattering Cross-section Sets</i>	195
L.G. Pérez, O. González and J. De Urquijo <i>Three-body Electron Attachment Processes In H₂O, CO₂, and Their Mixtures</i>	196

N. Pinhão <i>Fitting of Electron Collision Cross Sections from Swarm Data Using a Genetic Algorithm</i>	197
M. Ranković, R. Kumar T P, P. Nag, J. Kočišek and J. Fedor <i>Electron Induced Processes in Dielectric Insulation Gases</i>	198
Jacob Stephens, Max Flynn and Andreas Neuber <i>Multi-term Boltzmann Models: Engineering Tools for the Pulsed Power Community</i>	199
L. Vialetto <i>Particle Propagation and Electron Transport in Gases</i>	200
Boya Zhang, Mai Hao, Peiqiong Liu and Xingwen Li <i>Deriving Swarm Parameters from Ion Kinetics and Determining Collision Cross Sections Through Data-driven Methods for Eco-friendly Insulating Gases</i>	201
Authors' Index.....	203
Programme of the SPIG 2024.....	207

PREFACE

This special issue of the Publication of Astronomical Observatory in Belgrade (PubAOB) contains the contributed papers and abstracts of Plenary Lectures, Topical Invited Lectures, Progress Reports and Posters that will be presented at the 32nd International Symposium on the Physics of Ionized Gases (SPIG 2024) which will be held from 26st to 30th August 2024, in Belgrade, Serbia.

The SPIG 2024 is organized by the University of Belgrade – Faculty of Physical Chemistry and Serbian Academy of Sciences and Arts, with the support of the Ministry of Science, Technological Development and Innovation of the Republic of Serbia.

The 2nd Workshop on Swarm Physics and Gaseous Dielectrics (SPGD) and the 1st Workshop LIBS4fusion will be attached to the SPIG 2024 conference.

We expect to have regular participants (on site), who will present 11 plenary invited talks, 18 topical invited, 23 progress reports, and 58 posters within the main SPIG 2024 conference. Workshops will entail 11 invited talks within the 2nd SPGD, and 10 invited talks within the LIBS4fusion. Presentations will cover four main disciplines connected to physics of ionized gasses with strong mutual interactions and numerous applications: Atomic Collision Processes, Particle and Laser Beam Interactions with Solids, Low Temperature Plasmas and General Plasma (including Fusion and Astrophysical plasma).

The SPIG reflects the progress in plasma physics and related fields. The conference has a long tradition, starting with the first meeting in Belgrade in 1962, entitled: "1st Yugoslav Symposium on the Physics of Ionized Gases (SPIG)". As previous SPIG proceedings, this issue of PubAOB presents new results from theory, experiment and application in the broad area of ionized gasses phenomena.

Editors would like to thank the members of the Scientific and Advisory Committees of SPIG 2024 for their efforts in proposing the invited lectures and reviewing the contributed papers and abstracts. We would also like to thank the authors for their contribution, and to wish all participants a pleasant and productive stay in Belgrade. We are grateful to the Serbian Academy of Sciences and Arts for their long-term commitment to support this event as well as the Serbian Ministry of Science, Technological Development and Innovation for their continuing support.

Editors:

Bratislav Obradović, Jovan Cvetić,
Miroslav Kuzmanović and Nikola Cvetanović

Belgrade, August 2024

Section 1.

**ATOMIC COLLISION
PROCESSES**

MISSING IONS IN LABORATORY AND SPACE

O. ASVANY¹, P.C. SCHMID¹, S. THORWIRTH¹ and S. SCHLEMMER¹

¹*I. Physikalisches Institut, Universität zu Köln, Zùlpicher Str. 77, 50937 Köln, (Germany)
 E-mail schlemmer@ph1.uni-koeln.de*

Abstract. Molecular ions play a vital role in space because they are readily formed by the ubiquitous cosmic ray ionisation and often undergo rapid chemical reactions even at the low temperatures of the interstellar medium. It is an important task of laboratory astrophysics to provide astrophysicists with high resolution spectra of molecular ions. Action spectroscopy in cryogenic higher-order multipole ion traps as depicted in the insert of the Figure below was instrumental to overcome limitations of traditional ways of ion spectroscopy. Mass selection paired with low temperature storage and near unity ion detection efficiency are unique features of these techniques (McGuire et al., 2020). Today narrow band infrared lasers are commercially available and allow to record rotationally resolved vibrational spectra (see Fig.). In our newly developed leak-out spectroscopy (LOS) method the ions of interest are kicked-out from the trap based on a vibration-to-translation energy transfer (Schmid et al., 2022). We use the highly accurate THz radiation from amplifier multiplier chains (THz AMC, see Fig.) to employ THz-infrared double resonance schemes in order to also record pure rotational transitions (Asvany and Schlemmer, 2021). Based on these spectra several ionic species have been found in space. Examples as published in (Silva et al., 2023) will be discussed along with experiments beyond spectroscopy.

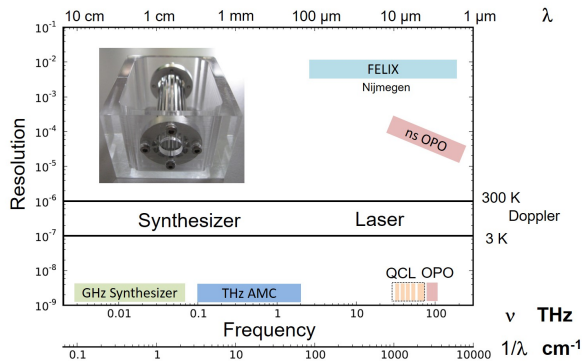


Figure 1: Spectral range and resolution of light sources for action spectroscopy in traps.

References

- B.A. McGuire, O. Asvany, S. Brünken, S. Schlemmer, *Nat. Rev. Phys.*, **2**, 402 (2020).
 P. C. Schmid, O. Asvany, T. Salomon, *et al.*, *J. Phys. Chem. A* **126**, 43 (2022).
 O. Asvany, S. Schlemmer, *Phys. Chem. Chem. Phys.*, **23**, 26602 (2021).
 W.G.D.P. Silva, J. Cernicharo, S. Schlemmer, *et al.*, *Astron. & Astrophys.* **676**, L1 (2023).

IMPACT SPECTROSCOPY AND CHRONOSCOPY OF GAS PHASE ATOMS, MOLECULES AND FULLERENES

HIMADRI CHAKRABORTY

*Department of Natural Sciences, Dean L. Hubbard Center for Innovation
Northwest Missouri State University, Maryville, USA
E-mail himadri@nwmissouri.edu*

Abstract. Studies of scattering and ionization by the positron/electron and photon impact on matters, the spectroscopy, involve a variety of structures in the reaction cross section as a function of the momentum transfer. These structures originate from hosts of resonant and diffraction processes which happen in ultrafast timescale in attoseconds (as). In fact, the resulting time delay or advancement of the product creation inherits structures but with additional nuances (Figure 1), the study of which is called the chronoscopy. I will present selected results of our computational research across these topics (see Madjet et al. 2021, Shaik et al. 2023, Aiswarya et al. 2024). Support from the US NSF is acknowledged.

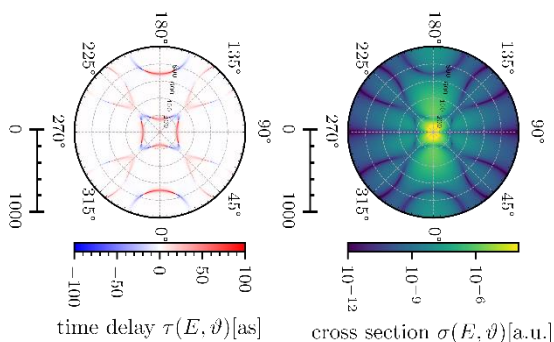


Figure 1: Delay and cross section diffractograms for the photoionization of $C_8F_8^-$.

References

- Aiswarya, R., Jose, J.....Chakraborty, H. S : 2024, *Phys. Rev. Lett.*, ([in press](#)).
Madjet, M. E, Ali, E.....Chakraborty, H. S : 2021, *Phys. Rev. Lett.*, **126**, [183002](#).
Shaik, R., Varma, H. R.....Chakraborty, H. S : 2023, *Phys. Rev. Lett.*, **130**, [233201](#).

ION PROCESSING OF MOLECULAR SYSTEMS: A WAY TO FORM COMPLEX SYSTEMS IN SPACE

ALICJA DOMARACKA

*Centre de Recherche sur les Ions, les Matériaux et la Photonique (CIMAP)
(CEA/CNRS/ENSICAEN/Université de Caen Normandie), Boulevard Henri
Becquerel, CS 65133 14076 Caen cedex 5, France
E-mail domaracka@ganil.fr*

Abstract. In space, the molecular matter is exposed to ionizing radiation and two scenarios are proposed to explain the emergence of new molecular species. On the one hand, the *bottom-up* approach proposes the growth of larger molecules from smaller subunits. On the other hand, the *top-down* scenario considers the emission of molecular species from a large piece of matter. In order to study the processes leading to the formation of complex organic molecules, we have considered ion interaction with molecular clusters or icy mantels.

Molecular systems in space are exposed to energetic ions e.g. solar wind or ions trapped in the Jupiter magnetosphere and cosmic rays. The GANIL facility (Grand Accélérateur National d'Ions Lourds, Caen, France), a unique tool to study ion interactions with matter, allow to study ion induced fragmentation and reactivity of such systems in a very large range of kinetic energies of projectiles (from keV to GeV, ions from He to U). During my talk, I will present examples of: i) intra-cluster molecular growth processes within of polycyclic aromatic hydrocarbons and amino acids molecular clusters induced by ion collisions (e.g. Delaunay R. et al. 2015, Domaracka A. et al. 2018, Rousseau P. et al. 2020) and ii) ion processing of astrophysical ice analogues and condensed complex organic molecules (e.g.: Rothard H. et al. 2017, Vignoli Muniz G. S. et al. 2017 and 2022).

References

- Delaunay, R. et al. 2015, *J. Phys. Chem. Lett.*, **6** 1536.
Domaracka, A. et al. 2018, *Phys. Chem. Chem. Phys.*, **20**, 15052.
Rothard, H. et al. 2017, *J. Phys. B*, **50**, 062001.
Rousseau, P. et al. 2020, *Nature Communications* **11**, 3818.
Vignoli Muniz G. S. et al. 2017, *Astrobiology*, **17**, 298.
Vignoli Muniz G. S. et al. 2022, *ACS Earth Space Chem.*, **511**, 2149.

EXPLORING QUANTUM EFFECTS IN THE ATTOSECOND DOMAIN

CARLA FIGUEIRA DE MORISSON FARIA

*Department of Physics and Astronomy, University College London, Gower Street,
London WC1E 6BT, United Kingdom
E-mail c.faria@ucl.ac.uk*

Abstract. Matter in strong laser fields poses many challenges, theoretically and experimentally. Not only are the field strengths comparable to the target's binding forces, but the attosecond (10^{-18} s) timescales involved are some of the shortest in nature. Although classical methods are hugely popular, the phenomena themselves seem to be inherently quantum. Here, I will exemplify my group's work on quantum effects in attoscience.

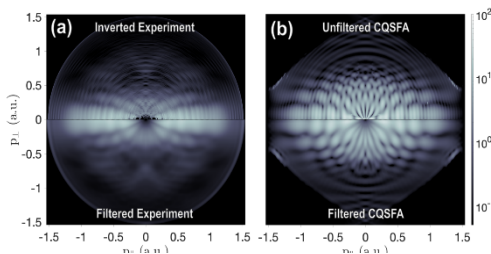


Figure 1: a) experimental and (b) theoretical photoelectron momentum distributions for argon, in a field of intensity of 2×10^{14} W/cm² and wavelength $\lambda = 800$ nm; from Werby et al 2021.

First, an orbit-based, UCL-developed approach that fully accounts for the laser field and the binding potentials, the Coulomb-Quantum Orbit Strong-Field Approximation (CQSFA) will be applied to ultrafast photoelectron holography. The CQSFA's huge predictive power allows to trace a myriad of holographic structures to specific types of quantum interference (Maxwell 2017, Maxwell 2020), assess the applicability range of standard theories (Rook 2024), revisit kinematic constraints using catastrophe theory

(Rook 2024b), and explore applications with experimental groups (Kang 2020, Werby 2021, Werby 2022). Subsequently, I will discuss quantum interference in laser-induced nonsequential double ionization (NSDI). We have challenged the long-standing view that NSDI is classical by showing that quantum interference may survive focal averaging and integration over several degrees of freedom (Maxwell 2016), derived analytic interference conditions for NSDI in arbitrary fields and identified their building blocks (Hashim 2024).

References

- Hashim, S., et al, 2024: *Phys. Rev. A*, **109**, 063110
Kang, H., et al, 2020: *Phys. Rev. A* **102**, 013109
Maxwell, A.S., and Faria, C., 2016: *Phys. Rev. Lett.* **116**, 143001
Maxwell, A.S., et al, 2017: *Phys. Rev. A* **96**, 023420
Maxwell, A.S., et al, 2020: *Phys. Rev. A* **102**, 033111
Werby, N., et al, 2021: *Phys. Rev. A* **104**, 013109; Werby, N., 2022: *Phys. Rev. A* **106**, 033118
Rook, T., et al, 2024: *Phys. Rev. A* **109**, 033115; Rook, T., et al, 2024b: *Phys. Rev. Research* **6**, 02332

EXTREME UV IMAGING WITH HIGH HARMONICS

G. G. PAULUS

Friedrich Schiller University, Max Wien Platz 1, 07783 Jena, Germany
Helmholtz Institute Jena, Fröbelstieg 3, 07743 Jena, Germany
E-mail gerhard.paulus@uni-jena.de

Abstract. I will discuss cross-sectional nanoscale imaging in the extreme ultraviolet (XUV) spectral region using high-harmonics produced by intense femtosecond laser radiation. The imaging method to be discussed is the XUV incarnation of optical coherence tomography (OCT). In recent years, OCT has become a major diagnostic method, especially in ophthalmology, where it allows cross-sectional imaging of the retina. The axial resolution is a few micrometers. XCT, in contrast, reaches resolutions of 20 nm and better. OCT and XCT alike are based on white-light interferometry. Nevertheless, due to the challenges of XUV optics, XUV coherence tomography (XCT) has to be implemented in a very different way — but it also offers special capabilities.

Most of these rely on the fact that it is possible to reconstruct the phase of the XUV radiation reflected at the sample. This in turn allows to determine the spectral *field* reflectivity, which can be used to determine various physical properties of the interfaces. These include the material composition, the thickness of layers even far below the nominal resolution, and the roughness of the boundary layers.

A particularly relevant application of XCT for the spectral range up to 100 eV are silicon-based samples. We have demonstrated depth resolutions of 20 nm and very high sensitivities. Buried oxide layers of a thickness of a few nanometers could be detected as well as buried monolayers of graphene. It is even possible to identify the material encapsulated in silicon and determine properties like layer roughness without destroying the sample. A unique perspective is ultrafast imaging.

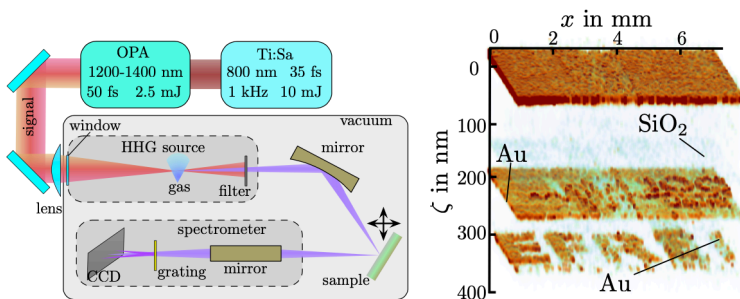


Figure 1: (left) Experimental setup of lab-based XCT; (right) Reconstructed 3D XCT measurement a structured sample consisting of two gold layers and an additional thin silicon dioxide layer buried in silicon. The axial resolution is 24 nm.

References

- Fuchs, S. et al.: 2017, *Optica*, **4**, 903.
- Wiesner, F. et al.: 2021, *Optica*, **8**, 230.
- Wiesner, F. et al.: 2022, *Optics Express*, **30**, 32267.
- Abel, J. J. et al.: 2022, *Optics Express*, **30**, 35671.
- Abel, J. J. et al.: 2024, *Materials Characterization*, **211**, 113894.

THEORY ON DYNAMICS OF ATOMS IN STRONG LASER FIELD

XIAO-MIN TONG

*Center for Computational Sciences, University of Tsukuba,
Tsukuba, Ibaraki 305-8577, Japan
E-mail tong.xiaomin.ga@u.tsukuba.ac.jp*

Abstract. Solving the time-dependent Schrödinger equation (TDSE) is a key procedure to understand most dynamics for atoms in strong field. In this talk, I will present a numerical method to solve TDSE using a second-order split operator combined with generalized pseudospectral method. Instead to solve the TDSE in differential form, I proposed a method to solve it in integral form (Tong et al, 2006). Mathematically the two equations are equivalent to each other while the proposed one can provide more physical insights. Based on this method, I will present three applications, which covers the main dynamics of atoms in strong laser fields.

The first one is the above threshold ionization. In this example, by restricting the ionization to a half cycle of the laser field and then propagating the liberated electron wave packet during the laser pulse, we show conclusively that low-energy-momenta structure in the photoelectron angular distribution originates from multiple scatterings of the tunnel-ionized electron with the ion (Tong et al. 2013).

The second is the high order harmonic generation (HHG). In this example, I will show how we simulated the atomic HHG efficiently and accurately since we need to integrate all the atomic HHGs at different positions in the gas target to get macroscopic HHG. In this step, we must solve TDSE hundreds or thousands of times for different laser intensities. The macroscopic HHG is obtained by summing over all the microscopic HHG with phase matching and self-absorption in two scales. One is in the laser wavelength scale, within which the laser peak intensity does not change while the propagation phase changes. Another is in the laser beam waist scale, within which the laser intensity and Gouy phase shift change. The details can be found in (Tong 2023).

The third one is an ongoing project on how to effectively produce more excited Ar atoms in a two-color laser field. Since the laser parameter space is very large so we use genetic algorithm to search the optimized laser parameters. All these rely on a fast and accurate TDSE solver as we proposed. The details will be present in the conference.

References

- Tong, X. M. et al. : 2006, *Phys. Rev. A*, **74**, 031405(R).
Tong, X. M. et al. : 2013, *Phys. Rev. A*, **88**, 013410.
Tong, X. M. : 2023, *Phys. Rev. A*, **108**, 023118.

Description of electron swarms in an electric field: a finite elements computation including third-order transport parameters

N. Pinhão

*Instituto de Plasmas e Fusão Nuclear, Instituto Superior Técnico,
Universidade de Lisboa, Av. Rovisco Pais, 1049-001 Lisboa, Portugal*

E-mail npinhao@ctn.tecnico.ulisboa.pt

Abstract In this communication we analyze the movement of an electron swarm drifting in an electric field, \bar{E} , under hydrodynamic conditions. We extend the analysis based on the effective ionization rate, v_{eff} , velocity, \bar{W} , and diffusion tensor, \bar{D} , to include a third-order transport parameter, \mathbf{Q} , related to the skewness of the swarm distribution. Using the density-gradients expansion of the velocity distribution function, $f(\vec{r}, \vec{v}, t)$, with $j_{\text{max}} = 3$,

$$f(\vec{r}, \vec{v}, t) = \sum_{j=0}^{j_{\text{max}}=3} F^{(j)}(\vec{v}) \odot^j (-\nabla)^j n(\vec{r}, t)$$

where the expansion coefficients $F^{(j)}$ are j -rank tensors and \odot^j a j -fold scalar product, on Boltzmann equation, we obtain a series of equations for the components of the expansion coefficients $F^{(0)}$ - $F^{(3)}$. These equations are solved using a finite element method on a (v, μ) grid (where $\mu = \cos(\theta)$ and θ is the angle between \bar{E} and \vec{v}). The algorithm used is an extension of [Segur 1983, 1984] to include third-order transport parameter, a more complete collision term and several optimizations to speed up the computation. Although for non-conservative conditions the method is iterative and depending on the reduced field value, the characteristic time for the computation of the set of expansion coefficients is on the order of seconds.

We discuss how the expansion coefficients $F^{(j)}$, with $j > 0$, integrated on μ , provide information on the velocity distribution within the swarm. E.g. $F^{(1)}$, represents the average position of electrons with velocity \vec{v} and the position of all electrons, (weighted by $F^{(0)}$). The transport parameters obtained are compared with those obtained with Monte Carlo and a multi-term Boltzmann codes [Simonović 2022].

References

- Segur, P, Bordage, M-C, Balager, J-P, Yousfi, M. 1983 *J. Comp. Phys.* **50** 116-137
Segur, P, Yousfi, M, Bordage, M-C. 1984 *J. Phys. D: Appl. Phys.* **17** 2199-2214
Simonović, I, Bošnjaković, D, Petrović, Z Lj, White, R D, and Dujko S, 2022 *Plasma Sources. Sci. Technol.* **31** 015003

VUV PHOTONIZATION OF INTERSTELLAR MOLECULES: MAKING SENSE OF OUR BEAUTIFULLY MYSTERIOUS UNIVERSE, MOLECULE BY MOLECULE

HELGI RAFN HRODMARSSON

*LISA UMR 7583 Université Paris-Est Créteil and Université Paris Cité, Institut Pierre et Simon Laplace, 61 Avenue du Général de Gaulle, 94010, Créteil, France
E-mail hhrodmansson@lisa.ipls.fr*

Abstract. VUV photons are important drivers of multiple chemical and physical processes in space. As different molecules can be used as tracers for different types of cosmic environments, it is important to characterize both qualitatively and quantitatively the processes induced by VUV photons in different radiation fields (Hrodmansson & van Dishoeck 2023). This contribution will focus on VUV photoionization of various molecules of astronomical interest, going from diatomics upward to fullerenes, using the light from the DESIRS beamline at the Synchrotron SOLEIL facility (Nahon *et al.* 2012). The talk will cover the importance of absolute photoionization cross sections of small molecules such as OH (Harper *et al.* 2019), SH (Hrodmansson *et al.* 2019), and NH₂ (Harper *et al.* 2021), the importance of dissociative photoionization of astrobiologically relevant molecules (Derbali *et al.* 2019, 2020; Hrodmansson *et al.* 2024a), the contribution of photoelectric heating by polycyclic aromatic hydrocarbons (PAHs) (Hrodmansson *et al. in prep*) and the photoionization of the fullerenes C₆₀ (Hrodmansson *et al.* 2020, 2024b, *in prep*) & C₇₀ (Hrodmansson *et al. in prep*) in space.

References

- Derbali, I., Hrodmansson, H. R., Gouid, Z., et al. : 2019, *Phys. Chem. Chem. Phys.*, **21**, 14053.
- Derbali, I., Hrodmansson, H. R., Schwell, M et al.: 2020, *Phys. Chem. Chem. Phys.*, **22**, 20394.
- Harper, O. J., Hassenfratz, M., Loison, et al. : 2019, *J. Chem. Phys.*, **150**, 141103.
- Harper, O. J., Gans, B., Loison, et al. : 2021, *J. Phys. Chem. A*, **125**(13), 2764.
- Hrodmansson, H. R., Garcia, G. A., Nahon, L., Loison, J.-C., Gans, B. : 2019, *Phys. Chem. Chem. Phys.*, **21**, 25907.
- Hrodmansson, H. R., Garcia, G. A., Linnartz, H., Nahon, L. : 2020, *Phys. Chem. Chem. Phys.*, **22**, 13880.
- Hrodmansson, H. R., & van Dishoeck, E. F. : 2023, *Astron. Astrophys.*, **675**, A25.
- Hrodmansson, H. R., Schwell, M., Fray, et al. : 2024, *Astrophys. J.*, **964**, 26.
- Hrodmansson, H. R., Rapacioli, M., Spiegelman, et al. : 2024, *J. Chem. Phys.*, **160**, 164314.
- Nahon, L., N. de Oliveira, N., Garcia, G. A., et al. : 2012, *J. Synchrotron Radiat.*, **19**(4), 508.

ELECTRON TRANSPORT AND NEGATIVE IONIZATION FRONTS IN STRONGLY ATTACHING GASES

JASMINA ATIĆ  and SAŠA DUJKO 

Institute of Physics Belgrade, Pregrevica 118, 11080 Belgrade, Serbia
E-mail jasmina.atic@ipb.ac.rs

Abstract. To optimize and understand the process of gas insulation in power transmission and distribution systems, we study electron transport, and the inception and propagation of negative ionization fronts in strongly attaching gases. The calculations are carried out not just for the familiar gaseous dielectrics, including SF₆, but also for the new generation of gaseous dielectrics that are known to have low global warming potentials and minimal impact on the Earth's atmosphere. Examples include CF₃I, C₃H₂F₄ and C₄F₇N.

Electron swarm transport coefficients are calculated using a multi term theory for solving the Boltzmann equation and Monte Carlo simulations (Dujko *et al.* 2010). We found significant discrepancies between the flux and bulk transport coefficients, which vary from a few percents to a few orders of magnitude. Perhaps the most striking phenomenon is the occurrence of negative differential conductivity in SF₆ and CF₃I only in the E/N -profile of the bulk drift velocity (Mirić *et al.* 2016). The mixture of C₃H₂F₄ and SF₆ exhibits positive synergy, with an increase in the critical electric field of the mixture to values higher than those for each gas separately. The inception and propagation of negative ionization fronts are studied by the classical fluid model in 1D and 1.5D setups. The classical model has been extended and generalized by expanding the source term in the equation of continuity in terms of powers of the number density gradient operator. We calculate the electron density, densities of positive and negative ions, electric field, and velocity of ionization fronts for a range of pure gases and gas mixtures at various E/N .

Acknowledgments: This work is supported by the Science Fund of the Republic of Serbia, Grant No. 7749560, Exploring ultra-low global warming potential gases for insulation in high-voltage technology: Experiments and modelling EGWIn.

References

- Dujko S., White R.D., Petrović Z.Lj., and Robson R.E. : 2010, *Phys. Rev. E*, **81**, 046403.
Mirić J., Bošnjaković D., Simonović I., Petrović Z. Lj., and Dujko S. : 2016, *Plasma Sources Sci. Technol.*, **25**, 065010.

LOKI-B C++: AN OPEN-SOURCE BOLTZMANN SOLVER FOR REPRODUCIBLE ELECTRON BOLTZMANN CALCULATIONS

DAAN BOER and JAN VAN DIJK

Elementary Processes in Gas Discharges, Department of Applied Physics and Science Education, Eindhoven University of Technology, The Netherlands
E-mail d.j.boer@tue.nl, j.v.dijk@tue.nl

Abstract. Boltzmann solvers are crucial in the simulation of low-temperature plasmas, where the electron energy distribution function (EEDF) is typically not Maxwellian, and thus needs to be computed separately. Input is provided in the form of a set of cross sections that measure the probability of the corresponding electron impact process as a function of the electron energy. Subsequently, output is in the form of swarm parameters, which in turn consist of transport and rate coefficients. These coefficients can then e.g. be used for further plasma modeling.

The Lisbon KInetics Boltzmann solver (LoKI-B), is a Boltzmann solver that is originally written in Matlab, see Tejero-del-caz et al. 2019. The project is open-source and available under a copyleft license on GitHub (<https://github.com/IST-Lisbon/LoKI>). The development of LoKI-B was instigated for two main reasons. The first reason is the desire to handle complex molecular gas mixtures that require explicit treatment of the ro-vibrational substructure of electronically excited states. LoKI-B solves this problem by explicitly treating the ro-vibrational substate relations, which allows for the user to assign population distributions to specific populations of states. The second reason is to provide a transparent and open-source alternative to the existing offer.

The choice for Matlab is understandable, as it is a high-level language that is often taught as part of a physics degree at university. However, it is also limiting, as it is hard to implement custom, performant algorithms, and to interop with complementary simulation tools that are not written in the same language. Moreover, usability is hampered as a Matlab license is required, and, whereas the code is open-source, LoKI-B is thus not free software. These observations lead to the development of a C++ version of LoKI-B.

This work presents LoKI-B C++, which will be open-source at the time of the conference. The code focuses on sound open-source practices, including test driven development, usage of code coverage metrics, and continuous integration and deployment. Community contributions are welcome and even encouraged. Additionally, this work presents benchmarks, numerical improvements; such as exploratory work on a nonuniform discretization of the electron energy, and improvements regarding data management and accessibility.

More specifically, usability and ease-of-access are strongly improved by providing a fully featured, free instance of LoKI-B C++ directly in the browser. This feat is made possible by compilation to WebAssembly. These developments, when combined with the recent developments in LXCat3 (Carbone et al. 2021, <https://github.com/LXCat-project/LXCat>), realize the capability to perform fully transparent and reproducible electron Boltzmann computations.

References

- Tejero-del-Caz, A., Guerra, V., Gonçalves, D., da Silva, M. L., Marques, L., Pinhão, N., Pintassilgo, C. D., & Alves, L. L. (2019). The LisbOn KInetics Boltzmann solver. *Plasma Sources Science and Technology*, **28**(4), 043001. <https://doi.org/10.1088/1361-6595/ab0537>
- Carbone, E., Graef, W., Hagelaar, G., Boer, D., Hopkins, M. M., Stephens, J. C., Yee, B. T., Pancheshnyi, S., van Dijk, J., & Pitchford, L. (2021). Data Needs for Modeling Low-Temperature Non-Equilibrium Plasmas: The LXCat Project, History, Perspectives and a Tutorial. *Atoms*, **9**(1), 16. <https://doi.org/10.3390/atoms9010016>

SYNCHROTRON RADIATION PHOTOELECTRON SPECTROSCOPY STUDY OF THE ELECTRONIC STRUCTURE OF Ag-Bi-I RUDORFFITE NANOPARTICLES

DANIJELA DANILOVIĆ¹ , DUŠAN K. BOŽANIĆ¹ ,
ALEKSANDAR R. MILOSAVLJEVIĆ², RADOVAN DOJČILOVIĆ¹  and
VLADIMIR DJOKOVIĆ¹ 

¹*Center of Excellence for Photoconversion, "Vinča" Institute of Nuclear Sciences - National Institute of the Republic of Serbia, University of Belgrade, P.O. Box 522, 11001 Belgrade, Serbia, danijelad@vin.bg.ac.rs*

²*Synchrotron SOLEIL, l'Orme des Merisiers, St.Aubin, BP48, 91192 Gif sur Yvette Cedex, France*

Abstract. Organic/inorganic lead halide perovskites are among the most studied materials for absorption layers in solar cells due to their optimal band gap, high charge carrier mobility, and valence band alignment with materials used for electron and hole transport (Milosavljević et al. 2018). However, there are several obstacles for large-scale production of these materials such as degradation in the presence of oxygen and moisture and lead toxicity. Silver-bismuth-iodide (Ag-Bi-I) rudorffites have garnered significant research interest as lead-free, chemically stable, and low-cost absorber materials. Fabricating Ag-Bi-I in nanocrystal form could facilitate their integration into solar cells and enhance the performance due to the quantum confinement effect. Here, we present the synthesis of ligand-free Ag-Bi-I rudorffite nanomaterials and a photoelectron spectroscopy study of the obtained systems. We fabricated Ag₃BiI₆ aerosol nanoparticles with an average size of ~ 100 nm (Danilovic et al. 2020) and colloidal nanoplatelets with lateral dimensions of approximately 110 nm and thickness ranging from 1 to 8 nm (Danilovic et al. 2022). The electronic structure of isolated nanoparticles was explored using synchrotron radiation X-ray aerosol photoelectron spectroscopy (XASP). By integrating XASP results with UV-Vis absorption spectroscopy and XPS data, the complete valence electronic structure of Ag-Bi-I nanosystems was reconstructed. Furthermore, an analysis that shows the relation between the positions of the bands in the Ag₃BiI₆ nanosheet absorption spectra and the thickness of the nanosheet will be discussed.

References

- Milosavljević, A. R., Božanić, D. K., Sadhu, S. : 2018, *J. Phys. Chem. Lett.* **9**, 3604.
Danilović, D., Božanić, D. K., Dojčilović R. : 2020, *J. Phys. Chem. C* **124**, 23930.
Danilović, D., Milosavljević A. R., Sapkota, P. : 2022, *J. Phys. Chem. C* **126**, 13739.

PHOTOELECTRON SPECTROSCOPY OF SOLVATED BIOLOGICAL INTEREST MOLECULES IN LIQUID JET CONFIGURATION

M. FOURNIER^{1,2}, J. PALAUDOUX², R. DUPUY², F. PENENT² and
C. NICOLAS¹

¹*Synchrotron SOLEIL, Saint-Aubin, France
marine.fournier@synchrotron-soleil.fr*

²*Laboratoire Chimie Physique – Matière et Rayonnement, Sorbonne Université,
UMR 7614, Paris, France*

Uracil is a RNA nucleobase and 5-bromouracil, one of its haloderivatives and known for its radiosensitizer property in DeoxyriboNucleic Acid (DNA) (Zimbrick J D et al. 1969). Incorporated in DNA, it can both be responsible of mutagenic effect (Kavli B et al. 2007). The cause of this effect is largely studied, but doubts still subsist about the deprotonation site and the tautomer form present in liquid water. Probing the electronic structure gives information on the local environment, and consequently lets us to study the effect of solvation and chemical environment changes. This type of measurement is possible combining an electron spectrometer with an under-vacuum liquid jet device. With this configuration, it is possible to probe three molecular layers at the surface of the liquid-jet, enough to be in complete solvation condition. The measurements presented in this work have been done on PLEIADES beamline (Renault J-P et al. 2022), synchrotron SOLEIL. The C 1s and N 1s photoelectron spectra of each molecule has been measured at different pH conditions (6.5, 10.8, 12.6), far enough from the pKa value. Thus, we obtain photoelectron spectra of protonated form of uracil comparable to the ones measured in water-clusters (Mattioli G et al. 2022), which not reveal differences between micro-solvation and complete solvation. The increase of pH in solutions induces a shift of the photoelectron peaks to lower binding energies. Peak attribution is completed by theoretical calculations (team of Majdi Ochlaf, Université Marne la Vallée and the team of Petr Slavicek, University of chemistry and technology of Prague). Interestingly, the 5-bromouracil behaves differently compared to uracil at the higher pH condition whose the interpretation is still to be confirmed. We have extended our liquid XPS measurements to biggest biological molecule with solvated prototypical (DNA). These measurements are relevant to the study of radiation damage on DNA at the physical stage.

References

- Kavli B, Otterlei M, Slupphaug G and Krokan H 2007 *DNA Repair* **6** 505–16
Mattioli G et al., 2020 *Sci. Rep.* **10** 13081
Renault J-P et al. 2022 *Int. J. Mol. Sci.* **23** 8227
Zimbrick J D, Ward J F and Myers L S 1969 *Int. J. Radiat. Biol. Relat. Stud. Phys. Chem. Med.* **16** 525–34

STRONG-FIELD PROCESSES INDUCED BY TAILORED LASER FIELDS

D. HABIBOVIĆ¹ and D. B. MILOŠEVIĆ^{1,2}

¹Faculty of Science, University of Sarajevo, Zmaja od
Bosne 35, 71000 Sarajevo, Bosnia and Herzegovina

²Academy of Sciences and Arts of Bosnia and Herzegovina,
Bistrik 7, 71000 Sarajevo, Bosnia and Herzegovina
E-mail dhfizika1@gmail.com

Abstract. When atoms or molecules are exposed to a strong laser field, many interesting processes can be induced. Particularly prominent examples include high-order above-threshold ionization (HATI) and high-order harmonic generation (HHG). The subtle control of the photoelectron and harmonic yields can be achieved by using tailored driving fields (see Habibović et al. 2021. and Habibović et al. 2024.). These fields provide various parameters which can be used as control knobs. We investigate different tailored fields with particular focus on the bichromatic linearly and elliptically polarized fields. These fields consist of two linearly or elliptically polarized components with commensurate frequencies. The components of the bichromatic linearly polarized field have mutually parallel polarizations, while for the bichromatic elliptically polarized field the semimajor axes of two components are orthogonal. Particularly useful parameter is the relative phase between the field components which can be employed as control parameter for both the HHG and HATI processes. The example presented in Figure 1 shows the dependence of the HHG yield on the phase between the laser-field components for long (left panel) and ultrashort (right panel) driving field.

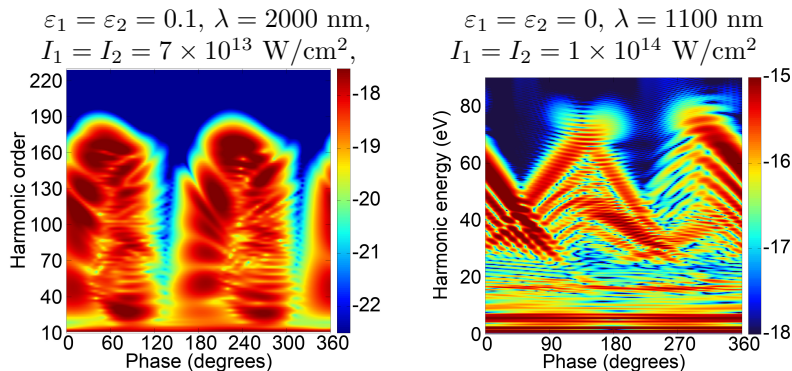


Figure 1: High-order harmonic yield as a function of the harmonic order and the phase between the field components for CO molecule exposed to ω - 2ω long bichromatic elliptically polarized field (left panel) and for the Ar atom exposed to ω - 2ω ultrashort (four cycles) linearly polarized pulse (right panel).

References

- Habibović, D., Becker, W., Milošević, D. B. : 2021, *Symmetry*, (13), 1566.
Habibović, D., Milošević, D. B. : 2024, *Phys. Rev. A*, (109), 043110.

TOWARDS DISTANT DEPENDENT INNER-SHELL PHOTOELECTRON CIRCULAR DICHROISM

EMILIA HEIKURA¹, CHRISTINA ZINDELL¹, DENIS KARGIN¹,
ALEKSANDAR MILOSAVLJEVIC², ANDREAS HANS¹,
RUDOLF PIETSCHNIG¹ and ARNO EHRESMANN¹

¹*University of Kassel, Heinrich-Plett-Straße 40, 34132 Kassel, Germany*

E-mail emilia.heikura@physik.uni-kassel.de

E-mail arno.ehresmann@physik.uni-kassel.de

²*Synchrotron Soleil, L'Orme des Merisiers Départementale 128, 91190 Saint-Aubin,
France*

E-mail aleksandar.milosavljevic@synchrotron-soleil.fr

Photoelectron circular dichroism (PECD) is one of the most powerful methods for investigating molecular chirality in the gas phase. PECD is a forward-backward asymmetry of emitted photoelectrons from chiral molecules after interaction with a circularly polarized light. The asymmetry can be observed even in randomly oriented chiral molecules. Site-selectivity of inner-shell photoelectrons enables the investigation on chirality as a function of a distance from a stereocenter. It is still unknown how the magnitude of PECD is evolving as a function of a distance between the emission site from the stereocenter. To be able to investigate this phenomenon, a series of specifically synthesized molecules was designed. In these molecules the distance between stereocenter and a marker atom can be increased while otherwise the structure of the molecule stays intact.

References

- Powis, I. : 2008, *Advances in Chemical Physics*, **138**, 267.
Herganhahn, U. et al. : 2004, *J. Chem. Phys.*, **120**, 4553.

EXPLORING BIOMOLECULAR PROPERTIES IN THE GAS PHASE BY USING ADVANCED LIGHT SOURCES

LAURA PILLE¹, BART OOSTENRIJK¹, JULIETTE LEROUX^{1,2},
CARLOS ORTIZ MAHECHA³, ROBERT MEIßNER³, DEBORA SCUDERI⁴,
SADIA BARI^{1,5} and LUCAS SCHWOB¹

¹*Deutsches Elektronen-Synchrotron DESY, Germany*

²*CIMAP, CEA/CNRS/ENSICAEN/Université de Caen Normandie, 14050 Caen, France*

³*Institute of Polymers and Composites, Hamburg University of Technology,
Hamburg, Germany*

⁴*Université Paris-Saclay, CNRS, Institut de Chimie Physique, UMR8000, 91405,
Orsay, France*

⁵*Zernike Institute for Advanced Materials, University of Groningen, Groningen,
The Netherlands*

Biomolecules such as proteins and peptides exhibit complex three-dimensional structures that are crucial for their biological functions. Non-covalent interactions within proteins, particularly those involving sulfur-containing residues like methionine and aromatic amino acids such as tyrosine and tryptophan, significantly contribute to stabilizing their folded structures (Valley et al. 2012). This specific interaction, referred to as S: π interaction, has been consistently identified in various protein database analyses, underscoring their important role in enhancing the structural stability of proteins (Meyer et al. 2003).

In this work, we study the electronic and structural properties of tailor-made gas-phase peptides that represent a model of the S: π interaction. By using electrospray ionization (ESI) in combination with synchrotron light sources we perform mass spectrometry-based action spectroscopy. We aim to indicate and characterize the S: π interaction by measuring the ionization potential (VUV) and investigating the resonant absorption processes occurring at the carbon K-edge (soft X-rays). Additionally, we explore fragmentation channels at specific absorption resonances as distinctive signatures of S: π interactions. We estimate the preferred orientation of the sulfur atom relative to the aromatic ring using Molecular dynamics (MD) simulations and density functional theory (DFT).

This experimental and computational approach offers a detailed understanding of the S: π interaction in our tailor-made peptides and contributes to a broader understanding of the structure-function relationship in biomolecules.

References

- Valley, C., Cembran, A., Perlmutter, J., Lewis A., Labello, N., Gao, J., Sachs, J., 2012, *J Biol Chem*, 287, 34979-34991.
Meyer, E.A., Castellano, R.K. and Diederich, F., 2003, *Angew. Chem. Int. Ed.* 42, 1210-1250.

DE-EXCITATION CASCADE CALCULATION FOR HIGHLY EXCITED HOLLOW ATOMS

M. WERL¹, T. KOLLER¹, P. HAIDEGGER¹, S. WRATHALL¹, L. EBLETZBICHLER¹,
 A. NIGGAS¹, F. AUMAYR¹, K. TÖKÉSI² and R.A. WILHELM¹
¹*TU Wien, Institute of Applied Physics, 1040 Vienna, Austria, EU*
E-mail werl@iap.tuwien.ac.at

²*Institute of Nuclear Research of the Hungarian Academy of
 Sciences (ATOMKI), 4001 Debrecen, Hungary, EU*

Abstract.

Hollow atoms (HAs) are an intricate type of particles, mainly having electrons in highly excited n -shells and no or only few electrons in core shells. They are formed upon highly charged ion impact on a conductive surface. Some Ångströms above the surface, electrons are resonantly captured by the projectile into states roughly equal to the incident charge state $n \sim q_{in}$, see Burgdörfer et al. 1991. Upon creation, the hollow atom deexcites (in free vacuum) via autoionising and radiative pathways, as sketched in Fig. 1 a). In this contribution, we discuss the lifetime of the hollow atom and assess how an experimental observation of an HA can be feasible. To do so, we apply a Monte-Carlo based code describing the formation and deexcitation of HAs through coupled rate equations. Input transition rates are obtained from the atomic structure code package FAC (Gu 2018). Our results show that, given suitable experimental conditions (projectile and target species, incidence angle and kinetic energy), it is possible to produce HAs with lifetimes of several tens of ps (see Fig. 1 b).

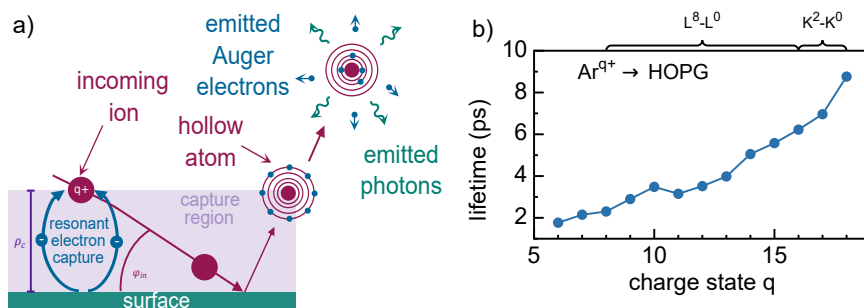


Figure 1: a) Schematics of the formation and subsequent deexcitation of a hollow atom. Electrons are captured by the surface into high- n states, before decaying via radiative and autoionising pathways. b) Hollow atom lifetimes formed by scattering of Ar^{q+} on a HOPG surface. Adapted from Werl et al. 2024.

References

- Burgdörfer, J., Lerner, P., Meyer, F.W. : 1991, *Phys. Rev. A*, **44**, 9.
 Gu, M.F. : 2008, *Can. J. Phys.*, **86**, 5.
 Werl, M., Koller T., Haidegger, P., Wrathall, S., Ebletzbichler, L., Niggas, A., Tökési, K., Wilhelm, R.A. : 2024, In preparation.

STUDIES ON STREAMER DISCHARGES IN ULTRA-LOW GWP GASES

DANKO BOŠNJAKOVIĆ , ILIJA SIMONOVIĆ  and SAŠA DUJKO 

Institute of Physics Belgrade, Pregrevica 118, 11080 Belgrade, Serbia

Abstract. In this work, we use a Particle-in-cell/Monte Carlo collision (PIC/MCC) model to investigate the inception and propagation of both positive and negative streamers in ultra-low GWP gases, including $C_3H_2F_4$ and C_3HF_5 . The modelling results can be used as a basis for assessing the performance of these gases in high-voltage insulation as eco-friendly alternatives to SF_6 .

The PIC/MCC model uses Velocity Verlet scheme to track individual electrons in 3D and a Monte Carlo null-collision technique to sample the electron-neutral collision parameters. The electric field is assumed to be axially symmetric and is computed on a 2D numerical grid coupled with a Poisson equation solver. The electric field solver is implemented using the iterative multigrid method provided by the AMReX software framework. AMReX is an open-source C++ library for massively parallel block structured adaptive mesh refinement applications. In addition to its in-built geometric multigrid solver, we use the programming abstractions that it provides to implement adaptive mesh refinement and to support MPI and OpenMP parallelization on multicore CPUs. We also employ a particle management technique in order to optimize the number of particles in a simulation and shorten the computation time. To study the propagation of positive streamers, we include a photoionization model and a stochastic background ionization as sources of free electrons.

Results of PIC/MCC simulations are presented as an evolution of electron and ion densities, electric field distribution, streamer radius and velocity, and are obtained as a function of the applied electric field strength. In addition to ultra-low GWP gases, calculations are also performed for artificial dry air so as to validate and compare our results with those from open source Afivo-pic code.

Acknowledgments: This work is supported by the Science Fund of the Republic of Serbia, Grant No. 7749560, Exploring ultra-low global warming potential gases for insulation in high-voltage technology: Experiments and modelling EGWIn.

ELECTRON TRANSPORT IN SIMPLE LIQUID MIXTURES

G. J. BOYLE¹, N. A. GARLAND², R. P. MCEACHRAN³ and R. D. WHITE¹

¹*James Cook University, Townsville, Australia*
E-mail gregory.boyle@jcu.edu.au

²*Griffith University, Nathan, Australia*

³*Australian National University, Canberra, Australia*

Abstract. The study of low-energy electrons in structured fluid systems, such as dense gases and liquids, underpins many areas of technology and scientific research. The 2021 European Committee for Future Accelerators Detector Research and Development Roadmap [Colaleo *et al.*2021] highlighted the importance of liquid detectors to dark matter searches, neutrino physics and astroparticle experiments. The use of dopants and liquid mixtures to improve detector operation is an active area of research and requires models of electron transport in liquid mixtures.

The behaviour of low-energy electrons in liquids is substantially more complex than in dilute gaseous systems. For example, when the de Broglie wavelength of the electrons (near thermal) energies is comparable to the interatomic spacing of atoms in the medium, scattering occurs from multiple (correlated) scattering centres simultaneously. This coherent scattering was incorporated into a kinetic theory framework by Cohen and Lekner [Cohen and Lekner 1967, Lekner 1967] and can lead to orders-of-magnitude difference in the calculated transport properties.

In a recent paper [Boyle *et al* 2023], the framework of Cohen and Lekner for pure liquids was extended to simple liquid mixtures, which accounted for the correlation between medium atoms of different types. In this work we investigate the dependence of transport properties, such as drift velocity and diffusion coefficients, on the structure of simple liquid admixtures, which nevertheless demonstrate complex relationships. We discuss the implications of using dopants and liquid mixtures in the development of liquid time projection chambers.

References

- Boyle, G. J., Garland, N. A., McEachran, R. P., Mirihana, K. A., Robson, R. E., Sullivan, J. P., White, R. D. : 2024, *J. Phys. B: At. Mol. Opt. Phys.* **57**, 015202.
Cohen, M. H., Lekner, J. : 1967, *Phys. Rev.* **158**, 130.
Colaleo, A., *et al.* : 2021, *The 2021 ECFA Detector Research and Development Roadmap* (CERN)
Lekner, J. : 1967, *Phys. Rev.* **158**, 130.

ELECTRON TRANSPORT IN RADIO-FREQUENCY ELECTRIC AND MAGNETIC FIELDS IN ULTRA-LOW GWP GASES

SAŠA DUJKO¹ , ILIJA SIMONOVIĆ¹ , DANKO BOŠNJAKOVIĆ¹ ,
JASMINA ATIĆ¹  and ZORAN LJ. PETROVIĆ² 

¹*Institute of Physics Belgrade, Pregrevica 118, 11080 Belgrade, Serbia*

²*Serbian Academy of Sciences and Arts, Knez Mihailova 35, 11001 Belgrade, Serbia*

Abstract. In this work, we study the transport of electrons in radio-frequency (RF) electric and magnetic fields in ultra-low global warming potential (GWP) gases. Calculations have been performed for electron swarms in $C_3H_2F_4$ and C_3HF_5 using a time-dependent multi-term technique to solve the Boltzmann equation and Monte Carlo simulation.

The progress and further improvements of plasma science require the most accurate modeling of charged particle transport under the influence of electric and magnetic fields in neutral gases. In this work, we study the transport of electrons in RF electric and magnetic fields in ultra-low GWP gases, including $C_3H_2F_4$ and C_3HF_5 . Electron swarm transport properties and distribution functions have been calculated using a unified time-dependent multi term theory to solve the Boltzmann equation and Monte Carlo simulation. The motivational factors for this study include the following: (1) understanding electron kinetics and electron heating mechanisms in inductively coupled plasmas, (2) understanding of the interaction between electromagnetic waves and ambient electrons inside gas-insulated switchgears used in electrical power transmission systems. We systematically investigate the explicit effects associated with the electric and magnetic fields including fields to density ratios, field frequency, field phases and field orientations. We also highlight the explicit modification of electron swarm transport coefficients by non-conservative collisions, including the electron attachment and ionization. We have observed a multitude of kinetic phenomena that are generally inexplicable with the conventional transport theory of electron swarms in direct-current (DC) fields. Phenomena of significant note include the increase of mean energy with increasing magnetic field, time-resolved negative differential conductivity, anomalous anisotropic diffusion, and transient negative diffusivity.

Acknowledgments: This work is supported by the Science Fund of the Republic of Serbia, Grant No. 7749560, Exploring ultra-low global warming potential gases for insulation in high-voltage technology: Experiments and modelling EGWIn.

STUDIES ON ELECTRON SWARMS AND STREAMER DISCHARGES IN ECO-FRIENDLY RPC GASES

SAŠA DUJKO¹ , ILIJA SIMONOVIĆ¹ , DANKO BOŠNJAKOVIĆ¹ ,
ZORAN LJ. PETROVIĆ²  and J. de URQUIJO³

¹*Institute of Physics Belgrade, Pregrevica 118, 11080 Belgrade, Serbia*

²*Serbian Academy of Sciences and Arts, Knez Mihailova 35, 11001 Belgrade,
Serbia*

³*Instituto de Ciencias Físicas, Universidad Nacional Autónoma de México, 62251
Cuernavaca, Morelos, Mexico*

Abstract. In this work, we study the transport of electrons and the propagation of streamers in resistive plate chambers (RPC). We are considering the performance of new eco-friendly gas mixtures instead of the currently used $C_2H_2F_4$ and SF_6 .

Resistive plate chambers are gaseous particle detectors often used for timing and triggering purposes in high-energy physics experiments. At the Large Hadron Collider (LHC) at CERN, all key experiments, including ALICE, ATLAS, CMS and LHCb employ RPC detectors. RPCs in these experiments are operated with gas mixtures in which the main component is $C_2H_2F_4$. $C_2H_2F_4$ is mixed with $i-C_4H_{10}$ and SF_6 in various percentages, to control the amount of liberated charge and the occurrence of violent discharges. However, $C_2H_2F_4$ and SF_6 are characterized by high global warming potentials. In this work, we study the performance of new eco-friendly RPC gas mixtures. The $C_2H_2F_4$ is replaced with a proper mixture of $C_3H_2F_4$ and CO_2 , while CF_3I , C_4F_7N and $C_5F_{10}O$ were considered as alternatives to SF_6 . We approach the problem at three stages: (1) First, we propose complete and consistent sets of cross sections for $C_3H_2F_4$ and strongly attaching gases, including CF_3I , C_4F_7N and $C_5F_{10}O$, (2) Second, we investigate the transport of electrons in various eco-friendly gas mixtures, and (3) Third, we simulate the inception and propagation of streamers in LHC-like conditions. Swarm analysis was performed using pulsed-Townsend measurements of swarm data, numerical solutions of Boltzmann's equation, and Monte Carlo simulations. The inception and propagation of streamers were simulated using the classical fluid model, which involves the drift-diffusion approximation and local field approximation. The model is implemented in 3D setup within the AMReX environment.

Acknowledgments: This work is supported by the Science Fund of the Republic of Serbia, Grant No. 7749560, Exploring ultra-low global warming potential gases for insulation in high-voltage technology: Experiments and modelling EGWIn.

AN ALIASING METHOD FOR DETERMINATION OF TRANSPORT DATA FOR EXOTIC CHARGED PARTICLES IN CROSSED ELECTRIC AND MAGNETIC FIELDS

N. A. GARLAND¹, R. D. WHITE², R. E. ROBSON² and M. HILDEBRANDT³

¹*School of Environment and Science, Griffith University, Nathan 4111, Australia*
E-mail n.garland@griffith.edu.au

²*College of Science and Engineering, James Cook University, Townsville 4810, Australia*

³*Paul Scherrer Institut, 5232 Villigen PSI, Switzerland*

Abstract. Understanding current and emerging particle physics experiments relies on quantifying the transport of exotic charged particles, such as muons. In some cases the fundamental scattering cross sections of exotic charged particles is not known, let alone the macroscopic transport data such as mobility or diffusion coefficients. As one path forward to remedy this dearth of data, we discuss an aliasing method that leverages the known transport data of well-studied ions to approximate the lacking, but much needed, transport of more challenging charged particles, such as positive muons as presented in this work.

1. INTRODUCTION

A good theoretical understanding of the behaviour of charged particles in gases is essential for modelling beam experiments. For some charged particles of interest, such as electrons, ions, or even positrons, there are well-established theory and experimental techniques to determine fundamental scattering cross sections and transport data to assist in modelling. For some exotic charged particles, such as muons, determining this transport data from theory or experiment is a more challenging task, and in some cases there may be no data at all.

This work presents an empirical approach to quantifying transport data of a beam of positive muons μ^+ in helium gas, subject to crossed electric and magnetic fields. A specific application of this scenario is central to the planned operation of the muCool experiment [Antognini *et al.*]. For understanding this experiment, one requires the input of (μ^+ , He) transport data, which is, however, unavailable. A similar problem also arises in fundamental simulations, which may require the input of thus far unknown (μ^+ , He) scattering cross sections. In this case, Taqqu recently argued that known (H^+ , He) cross sections could be adapted to the muon problem for simulation purposes, and in a similar spirit we adapt or “alias” known (H^+ , He) swarm experimental transport data as a method to approximate (μ^+ , He) transport. Such a procedure has already been discussed in the context of momentum transfer theory for muons in an electric field only [Robson *et al.*], while this present work extends the method to crossed electric and magnetic fields.

2. METHODS

With a need for transport coefficients of exotic particles in interpreting experiments or prescribing input for theory or simulation, there is the obvious question as to what data could be used when no swarm data, or fundamentally calculated data from interaction cross sections, is available. Specifically, for muon beams in gases a previously discussed method of determining a muon reduced mobility in a background electric field [Robson *et al.*] through aliasing motivates the development of aliasing of swarm transport data presented here.

In this aliasing method, we seek to determine the mobility of a charged particle species, termed species (1), purely from knowledge of known mobility data of a surrogate particle, species (2), in the same gas. Here, we assume species (1) and (2) are of the same charge, and that the nature of the interactions between both species (1) and (2) and the background gas molecule are similar. For example, in this study we will turn attention to obtaining transport data of μ^+ in He given known transport data of a surrogate particle, H^+ , in He [Ellis *et al.*]. Given that an introduction to aliasing swarm data in the absence of magnetic fields may be found in the work of Robson *et al.*, we will now briefly formulate the extension to the case of perpendicular magnetic and electric fields as relevant to the understanding of the muCool apparatus.

Critical to the aliasing procedure are assumptions about the collision dynamics in both the surrogate and desired systems. As outlined previously by Robson *et al.*, we assume that the elastic momentum transfer cross section (MTCS) of projectiles (1) and (2) evaluated at equivalent centre of mass (CoM) energies is the same,

$$\sigma_m^{(1)}(\varepsilon_{CM}^{(1)}) = \sigma_m^{(2)}(\varepsilon_{CM}^{(2)}). \quad (Eq. 1)$$

To connect to previous MTCS scaling concepts in literature [see Krstić and Schulz, Senba] we note that equivalent CoM energies implies a scaled velocity by some ratio of reduced masses, i.e. so called velocity scaling as often termed in literature. In contrast, some authors have identified so called energy scaling, by a ratio of reduced masses, to be appropriate for other cross sections such as total elastic, or viscosity cross sections.

In the limit of zero magnetic field, invoking equivalent MTCS at a given CoM energy is sufficient to constrain the problem and deduce an aliasing relationship from one particle's transport data to another, via reduced mass ratio scaling. Here we consider the case of an orthogonal, non-zero \mathbf{B} component. In order to limit the number of degrees of freedom in our problem, we must assume another constraint between the surrogate and desired scattering systems. Here, we assume equivalence of the Lorentz angles, ϕ , of particle (1) and (2), which are impinging upon a target atom with the same CoM energy. The Lorentz angle is defined as the angle, ϕ ,

between a particle beam's average velocity and the background electric field. This assumption is quite reasonable given the fixed orientation of electric and magnetic fields, and thus the Lorentz angle of a charged particle relative to a scattering target will be equivalent independent of what the particle is. With the two critical assumptions of equivalent CoM energy and Lorentz angle in our desired system (1) and a proposed surrogate system (2), we may then find that

$$\frac{K^{(1)}}{K^{(2)}} = \sqrt{\frac{\mu^{(2)}}{\mu^{(1)}}}. \quad (\text{Eq. 2})$$

Given a crossed field configuration we may invoke Tonks' theorem to propose $\varepsilon_{CM}(E, B, \theta) = \varepsilon_{CM}(E_{eff}, 0, 0)$, and $W(E, B, \theta) = W(E_{eff}, 0, 0)$, where an effective electric field in the sense of a conventional electric field only swarm experiment is given by

$$E_{eff} = E \sqrt{\frac{1 + (\Omega/\nu_m)^2 \cos^2 \theta}{1 + (\Omega/\nu_m)^2}}, \quad (\text{Eq. 3})$$

where θ is the angle between E and B , the cyclotron frequency is $\Omega = qB/m$. If the angle between E and B is $\theta = \pi/2$ we can simplify matters such that

$$E_{eff} = \frac{E}{\sqrt{1 + (\Omega/\nu_m)^2}}. \quad (\text{Eq. 4})$$

Assuming that the Lorentz angle is fixed between charged particle (1) and (2), i.e. $\tan \phi = K^{(1)}B^{(1)} = K^{(2)}B^{(2)}$, then it follows that

$$\frac{B^{(1)}}{B^{(2)}} = \sqrt{\frac{\mu^{(1)}}{\mu^{(2)}}}. \quad (\text{Eq. 5})$$

Making use of the Wannier energy relation, in the limit of low electron energies where inelastic collisions can be neglected, $\varepsilon_{CM} = \frac{3}{2}k_B T_g + \frac{1}{2}M\langle v \rangle^2$, after some algebra one can obtain

$$E^{(1)} = \sqrt{\frac{\mu^{(1)}}{\mu^{(2)}}} \sqrt{(E^{(2)})^2 + \frac{3k_B}{M} \left[\frac{1 + (K^{(2)}B^{(2)})^2}{(K^{(2)})^2} \right] [T_g^{(2)} - T_g^{(1)}]}.$$

3. DEMONSTRATION OF ALIASING

Given the proposed mapping between a desired $E^{(1)}, B^{(1)}, K^{(1)}$ data set and a known data set for an ion, $E^{(2)}, B^{(2)}, K^{(2)}$ we can consider constructing a set of data based on given swarm experiment data for H^+ in He in only an axial electric field. If we invoke the effective field assumption, we may consider known swarm data of an (E, K) pair from a swarm experiment to be an effective field $(E|_{eff}, K)$ that is then mapped to a possible $E^{(2)}, B^{(2)}$ orthogonal field pair, which then corresponds to a scaled reduced mobility, KN , surface for μ^+ in He as a function of local reduced fields. A surface plot of KN is shown in Figure 1 and demonstrates the utility and potential application of the proposed aliasing procedure in a crossed electric and magnetic field scenario for determination of positive muon reduced mobility in helium gas, where otherwise no prior data was available.

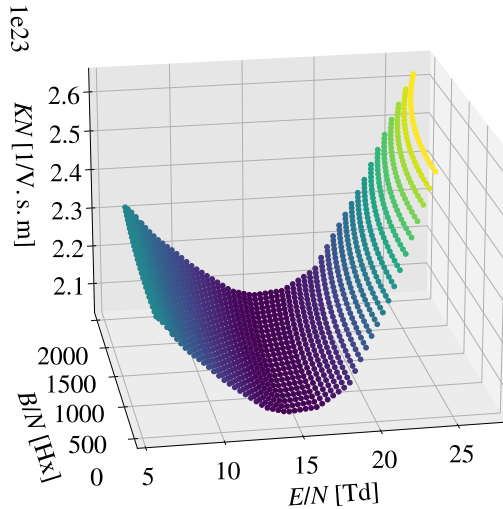


Figure 1 - Reduced mobility surface for μ^+ transport in He at 11 K, as a function of reduced electric and magnetic fields. Data generated by aliasing of swarm data measurements of H^+ in He [Ellis *et al.*].

References

- Antognini, A. *et al.* (muCool Collaboration) : 2020, *Phys. Rev. Lett.*, **125**, 164802.
 Ellis, H. W. *et al.* : 1984, *Atomic Data and Nuclear Data Tables*, **31**, 113–151.
 Krstić, P. S. and Schultz, D. R. : 2006, *Phys. Plasmas*, **13**, 053501.
 Robson, R. E. *et al.* : 2012, *J. Chem. Phys.*, **137**, 214112.
 Senba, M. : 1989, *J. Phys. B: At. Mol. Opt. Phys.*, **22**, 2027.
 Taqqu, D. : 2006, *Phys. Rev. Lett.*, **97**, 194801.

MONTE CARLO SIMULATION OF ELECTRON SWARMS IN PULSED TOWNSEND EXPERIMENT AND VALIDATION OF THE SWARM DATA DERIVED FROM WAVEFORM ANALYSIS

MAI HAO^{1,2}, GERJAN HAGELAAR², BOYA ZHANG¹ and XINGWEN LI¹

¹State Key Laboratory of Electrical Insulation and Power Equipment,
 Xi'an Jiaotong University, Xi'an 710049, China
 E-mail haomai_xjtu@hotmail.com

²LAPLACE, Université de Toulouse, CNRS, 31062 Toulouse, France
 E-mail gerjan.hagelaar@laplace.univ-tlse.fr

Abstract. The pulsed Townsend experiment (PT) is one of the swarm methods in active use to determine transport coefficients for fluid model. A shared characteristic of the PT experimental techniques is their initial recording of electron current waveform, followed by the fitting of electron swarm parameters using a theoretically derived electron current expression. However, the theoretically derived expressions are based on the hydrodynamic regime and involve truncation approximations of higher-order terms in the original diffusion equation. Therefore, it is necessary to investigate whether idealized analytical tools are applicable for analyzing measurements (usually in non-hydrodynamic conditions). In this work, Monte Carlo simulations with cross section set of Ar as input are used to describe electron transport at the kinetic theory level, fully accounting for the behavior of the electron swarm in the PT experiment. The simulation in this work is set within a finite boundary equivalent to the experimental setup, and it is capable of describing the behavior of electron swarm under non-equilibrium conditions. Additionally, the ideal “simulated experimental waveforms”, regarding as computer-based representations of actual experiments, are used to fit electron swarm parameters using previously established electron current expressions. By comparing the fitted electron swarm parameters with standard data from MCIG, a software for calculating transport coefficients based on the Monte Carlo method (In MCIG, the electron swarm evolves endlessly under boundless space and within the hydrodynamic regime, so the obtained transport coefficients are considered standard), we can gain a better understanding of the quality of these fitted data, as well as identify the circumstances under which the employed electron current expressions are inadequate for describing actual PT discharge.

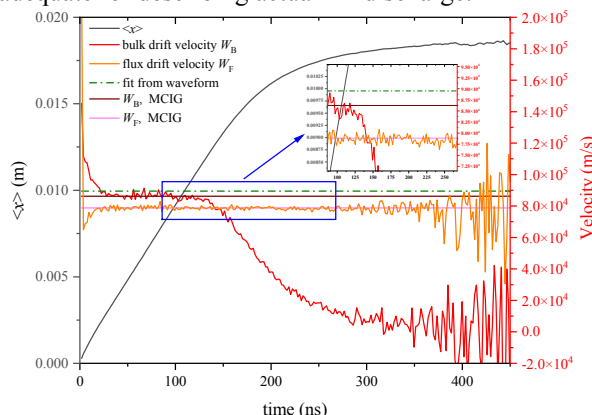





Fig.1 The evolution of the mean position for electrons and drift velocities, with the left axis representing position and the right axis representing velocity, for pressure $p = 500$ Pa, $E/N = 100$ Td in Ar.

INVESTIGATION OF ELASTIC ELECTRON SCATTERING BY ANAESTHETIC MOLECULES IN GASEOUS PHASE

JELENA B. MALJKOVIĆ¹ , JELENA VUKALOVIĆ^{1,2} ,
FRANCISCO BLANCO³, GUSTAVO GARCIA⁴ and
BRATISLAV P. MARINKOVIĆ¹ 

¹ *Institute of Physics Belgrade, University of Belgrade, Pregrevica 118,
11080 Belgrade, Serbia
E-mail: jelenam@ipb.ac.rs*

² *Faculty of Science, University of Banja Luka, Mladena Stojanovića 2,
78000 Banja Luka, Republic of Srpska, Bosnia and Herzegovina*

³ *Departamento de Física Atómica Molecular y Nuclear, Facultad de Ciencias
Físicas, Universidad Complutense, Avda. Complutense s/n, E-28040 Madrid, Spain*

⁴ *Instituto de Matemáticas y Física Fundamental, Consejo Superior de
Investigaciones Científicas, Serrano 121, 28006 Madrid, Spain*

Abstract. Driven by their significant impact on both global warming and ozone depletion, we conducted collaborative theoretical and experimental studies on the elastic electron scattering from anesthetic molecules (halothane, sevoflurane, isoflurane, and desflurane) at intermediate electron energies. Studies have revealed that most administered anesthetics are excreted unchanged from the patient's body into the lower atmosphere, with their release steadily rising over time. As halogenated compounds, anesthetics possess high Global Warming Potentials (GWP), and the majority among them exhibit substantial Ozone Depletion Potentials (ODP). Experimental investigations were conducted employing a crossed-beam setup, consisting of an electron gun, a single capillary gas needle, and a detection system equipped with a channeltron. To establish the absolute scale for the measured relative cross sections, the relative-flow method was employed, with argon gas serving as a reference. Theoretical calculations of the differential cross sections were conducted using the Independent Atom Model along with the Screening Corrected Additivity Rule, incorporating interference effects (IAM-SCAR+I).

This research was supported by the Science Fund of the Republic of Serbia, Grant No. 6821, Project title – ATMOLCOL.

References

- Langbein, T., Sonntag, H., Trapp, D., Hoffmann, A., Malms, W., Röth, E.P., Mörs, V., Zellner, R.: 1999, *Br. J. Anaesth.*, **82**, 66–73.
- Maljković, J.B., Vukalović, J., Pešić, Z.D., Blanco, F., García, G., Marinković, B.P.: 2023, *Eur. Phys. J. Plus*, **138**, 349.
- Vukalović, J., Maljković, J.B., Blanco, F., García, G., Predojević, B., Marinković, B.P.: 2022, *Int. J. Mol. Sci.*, **23**, 21.
- Vukalović, J., Marinković, B. P., Rosado, J., Blanco, F., García, G., Maljković, J. B.: 2024, *Phys. Chem. Chem. Phys.*, **26**, 985-991.

ELECTRON SCATTERING CROSS SECTIONS REPRESENTED IN BELGRADE ELECTRON-ATOM/MOLECULE DATABASE (BEAM)

BRATISLAV P. MARINKOVIĆ  and STEFAN Đ. IVANOVIĆ 

Institute of Physics Belgrade, University of Belgrade, Laboratory for Atomic Collision Processes, Pregrevica 118, 11080 Belgrade, Serbia

E-mail bratislav.marinkovic@ipb.ac.rs and stefan.ivanovic992@gmail.com

Abstract. Electron scattering cross sections have been maintained within BEAM database with the specific emphasis on the electron interactions with metal vapour atoms. Processes that have been covered are elastic scattering, electronic state excitations and ionization.

BEAM database was promoted in 2015 (Marinković *et al.* 2015) and from the beginning it was a part of Virtual Atomic/Molecular Data Centre (Albert *et al.* 2020). Different set of electron-scattering cross sections, either differential or integral, have been maintained and curated. Currently, 17 atomic species and 18 molecular species are included in BEAM database. The usefulness of database has been demonstrated in analyzing data from Rosetta Mission (Marinković *et al.* 2017) or showing collisional datasets of importance for molecular dynamics (Vujčić *et al.* 2023).

Acknowledgements

This research was supported by the Science Fund of the Republic of Serbia, grant #6821, project name: “Atoms and (bio)molecules-dynamics and collisional processes on short time scale” (ATMOLCOL).

References

- Albert, D., Antony, B., Ba, Y.A., et al. : 2020, *Atoms* **8**, 76.
Marinković, B.P., Bredehöft, J.H., Vujčić, V., Jevremović, D., Mason, N.J. : 2017, *Atoms* **5**, 46.
Marinković, B.P., Vujčić, V., Sushko, G., Vudragović, D., Marinković, D.B., Đorđević, S., Ivanović, S., Nešić, M., Jevremović, D., Solov'yov, A.V., Mason, N.J. : 2015, *Nucl. Instrum. Meth. B* **354**, 90-95.
Vujčić, V., Marinković, B.P., Srećković, V.A., Tošić, S., Jevremović, D., Ignjatović, Lj.M., Rabasović, M.S., Šević, D., Simonović, N., Mason, N.J. : 2023, *Phys. Chem. Chem. Phys.* **25**, 26972 – 26985.

EJECTED ELECTRON SPECTRA OF KRYPTON STUDIED BY HIGH AND LOW ENERGY ELECTRONS

BRATISLAV P. MARINKOVIĆ¹ , JOZO J. JURETA¹ and
LORENZO AVALDI²

¹*Institute of Physics Belgrade, University of Belgrade, Laboratory for Atomic Collision Processes, Pregrevica 118, 11080 Belgrade, Serbia*
E-mail bratislav.marinkovic@ipb.ac.rs and jozo.jureta@ipb.ac.rs

²*CNR-Istituto di Struttura della Materia, Area della Ricerca di Roma 1, CP10, 00015 Monterotondo Scalo, Italy*
E-mail lorenzo.avalidi@ism.cnr.it

Abstract. The spectra of ejected electrons of krypton have been investigated by using high resolution electron spectroscopy at high and low incident electron energies and at 40°, 90° and 130° scattering angles. The features in the spectra have been identified as singly and doubly excited states, correlation satellites, and double- Auger electrons.

The experiment was performed with the high-resolution electron spectrometer OHRHRA (Jureta et al. 2021). The spectra were obtained in the Constant Analyzer Energy (CAE) mode in which the analyzer pass energy was constant, while the kinetic energy was scanned by varying the retarding ratio of the lens stack. Measurements were performed at high (2019 eV) and low (28-50 eV) electron energies, while the ejected spectra were recorded from 3.5 eV to 25 eV. This is a continuation of our studies on Auger and Coster-Kronig spectra of krypton induced by electron impact (Jureta et al. 2021).

Acknowledgements

The work has been performed within the scope of bilateral project between Italy and Serbia of particular relevance (Grande Rilevanza) “Nanoscale insights in radiation damage”. This research was supported by the Science Fund of the Republic of Serbia, grant #6821, project name: “Atoms and (bio)molecules-dynamics and collisional processes on short time scale” (ATMOLCOL).

References

Jureta, J.J., Marinković, B.P. and Avaldi, L. : 2021, *J. Quant. Spectrosc. Radiat. Transf.* **268**, 107638.

POST-PRIOR DISCREPANCY IN THE CB1-4B METHOD FOR SINGLE-ELECTRON CAPTURE IN FAST $\text{Li}^{3+} + \text{He}$ COLLISIONS

NENAD MILOJEVIĆ¹, IVAN MANČEV¹, DANILO DELIBAŠIĆ¹ and
MILOŠ MILENKOVIĆ²

¹*Department of Physics, Faculty of Sciences and
Mathematics, University of Niš, Višegradska 33, 18000 Niš, Serbia
E-mail nenad.milojevic@pmf.edu.rs*

²*Faculty of Technology, University of Niš,
Bulevar oslobođenja 124, 16000 Leskovac, Serbia*

Abstract. Post-prior discrepancy in the four-body boundary-corrected first Born approximation (CB1-4B) is investigated. For this purpose, the state-selective Q_{nlm} and state-summed Q_{nl} , Q_n and Q_Σ total cross sections for single-electron capture at intermediate and high impact energies in $\text{Li}^{3+} + \text{He}$ collisions in post form of the CB1-4B approximation have been calculated. For state-summed total cross sections Q_Σ , the theoretically obtained results were compared with available measurements, and excellent agreement was observed. Examining the post-prior discrepancy is essential to determine whether the same physical assumptions are included in the prior and post forms of the CB1-4B approximations.

1. INTRODUCTION

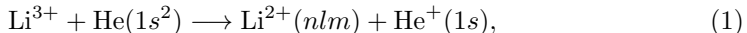
The systematic study of collision processes is one of the main sources of information about the structure of matter (atoms and molecules) as well as the interactions between the particles that make up these systems. On the other hand, charge-exchange collision processes are very important in assessing the energy loss of ions (e.g. protons and carbon nuclei) passing through tissue in the process of ion therapy for tumor tissue (Belkić 2010, Belkić 2013a, Belkić 2013b). Also, single-electron capture in collisions of fast projectiles with atomic and ionic targets, as one of the most extensively studied charge-exchange processes (Mančev et al. 2012, Mančev et al. 2013a, Mančev et al. 2013b, Milojević 2014, Milojević et al. 2017), is crucial for describing astrophysical phenomena (Heng et al. 2008), processes of neutralization and charging of plasma constituents (Thomas 2012), as well as in thermonuclear research (Marchuk 2014). Because of all these, single-electron capture remains a subject of significant theoretical investigation today (Milojević et al. 2020, Milojević et al. 2023).

In this paper, single-electron capture in collisions of fast lithium nuclei with helium atoms in the ground state is theoretically investigated. A four-body boundary-corrected first Born (CB1-4B) approximation in both prior and post forms is used. For this collision system, the results in the prior form of the CB1-4B approximation have already been calculated in previous work (Mančev et al. 2012), while in the post form of the CB1-4B approximation, the results for capture into the excited states of the projectile Li^{2+} in the exit channel are presented here for the first time.

Atomic units will be used throughout unless otherwise stated.

2. THEORY

The considered single-electron capture is schematically represented as:



where nlm is the usual set of three quantum numbers of hydrogenlike atomic systems Li^{2+} , while the symbol Σ denotes the capture into all final states of the projectile Li^{2+} in the exit channel. The parentheses symbolize the bound states.

The prior form of the state-selective transition amplitude for process (1) in the CB1-4B approximation read as (Mančev *et al.* 2012):

$$T_{nlm}^{\text{CB1-4B}^-}(\vec{\eta}) = 3 \iiint d\vec{x}_1 d\vec{x}_2 d\vec{R} \varphi_{nlm}^*(\vec{s}_1) \varphi_{100}^*(\vec{x}_2) (2/R - 1/s_1 - 1/s_2) \varphi_i(\vec{x}_1, \vec{x}_2) \\ \times e^{-i\vec{\alpha} \cdot \vec{R} - i\vec{v} \cdot \vec{x}_1} (vR + \vec{v} \cdot \vec{R})^{2i/v} \equiv T_{nlm}^-(\vec{\eta}), \quad (3)$$

while in the post form of the state-selective transition amplitude is given by (Mančev *et al.* 2013):

$$T_{nlm}^{\text{CB1-4B}^+}(\vec{\eta}) = \iiint d\vec{x}_1 d\vec{x}_2 d\vec{R} \varphi_{nlm}^*(\vec{s}_1) \varphi_{100}^*(\vec{x}_2) \left[3(1/R - 1/s_2) \right. \\ \left. + 1/R - 2/x_1 + 1/r_{12} \right] \varphi_i(\vec{x}_1, \vec{x}_2) e^{-i\vec{\alpha} \cdot \vec{R} - i\vec{v} \cdot \vec{x}_1} (vR + \vec{v} \cdot \vec{R})^{2i/v} \equiv T_{nlm}^+(\eta), \quad (4)$$

where $\vec{v} = v\hat{z}$ is the velocity of the projectile along the z -axis, with the unit vector \hat{z} , which is determined by the velocity of the projectile before the collision. In processes (1) and (2), two electrons are also involved, denoted as e_1 and e_2 , which are bound to the helium atom in the entrance channel. Quantities \vec{s}_1 and \vec{s}_2 (\vec{x}_1 and \vec{x}_2) represent the position vectors of the first and second electrons (e_1 and e_2) relative to the Li^{3+} (alpha particles, He^{2+}), respectively. The relative position of lithium Li^{3+} with respect to He^{2+} denoted as \vec{R} . The vector of the distance between the two electrons e_1 and e_2 is denoted by $\vec{r}_{12} = \vec{x}_1 - \vec{x}_2 = \vec{s}_1 - \vec{s}_2$, and we have $r_{12} = |\vec{r}_{12}|$. Here the $\vec{\alpha} = \vec{\eta} - (v/2 - (E_i + 9/[2n^2] + 2)/v)\vec{v}$ is the momentum transfer, while transverse momentum transfer is given by $\vec{\eta} = (\eta \cos \phi_\eta, \eta \sin \phi_\eta, 0)$ with the property $\vec{\eta} \cdot \vec{v} = 0$. The functions $\varphi_{nlm}(\vec{s}_1)$ and $\varphi_{100}(\vec{x}_2)$ represent the bound state wave functions of the hydrogenlike atomic systems Li^{2+} and He^+ in exit channel, respectively. The helium atom in the entrance channel is in the ground state $1s^2$ (1S_0), so we used the symmetric two-parameter wave function of Silverman *et al.* (Silverman *et al.* 1960), which corresponds to the singlet (antisymmetric) spin state: $\varphi_i(\vec{x}_1, \vec{x}_2) = N(e^{-\alpha_1 x_1 - \alpha_2 x_2} + e^{-\alpha_2 x_1 - \alpha_1 x_2})$, with variational parameters $\alpha_1 = 2.183171$ and $\alpha_2 = 1.18853$ where binding energy is $E_i = -2.8756614$. The normalization constant is $N = [(\alpha_1 \alpha_2)^{-3} + (\alpha_1/2 + \alpha_2/2)^{-6}]^{-1/2}/(\pi\sqrt{2})$.

The state-selective and state-summed total cross sections in the prior and post form CB1-4B approximation are given by:

$$Q_{nlm}^\pm(\pi a_0^2) = \frac{1}{2\pi^2 v^2} \int_0^\infty d\eta \eta |T_{nlm}^\pm(\vec{\eta})|^2, \quad Q_{nl}^\pm = \sum_{m=-l}^{+l} Q_{nlm}^\pm, \quad Q_n^\pm = \sum_{l=0}^{n-1} Q_{nl}^\pm. \quad (5)$$

Numerical calculations of the integrals (5) (five-dimensional in the case of post form, and three-dimensional in the case of prior form) are performed by means of the Gauss-Legendre (GL) and Gauss-Mehler (GM) quadratures. The numbers of integration

points, N_{GL} and N_{GM} , were $N_{\text{GL}} \leq 96$ and $N_{\text{GM}} = 20$. Namely, since the singlet spin state is in the entrance channel, the singlet spin state must also be in the exit channel because the perturbation is not spin-dependent. It follows that the total wave function in the configuration space must be symmetric in the exit channel:

$$\chi_f = N_1 [\varphi_{nlm}^*(\vec{s}_1) \varphi_{100}^*(\vec{x}_2) e^{-i\vec{\alpha} \cdot \vec{R} - i\vec{v} \cdot \vec{x}_1} + \varphi_{nlm}^*(\vec{s}_2) \varphi_{100}^*(\vec{x}_1) e^{-i\vec{\alpha} \cdot \vec{R} - i\vec{v} \cdot \vec{x}_2}] / \sqrt{2} \quad (6)$$

The transition amplitudes (3) and (4) are the same for both terms. Due to the non-triviality of calculating the generalized expression for the normalization constant N_1 , we can approximately assume it to be equal to 1. To account for this, the total cross sections $Q_{nlm}^{\pm}(\pi a_0^2)$ needs to be multiplied by 2. The previous consideration is entirely equivalent to the consideration in the spin-independent formalism where electrons e_1 and e_2 are distinguishable, and where the multiplication by two arises from the fact that the probability of capturing electron e_1 while electron e_2 remains in the target is the same as the probability of capturing electron e_2 while electron e_1 remains in the target. State-summed total cross sections for electron capture into all the final states are obtained by applying the Oppenheimer (n^{-3}) scaling law (Oppenheimer 1928, Belkić et al. 1987) via:

$$Q_{\Sigma}^{\text{CB1-4B}\pm} = Q_1^{\text{CB1-4B}\pm} + Q_2^{\text{CB1-4B}\pm} + 2.081 Q_3^{\text{CB1-4B}\pm}. \quad (7)$$

3. RESULTS AND DISCUSSION

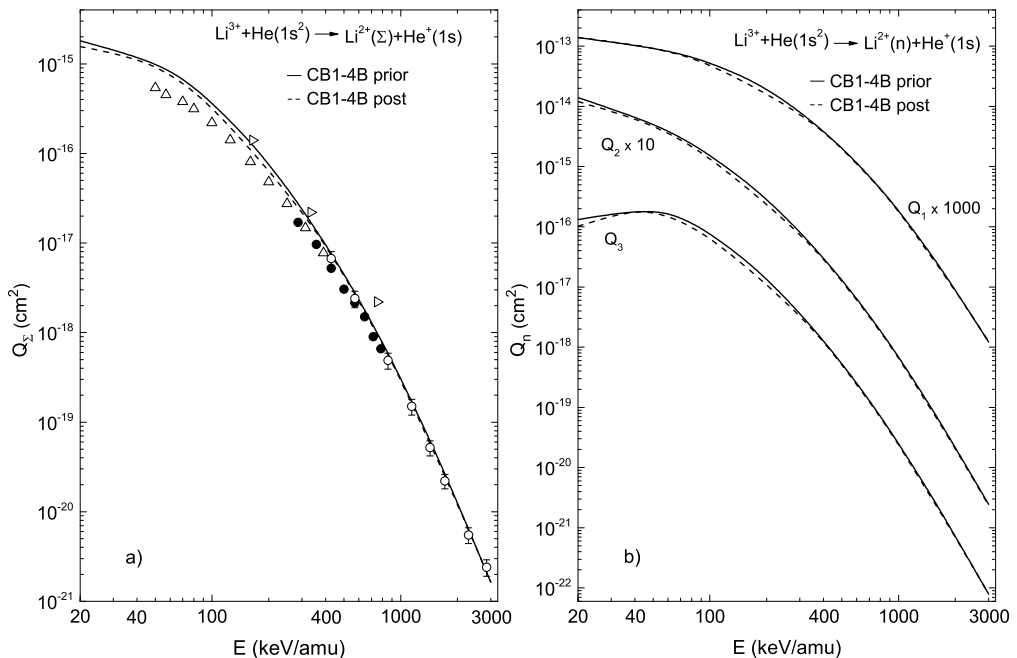


Figure 1: Panel a): Experimental data: \triangle (Shah and Gilbody 1985), \circ (Woitke et al. 1998), \triangleright (Nikolaev et al. 1961), \bullet (Sant'Anna et al. 2009).

For the study of single-electron capture (1) and (2), numerical results have been obtained in post form for the total cross sections Q_1 , Q_2 , Q_3 and Q_{Σ} in the energy

range from 20 keV/amu to 3000 keV/amu. These results, together with those from the prior form (Mančev *et al.* 2015), are presented in Figure 1, Q_Σ in panel (a) alongside available experimental data, and Q_1 , Q_2 , Q_3 in panel (b). As can be seen, the experimental data are well matched except for the measurements by Nikolaev *et al.* (Nikolaev *et al.* 1961), which exceed the others in the energy range of 164-752 keV. Both forms show excellent agreement with the measurements at energies above 300 keV/amu, while at lower energies better agreement is achieved in the post form, except for one measurement (Nikolaev *et al.* 1961) at an energy of 164 keV/amu, which is better described by the prior form. Additionally, the panels indicate that the post-prior discrepancy is almost negligible at higher energies.

4. CONCLUSIONS

The post-prior discrepancy in the CB1-4B approximation for the process of single-electron capture in fast collisions of lithium nuclei with helium atoms has been investigated. It has been shown that this discrepancy is small, almost negligible at high energies for the obtained state-summed cross sections. This means that the physical assumptions in the post and prior forms of the CB1-4B approximation are included in the same way (as we know, the exact transition amplitudes in the prior and post forms are equal on the energy shell). Additionally, the calculated stated-summed total cross sections Q_Σ are in excellent agreement with the experimental data at energies above 160 keV/amu.

Acknowledgements N. Milojević, I. Mančev and D. Delibašić acknowledge financial support from the Science Fund of the Republic of Serbia (# GRANT 6821, Project title - ATMOLCOL) and Ministry of Education, Science and Technological Development of the Republic of Serbia for support under Contract No. 451-03-65/2024-03/200124.

References

- Belkić, Dž.: 2010, *J. Math. Chem.* **47**, 1366.
 Belkić, Dž.: 2013a, *Fast Ion-Atom and Ion-Molecule Collisions*, World Scientific Publishing, Singapore.
 Belkić, Dž.: 2013b, *Adv. Quantum Chem.* 65.
 Mančev, I., Milojević, N., Belkić, Dž.: 2012, *Phys. Rev. A* **86**, 022704.
 Mančev, I., Milojević, N., Belkić, Dž.: 2013a, *Phys. Rev. A* **88**, 052706.
 Mančev, I., Milojević, N., Belkić, Dž.: 2013b, *Few-Body Syst.* **54**, 1889.
 Milojević, N.: 2014, *J. Phys.: Conf. Ser.* **565** 012004.
 Milojević, N., Mančev, I., Belkić, Dž.: 2017, *Phys. Rev. A* **96** 032709.
 Heng, K., Sunyaev, R. A.: 2008, *Astronomy & Astrophysics*, **481**, 117.
 Thomas, D. M.: 2012, *Phys. Plasmas* **19**, 056118.
 Marchuk, O.: 2014, *Phys. Scr.*, **89**, 114010.
 Milojević, N., Mančev, I., Belkić, Dž.: 2020, *Phys. Rev. A* **102** 012816.
 Milojević, N., Mančev, I., Belkić, Dž.: 2023, *Phys. Rev. A* **107** 052806.
 Mančev, I., Milojević, N., Belkić, Dž.: 2015, *At. Data Nucl. Data Tables* **102**, 6.
 Silverman, J. N., Platas, O., Matsen, F. A.: 1960, *J. Chem. Phys.* **32**, 1402.
 Oppenheimer, J. R.: 1928, *Phys. Rev.* **31**, 349.
 Belkić, Dž., Saini, S., Taylor, H.S.: 1987, *Phys. Rev.* **36**, 1601.
 Shah M.B., Gilbody, H.B.: 1985, *J. Phys. B* **18**, 899.
 Nikolaev, V.S., Dmitriev, I.S., Fateyeva, L.N., Teplova, Ya.A.: 1961, *Sov. Phys. JETP* **13**, 695; 1961, *Zh. Eksp. Teor. Fiz.* **40**, 989.
 Woitke, O., Závodszyk, P.A., Ferguson, S.M., Houck, J.H., Tanis, J.A.: 1998, *Phys. Rev. A* **57**, 2692.
 Sant'Anna, M.M., Santos, A.C.F., Coelho, L.F.S., Jalbert, G., de Castro Faria, N.V., Zappa, F., Focke, P., Belkić, Dž.: 2009, *Phys. Rev. A* **80**, 042707.

DIRECT ELECTRON-LIQUID ENERGY LOSS SPECTRA MEASUREMENTS USING A LIQUID MICRO-JET

D. L. MUCCIGNAT¹, D. B. JONES², J. R. GASCOOKE², G. J. BOYLE¹, N. A. GARLAND³
and R. D. WHITE¹

¹*College of Science and Engineering, James Cook University, Townsville 4810, Australia
E-mail dale.muccignat@my.jcu.edu.au*

²*College of Science and Engineering, Flinders University, Bedford Park 5042, Australia*

³*Centre for Quantum Dynamics, Griffith University, Nathan 4111, Australia &
School of Environment and Science, Griffith University, Nathan 4111, Australia*

Abstract. Electron transport through liquids plays a critical role in a number of emerging applications in medicine, particle detectors and nanomaterials. Currently, conducting direct electron-liquid scattering experiments in vacuum conditions poses significant challenges due to the high vapour pressure of liquids and multiple scattering effects. In this work, we present a new electron-liquid scattering experiment that utilises a liquid micro-jet to provide a stable scattering surface for an electron beam under vacuum conditions. Initial measurements are made and compared to existing theory using a Monte Carlo simulation and their limitations are discussed.

1. INTRODUCTION

The application of Low Temperature Plasmas (LTPs) to liquid surfaces forms the basis for a variety of important applications in environmental remediation, medicine and in the synthesis of nanomaterials [Adamovich *et al.* 2017]. LTPs exhibit typical electron temperatures that are much higher than its equilibrium ion and background neutral species. The resultant heat flux is then much lower when compared to conventional plasmas while maintaining electron energies sufficient to drive reactions within the plasma and into the applied surface [Lieberman and Lichtenberg 2005]. Crucially, this property then allows their application to heat sensitive biological matter under atmospheric conditions. Understanding electron transport across the gas-liquid interface and into the target liquid is thus critical to the application of LTPs to liquid targets and biological matter. In particular, low energy (< 10 eV) electrons play a key role in driving reactions at the plasma-liquid interface and modelling their transport is critical for the high-level optimisation of efficacy and selectivity of current and future generation plasma-liquid applications.

Theoretical approaches to describe electron scattering through non-polar liquids has recently reached some maturity [Boyle *et al.* 2015], but the same can not be said for polar liquids. Polar liquids exhibit trapped electron states and free electron

scattering from spatially, temporally and orientationally correlated dipoles. Given suitable theoretical descriptions of an electron’s motion through polar liquids, experimental measurements of electron scattering in liquid environments are also required as a validation step. However, the high vapour pressure and the volatile nature of liquids makes their study under experimental conditions, particularly in vacuums, difficult to achieve [Faubel *et al.* 1988]. Experiments generally measure either macroscopic properties of electron swarms in liquids [Kubota *et al.* 1982] or indirectly through photoelectron scattering from liquid beams [Thürmer *et al.* 2013].

Therefore, we have developed a new experiment to measure direct electron-liquid scattering in a vacuum environment through the use of a liquid micro-jet ($L\mu J$). Recently, we presented a feasibility study of such an experiment using a Monte Carlo simulation of model experimental conditions [Muccignat 2022]. A similar proof-of-principle experiment was conducted by Nag *et al.* using an aqueous solution of TRIS (2-Amino-2-(hydroxymethyl)propane-1,3-diol) [Nag *et al.* 2023]. Here, we present initial results from the experiment and compare them to simulated data and discuss future work.

2. EXPERIMENTAL SET-UP

The scattering chamber utilised here was built originally by Cavanagh and Lohmann [Cavanagh and Lohmann 1999] for coincidence detection of electron ionisation events from a gas beam. In this section, in the interest of brevity, we only detail the modifications made to suit the new $L\mu J$ apparatus.

In this work, a $L\mu J$ developed by Advanced Microfluidic Systems GmbH¹ replaces the original molecular beam source. An inlet capillary is passed through a Conflat flange into the chamber where it is attached to a crystal nozzle that produces the $L\mu J$. The inner diameter of the nozzle is tapered to produce a liquid beam of a desired size. Liquid samples are prepared in a glass bottle and degassed along with a few grains of salt that are added to reduce electrokinetic charging of the jet during operation [Preissler 2013]. A high pressure dosing pump is then used to draw liquid from the bottle and through the inlet capillary at 0.5 – 1.5 ml/min.

Figure 1 shows the $L\mu J$ with an electron gun and two hemispherical detectors positioned radially around the scattering region. In this experiment, nozzles with diameters of 15, 25 and 40 μm were available and 40 μm was used in this work for its stability. From the nozzle, liquid flows directly downward through the vacuum and into a 1 mm orifice in the centre of the catcher. From there, the liquid drains with gravity and the help of a diaphragm pump where it pools in a vacuum safe bottle submerged in an ice bath awaiting disposal. Both the nozzle and catcher are heated to reduce the risk of the sample freezing. The position of the jet can be externally controlled through two stepping piezo motors along the horizontal axis of the scattering plane. Additionally, the height of the jet can be adjusted manually.

From the catcher, a waste tube removes the expended sample from the chamber through a Conflat flange and into a vacuum safe glass catcher bottle. An additional tube extends from the bottle lid and is attached to a backing pump to prevent backflow into the chamber. Both of these tubes contain valves to allow emptying of the bottle during operation.

¹www.admisys-gmbh.com

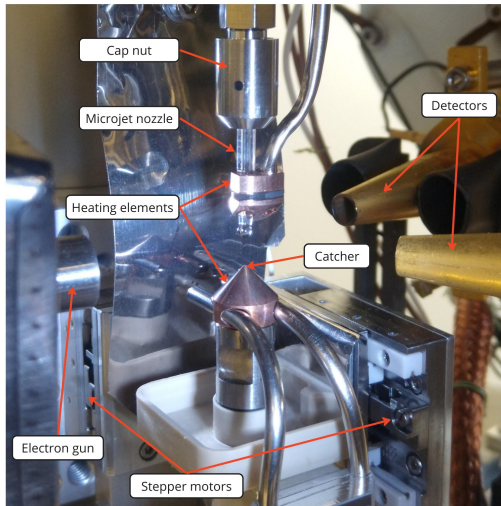


Figure 1: Photograph of the present liquid micro-jet apparatus along with labels for each device.

2. 1. RESULTS

During the initial set-up phase of the experiment, a Monte Carlo simulation was used to compare with measured scattering data to align the L μ J within the chamber. Here, we present preliminary measurements of electron-scattering from both the L μ J and from the background vapour.

Using an initial scattering beam of ≈ 250 eV, an energy loss spectra was measured from 251 eV to 220 eV. A strong elastic peak was found followed by a broad and tapering signal that results from inelastic and ionisation scattering processes. In Figure 2 we present the measured energy loss spectra for electrons scattered from the L μ J and compare that to spectra measured when the L μ J was moved outside of the interaction region. For comparison, each spectra is scaled by the maximum value of the liquid spectrum.

In addition, we present simulated spectra using the Monte Carlo simulation for both the liquid and gas scenarios. The simulation utilised the cross-section set proposed by Ness *et. al.*, along with approximate densities and a forward peaked analytic scattering angle function (differential cross-section). Broadly, for the gas density and scattering function selected, the simulation is able to reproduce the elastic peak observed. The most notable difference in each spectra can be found between 230 and 247 eV. In the simulated spectra there exists two small inelastic peaks that are followed by the broad ionisation signal while in the measured data only a single, broad, peak is obvious. Without additional measurements to validate the observed EELS and investigate the dependence upon initial energy and scattering angle, it is difficult to determine the cause for this discrepancy. Rotational processes were not included explicitly in the cross-section set and their inclusion may result in a similar broadening reflected in the simulated spectra. In addition, shifts in the energy loss threshold

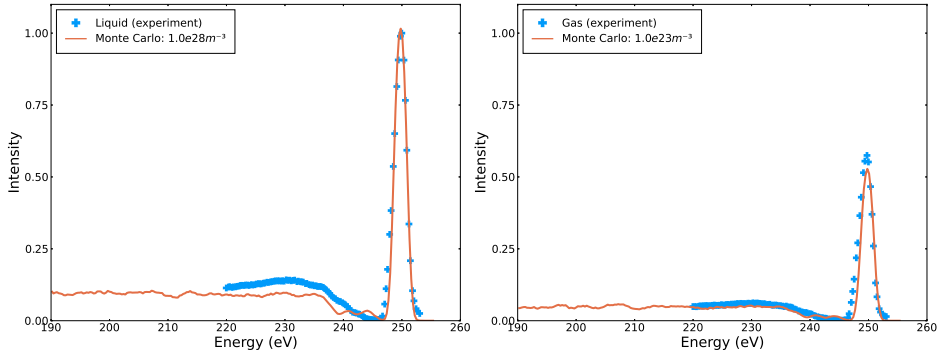


Figure 2: Electron energy loss spectra for a 250 eV electron beam incident upon a $40\ \mu\text{m}$ L μ J compared to ‘gas’ phase measurements where the L μ J was moved to the side. In addition, simulations were conducted using the H $_2$ O cross section set of Ness *et al.* using an approximate gas phase density and an analytic angular dependence of the differential cross sections. Each pair of liquid and gas spectra were scaled by the maximum value of the liquid spectra for comparison.

for excitation processes, resulting from interaction effects within the liquid, could result in each peak overlapping to more closely represent the measured data. We must note however that these measurements are preliminary by nature and require further investigation and additional measurements to verify.

Overall, we have conducted initial measurements of a new electron-liquid scattering experiment and compared them with existing theory. In future work we aim to leverage the unique nature of this experiment to further our understanding of electron-liquid transport through non-polar liquids.

References

- Adamovich, I. *et al.* : 2017, *J. Phys. D: Appl. Phys.*, **50**, 323001
 Boyle, G. J. *et al.* : 1988, *The J. of Chem. Phys.*, **142**, 154507 Faubel, M. *et al.* *Zeitschrift für Physik D: Atoms, Molecules and Clusters*, **10**, 269–277
 Cavanagh, S. J. and Lohmann, B. : 1999, *J. Phys. B: At. Mol. Opt. Phys.*, **32**, L261
 Kubota, S. *et al.* : 1982, *Journal of the Physical Society of Japan*, **10**, 3274-3277
 Lieberman, M. A. and Lichtenberg, A. J. : 2005, *Principles of Plasma Discharges and Materials Processing*, John Wiley & Sons
 Nag, P. *et al.* : 2023, *J. Phys. B: At. Mol. Opt. Phys.*, **56**, 215201
 Ness, K. F. *et al.* : 1988, *Phys. Rev. A.*, **38**, 1446-1456
 Preissler, N. *et al.* : 2013, *J. Phys. Chem. B*, **117**, 2422-2428
 Thürmer, S. *et al.* : 2013, *Phys. Rev. Let.*, **17**, 173005

DIFFUSION COEFFICIENTS OF H_2^+ IONS IN H_2 GAS

ŽELJKA NIKITOVIĆ  and ZORAN RASPOPOVIĆ 

*Institute of Physics, University of Belgrade, Pregrevica 118, 11080 Belgrade,
Serbia*

E-mail zeljka@ipb.ac.rs

zr@ipb.ac.rs

Abstract. In this work we present a complete cross sections set and transport properties of H_2^+ in H_2 gas. Ionic charge transfer reactions with molecules are indispensable elementary processes in the modeling of kinetics in terrestrial, industrial and astrophysical plasma in the detection of dark matter. A Monte Carlo simulation method is applied to accurately calculate transport parameters in hydrodynamic regime. We discuss new data for H_2^+ ions in H_2 gas where the mean energy, longitudinal and transversal diffusion coefficients are given as a function of low and moderate reduced electric fields E/N (E -electric field, N -gas density).

1. INTRODUCTION

Transport properties of species in gas plasmas are of great importance in understanding the nature of molecular and ionic interactions in gas mixtures (Todd et al. 2002, Mason 1957, Golzar et al. 2014). These properties include the mean energy, drift velocity, diffusion coefficients, ionization and chemical reaction coefficients, chemical reaction coefficients for ions and (rarely) excitation coefficients, and they are very useful in chemical industries for the design of many types of transport and process equipment.

We notice the importance of obtained results as atomic and molecular data which are input parameters for modeling of various environments. Low temperature can change the state of metals, gases, liquids and solids, cause damage to organisms depending on length of exposure, and change the functionality of mechanized processes. Quantum-mechanical calculation of a certain cross-section is a required task that requires knowledge of the surface potential energy of ions and molecules to be constructed from the structure of the reactants. Less intensive computational methods, such as the Denpoh-Nanbu theory (Denpoh and Nanbu 1998, Nikitović et al. 2014, Petrović et al. 2007), require knowledge of thermodynamic formation data and are applicable to a range of molecules.

2. CROSS SECTION SETS

Ion charge transfer reactions with molecules are important elementary processes in modeling kinetics in all types of plasma. In many cases, it is known

that the cross section for these reactions represents the most important part of the set of cross section. Transport properties needed for modeling H_2 discharges containing H_2^+ ions are calculated by the Monte Carlo method. A code that properly takes into account thermal collisions was used (Ristivojević and Petrović 2012). The cross-section set describes the total collision cross-section between an ion and a gas particle. The total collision cross-section between an ion and a gas particle is described at low energies using Langevin's cross-section and at higher energies using the collision of rigid spheres, as demonstrated in paper (Nikitović et al. 2016, Nikitović et al. 2019).

Figure 1 presents a complete set of cross sections for ion- H_2 molecule interactions as a function of collision energy. The provided cross sections by (Denpoh and Nanbu, 2022) are presented, except for those for proton transfer, H^+ production, and charge exchange, for which the cross sections were obtained from Phelps' work (Phelps 1990, Phelps 2011). The set encompasses rotational ($H_2^+ + H_2$, Rot.), vibrational ($H_2^+ + H_2$, Vib.), electronic ($H_2^+ + H_2$, El. ex.), and dissociative ($H_2^+ + 2H$, Diss. ex.) excitations, in addition to Neutral dissociation ($H_2^+ + 2H$, Neutral dissociation) and Ionization ($H_2^+ + H_2^+ + e$, Ionization), as well as dissociative ionization ($H_2^+ + H^+ + H + e$, Diss. Ionization) along with the other mentioned processes. The reaction products of $H_2^+ + H_2$ shown in parentheses, along with the corresponding labels on the Figure 1.

Non-elastic excitation processes are treated isotropically. In the case of ionization processes, the secondary ion H_2^+ is also tracked, which shares the incoming kinetic energy with the primary ion reduced by the reaction threshold. The partition of kinetic energy between the primary and secondary ions is determined randomly. In the case of proton transfer processes, the resulting ion H_3^+ is not tracked in the simulations, nor is the H^+ ion in the case of H^+ production.

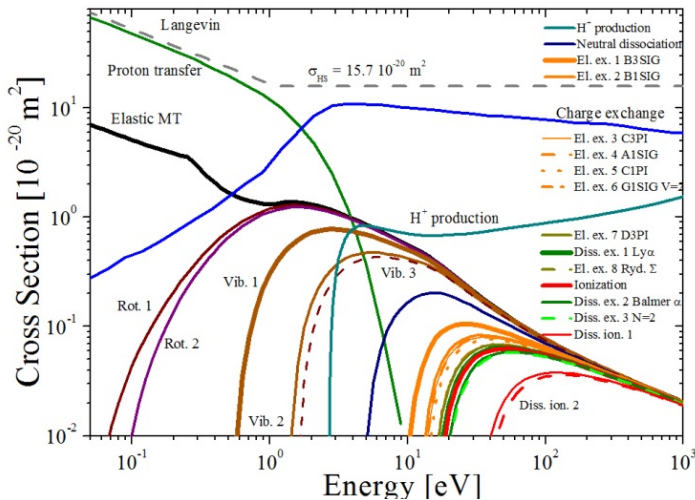


Figure 1: Complete set of cross sections for ion (H_2^+) and molecule (H_2) interactions as a function of collision energy.

2. RESULTS AND DISCUSSION

Proton transfer reactions deplete the swarm of low-energy H_2^+ ions, resulting in a mean ion energy of 0.37 eV at $E/N = 1$ Td, which is significantly higher than the thermal energy of H_2 molecules at $T = 300$ K in Figure 2. The rise in mean energy is strongly resisted by charge exchange, rotational and vibrational excitation as the electric field increases. With increasing energy, the rate of charge exchange reactions decreases, allowing the mean energy to rise more quickly after $E/N > 200$ Td.

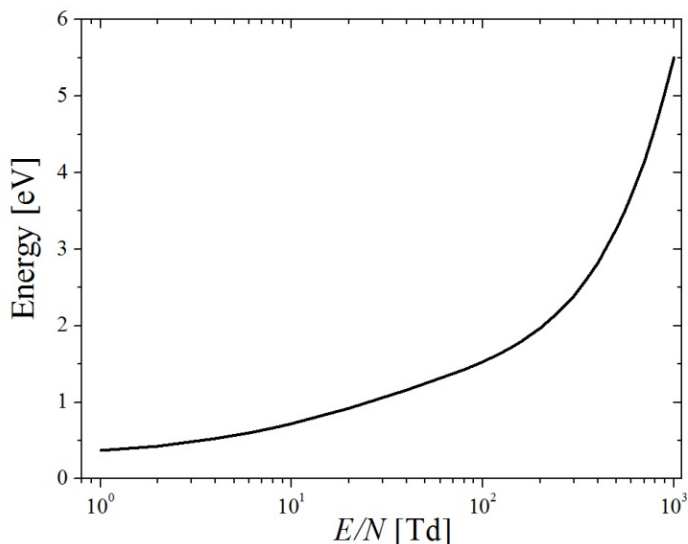


Figure 2: Mean energy of H_2^+ ions a function of E/N at 300 K.

In Figure 3, the bulk and flux values of longitudinal and transverse diffusion coefficients, multiplied by the gas concentration, are shown as a function of E/N . For $E/N < 100$ Td, the significantly lower D_L than D_T indicates highly anisotropic diffusion of the swarm, which spreads four times slower in the direction of the field, deforming the swarm's spherical shape into a highly ellipsoidal shape.

The reduction of diffusion coefficients with increasing E/N is attributed to the rising number of charge exchange reactions with energy that produce slow H_2^+ ions. While there are minor differences between the bulk and flux values of diffusion coefficients, as evident in Figure 3, except for transverse diffusion at low fields, where the bulk values surpass the flux values.

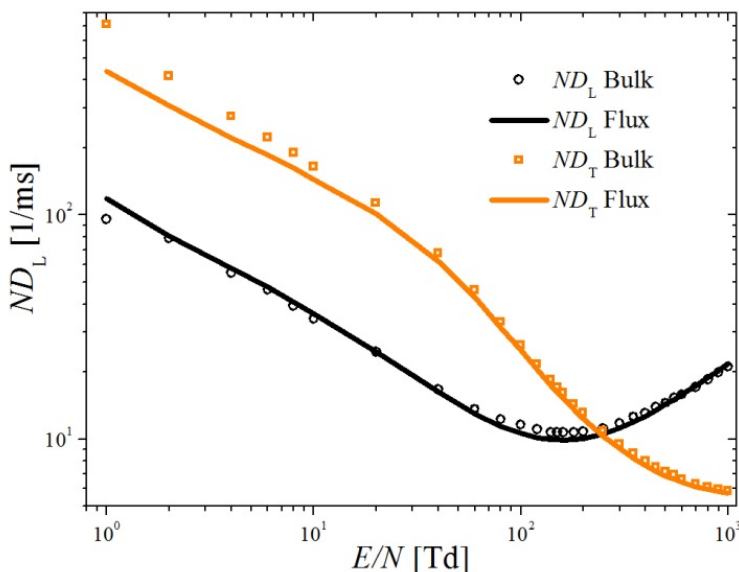


Figure 3: Bulk and flux longitudinal and transverse diffusion coefficients as a function of E/N at 300K.

Acknowledgements

The authors acknowledge funding provided by the Institute of Physics University Belgrade, through the grant by the Ministry of Education, Science and Technological Development of the Republic of Serbia.

References

- Denpoh K. and Nanbu K. : 1998, *J. Vac. Sci. Technol.* **A 16 (3)** 1201.
 Denpoh K. and Nanbu K.: 2022, *Journal of Vacuum Science & Technology A* **40** 063007.
 Golzar K., Amjad-Iranagh S., Amani M., Modarress H.: 2014, *J. Membrane Science* **451** 117.
 Mason E.: 1957, *J. Chem. Phys.* **27** 782.
 Nikitović Ž., Raspopović Z., Stojanović V. and Jovanović J.: 2014, *EPL* **108** 35004.
 Nikitović Ž. D., Stojanović V. D. and Raspopović Z. M.: 2016, *EPL* **114** 25001.
 Nikitović Ž., Raspopović Z. and Stojanović V.: 2019, *EPL* **128** 15001.
 Petrović Z. Lj., Raspopović Z. M., Stojanović V. D., Jovanović J. V., Malović G., Makabe T. and de Urquijo J.: 2007, *J. Appl. Surf. Sci.* **253** 6619.
 Phelps A. V.: 1990, *J. Phys. Chem. Ref. Data* **19** 653.
 Phelps A. V.: 2011, *Plasma Sources Sci. Technol.* **20** 043001.
 Ristivojević Z. and Petrović Z. Lj. : 2012, *Plasma Sources Sci. Technol.* **21** 035001.
 Todd B., Young J. B.: 2002, *J. Power Sources* **110** 186.

INFLUENCE OF CATASTROPHES AND HIDDEN DYNAMICAL SYMMETRIES ON ULTRAFAST BACKSCATTERED PHOTOELECTRONS

T. ROOK, L. CRUZ RODRIGUEZ and C. FIGUEIRA DE MORISSON FARIA

Department of Physics and Astronomy, University College London, Gower Street, London, WC1E 6BT, UK

E-mail thomas.rook.20@ucl.ac.uk

Abstract. We discuss the effect of using potentials with a Coulomb tail and different degrees of softening in the photoelectron momentum distributions (PMDs) using the recently implemented hybrid forward-boundary CQSFA (H-CQSFA). We show that introducing a softening in the Coulomb interaction influences the ridges observed in the PMDs associated with backscattered electron trajectories. In the limit of a hard-core Coulomb interaction, the re-scattering ridges close along the polarization axis, while for a soft-core potential, they are interrupted at ridge-specific angles. We analyze the momentum mapping of the different orbits leading to the ridges. For the hard-core potential, there exist two types of saddle-point solutions that coalesce at the ridge. By increasing the softening, we show that two additional solutions emerge as the result of breaking a hidden dynamical symmetry associated exclusively with the Coulomb potential. Further signatures of this symmetry breaking are encountered in subsets of momentum-space trajectories. Finally, we use scattering theory to show how the softening affects the maximal scattering angle and provide estimates that agree with our observations from the CQSFA. This implies that, in the presence of residual binding potentials in the electron's continuum propagation, the distinction between purely kinematic and dynamic caustics becomes blurred (see Rook et al. 2024).

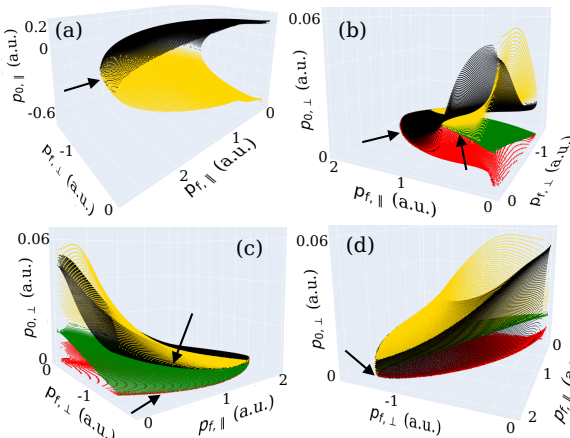


Figure 1: Three dimensional representation of the saddle point trajectories which correspond to the backscattered photoelectrons for a hard-core potential (a) and a soft-core potential (b-d). When a Coulomb softening is introduced, the number of sheets of solutions increases from two to four. The four distinct folds which connect these sheets all intersect at the singular point indicated by the black arrow in panel (d). The folds are indicated by the arrows in panels (a-c).

References

Rook, T., Cruz Rodriguez, L., Faria, CfdM.: 2024, [arXiv:2403.02264](https://arxiv.org/abs/2403.02264) [*physics.atom-ph*]

THREE-DIMENSIONAL STREAMER MODEL IN THE AMREX ENVIRONMENT

ILIJA SIMONOVIĆ^{id}, DANKO BOŠNJAKOVIĆ^{id} and SAŠA DUJKO^{id}

Institute of Physics Belgrade, Pregrevica 118, 11080 Belgrade, Serbia

Abstract. Streamers appear in nature as sprite discharges in the upper-planetary atmospheres, and as precursors of lightning, see Teunissen and Ebert 2017. They have a wide variety of applications in technology including the ignition of high-intensity discharge lamps and the purification of gases and liquids from harmful organic pollutants. The further development of these applications requires a joint effort of experimental investigations and computer modelling of streamer discharges.

We have developed a 3D streamer model in the AMReX environment. AMReX is an open-source C++ library for massively parallel block structured adaptive mesh refinement applications, see Zhang et al. 2019. AMReX has inbuilt geometric multigrid solvers for solving elliptic differential equations, and it allows both MPI and OpenMP parallelization on CPUs as well as parallelization on GPUs. AMReX also has many inbuilt classes which enable a convenient implementation of both grid and particle data.

Our model is based on the first-order fluid model with local field approximation. The time integration in our code is performed by employing the second order Runge-Kutta method. The spatial discretization is performed by using the finite volume method. In our model, the non-local source term due to photoionization is represented by solving a set of Helmholtz equations, and we apply the Bourdon three term parametrization for representing the photon absorption function, see Bourdon et al. 2007. The verification of our code is performed by comparing its results to the results of the Afivo-streamer open-source code, see Teunissen and Ebert 2017.

Acknowledgments: This work is supported by the Science Fund of the Republic of Serbia, Grant No. 7749560, Exploring ultra-low global warming potential gases for insulation in high-voltage technology: Experiments and modelling EGWI.

References

- Bourdon A., Pasko V. P., Liu N. Y., Célestin S., Ségur P. and Marode E.: 2007, *Plasma Sources Sci. Technol.* **16**, 656
Teunissen, J. and Ebert, U.: 2017, *Journal of Physics D: Applied Physics* **50**, 474001
Zhang, W. et al.: 2019, *Journal of Open Source Software*, **4**, 1370

EXCITATION OF ACETONE INDUCED BY ELECTRON IMPACT

BARBORA STACHOVÁ, JURAJ ORSZÁGH and ŠTEFAN MATEJČÍK

Comenius University in Bratislava, Faculty of Mathematics, Physics and Informatics, Bratislava, Slovak Republic
E-mail barbora.stachova@fmph.uniba.sk

Abstract. Acetone [(CH₃)₂CO] is the simplest ketone and it is one of the organic compounds that can be found in outer space. The detection of acetone in the interstellar space was first reported by Combes et al. [Combes et al., 1987], who detected this molecule in Sagittarius B2. It has also been detected in the mass spectra from 67P/Churyumov Gerasimenko, by the COSAC mass spectrometer at the comet's surface [Goesmann et al., 2015].

The emission spectrum following electron impact on acetone was studied in a crossed-beam experiment [Országh et al., 2017]. The spectrum was measured at several electron energies ranging from 7 to 102 eV within the wavelengths of 280 - 950 nm. The emission bands of CH (A-X), CH (B-X) and CH (C-X) along with emission lines of hydrogen's Balmer series were detected. Relative emission cross sections of identified transitions were measured at electron energy range within 7 – 102 eV. The experimental results are also complemented by theoretical calculations based on enthalpies of formation and excitation energies of detected fragments. The comparison of experimental and theoretical data can be used as a basis for suggesting dissociative excitation channels for selected transitions.

Acknowledgement

This work was supported by Slovak Research and Development Agency within projects nr. APVV-19-0386, SK-PL-23-0050, and by Slovak grant agency VEGA within the projects nr. 1/0489/21, 1/0553/22.

References

- Combes, F., Gerin, M., Wootten, A., Wlodarczak, G., Clausset, F., Encrenaz, P. J. : 1987, *Astronomy and Astrophysics*, 180, L13.
Goesmann, F., et al. : 2015, *Science*, 349, 6247.
Országh, J., Danko, M., Čechvala, P., Matejčík, Š. : 2017, *The Astrophysical Journal*, 841:17, (10pp).

SMALL MOLECULES ESSENTIAL TO ASTROPHYSICS: COLLISIONAL AND RADIATIVE PROCESSES

SANJA TOŠIĆ¹ , VLADIMIR SREČKOVIĆ²  and VELJKO VUJČIĆ² 

¹*Institute of Physics Belgrade, University of Belgrade, Pregrevica 118, Belgrade, Serbia*

E-mail seka@ipb.ac.rs, vlada@ipb.ac.rs

²*Astronomical Observatory, Volgina 7, 1100 Belgrade, Serbia*

E-mail veljko@aob.rs

Atomic/molecular collisions and radiation are crucial for understanding the different environments within our universe. These processes control molecular energy transfer, excitation, and de-excitation, which affects the spectra of many astrophysical sources, including planetary atmospheres, interstellar clouds, and circumstellar envelopes (see e.g. Sreckovic et al. 2022). Data and databases related to atomic and molecular processes have become increasingly important for developing models and simulations of complex physical/chemical processes, as well as for interpreting observations and results of measurements in various fields (Vujcic et al. 2023). The data can be used for a variety of other applications, such as modeling non-local thermal equilibrium of the early universe's chemistry, modeling of the solar atmosphere, modeling of white dwarf atmospheres etc. A new generation of methods and models needs to be developed along with improvements to the existing ones in order to include as many processes as possible and to use more accurate data which can be used in modern codes. For conditions that exist in laboratory plasmas, planetary atmospheres, the ionosphere and other areas of science, it is primarily aimed at obtaining cross sections and rates coefficients for certain collisional and radiative processes (Albert et al. 2020). In this contribution we present that kind of data.

Acknowledgments: This research was supported by the Science Fund of the Republic Serbia [Grant no. 3108/2021, NOVA2LIBS4fusion and Grant No. 7749560, EGWIn]

References

- Albert, D., Antony, B. K., Ba, Y. A., ... & Zwölf, C. M. : 2020, *Atoms*, **8(4)**, 76.
Sreckovic, V. A., Ignjatovic, L. M., Kolarski, A., Mijic, Z. R., Dimitrijevic, M. S., & Vujcic, V. : 2022, *Data*, **7**, 129.
Vujčić, V., Marinković, B. P., Srećković, V. A., Tošić, S., Jevremović, D., Ignjatović, L. M., ... & Mason, N. J. : 2023, *Phys. Chem. Chem. Phys.*, **25(40)**, 26972-26985.

DISSOCIATIVE ELECTRON ATTACHMENT TO CO₂ IN ELECTRIC AND MAGNETIC FIELDS

MIRJANA M. VOJNOVIĆ¹ , MIROSLAV M. RISTIĆ² ,
VIOLETA V. STANKOVIĆ-MALIŠ¹  and GORAN B. POPARIĆ¹ 

¹*University of Belgrade, Faculty of Physics, Belgrade, Serbia*
E-mail mvojnovic@ff.bg.ac.rs

²*University of Belgrade, Faculty of Physical Chemistry, Belgrade, Serbia*

Abstract. Rate coefficients for the production of O⁻ from CO₂ by dissociative electron attachment in the presence of constant electric and magnetic fields are presented. Monte Carlo simulation was used in order to obtain electron energy distribution functions for different values of density normalized electric and magnetic fields and angles between the fields. Results for two choices of E/N (500 Td and 700 Td) and three values of B/N (1000 Hx, 2000 Hx and 3000 Hx) are grouped and analyzed.

Acknowledgements

This work is partially supported by the Ministry of Education, Science and Technological Development of the Republic of Serbia by the Project No. 451-03-66/2024-03/ 200162.

INVESTIGATION OF ELASTIC ELECTRON SCATTERING FROM DESFLURANE MOLECULE AT INTERMEDIATE ELECTRON ENERGY

JELENA VUKALOVIĆ^{1,2} , JELENA B. MALJKOVIĆ¹ ,
FRANCISCO BLANCO³, GUSTAVO GARCIA⁴ and
BRATISLAV P. MARINKOVIĆ¹ 

¹ *Institute of Physics Belgrade, University of Belgrade, Pregrevica 118,
11080 Belgrade, Serbia*

E-mail jelena.vukovic@pmf.unibl.org

² *Faculty of Science, University of Banja Luka, Mladena Stojanovića 2,
78000 Banja Luka, Republic of Srpska, Bosnia and Herzegovina*

³ *Departamento de Física Atómica Molecular y Nuclear, Facultad de Ciencias
Físicas, Universidad Complutense, Avda. Complutense s/n, E-28040 Madrid, Spain*

⁴ *Instituto de Matemáticas y Física Fundamental, Consejo Superior de
Investigaciones Científicas, Serrano 121, 28006 Madrid, Spain*

Abstract. Our investigation focuses on the elastic electron scattering phenomenon involving the anaesthetic molecule, desflurane, specifically at a medium energy of 250 eV. Utilizing an experimental setup employing a crossed beam technique, comprising an electron gun, a single capillary gas needle, and a detection system equipped with a channeltron, we measured the differential cross sections. To establish the absolute scale for these cross sections, we employed the relative-flow method, using argon gas as a reference. Our calculations are rooted in the Independent Atom Model (IAM), incorporating the screening corrected additivity rule (SCAR) technique, and account for interference effects.

This research was supported by the Science Fund of the Republic of Serbia, Grant No. 6821, Project title – ATMOLCOL.

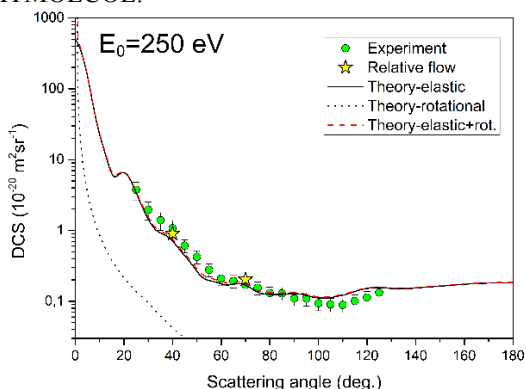


Figure 1: Differential cross section for elastic electron scattering from desflurane at 250 eV.

References

Vukalović, J., Marinković, B. P., Rosado, J., Blanco, F., García, G., Maljković, J. B.: 2024, *Phys. Chem. Chem. Phys.*, **26**, 985-991.

TRANSPORT PROPERTIES OF TWO-TEMPERATURE SF₆ AND ITS ALTERNATIVE GASES

GUANYU WANG, BOYA ZHANG and XINGWEN LI

*State Key Laboratory of Electrical Insulation and Power Equipment,
Xi'an Jiaotong University, Xi'an 710049, China.
E-mail wangguanyu@stu.xjtu.edu.cn*

Abstract. Non-local thermodynamic equilibrium (NLTE) phenomena in plasmas typically have a significant impact on dissociation and ionization reactions, thereby altering the macroscopic transport properties of gases. This study calculates the transport coefficients of SF₆ and environmentally friendly alternative gases such as C₄F₇N, CO₂, and dry air under two-temperature conditions, exploring the influence of NLTE conditions on ionized gases. The results indicate that non-equilibrium phenomena alter the dominant sequence of ionization reactions within the plasma, consequently affecting its transport characteristics. Due to the complexity of the C₄F₇N molecule, it is more significantly affected by NLTE conditions, whereas CO₂ and dry air are relatively less affected. The two-temperature state influences the transport properties of gases from both the chemical reaction and interaction intensity perspectives; some examples are presented.

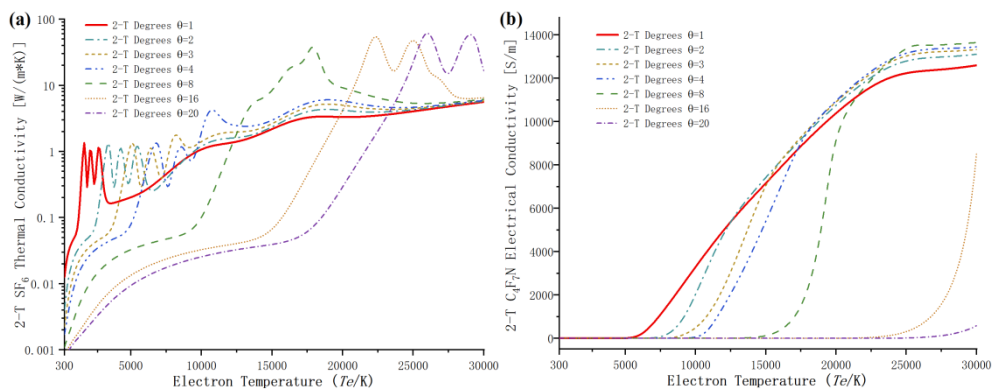


Figure 1: Two-Temperature Transport Properties at 0.1MPa.
(a) Thermal Conductivity, SF₆. (b) Electrical Conductivity, C₄F₇N.

Section 2.

PARTICLE AND LASER BEAM INTERACTION WITH SOLIDS

PLASMA MODIFICATION OF NATURAL FIBRES TO IMPROVE ADHESION IN BIO-COMPOSITES

MARIJA GORJANC

*University of Ljubljana, Faculty of Natural Sciences and Engineering,
Aškerčeva 12, 1000 Ljubljana, Slovenia
E-mail marija.gorjanc@ntf.uni-lj.si*

Abstract. Due to environmental and sustainability concerns, natural fibers have become an important class of reinforcing materials in composites. The biggest problem in the development of composites is the poor adhesion of the fibers in the matrix. Plasma technology has been proven many times to be a suitable method for improving the interfacial properties of composites. However, most of these studies have been carried out on synthetic polymers. The most used pretreatments of natural fibers for reinforcing materials are alkali or acetylation treatments. To reduce or even eliminate the use of synthetic polymers in the development of textile bio-composites and eliminate the wet chemical pretreatments of reinforcing materials, it is crucial to conduct extensive research on plasma treatment of natural reinforcing materials to improve adhesion within the bio-composite. Plasma-induced chemical, physical and chemical changes on flax, coir and cotton fibers for their incorporation into bio-composites will be discussed. In addition, the importance of plasma pretreatment in all-cellulose composites will be discussed in detail.

References

- Kert, M., Forte-Tavčer, P., Hladnik, A. Spasić, K. Puač, N., Petrović, Z.Lj., Gorjanc, M. : 2021, *Coatings*, **11**, 16p.
Ogrizek, L., Lamovšek, J., Čuš, F., Leskovšek, M., Gorjanc, M. : 2021, *Processes*, **9**, 15p.
Preveen, K.M, Prime, G., Simončič, B., Gorjanc, M., Vesel, A., Mozetič, M. et al. : 2022, *Surf Innov*, **10**, 128.

INTEGRATING PULSE LASER DEPOSITION AND ADVANCED SPECTROSCOPY: UNVEILING HIDDEN PHENOMENA IN TRANSITION METAL OXIDES

MILAN RADOVIĆ 

*Paul Scherrer Institut
E-mail milan.radovic@psi.ch*

Abstract. Transition Metal Oxides (TMOs) exhibit unique, multifunctional phenomena due to the interplay between spin and orbital degrees of freedom and the lattice. Controlling the electronic structure of TMO thin layers is essential for designing heterostructures where new phases and phenomena emerge. Combining Pulse Laser Deposition (PLD) with advanced spectroscopy techniques like Angle-Resolved Photoemission Spectroscopy (ARPES) and Resonant Inelastic X-ray Scattering (RIXS) has been pivotal for understanding and manipulating TMOs. This synergy enhances fundamental insights and optimizes material properties for specific functionalities.

Two examples will illustrate the power of this experimental platform. Firstly, controlling the Metal-Insulator Transition (MIT) via dimensionality crossover will be presented. A RIXS study on CaVO₃ demonstrated that MIT is influenced by electronic bandwidth and the local site environment, showcasing precise manipulation of TMO electronic properties.

Secondly, the induced ferromagnetic order in thin NdNiO₃ (NNO) films, in proximity to a magnetic layer, will be discussed. This study shows how magnetic interactions can be harnessed to influence TMO electronic behavior.

Both examples highlight functional approaches to manipulating TMO electronic and magnetic properties.

References

- McNally E. D., Lu X., Pellicciari J., Beck S., Dantz M., Naamneh M., Shang T., Medarde M., Schneider W. Ch., Strocov N. V., Pomjakushina V. E., Ederer C., Radovic M., Schmitt T., 2019, *npj Quantum Materials* **4:6**.
- Caputo M., Ristic, Z., Dhaka S. R., Das T., Wang Z., Matt E. C., Plumb C. N., Guedes B. E., Jandke J., Naamneh M., Zakharova A., Medarde M., Shi M., Patthey L., Mesot J., Piamonteze C., Radovic M., 2021 *Advanced Science* **8**, 2101516.

CHARACTERIZING IONIZATION AND ELECTRON DYNAMICS IN BIOLOGICAL MATERIALS: THEORETICAL AND NUMERICAL INSIGHTS INTO PULSED LASER-INDUCED BREAKDOWN PROCESSES

HRISTINA DELIBAŠIĆ-MARKOVIĆ 

*Faculty of Science, Department of Physics, University of Kragujevac, Serbia
E-mail hristinadelibasic@gmail.com*

Abstract. This research presents an analysis of free electron generation in biological materials subjected to intense laser radiation. The study significantly deepens the existing models by integrating a range of ionization mechanisms - photoionization, cascade ionization, thermal ionization, and chromophore ionization - alongside a detailed consideration of electron diffusion, attachment, and recombination kinetics. The model also introduces quantum mechanical considerations to address the energy state transitions and sub-atomic interactions within the material, which are crucial for accurately predicting ionization outcomes. Additionally, non-linear optical phenomena such as multiphoton absorption and the Kerr effect are incorporated to assess their influence on the overall ionization process and the spatial-temporal distribution of free electrons. The accuracy and applicability of the model are further enhanced by systematically varying external laser parameters - wavelength, pulse duration, and pulse energy - and examining their effects in conjunction with the intrinsic optical properties and surface characteristics of the biological materials. This approach allows for a precise manipulation of the laser-material interaction to achieve desired modification outcomes. The model's predictions are validated against a range of experimental data, including recent developments in time-resolved spectroscopy that provide a high-resolution view of electron dynamics. This validation not only confirms the model's robustness but also identifies areas for parameter optimization to improve the efficiency and precision of laser applications in biological media. This research thus extends the fundamental understanding of laser-material interactions, providing a solid foundation for further developments in medical and biotechnological applications.

Acknowledgements: Author would like to acknowledge the support received from the Science Fund of the Republic of Serbia, #GRANT 6821, Atoms and (bio)molecules-dynamics and collisional processes on short time scale—ATMOLCOL. Appreciation also goes to the Serbian Ministry of Education, Science and Technological Development (Agreement No. 451-03-66/2024-03/ 200122).

INTERACTION OF IONS WITH GRAPHENE-INSULATOR-GRAPHENE COMPOSITE SYSTEMS

ANA KALINIĆ¹ , IVAN RADOVIĆ¹ , V. DESPOJA²,
LAZAR KARBUNAR³  and Z. L. MIŠKOVIĆ⁴

¹*Department of Atomic Physics, "VINČA" Institute of Nuclear Sciences - National Institute of the Republic of Serbia, University of Belgrade, P.O. Box 522, Belgrade 11001, Serbia*

E-mail ana.kalinic@vin.bg.ac.rs

E-mail iradovic@vin.bg.ac.rs

²*Centre for Advanced Laser Techniques, Institute of Physics, Bijenička 46, Zagreb 10000, Croatia*

E-mail vdespoja@ifs.hr

³*School of Computing, Union University, Knez Mihailova 6, Belgrade 11000, Serbia*

E-mail lkarbunar@raf.rs

⁴*Department of Applied Mathematics, and Waterloo Institute for Nanotechnology, University of Waterloo, Waterloo, Ontario N2L 3G1, Canada*

E-mail zmiskovi@uwaterloo.ca

Abstract. The hybridization between Dirac plasmons from graphene and surface optical phonons from the Al₂O₃ layer is investigated. The analysis focuses on the interaction of ions moving parallel and above graphene-insulator-graphene systems with the mentioned composites. Specifically, it examines the impact of this hybridization on the induced wake potential in the top surface of the system (Despoja et al. 2019 and Kalinić et al. 2021), as well as on the stopping and image forces acting on the incident particle (Kalinić et al. 2022). The effective dielectric function required to calculate these quantities is derived using two methods: one based on massless Dirac fermions and the other on the extended hydrodynamic model. A comparison with the *ab initio* method is given. The study demonstrates how various factors such as the doping density of graphene, the thickness and dielectric properties of the Al₂O₃ layer, the damping factor of Dirac plasmons, particle speed, and distance from the system influence the induced wake potential, stopping force, and image force.

References

- Despoja, V., Radović, I., Karbunar, L., Kalinić, A., Mišković, Z. L.: 2019, *Phys. Rev. B*, **100**, 035443.
- Kalinić, A., Radović, I., Karbunar, L., Despoja, V., Mišković, Z. L.: 2021, *Phys. E Low-dimens. Syst. Nanostruct.*, **126**, 114447.
- Kalinić, A., Despoja, V., Radović, I., Karbunar, L., Mišković, Z. L.: 2022, *Phys. Rev. B*, **106**, 115430.

MODELING THE SURFACE INTERACTION OF CELLULOSIC MATERIALS WITH CO₂ PLASMAS

VIOLETA V. STANKOVIĆ MALIŠ  and GORAN B. POPARIĆ 

*University of Belgrade, Faculty of Physics, Studentski Trg 12, P.O.Box 44,
11000 Belgrade, Serbia*

E-mail violeta.stankovic@ff.bg.ac.rs

Abstract. Within this research, the modeling of the interaction of plasma ions with the surfaces of cellulose samples, i.e. with the molecules of repeating cellulose structures, is presented. Low pressure RF plasma in a working CO₂ gas atmosphere was modeled using the “Particle in cell” method. The mentioned method represents a modified computer code of the group from Berkeley, University of California see Verboncoeur et al.1993 in terms of the database of CO₂ effective cross sections which is presented in detail in the earlier work of our group see Stankovic et al.2020. The calculations were performed within the cylindrical spatial geometry of the CCP reactor (plasma sheath), which is characterized by a significant drop in the cathode potential that favors the acceleration of plasma ions towards the electrode. The main data obtained by the simulation were the volume of the cylindrical area (cathode potential gradient of the plasma sheath) as well as the concentration of electrons in a unit volume of the plasma sheath. In the next stage the total and partial ionization rate coefficients were obtained by the Monte Carlo method and averaged over the half-period of the reduced RF electric field oscillation see Stankovic et al.2020. This enabled us to calculate the number of ions that act on the cellulose sample surface per unit of time by using the probability for the ionization collision process. In final stage the physical breaking of certain chemical bonds in repeating cellulosic structures of the sample (paper) is modeled by semiquantum simulation of the interaction where the major role has impact electric field influence of the accelerated ions ensemble on cellulose chains. The breaking of chemical bonds is modeled as a consequence of extreme deformation of their electron clouds induced by interaction with fast accelerated ions. In order to verify the modeling of the plasma-sample interaction, paper samples were also experimentally treated in a RF CCP reactor in the power range from 20 to 100 W and then subject the treated surfaces to the FTIR test method. Comparative analysis showed good agreement between experimental and simulation data of modeled plasma-surface interaction.

References

- Verboncoeur, J.P. et al.: (1993), *J. Comp. Physics*, 104, pp. 321-328.
Stanković V.V., Ristić M. M., Vojnović M. M., Aoneas M. M., Poparić G. B.: (2020) *Plasma Chem. and Plasma Process.* **40** (6), 1621-1637.

LOW ENERGY HEAVY ION RAINBOW SCATTERING BY GRAPHENE

MILIVOJE HADŽIJOJIĆ¹  and MARKO ĆOSIĆ² 

*Laboratory of Physics, "Vinča" Institute of Nuclear Sciences
National Institute of the Republic of Serbia, University of Belgrade,
P.O. Box 522, 11001 Belgrade, Serbia*

E-mail ¹milivoje@vin.bg.ac.rs

E-mail ²mcosic@vinca.rs

Abstract. We studied low-energy heavy-ion scattering on graphene. Ion trajectories were obtained by numerically solving Newton's equations of motion. To incorporate electron capture processes, we have used time dependent interaction potential. Graphene thermal motion was included by averaging time-dependent interaction potential over the distribution of atomic displacements. We demonstrate that electron capture process does not disrupt rainbow effect.

1. INTRODUCTION

It is known that the rainbow effect accompanies the scattering of light, atom, and ion collisions. Rainbow scattering occurs in ion transmission through thin crystals and nanotubes in the channeling mode [Nešković et al. 2017] and transmission of protons through graphene [Ćosić et al. 2018]. It was shown that the shape of the rainbow pattern contains sufficient information for the determination of the accurate proton-Si interaction potential [Petrović et al. 2015] and proton-cubic crystal interaction potential in general [Petrović et al. 2019, Starčević et al. 2021 and 2023], investigation of the graphene thermal vibrations [Ćosić et al. 2019], and point defects [Hadžijojić et al. 2021]. For these reasons, we investigate how the electron (e^-) capture process affects rainbow scattering in the case of highly charged ion scattering through graphene.

2. THEORY

To study ion transmission through graphene, we have modified the interatomic potential introduced in [Wilhelm et al. 2019], which in atomic units reads

$$\begin{aligned}
 V(\mathbf{R}, t) = & \frac{(Z_1 - Q_{in} + N_{stab}(t)) Z_2}{R} \phi \left(\frac{R}{a_2(N_{core} + N_{stab}(t), Z_2)} \right) \\
 & + \frac{N_{cap}(t) Z_2}{R} \phi_{hollow}(R, r_0) \\
 & + \frac{(Q_{in} - N_{stab}(t) - N_{cap}(t)) Z_2}{R} \phi \left(\frac{R}{a_1(Z_2)} \right).
 \end{aligned} \tag{1}$$

R is ion-atom distance, ϕ and ϕ_{hollow} are screening functions:

$$\begin{aligned}
 \phi \left(\frac{R}{a} \right) &= \sum_{k=1}^3 \alpha_k \exp \left[-\frac{\beta_k R}{a} \right], \\
 \phi_{hollow}(R, r_0) &= \sum_{k=1}^3 \alpha_k \left(e^{-\frac{\beta_k R}{a_1(Z_2)}} - \frac{\sinh(\beta_k r_{<}/a_1(Z_2))}{\beta_k r_{<}/a_1(Z_2)} e^{-\frac{\beta_k r_{>}}{a_1(Z_2)}} \frac{R}{r_{>}} \right).
 \end{aligned} \tag{2}$$

Here $r_0 = 3.42 + 3.02\sqrt{Q_{in}}$, $\alpha_k = (0.190945, 0.473674, 0.335381)$ and $\beta_k = (0.278544, 0.637174, 1.919249)$, $r_{<} = \min(R, r_0)$, and $r_{>} = \max(R, r_0)$, $a_1(Z_2) = 0.8854/(Z_2/\xi)^{(1/3)}$, and $a_2(Z_1, Z_2) = \frac{0.8854}{Z_1^{0.23} + (Z_2/\xi)^{0.23}}$, parameter ξ was modeled according to the Ref. [Wilhelm et al. 2019], N_{cap} is the number of e^- captured into Rydberg states, N_{stab} is the number of e^- stabilized via Auger decay or via extremely fast interatomic coulombic decay (ICD). These are obtained by solving equations [Wilhelm et al. 2019]:

$$\begin{aligned}
 \frac{dN_{cap}}{dt} &= \lambda(t) (Q_{in} - N_{cap}(t) - N_{stab}(t)) - \gamma(t)N_{cap}(t), \quad N_{cap}(-\infty) = 0 \\
 \frac{dN_{stab}}{dt} &= \gamma(t)N_{cap}(t), \quad N_{stab}(-\infty) = 0.
 \end{aligned} \tag{3}$$

Initially e^- are captured at a rate λ . Close to the membrane they are stabilized by ICD which take place at rate γ , given by the following expression:

$$\gamma(R) = \frac{\gamma_{max}}{1 + (R/\gamma_o)^8}. \tag{4}$$

Parameters γ_{max} and γ_o were obtained by fitting the experimental data taken from Ref. [Wilhelm et al. 2019]. Thermal effects were incorporated by averaging interaction potential (1) over the atomic displacements [Ćosić et al. 2018]. The scattering law is a mapping of the impact parameter plane $\mathbf{b} = (b_x, b_y)$ to the scattering angle plane $\boldsymbol{\theta} = (\theta_x, \theta_y)$. The differential cross-section σ_{diff} of the scattering process is in the small angle approximation given by the relation

$$\sigma_{\text{diff}}(\boldsymbol{\theta}) = \sum_i \frac{1}{|J_{\boldsymbol{\theta}}^{(i)}(\mathbf{b}(\boldsymbol{\theta}))|}, \quad (5)$$

where $J_{\boldsymbol{\theta}}^{(i)}(\mathbf{b}(\boldsymbol{\theta}))$ is the Jacobian of the i -th branch of the map $\boldsymbol{\theta} \rightarrow \mathbf{b}$. The differential cross-section is infinite along lines

$$J_{\boldsymbol{\theta}}(\mathbf{b}(\boldsymbol{\theta})) = 0, \quad (6)$$

called *rainbows*. Note that rainbows dominantly determine the shape of the angular distribution.

3. RESULTS

Descartes's coordinate system was attached to the graphene plane, with the z-axis aligned along the direction of the incident beam. The initial energy of Xe^{32+} was set to 40 keV. Classical equations of motion for thermally averaged potential (1) were solved together with rate equations (3) numerically using Runge-Kutta 8-3 algorithm. In the next step, trajectories were used to determine Jacobian using the Richardson extrapolation method. Rainbow lines were found as the numerical solution of equation (6) using the marching-square algorithm. Figure 1(a) shows the dominant rainbow in the scattering angle plane. The charge state of ions forming this line is indicated by different colors ranging from deep blue to yellow. Obtained rainbow has the shape of a cusped hexagonal line already observed in theoretical calculations of proton transmission through graphene [Ćosić et al. 2018], and experimentally [Watanabe et al. 2024]. Interestingly, e^- capture does not disrupt the rainbow effect. The obtained distribution has a hexagonal shape in the region of small scattering angles and is circular toward the edge. Besides maxima at the zero scattering angle, dominant maxima correspond to the curve in Fig. 1(a). Figure 1(b) shows an exit charge distribution corresponding to the scattering of 100 Xe^{32+} ions with impact parameters lying along a horizontal cross section of the impact parameter plane connecting two neighboring carbon atoms. Notice that most of the ions have exit charge 2. This value is significantly different from the mean charge of the rainbow in Fig. 1(a). This suggests that e^- capture processes affect ions forming rainbow less than the others. Using the crystal rainbow theory, one may determine which impact parameters correspond to the observed scattering angles. Hence, one may determine how e^- capture depends on the ion impact parameter. Tilting graphene displaces rainbow line, which could enable scanning of the entire graphene impact parameter plane in this way [Ćosić et al. 2021].

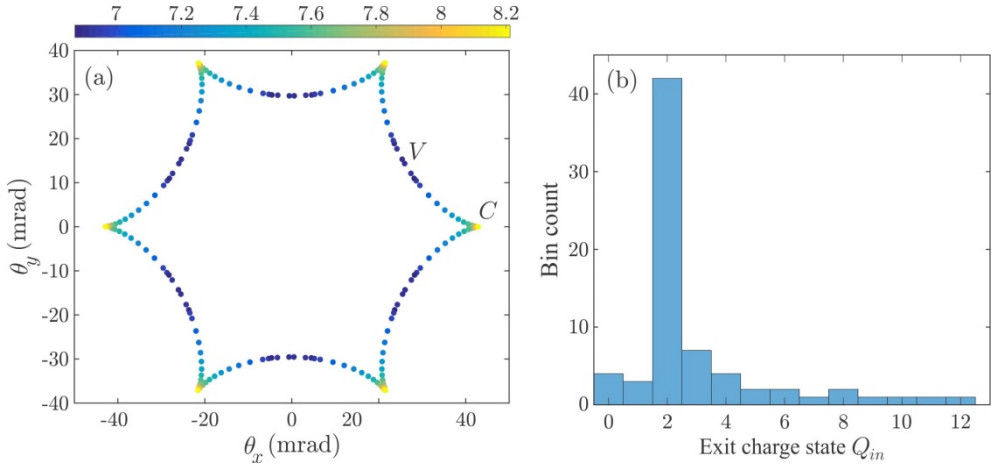


Figure 1: (a) Rainbow line in the scattering angle plane generated by the 40 keV Xe^{32+} ions scattered by graphene. The corresponding exit charge state colors are rainbow. (b) Exit charge state distribution of 40 keV Xe^{32+} ions with impact parameters along a line in the impact parameter plane connecting the center of a graphene hexagon and a midpoint between two adjacent C atoms.

Being structurally stable, rainbow shape is noise immune, and could be used to determine more accurately or reduce the number of model parameters. Note that maximal difference of the rainbow exit charges occurs for points marked in Fig. 1 by C and V . Subsequent trajectory analysis showed that distance of the corresponding impact parameters from the graphene hexagon center are 79.9 pm, and 83.4 pm respectively. Therefore analysis of the rainbow shape provides insight in the neutralization process at picometer scale.

References

- Ćosić, M., Petrović, S., Nešković, N. : 2018, *Nucl. Instrum. Meth. Phys. Res. B*, **422**, 54.
- Ćosić, M., Hadžijojić, M., Petrović, S., Rymzhanov, R., Bellucci, S. : 2019, *Carbon* **145**, 161.
- Ćosić, M., Hadžijojić, M., Petrović, S., Rymzhanov, R. : 2021, *Chaos* **31**, 093115.
- Hadžijojić, M., Ćosić, M., Rymzhanov, R. : 2021, *J. Phys. Chem. C* **125**, 38.
- Nešković, N., Petrović, S., Ćosić, M. : 2017, *Rainbows in Channeling of Charged Particles in Crystals and Nanotubes*. Springer.
- Petrović, S., Nešković, N., Ćosić, M., Motapothula, M., Breese, M.B.H. : 2015, *Nucl. Instrum. Meth. Phys. Res. B* **360**, 23.
- Petrović, S., Starčević, N., Ćosić, M. : 2019, *Nucl. Instrum. Meth. Phys. Res. B*, **447**, 79.
- Starčević, N., Petrović, S. : 2021, *Nucl. Instrum. Meth. Phys. Res. B*, **499**, 39.
- Starčević, N., Petrović, S. : 2023, *Eur. Phys. J. D*, **77**, 61.
- Watanabe, N., Otsuka, M., Kumagai, Y., Ishii, K. : 2024, *Nucl. Instrum. Meth. Phys. Res. B*, **553**, 165380.
- Wilhelm, R. A. et al. : 2019, *Communications Physics* **89**, 2.

INTERACTION OF IONS WITH DRIFT-CURRENT BIASED SUPPORTED GRAPHENE

ANA KALINIĆ¹ , IVAN RADOVIĆ¹ , LAZAR KARBUNAR²  and
Z. L. MIŠKOVIĆ³

¹*Department of Atomic Physics, "VINČA" Institute of Nuclear Sciences - National Institute of the Republic of Serbia, University of Belgrade, P.O. Box 522, Belgrade 11001, Serbia*

E-mail ana.kalinic@vin.bg.ac.rs

E-mail iradovic@vin.bg.ac.rs

²*School of Computing, Union University, Knez Mihailova 6, Belgrade 11000, Serbia*

E-mail lkarbunar@raf.rs

³*Department of Applied Mathematics, and Waterloo Institute for Nanotechnology, University of Waterloo, Waterloo, Ontario N2L 3G1, Canada*

E-mail zmiskovi@uwaterloo.ca

Abstract. In our previous publications we studied the electron energy loss function (EELS, Despoja et al. 2017) and calculated the stopping force acting on a charged particle moving parallel to a graphene-insulator-graphene composite system (Kalinić et al. 2022). In this work we investigate the EELS and evaluate the stopping force on a charged particle moving parallel to a graphene layer biased with a drift electric current supported by an insulating substrate. The dielectric function of the system is expressed in terms of the bulk dielectric function of the substrate and the response function of graphene. Focusing on the range of frequencies from THz to mid-infrared, the response function is written in terms of a frequency-dependent conductivity of graphene (Despoja et al. 2017). The conductivity with the drift current is connected with the conductivity with no drift by using the Galilean Doppler shift model (Morgado et al. 2017 and 2019). The EELS (the imaginary part of the negative value of the inverse dielectric function) and the stopping force (the dissipative force which opposes the particle's motion) are presented in the cases without and with drifting electrons. The stopping force is also calculated when the drift and particle velocities have the same and opposite signs.

References

- Despoja, V., Djordjević, T., Karbunar, L., Radović, I., Mišković, Z. L.: 2017, *Phys. Rev. B*, **96**, 075433.
- Kalinić, A., Despoja, V., Radović, I., Karbunar, L., Mišković, Z. L.: 2022, *Phys. Rev. B*, **106**, 115430.
- Morgado, T. A., Silveirinha, M. G.: 2017, *Phys. Rev. Lett.*, **119**, 133901.
- Morgado, T. A., Silveirinha, M. G.: 2019, *Phys. Rev. Lett.*, **123**, 219402.

FORMING NANOCRYSTALLINE SnO₂ FILMS ON SILICON AND SILICON DIOXIDE BY LASER-PLASMA DEPOSITION METHOD

F. KOMAROV, O. MILCHANIN, M.V. PUZYREV and I.S. RAHAVAYA

*A.N.Sevchenko Institute of Applied Physics Problems, Belarusian State
University
7 Kurchatov St., 220045, Minsk, Belarus,
E-mail puzyrev@bsu.by*

Abstract. The method of laser-plasma deposition of a tin thin layer on silicon substrates and SiO₂/Si structures in the combination with subsequent two-stage heat treatment to form a thin nanocrystalline layer of tin dioxide was used. This procedure can be valuable one for the fabrication of transparent conductive coatings and other optoelectronic devices.

1. INTRODUCTION

Tin dioxide (SnO₂) has a number of specific and unique properties, which makes this material suitable for various applications (Wang H. and Rogach A.L., 2014). It is often used to make conductive coatings on solar cells and other optoelectronic devices because it is a wide-gap semiconductor that is optically transparent in the visible wavelength range. The surface of grains in SnO₂ films has high absorption properties and reactivity, which is due to the presence of free electrons and oxygen vacancies in the crystal lattice of SnO₂. Therefore, nanocrystalline tin dioxide films are sensitive to the presence of various organic and some biological molecules in the surrounding atmosphere. Gas-sensitive SnO₂ layers are widely used in the production of sensors for monitoring poisonous and flammable gases (Gorley P.M et al., 2005). It is known that the optical, electrophysical and sensor properties of SnO₂ strongly depend on its structural and phase characteristics. This is depended on the conditions of its formation: type of substrate, deposition method, temperature and annealing environment.

In this work, for the first time, the method of laser-plasma deposition of a tin layer on silicon and a SiO₂/Si structure was used in combination with subsequent two-stage heat treatment to form a thin nanocrystalline layer of tin dioxide. The

advantages of the laser-plasma method for applying nanocoatings include high sterility, the ability to obtain plasma from any substance, and guaranteed reproducibility of conditions during the deposition of coatings, which allows you to control their composition and structure (Pulsed laser deposition of thin films, 2007, Goncharov V.K et al., 2021).

2. INSTRUMENTS AND TECHNIQUE OF EXPERIMENT

The LOTIS-TII pulsed YAG:Nd³⁺ laser with a wavelength $\lambda = 1064$ nm and a pulse duration $\tau = 20$ ns (as a full width at half maximum - FWHM) was used for experiments. Laser pulse was focused on a target which is placed in a vacuum chamber under pressure of 2.6×10^{-3} Pa. The target was mounted at angle of 45° with respect to the laser beam propagation and was constantly rotated to provide initial surface for ablation. The laser beam intensity was 3.8×10^8 W/cm² and the diameter was about 2 mm. The sample deposition was carried out at room temperature. The target was made from technically pure tin. The laser pulse frequency was 5 Hz. The optically transparent silicon wafers in IR range (polished front and back sides) and the SiO₂(100 nm)/Si structures were used as substrates.

The control of electron and ion flows in erosive laser plasma was carried out according to the scheme (Goncharov V.K et al., 2021). The distance between the substrate and the target was 12 cm. The grid for cutting off the flow of electrons was located at a distance of 6 cm from the target surface. The transparency of the grid was 90%. The exposition of tin films deposition on various samples was lasted for 30-60 minutes. The experimental scheme is shown in Figure 1.

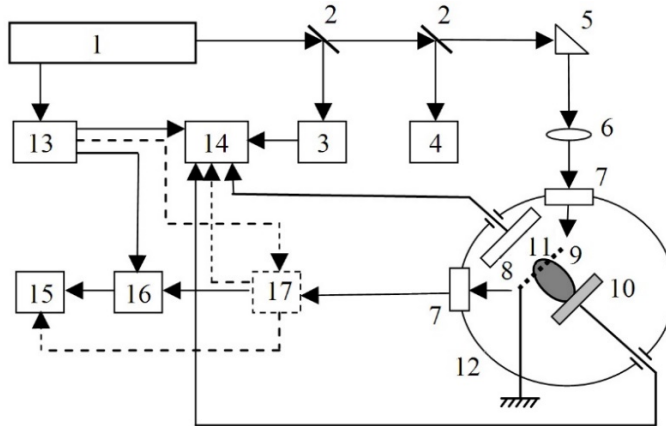


Figure 1. 1 – laser; 2 – beam splitting plates; 3 – photodiode; 4 – energy meter; 5 – total internal reflection prism; 6 – lens; 7 – windows; 8 – substrate; 9 – mesh; 10 – target; 11 – plasma torch; 12 – vacuum chamber; 13 – synchronization block; 14 – oscilloscope; 15 – computer; 16 – CCD - camera; 17 – spectrometer

The topological and structural-phase characteristics of the tin oxide layer were studied by transmission and scanning electron microscopy using a Hitachi H-800 transmission microscope with a Hitachi H-8010 raster attachment. Optical spectra (reflection, transmission) were recorded using a Lambda 1050WB spectrometer.

3. RESULTS AND DISCUSSION

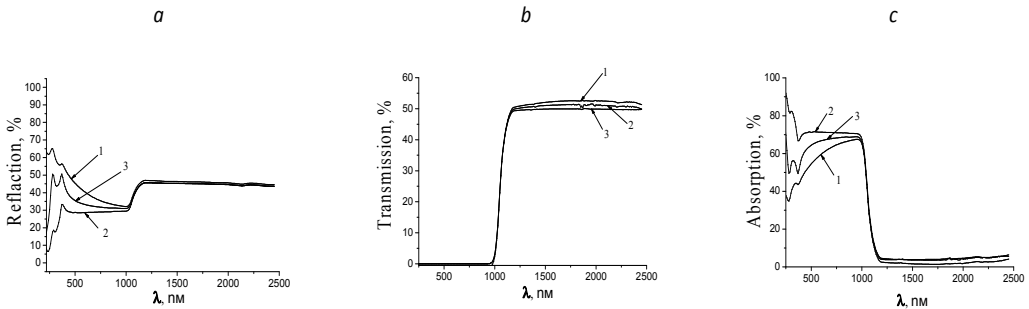


Figure 2. Optical spectra of reflection *a*, transmission *b* and absorption *c* from structures: Si, Sn/Si, SnO₂/Si

1- original Si, 2- film Sn on Si, 3- annealing 200°C 120 min +500°C 120 min

Figure 3 shows the results of optical studies of the formed structures: Si, Sn/Si, SnO₂/Si. The reflection and transmission spectra were measured, and the absorption spectra were calculated using the formula: $A = 100\% - T - R$ (where *A* is absorption, *T* is transmission, *R* is reflection). Films of amorphous tin and nanocrystalline tin dioxide are almost completely (98%) transparent in the near-IR range. In the ultraviolet and visible ranges, due to absorption, the transparency of the SnO₂ layer is about 80%.

Structural studies has shown that the tin layer after laser deposition has a high degree of thickness uniformity over a large area of the substrate. The droplet fraction was not detected on the surface of the samples. The formed films had an amorphous structure. It has been, found the formation of a nanocrystalline SnO₂ phase for two types of substrates: Si and SiO₂/Si after annealing. Figure 3 presents the results of structural studies.

The thickness of the SnO₂ layers was in the range from 20 to 40 nm, depending on the duration of deposition (Figure 3, *a*). It can be noted that when using a silicon wafer as a substrate, the structure of the SnO₂ film was more perfect: faceted crystals with an average size of 5-10 nm are observed (Figure 3, *b*). A detailed analysis of electron diffraction patterns showed that the crystal structure of the SnO₂ layer corresponds to a tetragonal system with the space group P4₂/mnm (Figure 3, *c*).

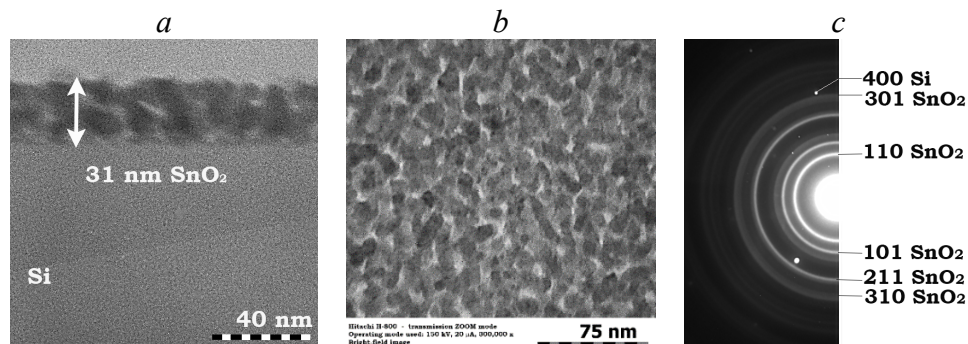


Figure 3. TEM micrographs of cross section *a* and planar *b* sections of the SnO₂/Si structure. *c* – electron diffraction pattern from the SnO₂ layer

CONCLUSION

Thus, the presented work shows the fundamental possibility of using the method of laser-plasma deposition of thin layers of tin on silicon structures, followed by two-stage annealing to form high-quality, in terms of structure (high uniformity in thickness, homogeneity of grain sizes) transparent layers of nanocrystalline tin dioxide.

References

- Wang H., Rogach A.L.: 2014, *Chemistry of Materials*, **26**, 123.
- Gorley P.M., Khomyak V.V., Bilichuk S.V., Orletsky L.G., Horley P.P. and Grechko V.O. SnO₂: 2005, *Materials Science and Engineering*, **118**, 160.
- Pulsed laser deposition of thin films* / Ed.: R. Eason. – Hoboken, New Jersey: Wiley-Interscience, 2007. – 682 p.
- Goncharov V.K., Pekhota A.A., Puzyrev M.V.: 2021, *Journal of Engineering Physics and Thermophysics*, **94**, No. 2, 503.

TARGET SELECTION FOR LIBS STUDIES OF HYDROGEN ISOTOPE RETENTION

DRAGAN RANKOVIĆ¹ , BILJANA STANKOV² , IVAN TRAPARIĆ² ,
MIROSLAV KUZMANOVIĆ¹  and MILIVOJE IVKOVIĆ^{2*} 

¹Faculty of Physical Chemistry, University of Belgrade, 11158 Belgrade, Serbia

²Institute of Physics, University of Belgrade, Pregrevica 118, 11080 Belgrade, Serbia

*E-mail ivke@ipb.ac.rs,

Abstract. The study of the hydrogen's isotope retention in the first wall of the fusion reactors is the main task in diagnostics of plasma facing components (PFC). Laser Induced Breakdown Spectroscopy (LIBS) enables in-situ PFC diagnostics without any sample preparation making it a most promising technique for this purpose, see H.J. van der Meiden et al, 2021. The basis of this diagnostics is the measurement of the emission of hydrogen isotopes Balmer alpha lines. The most challenging task is the resolving of these lines. Therefore, the first task was the selection and preparation of the targets from which, due to the laser irradiation and consequent plasma formation, hydrogen and deuterium spectral lines will be emitted. Such targets should be substitutes of the hydrogen isotopes enriched components of PFC of future fusion reactors. The main idea was to use the heavy water D₂O embedded in various substrates that are good absorbers of water. For this purpose, following substrates were tested: NaCl - salt, copper sulfate pentahydrate CuSO₄•5H₂O - known as blue vitriol or blue stone, active coal - charcoal, microporous aluminosilicates - zeolites, calcium carbonate CaCO₃ - quicklime, CaSO₄•2H₂O – gypsum. Several forms of graphite were also considered: factory made graphite discs, electrodes with controlled amount of the D₂O on it and spectroscopically pure (or mixed with silica gel) graphite powder, which was doped with water before or after pressing it by hydraulic press. Testing was performed using a 6 ns Q – switched Nd:YAG and TEA CO₂ laser (having 80 ns pulse with 2 μs long tail) in low pressure argon or helium atmosphere. The best results are obtained using gypsum and graphite doped with silica gel, see Traparic et al 2024.

Acknowledgements. The research was funded by the Ministry of Science, Technological Development and Innovations of the Republic of Serbia, Contract numbers: 451-03-68/2022-14/200024 and 451-03-65/2024-03/200146, and supported by the Science Fund of the Republic Serbia, Grant no. 7753287 "NOVA2LIBS4fusion".

References

Van der Meiden, H.J. et al. : 2021, *Nucl. Fusion*. **61** 125001
Traparic, I et al.: 2024, submitted to *Spectrochimica Acta B*

EQUILIBRIUM COMPOSITION OF PLASMA OBTAINED BY LASER ABLATION OF GLASS

MIROSLAV RISTIĆ , ALEKSANDRA ŠAJIĆ , JOVANA BABIĆ  and
MIROSLAV KUZMANOVIĆ 

*University of Belgrade, Faculty of Physical Chemistry,
Studentski Trg 12, P. O. Box 47, 11000 Belgrade, Serbia*

E-mail ristic@ffh.bg.ac.rs

E-mail aleksandra.sajic@ffh.bg.ac.rs

E-mail miroslav@ffh.bg.ac.rs

Abstract. In addition to standard glass analysis techniques, laser induced breakdown spectroscopy (LIBS) emerged in past decades as a powerful tool for glass analysis. Calculation of the composition of plasma created by laser ablation of common glass sample is performed, assuming the existence of the local thermodynamical equilibrium. Elemental composition of glass (in molar percentages) is assumed to be the following: 60.7 % oxygen, 27.6 % silicon, 9.59 % sodium, 0.78 % aluminum, 0.62 % sulfur, 0.51 % potassium and 0.32 % calcium. Plasma is considered to be under the constant pressure of 1 atm, while the considered temperature range was from 5,000 to 20,000 K. The possibility of finding elements in multiple ionization stages is taken into account. Continuum lowering is not accounted at this level of calculation, while mixing with background gas is neglected. Obtained results are expected to be very useful in the practical analysis of glasses, in terms of spectrum synthesis based on calculated compositions.

References

- Gerhard C., J. Hermann J., Mercadier L., Loewenthal L., Axente E., Luculescu C. R., Sarnet T., Sentis M., Viöl W. : 2014, *Spectrochimica Acta Part B*, **101**, 32.
- Kramida A., Ralchenko Y., Reader J., and NIST ASD Team : 2023, *NIST Atomic Spectra Database* (version 5.11), National Institute of Standards and Technology, Gaithersburg, MD.
- Семенова О. П. : 1958, *Изв. вузов. Физика*, **1**, 95.
- Yun J.-I., Klenze R., Kim J.-I. : 2002, *Applied Spectroscopy*, **56** (7), 852.

SEMIQUANTUM SIMULATION OF CELLULOSIC MATERIALS INTERACTION WITH CO₂ PLASMAS

VIOLETA V. STANKOVIĆ MALIŠ  and GORAN B. POPARIĆ 

*University of Belgrade, Faculty of Physics, Studentski Trg 12, P.O.Box 44,
11000 Belgrade, Serbia*

E-mail violeta.stankovic@ff.bg.ac.rs

Abstract. The interaction of the generated ions in the gas discharge, which was modeled by using the “Particle in the cell” method see Verboncoeur et al.1993, with the surfaces of cellulose material samples (paper) exposed to CO₂ plasma treatment, i.e. the effect of fast ions near the cathode area, was quantitatively determined using a new computer code. The simulation of mentioned semiquantum plasma-ion interaction have been developed in our group and involves the breaking of interatomic chemical bonds of certain molecules, the building blocks of cellulose chains, under the influence of the electric field created by the ensemble of electrons. Since there are currently no known probabilities for the collisional interaction of an ensemble of ions and molecules of cellulose structures, the way to overcome this kind of challenge is to simulate the deformation of the electronic states of cellulose molecules by the influence of the electric field of the simulated ion created in the near-cathode CO₂ plasma region. Taking into account the ionization rate coefficients see Stankovic et al.2020, the volume of the cylinder membrane that corresponds to a certain part of the cathode potential drop, and then the concentration of electrons that occur in the modeled plasma, the number of ions that act per unit of time and per unit of the cellulose sample’s surface is obtained. This data, in addition to the effective electric field strength, represents the input data of this semiquantum simulation. The obtained results show that with the increase in the intensity of the RF power supply, the percentage of breaking chemical bonds, i.e. the deformation of the molecule’s electronic states of the cellulose sample’s structures, also increases. Apart from the mentioned conditions, the percentage of bond breaking in polymer chains also depends on the percentage of certain molecule’s presence in cellulose structures.

References

- Verboncoeur, J.P., Alves M.V., Vahedi V., and Birdsall C.K.: (1993), *J. Comp. Physics*, **104**, pp. 321-328.
Stanković V.V., Ristić M. M., Vojnović M. M., Aoneas M. M., Poparić G. B.: (2020) *Plasma Chemistry and Plasma Processing* **40** (6), 1621-1637.

RAINBOWS IN TRANSMISSION OF PROTON THROUGH THIN SILICON CARBIDE CRYSTAL

NIKOLA STARČEVIĆ  and SRDJAN PETROVIĆ 

Laboratory of Physics, "Vinča" Institute of Nuclear Sciences National Institute of the Republic of Serbia, University of Belgrade, P.O. Box 522, 11001 Belgrade, Serbia

E-mail nikolas@vin.bg.ac.rs

E-mail petrovs@vin.bg.ac.rs

Abstract. We propose the application of ion rainbows for the characterization of innovative functional materials. Thin silicon carbide (SiC) crystals exhibit highly promising qualities as a novel functional material, featuring unique physical and chemical properties suitable for applications in nanoelectronics, energy systems, and high-frequency, high-power devices. We aim to develop a theoretical framework for a novel materials characterization technique capable of visualizing crystalline structures. It will complement existing techniques in the field, offering a distinct advantage in directly characterizing both crystalline structure and composition.

1. INTRODUCTION

Characterization of crystals is an important part of materials science and engineering, crucial for understanding their structural, mechanical, electrical, and optical properties. By employing a variety of techniques, researchers unravel the intricate atomic arrangements and defects within crystalline materials, shedding light on their behavior and performance in various applications. From traditional methods like X-ray diffraction to cutting-edge approaches such as electron microscopy and atomic force microscopy, each characterization technique offers unique insights into the crystals' composition, orientation, and morphology. In this study, we introduce ion channeling through very thin crystals as a method for characterizing the crystallographic structure of materials. Ion channeling offers a unique approach to probe the structural properties of materials with high sensitivity and resolution. The ion channeling transmission characterization, based on the rainbow theory, presents a novel methodology specifically designed for analysis of the atomic arrangement and orientation within crystalline samples.

The ion channeling is an effect that occurs when a collimated ion beam is directed at a thin crystal oriented along a major crystallographic axis relative to the direction of the ion beam (see Gemmell 1974). In this phenomenon, ions traveling along specific crystallographic directions experience reduced scattering and can penetrate deeper into the crystal lattice, resulting in enhanced transmission through the material. This effect arises due to the alignment of the crystal lattice with the incident ion beam, allowing ions to travel through the open crystals' channels. If a crystal is sufficiently thin, ions will be transmitted through it and their scattering angles are subsequently detected, providing valuable information about the crystal's atomic structure and orientation. Additionally, in channeling, a significant effect occurs known as the crystal rainbow effect (see Petrović et al. 2000). This effect arises due to the singularity of the classical differential cross-section in particle scattering. It is characterized by strong focusing at a rainbow angle and an abrupt change in intensity/yield around it. Analysis shows that mathematically, the rainbows are singularities of the 2D mapping from the impact parameter (IP) plane to the scattering angle (SA) plane. Utilizing crystal rainbows, it is physically possible to describe the angular distribution of channeled ions in a way that rainbow lines represent its "skeleton" (see Motapothula 2012), while this theory simplifies the characterization process by providing a comprehensive framework for analyzing ion channeling patterns (see Čosić et al. 2019 and 2021, Hadžijojić et al. 2021 and 2023, Petrović et al. 2019, Starčević et al. 2021). In this work, we propose that the rainbow effect can be applied to the characterization of the SiC crystal.

2. RESULTS

The calculated rainbow patterns of channeled protons through thin Si, diamond, and SiC-3C crystals are presented. The method for their calculation is presented in Ref. (see Petrović et al. 2000). The thickness of all crystals was 24 nm, and the proton energy was 2 MeV. Si and C are cubic diamond-type monocrystals with a square crystal channel in the (001) orientation. The SiC polytype of interest in this work is SiC-3C, which forms a square channel in the (001) orientation. SiC-3C is a compound semiconductor characterized by rigid stoichiometry, where only a 50% Si and 50% C composition is allowed, meaning each Si atom has exactly four neighboring C atoms and vice versa. As already mentioned, the most prominent and intriguing aspect of the rainbow lines pattern is its representation as a "skeleton" of the ions' angular distribution. This indicates that all values of channeled ions' exit angles are constrained within rainbow lines, thereby defining the envelope of observable angular distributions.

Figs. 1(a) and (b) represent the rainbow lines in the IP and SA planes for the Si crystal, respectively, Figs. 1(c) and (d) depict the rainbow lines in the IP and SA for the diamond crystal, respectively, while Figs. 1(e) and (f) present the rainbow lines in the IP and SA planes for the SiC-3C crystal, respectively.

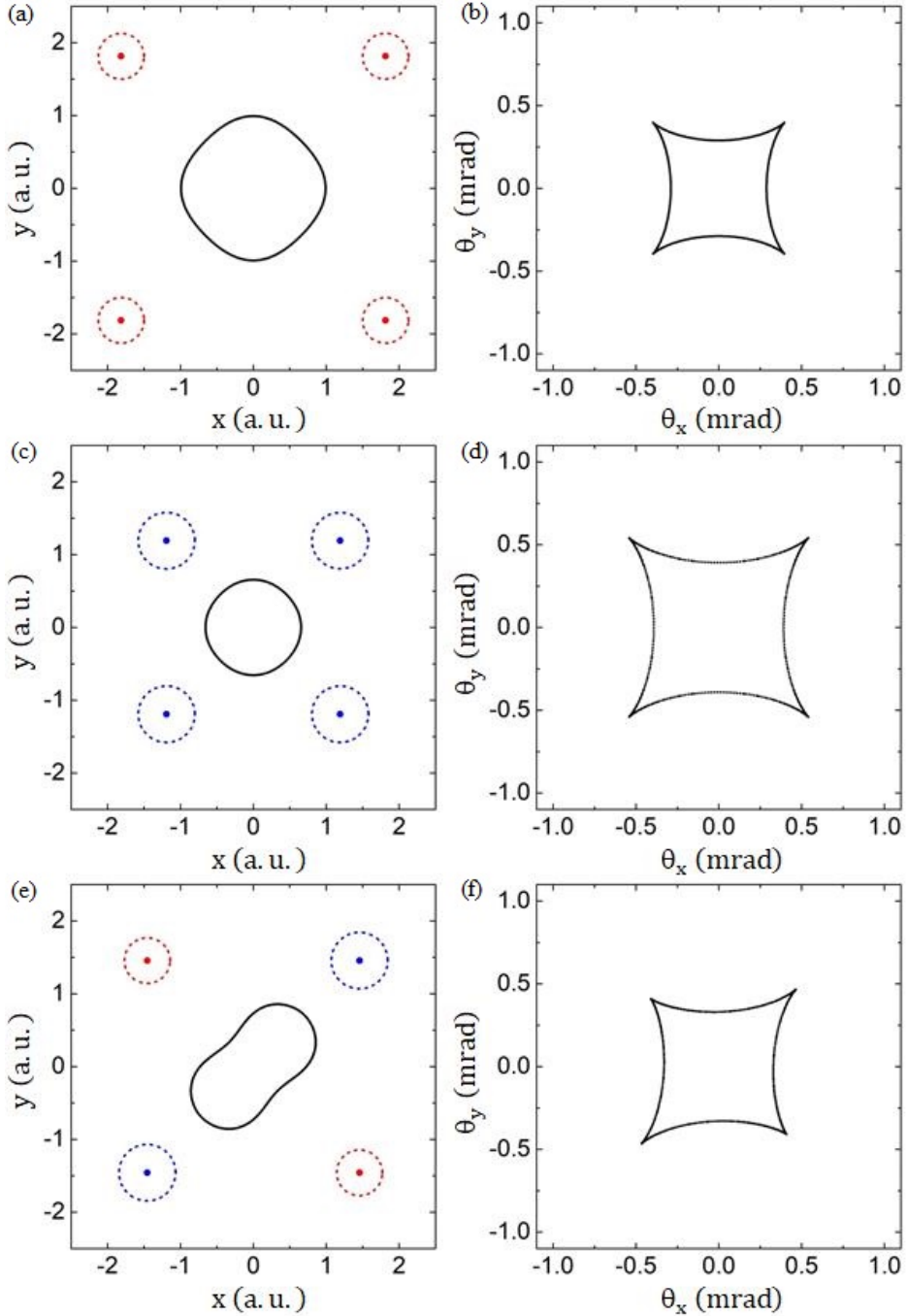


Figure 1: Rainbow lines in IP (left) and SA (right) plane for 2 MeV protons channeled through very thin Si (top), C (middle), and SiC (bottom) crystals. For all crystals, the rainbow lines are designated by black color. For the Si crystal, in the IP plane, the positions of atomic strings forming the square channel

are shown as red dots, with red dotted circles indicating the Si atomic screening radius. In the SA plane, the rainbow line is in the shape of a square with cusped corners directed towards the atomic strings. For the diamond crystal, the blue dots indicate the positions of atomic strings defining the channel, while the blue dotted circles represent the C atomic screening radius. It is interesting to note that, as a consequence of a much smaller square channel of a diamond crystal in comparison with the Si one, the rainbow line for a diamond crystal is larger than for a Si crystal. This implies that the proton-diamond interaction in a square channel is effectively larger, although the proton-silicon atom interaction is larger than the proton-carbon atom interaction. Thus, we can conclude that the size of the rainbow line and the magnitude of its cusps vary for different crystals of the same thickness, allowing for the analysis and identification of crystal types using the crystal rainbow theory. As for the SiC-3C crystal, a deformed rainbow line occurs in the IP plane compared to the corresponding rainbow line for silicon and diamond crystals. Clearly, this is a result of the fact that the silicon repulses the rainbow line more than the C atom. Consequently, the rainbow line in the SA plane takes the shape of a 45-degree tilted cusped rhomb, with the longer cusps directed toward the positions of the C atomic strings. From these results, we can conclude that the shape and magnitude of the rainbow lines, which depend on the type and spatial positions of atomic strings, enable precise determination of the structural properties of the SiC crystal using the crystal rainbow theory.




3. CONCLUSIONS

Utilizing the principles of crystal rainbow theory that rainbow lines determine angular distributions of channeled ions, we showed that the shape of these lines depends on the type and spatial positions of atomic strings defining crystal channel and also that it is highly sensitive to the structure of compounds like in the case of the SiC-3C crystal. We demonstrate that by using the crystal rainbow theory, it is possible to determine atomic compositions and crystal structures, which makes this technique highly valuable in the field of crystal characterization.

References

- Čosić, M., Hadžijojić, M., Rymzhanov, R., Petrović, S., Beluci, S. : 2019, *Carbon*, **145**, 161.
 Čosić, M., Hadžijojić, M., Petrović, S., Rymzhanov, R.: 2021, *Chaos*, **31**, 093115.
 Gemmell, D. S. : 1974, *Rev. Mod. Phys.*, **46**, 129.
 Hadžijojić, M., Čosić, M., Rymzhanov, R. : 2021, *J. Phys. Chem. C*, **125**, 21030.
 Hadžijojić, M., Čosić, M. : 2023, *Eur. Phys. J. D*, **77**, 86.
 Motapothula, M., *et al* : 2012, *Phys. Rev. B*, **86**, 205426.
 Petrović, S., Miletić, L., Nešković, N. : 2000, *Phys. Rev. B*, **61**, 184.
 Petrović, S., Starčević, N., Čosić, M. : 2019, *Nucl. Instrum. Meth. Phys. Res. B*, **447**, 79.
 Starčević, N., Petrović, S. : 2021, *Nucl. Instrum. Meth. Phys. Res. B*, **499**, 39.

PROPERTIES OF Cu/Zn OXIDE NANOSTRUCTURES FORMED BY PLASMA-ACTIVATED ELECTROLYSIS

N. TARASENKO¹, V. KORNEV¹, M. NEDELKO¹, A. RADOMTSEV¹,
N. TARASENKA^{1,3}, JOVAN CIGANOVIC² , SANJA ZIVKOVIC²  and
MILOŠ MOMCILOVIC² 

¹*B.I. Stepanov Institute of Physics, National Academy of Sciences of Belarus,
Minsk, Belarus*

²*Vinca Institute of Nuclear Sciences, University of Belgrade, Serbia*

³*Nanotechnology and Integrated Bio-Engineering Centre, Ulster University,
Belfast, UK*

E-mail n.tarasenko@ifanbel.bas-net.by

Abstract. In this work, the low-temperature plasma-activated electrolysis method has been developed and implemented for the synthesis of metal oxide (CuO, ZnO) nanoparticles (NPs) and oxide-based composite thin films.

1. INTRODUCTION

The development of novel composite nanomaterials has recently significantly contributed to the advances reached in the fields of electrochemical sensors and biosensors. The efficiency of the sensors produced is determined by several major parameters, including composition, structure and morphology of the constituent nanoparticles (NPs) and their surface. All these parameters are largely determined by the synthesis conditions of nanocomposites. Among the different techniques for NPs synthesis, plasma assisted processes in liquids have received much attention last years due to the combination of such advantages, as high production rate, versatility with the possibility of control over the NPs formation process. In this work, the low-temperature plasma-activated electrolysis method has been developed and implemented for the synthesis of metal oxide (CuO, ZnO) nanoparticles (NPs) and oxide-based composite thin films. A simultaneous anodic dissolution of the metal foils served as solid precursors was discovered followed by further assembly of the formed metal components into nanoparticles under reactions with plasma-produced species. As a result, the developed method does not require addition of any

toxic precursors and therefore benefits from the absence of further purification steps. Moreover, no additional annealing is required as compared to the existing methods. The further modification of the method has been demonstrated for simultaneous assembly of the synthesized oxides nanoparticles from colloidal solution on a substrate that emphasizes the versatility of the developed approach.

2. EXPERIMENTAL

The scheme of the experimental setup developed for the formation of composite nanoparticles both in colloid and as thin films are presented in Figure 1a. In the proposed approach, NPs formation occurs in result of dissolution of solid combined anode, composed of Cu and Zn foils, after high voltage application (1.5-3 kV) between the combined anode and a hollow capillary cathode with Ar flowing through it. For their dissolution, the anodes are submerged into the distilled water used as a solvent. The argon flow rate was about 20 mL/min. The cathode was made of stainless steel, its outer diameter is 800 μm , and the inner diameter is 500 μm and is located at a distance of 3-8 mm from the liquid surface. The advantage of this approach is that it operates under normal atmospheric conditions and does not require a sealed chamber. As the power source voltage increased, a breakdown of the discharge gap between the liquid surface and the end of the opposite electrode occurred, and a glow discharge of atmospheric pressure was ignited. The magnitude and stability of the discharge current characteristics depended on the source voltage and the argon pumping rate. To assembly the growing nanomaterial into thin-film structures, an additional substrate was placed in the cuvette, which was a copper plate or carbon cloth. This substrate was connected to the power source through an additional ballast resistance (6.8 M Ω). The composition, morphology, and optical properties of the resulting nanoparticles and films have been studied in dependence on the experimental conditions. The morphology and structure of the formed NPs were evaluated using scanning electron microscopy (SEM) technique with a SEM microscope SUPRA 55WDS (Carl Zeiss, Germany). Additional information on the phase composition, crystal and defect structure of the prepared NPs was obtained from the results of X-ray diffraction (XRD) and Raman spectroscopy. For Raman spectroscopy, the colloidal solution was deposited onto an aluminum foil and dried at 80 $^{\circ}\text{C}$ to remove excess of water. Raman spectra were registered in the range of 100–1000 cm^{-1} using a scanning probe confocal microscope\spectrometer NanoFlex (Solar LS, Belarus) with a laser excitation source at 470 nm.

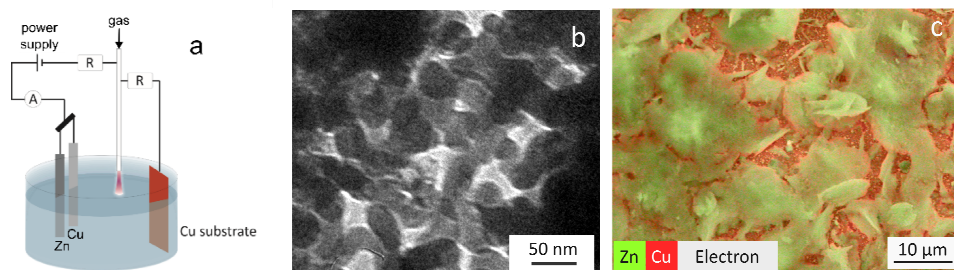


Figure 1. Plasma activated electrolysis synthesis and properties of Cu/Zn oxides nanostructures: a – scheme of the experimental setup, b –TEM and c - SEM image of the NPs deposited on the copper substrate with EDX mapping of Cu and Zn

3. RESULTS AND DISCUSSION

The morphology of the prepared Cu/Zn nanoparticles was investigated by transmission (TEM) and scanning (SEM) electron microscopies (Fig. 1 b,c). The TEM results indicate that plasma-assisted synthesis results in the production of elongated elliptically shaped nanoparticles that however are prone to agglomeration into the elongated branched structures depicted in more details in Figure 1c (SEM image). The elemental maps performed to find the distribution of the constituent elements in the prepared samples, were acquired using the EDX technique coupled with SEM. The results of the EDX mapping showed that the prepared nanoparticles mainly consist of copper, zinc and oxygen with Cu:Zn atomic ratio close to 1:1. This result is indicative of Cu, Zn and O being bound in a composite as will be further proved by XRD and Raman techniques.

Additional information about the crystal and defect structure of the prepared nanomaterial was obtained from Raman spectroscopy performed at room temperature in the range $100\text{--}1000\text{ cm}^{-1}$, as shown in Figure 2. The results of Raman spectroscopy and absorption spectra of the synthesized nanomaterial confirmed the formation of composite heterostructures. A typical Raman spectrum of the synthesized nanostructures reveals bands associated with the presence of copper and zinc oxide phases that are simultaneously present in the spectrum. Namely, the spectrum contains bands at 220 and 323 cm^{-1} , corresponding to the vibrational bands of the Cu_2O and CuO structures (Wang J et al. 2011). The other characteristic peaks of copper oxides that are typically observed at around $600\text{--}630\text{ cm}^{-1}$ most probably appear as shoulders to a broad band with a maximum at 561 cm^{-1} . The latter band is attributed to the LO phonon mode of ZnO wurtzite structure (Wang J et al. 2011, Pal U et al. 2006, Song Y et al. 2019). In addition, band at 431 cm^{-1} is observed (E_2^{high} mode) (Pal U et al. 2006, Song Y et al. 2019), that together with above-mentioned band at 561 cm^{-1}

proves the presence of ZnO in the nanocomposite. Thus, coexistence of the Raman modes of ZnO and CuO in the Raman spectra confirms the formation of a composite ZnO/CuO nanostructure.

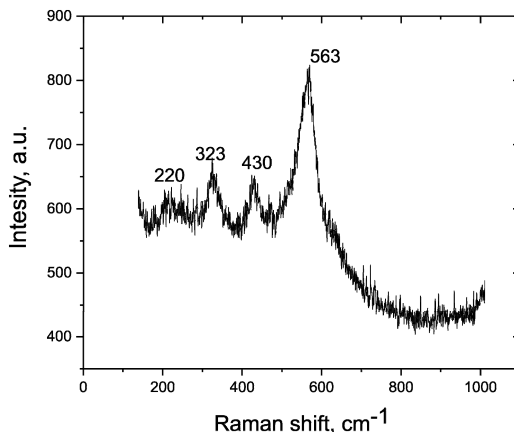


Figure 2. Raman spectrum of the ZnO/CuO composites deposited on the Cu substrate during the plasma activated electrolysis synthesis

To conclude, a novel approach based on simultaneous plasma-assisted anodic dissolution of constituent metals was proposed and tested towards the synthesis of composite CuO/ZnO NPs and thin films. The results demonstrate a simple versatile approach for composite multi-element oxides formation that can be expanded for the production of a broader range of nanomaterials.

Acknowledgement

The work was partially financed by the National Academy of Sciences of Belarus under project Convergence 2.2.05 and by the Belarusian Foundation for Fundamental Researches under Grant No. F 22SRBG-008. Authors from Serbia thank the Ministry of Science, Technological Development and Innovation of the Republic of Serbia for the financial support to the research through institutional funding (Contract number: 451-03-66/2024-03/200017) and bilateral project between Serbia and Belarus (contract number: 337-00-0230/2022-09/08).

References

- Pal, U., Serrano, J. G., Santiago, P., Xiong, G., Ucer, K. B., Williams, R. T.: 2006, *Opt. Mater.*, **29**, 65.
- Song, Y., Zhang, S., Zhang, C., Yang, Y.; Lv, K.: 2019, *Crystals*, **9**, 395.
- Wang, J., Sun, X., Yang, Y., Kyaw, A., Yin, J., Wei, J., Demir, H.: 2011, *Nanotechnol.* **22**, 325704.

Section 3.

LOW TEMPERATURE PLASMAS

OPPORTUNITIES AND CHALLENGES IN LOW-TEMPERATURE PLASMA SCIENCE FOR ATOMIC-LAYER PROCESSING

SATOSHI HAMAGUCHI

*Division of Materials and Manufacturing Science, Graduate School of Engineering,
Osaka University,
2-1 Yamadaoka, Suita, Osaka 565-0871, Japan
E-mail hamaguch@ppl.eng.osaka-u.ac.jp*

Abstract. Plasma processing technologies, which are widely used for semiconductor device manufacturing, are now facing a paradigm shift as Moore's law of device-scale shrinkage is near its end and new three-dimensional structures and nonconventional materials are employed in advanced semiconductor devices. As the complexity of structures increases and more unconventional materials are used, semiconductor manufacturing technologies, including plasma processing, also require further innovations. One of the most promising semiconductor technologies that have contributed significantly to the fabrication of such device structures with atomic-scale accuracy is atomic-layer processing (ALP) (K. Arts, et al. 2022) such as atomic-layer deposition (ALD) and atomic-layer etching (ALE). Unlike conventional chemical/physical vapor deposition (CVD/PVD) or reaction ion etching (RIE), ALP deposits or etches materials layer by layer. In this presentation, the author first discusses the necessity of ALP in modern semiconductor process technologies. In ALP, "self-limiting" surface reactions play key roles in achieving layer-by-layer processes. Plasmas are often used to allow self-limiting surface reactions to take place at relatively low surface temperatures. Therefore, second, the author presents atomic-scale numerical simulation as a means to analyze the fundamental reaction mechanisms in plasma-enhanced and thermal ALP techniques, using examples of plasma-enhanced ALE of Si-based materials (Tinacba, E.T.C. et al., 2021; Hirata, A. et al., 2023; Tercero, J. U. et al., 2024) and thermal ALE of metals (Basher A.H. et al., 2020; 2020; 2021) and discusses the nature of self-limiting reactions in such processes.

References

- Arts K., et al.: 2022, *Plasma Sources Sci. Technol.* **31**, 103002.
Tinacba, E.T.C., et al.: 2021, *J. Vac. Sci. Technol.* **A39**, 042603.
Hirata, A. et al.: 2023, *Jpn. J. Appl. Phys.* **62** S11015.
Tercero J. U. et al.: 2024, *Sur. Coating Technol.* **477**, 130365.
Basher, A.H. et al.: 2020, *Jpn. J. Appl. Phys.* **59**, 090905.
Basher, A. H. et al.: 2020, *J. Vac. Sci. Technol.* **A38**, 052602; 2021, *J. Vac. Sci. Technol.* **A39**, 057001.

LXCAT 3 AND BEYOND – FOSTERING REPRODUCIBILITY IN LOW-TEMPERATURE PLASMA SCIENCE

JAN VAN DIJK and DAAN BOER

Elementary Processes in Gas Discharges, Department of Applied Physics and Science Education, Eindhoven University of Technology, The Netherlands
E-mail j.v.dijk@tue.nl, d.j.boer@tue.nl

Abstract. The LXCat project (Pitchford et al. 2017, Carbone et al. 2021) provides electron-impact cross sections, swarm parameters, interaction potentials and other data that are required for low-temperature plasma (LTP) modeling and simulation. It is a community-driven project that contains approximately 30 000 cross sections, and welcomes in the order of 40 000 visitors per year. Version 2 of the website can be found at <https://lxcat.net/home/>. In spite of its success, a number of issues have been identified in recent years that stand in the way of further progress (sec. 6, 7 of Carbone et al. 2021). These concern the data format, the choice for the (SQL) database and the design of the software stack.

In this contribution, the authors report on the status of “LXCat 3”. This new version of the LXCat database is scheduled to be made available to the general public in September 2024 and addresses all of the above-mentioned concerns. It is based on a standard (JSON) file format that is underpinned by a well-defined data model that is encoded in JSON-Schema, it uses the multi-model ArangoDB database and features a design that allows interaction with the data other than through the LXCat website. LXCat3 is free software, available from the Github repository <https://github.com/LXCat-project/LXCat>. Special attention has been paid to a proper versioning of data items and combinations thereof, and references to particular data can now be made unambiguously using so-called “permalinks”. This feature will have a great impact on the reproducibility of studies in LTP science, especially when complex mixtures of molecular gases are involved and the input data needs are excessive.

After an introduction to the LXCat project and a discussion of the features of LXCat3, live demonstrations of the new platform will be given. The presentation will conclude with a discussion of recent developments, in particular the application of the framework to full plasma chemistries, including non-electronic processes.

References

- Carbone E.A.D. et al.: 2021, *Atoms* **9**, 16, <https://doi.org/10.3390/atoms9010016>
Pitchford L.C. et al. : 2017, *Plasma Processes and Polymers*, **14**, 1600098, <https://doi.org/10.1002/ppap.201600098>

USING DUST PARTICLES AS PROBES IN LOW PRESSURE GAS DISCHARGES

PETER HARTMANN

HUN-REN Wigner Research Centre for Physics, Budapest, Hungary
E-mail hartmann.peter@wigner.hu

Abstract. Conventional plasma diagnostic techniques can be classified as either invasive or non-invasive. Invasive techniques provide information about multiple local plasma parameters, whereas non-invasive techniques are typically optical and have limited spatial resolution. The primary disadvantage of invasive techniques is that the presence of the probe alters the plasma parameters that are intended to be measured, resulting in a systematic error in the results. One way to minimize the disturbance is achieved by reducing the size of the probe. A practical limit is the use of a single micrometer-sized solid grain, often referred to as a dust particle. A dust particle in plasma interacts with the electrons and ions and acquires a significant electric charge, as a result of which it can respond to the variations of the electric field in the discharge. By tracing the trajectory of the particle and deriving the acceleration, one can map the net force distribution along its trajectory. By introducing a precisely regulated external force, it is possible to set the initial conditions of the particle's motion in order to maximize the volume traversed by the particle.

In the presentation I will introduce the concept in detail and show examples based on works of several research groups including recent results from our own laboratory.

References

- Beckers, J.: 2011, Dust particle(s) (as) diagnostics in plasmas., *Proefschrift TU/E*
- Maurer, H.R., Schneider, V., Wolter, M., Basner, R., Trottenberg, T. and Kersten, H.: 2011, Microparticles as Plasma Diagnostic Tools. *Contrib. Plasma Phys.*, 51: 218-227.
- Ramazanov, T.S., et.al.: 2012, The Behavior of Dust Particles Near Langmuir Probe. *Contrib. Plasma Phys.*, 52: 110-113.
- Douglass A, Land V, Qiao K, Matthews L, Hyde T. : 2016, Using dust as probes to determine sheath extent and structure. *Journal of Plasma Physics.* 82(4):615820402.
- Hartmann, P., Kovács, A.Zs., Reyes, J.C., Matthews, L.S., Hyde, T.W.: 2014, Dust as probe for horizontal field distribution in low pressure gas discharges, *Plasma Sources Sci. Technol.* 23 045008

ATMOSPHERIC PRESSURE PLASMA IN PROCESSING OF CELLULOSE FIBERS: FROM SURFACE CLEANING TO TAILORED PROPERTIES

MIRJANA KOSTIC¹ , ANA KRAMAR² , BRATISLAV OBRADOVIC³  and
MILORAD KURAICA³ 

¹*University of Belgrade, Faculty of Technology and Metallurgy, Belgrade, Serbia*
E-mail kostic@tmf.bg.ac.rs

²*Novel Materials and Nanotechnology Group, Institute of Agrochemistry and Food
Technology, Spanish Council for Scientific Research, Paterna, Spain*
E-mail akramar@iata.csic.es

³*University of Belgrade, Faculty of Physics, Belgrade, Serbia*
E-mail obrat@ff.bg.ac.rs (BO), kuki@ff.bg.ac.rs (MK)

Abstract. Plasma processing of textile materials, especially ones from cellulose (natural and man-made (or regenerated) cellulose fibers), has been the focus of many researchers in the past three decades (Shishoo 2007, Ul Islam & Haji 2024). Plasma treatments, as an alternative to conventional wet treatments in textile processing used to clean fiber surfaces or to tailor fiber surface chemistry and morphology, have many advantages, such as small energy consumption, short time of treatment, and small chemical consumption, which makes this process environmentally friendly. Among many different plasma configurations available, which can be classified according to several criteria, such as the type of energy supply (direct or alternating with different frequencies), temperature (hot (thermal) and cold (non-thermal) plasma), and pressure (low-pressure and atmospheric pressure plasma), atmospheric pressure plasma, especially dielectric barrier discharge (DBD), is highly promising for textile material modification thanks to its simple arrangements and adaptability of electrodes' shape, more homogeneous surface discharge with lower temperature electrons preventing localized overheating and damage of treated material as well as its potential for up-scaling and implementation in existing industrial facilities and continuous processes. In this paper, we present a comparative study on the functionalization of cellulose fibers by DBD treatment with special emphasis on the aging effect as an additional treatment parameter. By controlling the DBD variables, such as the nature of gas (air, oxygen, and nitrogen), discharge power, frequency, and exposure time, a great variety of surface effects can be achieved, such as surface cleaning and etching, introduction of new functional groups, increase or decrease surface energy, cross-linking, etc.

References

- Shishoo, R. (Ed.): 2007, *Plasma Technologies for Textiles*, Woodhead Publishing Ltd., England.
- Ul Islam, S., Haji A. (Eds.): 2024, *Advances in Plasma Treatment of Textile Surfaces*, Woodhead Publishing Ltd., England.

LIBS SPECTROSCOPY: WHAT WE CAN MEASURE, AND HOW?

VIOLETA LAZIC

ENEA, Dept. NUC-TECFIS-DIM, Via Enrico Fermi 45, 00044 Frascati (RM), Italy
E-mail violeta.lazic@enea.it

Abstract. Laser Induced Breakdown Spectroscopy (LIBS) is a versatile technique for rapid elemental analysis of samples in various environments. At ENEA's laboratories of Frascati, we have built and tested different LIBS instruments, among them a portable static or handheld sensor for forensic examinations on a crime scene (Lazic et al. 2024), a compact LIBS tool mounted on a robotic arm (Almaviva, et. al. 2019) and the Integrated Laser Sensor (ILS) for sequential stand-off target scanning by laser scattering and Laser Induced Fluorescence (LIF), Raman, and LIBS techniques (Lazic et al. 2019). This presentation briefly reports the methods used for LIBS sampling, the implemented data processing, and the obtained analytical results for various case studies. The examples include: the depth profiling of multi-layered solid targets (coatings, paints and inks), measurements on liquid droplets (oils or water solutions), on particles in traces (e.g. soils, explosives), underwater analysis of the medium and of submerged solid or soft (e.g. sediment) targets. Beside the optimized experimental approach, the retrieval of correct information about samples starting from the LIBS spectra requires a proper use of the atomic databases, then identification of sources of the signal fluctuations and their minimization also through the data processing. In many cases, taking into account shot-to-shot variations of the plasma parameters during the LIBS measurements is of the outmost importance for obtaining element quantifications in samples.

References

- Lazic, V., Andreoli, F., Almaviva, S., Pistilli, M., Menicucci, I., Ulrich, C., Schnürer, F., Chirico, R., 2024, *Sensors*, **24**, 1469.
Almaviva, S., Caneve, L., Colao, F., Lazic, V., Maddaluno, G., Mosetti, P., Palucci, A., Reale, A., Gasiór, P., Gromelski, W., Kubkowska, M., 2020, *Fus. Eng. Des.* **169**, 112638
Lazic, V., Palucci, A., De Dominicis, L., Nuvoli, M., Pistilli, M., Menicucci, I., Colao, F., Almaviva, S., 2019, *Sensors*, **19**, 4269.

MICRO HOLLOW CATHODE DISCHARGES IN ARGON/NITROGEN USED FOR BORON NITRIDE PECVD

C. LAZZARONI¹, A. REMIGY, M. JACQUEMIN, H. KABBARA, S. KASRI,
B. MENACER, K. GAZELI, V. MILLE and G. LOMBARDI

*Université Sorbonne Paris Nord, Laboratoire des Sciences des Procédés et des
Matériaux, LSPM, CNRS, UPR 3407, F-93430, Villetaneuse, France*

¹*E-mail claudia.lazzaroni@lspm.cnrs.fr*

Abstract. A Plasma Enhanced Chemical Vapor Deposition (PECVD) process based on Micro Hollow Cathode Discharges (MHCDs) (Schoenbach K. H. et al., 1996) in Ar/N₂ mixture has been developed to deposit hexagonal boron nitride (h-BN), a material of choice for electronic and optoelectronic applications. We have shown the feasibility of h-BN deposition on large area substrates (2 inches) at relatively low temperature (800°C) compared to conventional processes (Kabbara H. et al., 2020). To optimize and better understand the deposition process, the discharge is characterized experimentally and through modelisations. In particular, we use Two-photon Absorption Laser Induced Fluorescence (TALIF) to measure the nitrogen atom density, a key parameter in the process. TALIF measurements show that the atomic nitrogen is produced inside the MHCD hole and can be transported over long distances using a pressure differential between the two sides of the MHCD. To achieve the h-BN deposition, the substrate holder must be polarized which involves a homogenization of the density profile along the substrate's surface (Remigy A. et al., 2024). The introduction of an electric field and the secondary discharge is the trigger for nitride deposition and not, as would be expected, the N atoms density in the vicinity of the substrate.

References

- Kabbara H., Kasri S., Brinza O., Bauville G., Gazeli K., Santos Sousa J., Mille V., Tallaire A., Lombardi G. and Lazzaroni C. : 2020, *Appl. Phys. Lett.*, **116** 171902.
Remigy A., Menacer B., Kourtzanidis K., Gazeli O., Gazeli K., Lombardi G. and Lazzaroni C. : 2024, *Plasma Sources Sci. Technol.*, **33**, 025013.
Schoenbach K. H., Verhappen R., Tessnow T., Peterkin F. E. and Byszewski W. W. :1996 *Appl. Phys. Lett.* **68**, 13.

LIQUID MICRODROPLETS IN A MICROPLASMA: PHENOMENA AND TECHNOLOGICAL APPLICATIONS

P. MAGUIRE, N. HENDAWAY, H. MCQUAID and D. MARIOTTI

Ulster University, Belfast, Ireland
E-mail pd.maguire@ulster.ac.uk

Abstract. The acceleration of chemical reactions in confined microvolumes has inspired considerable interest in the potential of charged microdroplets as chemical microreactors with further enhanced capability. The use of plasma-generated free electrons as a charge source opens the possibility of generating very high levels of surface charge and high interfacial electric fields in such microdroplets. To fully exploit their potential as gas-phase reactors, microdroplets need to be relatively long-lasting in order to deliver a continuous stream of reaction products to a remote target and therefore evaporation during plasma exposure needs to be optimised. Potential applications of charged liquid microreactors are many and varied, including direct medical treatment by delivering elevated levels of radicals, e.g. OH^\bullet , or on-demand synthesised nanoparticles to target cancers, possibly *in-vivo* via endoscopic access. Other nanomaterials advances include on-demand ink-jet patterns for photonic sensors, surface catalysis, biocides, nanofertilisers and polymer nanocomposites. Plasma physics and chemistry of such a multiphase system comprising gas, plasma, saturated vapour, gas-phase clusters, solid nanoparticles and liquid are extremely complex and little explored.

Free electron fluxes to liquid provide a rich source of solvated electrons capable of initiating rapid reduction reactions in precursor-loaded droplets. To supply such electrons requires a high density but low temperature plasma operating at atmospheric pressure under non-equilibrium conditions and capable of tolerating droplet injection without excess evaporation or electron loss. Although, from theoretical considerations, microscale particles in such a plasma are expected to acquire a net charge, this has yet to be demonstrated. We report the first measurements of particle charge acquired by microparticles in a fully collisional atmospheric pressure low temperature plasma. Estimates of areal electron flux to the droplet surface were obtained from simulation coupled with experimental observation of *in-droplet* reduction reactions. Results demonstrate a 2 – 3 orders of magnitude increase in charge levels compared to ion charging in corona systems or electron charging in low pressure plasmas while electron fluxes are many orders of magnitude higher than in gamma radiolysis.

ION INDUCED REACTIONS IN IMS STUDIED BY DFT

PETER PAPP, SAMUEL PETER KOVÁR, LADISLAV MORAVSKÝ and
ŠTEFAN MATEJČÍK

*Department of Experimental Physics, Faculty of Mathematics, Physics and
Informatics, Comenius University in Bratislava, Mlynská dolina F2, 842 48
Bratislava, Slovakia
E-mail peter.papp@uniba.sk*

Abstract. Sulfur containing hydrocarbons are being studied both experimentally and theoretically. Electron and ion induced processes are of main interest, represented by ionization reactions, electron attachment, as well as charge transfer reactions. In industry, the sulfur containing compounds (thiophenes) in crude oil are among the most abundant constituents, in some cases as high as 10% (Hua et al. 2004). On the other hand, sulfur is the tenth most abundant element in the universe and is known to play a significant role in biological systems, investigation of sulfur containing astrochemical molecules is therefore of high interest (Mifsud et al. 2021). Either sulfur containing hydrocarbons considered as industrial contaminant or highly important astrochemical molecules, among all possible chemicals five- or six-member rings containing sulfur atom are of interest as well. In this work Atmospheric Pressure Chemical Ionization of thiophen, its methyl-, dimethyl- and benzo- derivatives are studied with Ion Mobility Spectrometry (IMS) combined with Mass Spectrometry (Michalczuk et al. 2020). Quantum chemistry is used to model the thermochemical properties, ionization energies, electron affinities, bond energies in ions, proton affinities and reactions leading to formation of clusters of the studied analytes with reactant ions in IMS, produced with corona discharge source in ambient air.

This work was supported by the Slovak Research and Development Agency under the Contract no. APVV-19-0386, APVV-22-0133 and the Slovak Grant Agency for Science (contract no. VEGA 1/0553/22). Comenius University in Bratislava supported with CLARA@UNIBA.SK high-performance computing facilities, services and staff expertise of Centre for Information Technology (<https://uniba.sk/en/HPC-Clara>).

References

- Hua, R. X., Wang, J. H., et al. : 2004, *J. Separ. Sci.*, **27** (9), 691.
Mifsud, V. D., Kaňuchová, Z., et al. : 2021, *Space. Sci. Rev.*, **217** (14), 1.
Michalczuk, B., Moravský, L., et al. : 2020, *Int. J. Mass Spectrom.*, **449**, 116275.

INACTIVATION OF VIRUSES IN WATER BY PLASMA TREATMENT

G. PRIMC^{1,2}, M. ZVER¹, R. ZAPLOTNIK^{1,2}, A. FILIPIČ³, D. DOBNIK³ and
M. MOZETIČ^{1,2}

¹*Department of Surface Engineering, Jožef Stefan Institute, Jamova cesta 39,
Ljubljana, Slovenia*

E-mail miran.mozetic@guest.arnes.si

²*Plasmadis Ltd., Teslova ulica 30, Ljubljana, Slovenia*

E-mail gregor.primc@plasmadis.com

³*National Institute of Biology, Večna pot 121, Ljubljana, Slovenia*









E-mail arijana.filipic@nib.si

Abstract. Alternative methods for the inactivation of viruses in water have recently attracted enormous attention. The methods should enable rapid inactivation at room temperature and should be free from chemicals. The application of gaseous plasma fulfills these regulations but may be impractical because plasma sustained at atmospheric pressure is limited to the volume of the large electric field. A useful method for sustaining plasma at low pressure despite the water being at atmospheric pressure is the application of hydrodynamic cavitation. The saturated water vapor pressure at room temperature is established in a stable super-cavitation bubble of volume several cm³, and the electrodes are immersed into the bubble and powered with a suitable voltage supply to sustain the non-equilibrium gaseous plasma in a glow discharge mode. Plasma sustained in water vapor at the pressure of a few 10 mbar is a rich source of OH radicals, which are dissolved in the liquid. The high speed of liquid water passing the cavitation nozzle enables optimal mixing, so a few passages of water through the device enable the inactivation of viruses for 5 decades by an irreversible interaction of OH radicals with the organic matter. The water pH does not change significantly, and the concentration of hydrogen peroxide remains below 1 mg/L, so the effect of H₂O₂ on virus inactivation is marginal. The preferred discharge power is between 10 and 100 W, so the energy consumption is minimal.

References

Primc, G., Zaplotnik, R., Mozetič, M., Filipič, A., Gutiérrez-Aguirre, I., Dobnik, D., Dular, M., Petkovšek, M.: (2023) Method and device for disinfection of liquid, US 11,807,555 B2.

DIAGNOSTICS AND APPLICATIONS OF ATMOSPHERIC PRESSURE PLASMAS FOR TRIGGERING OF CELL MECHANISMS

NEVENA PUAC¹ , NIKOLA ŠKORO¹ , SERGEJ TOMIĆ² ,
ANDJELIJA MARKOVIĆ¹ , NEDA BABUČIĆ¹ ,
OLIVERA JOVANOVIĆ¹ , A. MORINA³, GORDANA MALOVIĆ¹ ,
MIODRAG ČOLIĆ⁴  and ZORAN LJ. PETROVIĆ^{4,5} 

¹*Institute of Physics, University of Belgrade, Pregrevica 118, 11080 Belgrade, Serbia*

²*Institute for the Application of Nuclear Energy, University of Belgrade, Banatska 31b, 11080 Belgrade, Serbia*

³*Faculty of Science and Natural Resources, University of Malaysia, Malaysia*

⁴*Serbian Academy of Sciences and Arts, Knez Mihailova 35, Belgrade, Serbia*

⁵*School of Engineering, Ulster University, Jordanstown, Co. Antrim, BT37 0QB UK*

E-mail nevena@ipb.ac.rs

Abstract. Cold plasmas with their rich plasma chemistry with ample amounts of Reactive Oxygen and Nitrogen Species (RONS) are driving the development of applications in the fields of Plasma Medicine and Plasma Agriculture (see Adamovic et al. 2022). One of the applications is by using Plasma Treated Liquids (PTLs). When aqueous solutions (water, cell medium, saline solution etc.) are exposed to cold plasma, reactions occurring in the gaseous phase and at the gas-liquid interface, introduce short and long-living RONS, such as OH, O, O₃, H₂O₂, NO₂⁻, NO₃⁻, into the aqueous phase (see Bradu et al. 2020). We have used several configurations of atmospheric pressure plasma sources that were powered in the range of frequencies from kHz to GHz. They were chosen according to the application and characterized in detail by optical emission spectroscopy, electrical characterization, ICCD imaging, mass spectrometry etc. The applications by using PTLs of these sources include decontamination of bacteria, cancer cell treatment, wound treatments and toxicity tests.

Acknowledgement: This work was supported by the Science Fund of the Republic of Serbia, 7739780, APPerTAin-BIOM project and by MSTDI Republic of Serbia grant number 451-03-66/2024-03/200024.

References

- Adamovich, I. et al. : 2022, *J. Phys. D: Appl. Phys.* **55**(37), 373001.
Bradu, C., Kutasi, K., Magureanu, M., Puač N., Živković, S. : 2020, *J. Phys. D: Appl. Phys.*, **53**(22), 223001.

FLUID MODELLING OF SINGLE-FILAMENT DBD AND SELF-PULSING DISCHARGES AT ATMOSPHERIC PRESSURE USING FEDM

A. P. JOVANOVIĆ¹, H. HÖFT¹, D. LOFFHAGEN¹, T. GERLING^{1,2,3} and M. M. BECKER¹

¹*Leibniz Institute for Plasma Science and Technology (INP), Greifswald, Germany*

²*Diabetes Competence Centre Karlsburg (KDK), Karlsburg, Germany*

³*ZIK Plasmatis, Greifswald, Germany*

Abstract. Non-thermal atmospheric-pressure plasmas have found many applications in various areas of science and technology in recent years (Keidar et al., 2021). An efficient way to generate these plasmas is often achieved either by limiting the current amplitude by introducing a dielectric layer over the electrode(s) in dielectric barrier discharges (DBDs) (Brandenburg et al., 2023) or the duration of the discharge using well-designed circuits in self-pulsing transient spark discharges (Janda et al., 2011 and Gerling et al., 2013). This work presents the fluid-Poisson modelling of these discharges using the Finite Element Discharge Modelling (FEDM) code (Jovanović et al., 2023), which is based on FEniCS (Logg et al., 2012). The first study focuses on a pulsed-driven single-filament DBD with two hemispherical alumina-covered electrodes with a 1 mm gas gap. The modelling is carried out at atmospheric pressure in N₂ with an admixture of 0.1 vol. % of O₂ (Höft et al., 2018) to analyse different features during discharge inception and streamer propagation. The comparison of modelling results with measured current and streamer velocity shows their good agreement with the experiment. The second study presents modelling results of a self-pulsing transient spark discharge in argon at atmospheric pressure. For this study, the model includes an additional equivalent circuit equation to describe the self-pulsing behaviour and the heat equation to account for the gas heating. The model reproduces a self-pulsing behaviour well and enables the prediction of the charge carrier densities and gas temperature during the discharge.

This work was funded by the Deutsche Forschungsgemeinschaft (DFG, German Research Foundation)—project number 466331904.

References

- Brandenburg, R. et al. : 2023, *Plasma Chem. Plasma Process.*, **43**, 1303.
Gerling, T. et al. : 2013, *Plasma Sources Sci. Technol.*, **22**, 065012.
Höft, H. et al. : 2018, *Plasma Sources Sci. Technol.*, **27**, 03LT01.
Janda, M., Martišovitiš, V., Machala, Z. : 2011, *Plasma Sources Sci. Technol.*, **20**, 035015.
Jovanović, A. P. et al. : 2023, *Plasma Sources Sci. Technol.*, **32**, 044003.
Keidar, M., Weltmann, K.-D., Macheret, S. : 2021, *J. Appl. Phys.* **130**, 080401.
Logg, A., Mardal, K. A. and Wells, G. : 2012, *Automated Solution of Differential Equations by the Finite Element Method: The Fenics Book*, Springer, Berlin.

THERMAL AND ACOUSTIC PROPERTIES OF CELLULOSE FIBROUS MATERIALS

SANJA PAVLOVIC¹ and GORAN POPARIĆ² 

¹ *College of Applied Studies Aviation Academy, Bulevar vojvode Bojovica 2, 11158 Belgrade*

E-mail pavlovic.s@vakademija.edu.rs

² *Faculty of Physics, University of Belgrade, Studentski Trg 12, P.O. Box 44, 11000 Belgrade, Serbia*

E-mail goran_poparic@ff.bg.ac.rs

Abstract. In the present research, the thermal and acoustic characteristics of cellulose fibrous materials with different structural and physical properties, made of cotton, hemp, viscose and their mixture were studied and also examined their acoustic characteristics after plasma treatment. The obtained experimental results of sound absorption coefficient (SAC) for cellulose fibrous materials before and after argon plasma treatment and the results of the additional investigation and measurements of the treated cellulose material surface are presented.

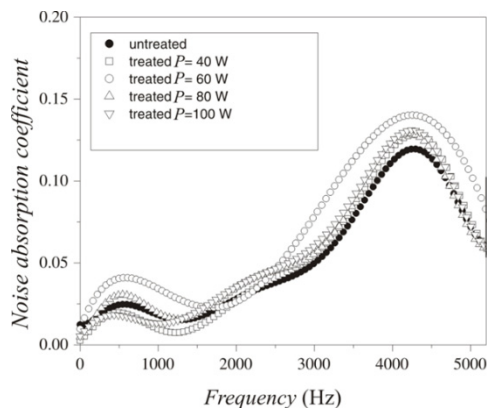


Figure 1: Sound absorption coefficient for untreated and plasma treated sample (Sanja S. Pavlovic at al.: 2019)

References

- Aoneas MM, Vojnović MM, Ristić MM, Vičić MD, Poparić B : 2017 Phys Plasma 24, 023502
Sanja S. Pavlovic at al.: 2019, Cellulose, Springer Nature, **26**, 6543.
Sanja S. Pavlovic at al: 2014, Polymer Testing **34**

ANALYSIS OF DIELECTRIC BARRIER DISCHARGES IN AR-MONOMER MIXTURES USING A STANDARDIZED FLUID MODELLING APPROACH

M. STANKOV¹, M. M. BECKER¹, L. BRÖCKER², C.-P. KLAGES² and D. LOFFHAGEN¹

¹*Leibniz Institute for Plasma Science and Technology
(INP), Felix-Hausdorff-Straße 2, 17489 Greifswald, Germany
E-mail marjan.stankov@inp-greifswald.de*

²*Institute for Surface Technology (IOT), Technische Universität
Braunschweig, Bienroder Weg 54 E, 38108 Braunschweig, Germany*

Abstract. Thin film deposition enhanced by atmospheric-pressure plasmas has been widely studied over the past two decades (Massines et al. 2012). Nevertheless there is still a lack of comprehensive understanding, especially in identifying the particle species responsible for film formation. To address this issue, a study which combines fluid-Poisson modelling and experimental analysis of dielectric barrier discharges in argon with small amounts of siloxanes, organosilanes, or hydrocarbons is reported.

The applied fluid-Poisson model is a time-dependent, spatially one-dimensional model comprising balance equations for particle number densities and electron energy density coupled with Poisson's equation. Given the complexity of the reaction kinetic models under consideration, which involve hundreds of reactions, building the model by manually setting up each equation is laborious and prone to error. To overcome this, the model is generated automatically using standardized input files containing lists of the plasma species and plasma chemical reactions, together with the corresponding rate and transport coefficients, similarly as described in (Jovanović et al. 2021).

The present study investigates the behaviour of a single-filament discharge powered by sinusoidal voltages of a few kV at a frequency of 19 kHz. The analysis shows that Penning ionisation involving monomer molecules and excited argon species significantly influences the discharge characteristics. The analysis of surface fluxes of particle species emphasises the essential role of cations in the film formation process. The investigation further focuses on the contributions of specific cations and their correlation with the measured average mass of deposited ions. In addition, the influence of various chemical processes on the cation formation is discussed.

Funded by the Deutsche Forschungsgemeinschaft (DFG, German Research Foundation) – project number 504701852.

References

- Jovanović, A. P., Stankov, M. N., Loffhagen, D., Becker, M. M.: 2021, *IEEE Trans. Plasma Sci.*, **49**, 3710.
Massines, F., Sarra-Bournet, C., Fanelli, F., Naudé, N. and Gherardi, N.: 2012, *Plasma Process. Polym.*, **9**, 297.

“AIR-PLASMA-WATER” ELECTROPHYSICAL SYSTEM BASED ON DBD PLASMA JET: PROSPECTS AND PROBLEMS

OLGA STEPANOVA¹, VADIM SNETOV¹, OLEG GRUSHKO¹,
DMITRY SUBBOTIN¹, ILYA RUCHKIN^{1,2} and MIKHAIL PINCHUK¹

¹*Institute for Electrophysics and Electric Power of the Russian Academy of
Sciences, 18 Dvortsovaya emb., St.Petersburg, 191186, Russia
E-mail omstepanova@ieeras.ru*

²*Ioffe Institute, 26 Polytekhnicheskaya str., St.Petersburg, 194021, Russia*

Abstract. Electrophysical systems with plasma-liquid interaction are intensively studied because of their numerous practical applications based on using reactive oxygen and nitrogen species to provide chemical and biological activity of a treated liquid (e.g., see Kovačević, Vesna V., et al. 2022). An original experimental setup based on dielectric-barrier discharge in an ambient air to produce biologically active mediums will be presented. It includes a coaxial electrode system applied by a sinusoidal power supply with a signal frequency of 26.5 kHz, gas supply system with control of temperature and humidity of the air passing through the discharge gap. A liquid is treated by its bubbling with gas discharge products due to volume absorption. Gas and liquid phases of the system “air-plasma-water” will be considered depending on a value of an applied voltage and relative humidity of the air in the discharge gap. Some revealed drawbacks in the system’s work will be analyzed in terms of reproducibility of NO_x^- and H_2O_2 concentrations. Different conditions of bubbling gas products will be considered to solve the problem of enhancing an efficiency of reactive oxygen and nitrogen species’ dissolution in water. The potential prospects on biomedical and environmental applications of the presented electrophysical system will be proposed.

The study has been supported by a grant from the Russian Science Foundation № 24-29-00816, <https://rscf.ru/en/project/24-29-00816/>.

References

Kovačević, V. V., Sretenović, G. B., Obradović, B. M., & Kuraica, M. M. : 2022, *J. Phys. D Appl. Phys.*, **55**(47), 473002.

APPLICATION OF MACHINE LEARNING AND ARTIFICIAL INTELLIGENCE IN PLASMA SPECTROSCOPY

IVAN TRAPARIĆ 

Institute of Physics Belgrade, Pregrevica 118, 11080, Serbia
E-mail traparic@ipb.ac.rs

Abstract. Plasma spectroscopy represents the non-contact and non-perturbative plasma diagnostics tool that is widely used. One such application, considered in this work, is the determination of electron density from Stark broadening of emitted spectral lines. The other, laser-induced breakdown spectroscopy (LIBS) is often used for quantitative analysis of sample constitution. Finally, to track impurity transport mechanisms, extreme ultraviolet (EUV) and vacuum ultraviolet (VUV) plasma spectroscopy are used in many fusion devices to monitor highly charged impurity ions. Over the years many approximative formulae and robust models were developed to simulate the shape of emitted spectral lines due to the Stark effect from which line width and shift can be determined. Since a lot of these codes request substantial computational resources, the application of machine learning (ML) for quick estimation of line width was considered (Tapalaga et al. 2022). Usually, the usage of ML in LIBS quantitative analysis is followed by the recording of a large enough database with enough variance in it for precise analysis. Therefore, the usage of an already recorded database for training of the ML model was investigated for additional acceleration of the procedure, and its potential was discussed (Traparic and Ivkovic. 2023). Last but not least, variational autoencoder (VAE) was employed to model the so-called Unresolved Transition Array (UTA) structure, that rises due to the emission from highly charged tungsten ions. The application considered here is the validation of collisional radiative models and estimation of plasma core temperature and electron temperature profile in devices that don't have advanced diagnostics for this purpose.

References

- Tapalaga, I., Traparić, I., Trklja Boca, N. *et al.*: 2022 *Neural Comput & Applic* **34**, 6349–6358
- Traparić, I., Ivković, M. : 2023 *Eur. Phys. J. D* **77**, 30.

LUMINESCENT ANALYSIS OF E-BEAM INDUCED TRANSFORMATION OF PHENOL IN THE PRESENCE OF HUMIC SUBSTANCES

E.N. BOCHARNIKOVA¹, O.N. TCHAIKOVSKAYA^{1,2}, S.A. CHAYKOVSKY^{2,3},
V.I. SOLOMONOV², A.S. MAKAROVA² and I.V. SOKOLOVA¹

¹ *Tomsk State University, Tomsk, Russia*
E-mail tchon@phys.tsu.ru

² *Institute of Electrophysics of the Ural Division of the Russian Academy of
Sciences, Ekaterinburg, Russia*
E-mail plasma@iep.uran.ru

³ *The Lebedev Physical Institute of the Russian Academy of Sciences, 19991
Moscow, Russia*
E-mail chaikovsky@iep.uran.ru

Abstract. Using luminescence spectroscopy and absorption spectra, the conversion of phenol in aqueous solution without and with the present of humic and fulvic acids under electron beam was studied. The UV technology and electron beam were evaluated using the energy efficiency index. The phenol conversion efficiency values were higher after electron beam treatment than after UV treatment.

1. INTRODUCTION

Phenols are a very common type of industrial wastewater contaminants. Many studies have shown that the presence of humic acids can reduce the removal kinetics of contaminants at environmentally significant concentrations. However, there are other studies with opposite results. But the mechanism of interaction between the transformation of humic substances and pollutants remains unclear and deserves further study. Plasma-chemical processes occurring under the influence of a pulsed electron beam on organic compounds in water, including at the liquid-air interface, are poorly studied. Under the influence of the beam, active centers (free radicals, ions, or excited molecules) appear and conditions favorable for chain [see Solomonov et al., 2006] and branched chain processes in air are formed [see Mesyats et al., 2001]. Electron beam irradiation is a form of non-thermal technology that is widely used to solve various agricultural problems such as inactivating foodborne pathogens, suppressing tuber germination, delaying

ripening of harvested produce, and controlling postharvest losses caused by insect and fungal infections [see Nguyen *et al.*, 2021; Villarreal-Lozoya *et al.*, 2009; Gul *et al.*, 2022; Elias *et al.*, 2020]. Scientific articles concerning irradiation of various biological systems with electron-beam (e-beam) doses have become quite frequent today. This is due to the search for optimal storage conditions for agricultural products and the evaluation of the effect of the e-beam on the health of living organisms.

2. MATERIALS AND METHOD

In our research, we irradiated a 1mM aqueous solution of phenol with electron beam. Then the phenol transformation in aqueous solution without and with the addition of humic and fulvic acids under electron beam was studied using luminescence spectroscopy and absorption spectra. Humic substances sample MK-2-1 (humic and fulvic acids, degree of dehydration 15%) was isolated from the upper peat from the high-marsh part of the deposit (Mezensky district, Arkhangelsk region, Russia). The debituminized peat was poured with 0.1 N NaOH (in a ratio of 1: 50) and infused for 24 hours without heating under constant stirring on a laboratory shaker, then humates were separated from the solid residue by filtration and purified from excess NaOH by dialysis on cellophane membranes to pH 7.5-8.0. The concentration of the working solutions was brought to a value of 25 mg/L by dilution with distilled water. We expected that phenol would react with point OH-radicals formed during redox reactions in humic substances.

The irradiation experiments were carried out with a vertical e-beam from the RADAN-303 accelerator installed in the quantum electronics laboratory of the Institute of Electrophysics, Ural Branch of the Russian Academy of Sciences (Ekaterinburg, Russia). The electron energy was 170 keV, the number of irradiation pulses with a repetition rate of 1 Hz varied from 50 to 800. The design of the experimental setup for studying the effect of an electron beam on aqueous solutions of organic substances is given in detail in [see Tchaikovskaya *et al.* 2023; Solomonov *et al.*, 2016]. In the laboratory apparatus, solutions were exposed to a vertically scanned beam in a continuous flow reactor (solution depth: 2 mm, width: 1.5 cm). When distilled water is replaced by phenol and phenol solution in the presence of humic acid MK-2-1, no new bands appear in the pulse cathodoluminescence spectrum. This indicates that the solution does not luminesce under electron irradiation in the region of 300÷900 nm. However, a decrease in the intensity of the above bands with increasing number of irradiation pulses was recorded.

3. RESULTS AND DISCUSSION

Fluorescence spectra of an aqueous solution of phenol in the presence of humic acid MK-2-1 15% before and after electron beam irradiation are shown in Figure 1. With increasing number of irradiation pulses there is a consistent decrease in fluorescence intensity at 300, 475 and 575 nm (Figure 1). The band around 300 is

the fluorescence of phenol. The band around 475 nm is the fluorescence of the complex of humic and fulvic acids (Figure 2).

We did not notice any changes in the fluorescence intensity of this band after exposure to the electron beam. Therefore, we can claim that humic and fulvic acids MK-2-1 can be easily processed. According to data obtained from fluorescence excitation spectra, the fluorescence band around 475 nm is formed mainly by structures in MK-2-1 absorbing in the region at 325 and 250 nm. The band around 575 nm is the fluorescence of the phenol complex with humic and fulvic acids MK-2-1 (Figure 1). According to fluorescent analysis it was found that during irradiation with an e-beam, the addition of MK-2-1 promoted a 2-fold increase in phenol transformation compared to aqueous solution (Figure 1).

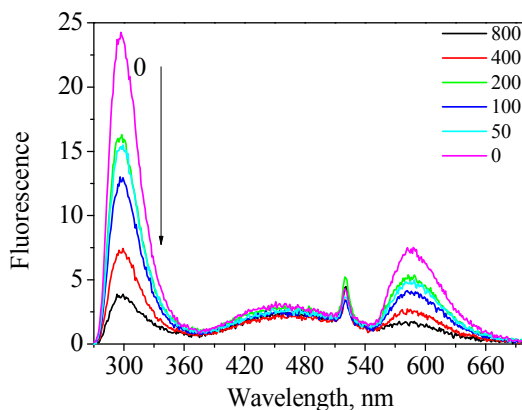


Figure 1: Fluorescence spectra of aqueous solution of phenol in the presence of humic acid MK-2-1 before irradiation (0 pulse) and after e-beam irradiation. The number of pulses is indicated in the inset. The arrow indicates the direction of change in fluorescence intensity. Fluorescence excitation wavelength is 260 nm.

UV technology and electron beam were evaluated by us using the electrical energy efficiency index. The two treatments were compared for the same systems: phenol+water, phenol + water + MK-2-1 at the same concentration. The phenol transformation efficiency values were higher after electron beam than after UV treatment. Moreover UV radiation was not at all effective for phenol attrition. Addition of MK-1 to the aqueous phenol solution did not result in any phenol transformation under UV treatment. The electron beam method had the disadvantage that constant power was required to operate the device, even when the beam was turned off. Nevertheless, compared to the UV treatment, we achieved phenol transformation under the action of the electron beam in the presence of MK-2-1.

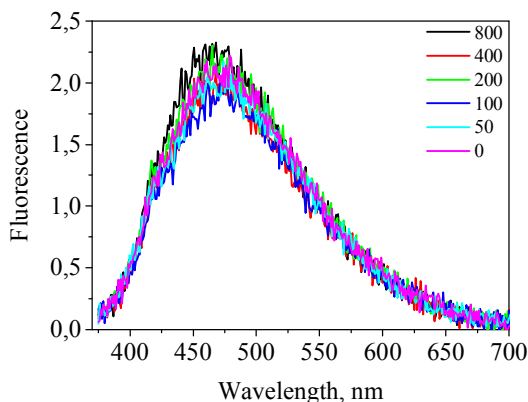


Figure 2: Fluorescence spectra of aqueous solution of humic acid MK-2-1 before irradiation (0 pulse) and after e-beam irradiation. The number of pulses is indicated in the inset. Fluorescence excitation wavelength is 365 nm.

This work was supported by the Russian Science Foundation (project no. 24-1920031). The sample MK-2-1 provided by Selyanina S.B. (Laverov Federal Center for Integrated Arctic Research of the Ural Branch of the Russian Academy of Sciences).

References

- Elias, M. I., Madureira, J., Santos, P. M. P., Carolino, M. M., Margaça, F. M. A., Cabo Verde, S. : 2020, *Innovative Food Science & Emerging Technologies*, **66**, 102487.
- Gul, M. M., Ahmad, K. S. : 2022, *Journal of Materials Science*, **57**, 7290.
- Mesyats, G. A., Novoselov, Yu. N., Filatov, I. E. : 2001, *Technical Physics Letters*, **27**, 813.
- Nguyen, T. T., Uthairatanakij, A., Srilaong, V., Laohakunjit, N., Kato, M., Jitareerat, P. : 2021, *Applied Biological Chemistry*, **64**, 19.
- Solomonov, V. I., Michailov, S. G., Lipchak, A. I., Osipov, V. V., Shpak, V. G., Shunailov, S. A., Yalandin, M. I., Ulmaskulov M. R. : 2006, *Laser Physics*, **16**, 126.
- Solomonov, V. I., Spirina, A. V., Popov, M. P., Kaigorodova, O. A. : 2016, *Journal of Optical Technology*, **83**, 494.
- Tchaikovskaya, O. N., Solomonov, V. I., Bocharnikova, E. N., Makarova, A. S., Mayer, G. V., Osipov, V. V., Chaikovskiy, S. A. : 2023, *IEEE Transactions on Plasma Science*, **61**, 2765.
- Villarreal-Lozoya, J. E., Lombardini, L., Cisneros-Zevallos, L. : 2009, *J. Agric. Food Chem.*, **57**, 10732.

COMPACT PIEZOTRANSFORMER SOURCE OF THE COLD ATMOSPHERIC PLASMA WITH THREE TYPES OF DISCHARGES

N.N. BOGACHEV¹, A.S. BAKSHAEV², L.V. KOLIK¹, E.M. KONCHEKOV¹ and
A.S. KONKOVA¹

¹*Prokhorov General Physics Institute of the Russian Academy of Sciences,
Moscow, Russia
E-mail bgniknik@yandex.ru*

²*MIREA – Russian Technological University, Moscow, Russia
E-mail alexbakshaev@bk.ru*

Abstract. In recent years, low-temperature atmospheric pressure plasma (cold atmospheric plasma, CAP) has received increasing attention from the scientific and engineering community, see Adamovich I, et al. 2017. This is due to the wide possibilities of creating and using such plasma for processing various solid and liquid materials, especially in biology and medicine. In studies on the use of low-temperature nonequilibrium atmospheric pressure plasma in medicine and biology, dielectric barrier discharges (DBDs), plasma jets, and corona discharges with various types of sources and electrode configurations are most often chosen. In recent years, there has been increasing interest in the creation of small-sized mobile CAP sources using piezoelectric transformers as a compact high-voltage element, see Itoh H., et al. 2006. It is important to consider that a piezotransformer is a resonant element with a strong dependence of the resonant frequency on the electrical parameters of the load. The report presents the developed compact CAP source for biomedical applications based on a piezotransformer with an E-class driver. The developed piezotransformer power supply has an output voltage of $V_{pp} = 5$ kV, $V_{RMS} = 2.3$ kV. The source allows you to create CAP with different types of discharge depending on the tip used: direct piezoelectric discharge, dielectric barrier discharge, discharge in a plasma jet with a flow of intertwined gases. The developed source with E-class driver can be programmed to automatically adjust the frequency of the voltage at the transformer input, which allows it to work with different loads. The research was financially supported by the Russian Science Foundation, project No. 24-29-00842.

References

- Adamovich I, et al. 2017, *J. Phys D Appl Phys.*, **50** (32), 323001.
Itoh H., Teranishi K., and Suzuki S. . 2006 *Plasma Sources Sci.Technol.*, **15** (2), 51.

IONIZATION OF A PLASMA ANTENNA CHANNEL IN A DIELECTRIC GAS-DISCHARGE TUBE

N.N. BOGACHEV, I.L. BOGDANKEVICH, V.I. ZHUKOV,
D.M. KARFIDOV, V.P. STEPIN and N.G. GUSEIN-ZADE

*Prokhorov General Physics Institute of the Russian Academy of Sciences, Moscow,
Russia*

E-mail bgniknik@yandex.ru

Abstract. Plasma antennas are a pressing topic for research at the intersection of gas discharge, plasma physics and antenna engineering. The most popular type of plasma antennas are those made from gas-discharge tubes with ionization by a surface electromagnetic wave. Many studies have been generated on the performance of various configurations of such plasma antennas. There are also many works on the study of the parameters and characteristics of discharges on a surface wave. An important fundamental task in the study of a plasma asymmetrical dipole antenna with a gas-discharge tube is the construction of a physical model and a description of the processes occurring in it and affecting its operation.

In this work, the process of the formation of a plasma antenna channel was studied using numerical simulation. Numerical simulations were carried out in the electromagnetic code KARAT, see Tarakanov V.P. 1992, using the finite difference time domain method for calculating the electromagnetic field and the Particle-in-Cell method for plasma. In 2.5D geometry, a model of a plasma asymmetric dipole antenna was created from a glass tube filled with argon with low local preionization, a metal screen and a coaxial cable (without using a surfatron). For argon pressures in the range from 0.1 Torr to 1 Torr, a stationary discharge mode was achieved, the discharge rates were determined, the distributions of electrons, ions and current in the plasma, the field distributions inside the gas discharge tube and in the near zone were obtained, and the antenna radiation patterns were calculated. The obtained discharge rates correspond to known theoretical estimates and experimental data.

References

Tarakanov V.P., User's manual for code KARAT, *Springfield: BRA* (1992)

ESTIMATION OF NITROGEN IMPURITY LEVEL IN HELIUM ATMOSPHERIC DISCHARGE VIA EMISSION SPECTROSCOPY

NIKOLA CVETANOVIĆ¹ , SAŠA S. IVKOVIĆ²  and
BRATISLAV M. OBRADOVIĆ² 

¹ *University of Belgrade, Faculty of Transport and Traffic Engineering,
11010 Belgrade, Serbia
E-mail nikola@ff.bg.ac.rs*

² *University of Belgrade, Faculty of Physics, 11001 Belgrade, Serbia*

Abstract. In the last two decades nonthermal atmospheric pressure discharges have emerged as the most investigated and most promising laboratory plasma sources (see e.g. Brandenburg, 2019). These discharges are predominantly dielectric barrier discharges (DBDs) operating in noble gases. Research has shown that presence of gas impurities within the working gas can be crucial for DBD operation, in some cases even for providing its sustenance. Numerous models have shown the influence of gas impurity level on discharge parameters (see e.g. Martens et al. 2010, Wang and Wang 2005, Zhanf et al. 2019). Therefore, the knowledge of impurity level is required both in experimental work and for reactor design. Here we propose a spectroscopic method for the estimation of nitrogen molecular impurity in discharge operating in helium, which is a typical working gas/impurity combination. The method is based on the intensity ratio of the prominent N₂ band (C³Πu–B³Πg, 0-0) at 337 nm, and the strong atomic line HeI (3³S–2³P) at 706 nm. A collisional-radiative model was developed to obtain a functional dependance of intensity ratio on the impurity level, at a given reduced electric field. In connection, an experimental study was performed to investigate the influence of gas flow rate on a closed chamber helium DBD (Ivković et al. 2022). Namely, the aim of the experiment was to investigate the presumed connection between the gas flow rate and the impurity level, and consequential change of the discharge operation. Using the abovementioned spectroscopic method, a strongly non-linear decrease of impurities concentration with increasing working gas flow rate was observed.

References

- Brandenburg R. et al., 2019 *Plasma Process. Polym.* **16**, 1
Martens T., Bogaerts A., Brok W. J. M. and Van Dijk J., 2010, *Appl. Phys. Lett.* **80** 091501
Wang Y and Wang D., 2005, *Phys. Plasmas* **12** 023503
Zhang Y., Ning W. and Dai D. 2019 *J. Phys. D. Appl. Phys.* **52** 045203
Ivković S.S., Cvetanović N. and Obradović B.M. 2022 *Plasma Sources Sci. Technol.* **31** 095017

MEASUREMENT OF THE VELOCITY OF THE PLASMA JET APPEARING FROM A WALL STABILIZED ARC

LAZAR GAVANSKI , NATAŠA SIMIĆ  and STEVICA DJUROVIĆ 

*University of Novi Sad, Faculty of Sciences, Department of Physics,
Trg Dositeja Obradovića 4, 21000 Novi Sad, Serbia
E-mail lazar.gavanski@df.uns.ac.rs*

Abstract. In this paper we report results of argon plasma jet velocity measurements. The jet is formed at atmospheric pressure.

1. INTRODUCTION

High temperature plasma jets are used for various material productions and processing, for example for synthesis of new materials, cutting and welding, plasma sintering (Spores and Pfender 1989), producing carbon nanotubes (Hahn et al. 2004), plasma-aided metallurgy, industrial plasma chemistry, hardening and nitriding of steels (Belevtsev et al. 2006), or material transformation such as melting, vaporization, and also applications in nanomaterial fabrication (Kim and Kim 2019). In this experiment, an argon plasma jet was produced by using a modified wall stabilized electric arc. For the application of plasma jets, some parameters, such as plasma temperature and jet velocity, are very important. Here we report the plasma jet velocity measured at atmospheric pressure.

2. CURRENT PULSE SOURCE

The basic plasma source is an atmospheric pressure wall stabilized arc (Nikolić et al. 2004). The arc channel, 5 mm in diameter and 70 mm in length, is formed by six copper discs, 7.1 mm in thickness. The discs are separated by 0.5 mm thick Teflon gaskets and were cooled by water. Pure argon is introduced into the arc channel through holes in tungsten electrodes with a flow rate of 3 l/min. The wall stabilized arc is usually used with closed ends behind the electrodes in direct current (DC) regime, with a current of 30 A. This current provides a plasma with electron temperatures between 10000 and 11000 K and electron densities of a few

times 10^{16} cm^{-3} (Djurović *et al.* 1997, 2002). In that case, the plasma column is formed between the electrodes. For the purpose of this experiment, the end behind the hollow anode is opened and high current pulses are applied. During the pulses, a two cm long plasma jet appeared on the open side of the wall stabilized arc (Ćirišan *et al.* 2006). The block scheme is given in Fig. 1a. A DC current source is connected to the arc via a diode, in order to protect the DC power supply from high current pulses. High current pulses, with a current maximum of 180 A, are obtained from the civil AC network of 220 V by using an appropriate high current switch and a trigger unit. Every 16th of the 50 Hz cycle was used to produce a high current pulse. The current intensity (Fig. 1b) was controlled by a current limiting resistor. In that case, the repetition rate of high current pulses was 3.13 Hz. The electron temperature in the plasma jet varied between 9400K and 10200 K during the plasma life (Ćirišan *et al.* 2006). The current pulses were controlled by means of a Rogowski coil and a digital oscilloscope.

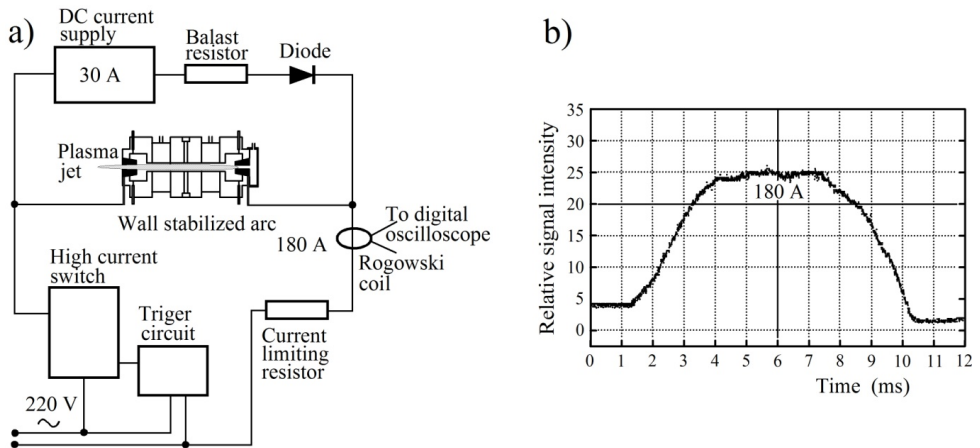


Figure 1: a) Block scheme of the electrical circuit and b) High current pulse.

3. JET VELOCITY MEASUREMENTS

For jet velocity measurements, the optical system shown in Fig 2 was assembled. Optical signals are led to the digital oscilloscope through an optical fiber and a photomultiplier. The signals are taken at two positions with a distance of 1 cm between them. Precise positioning of the end of the optical fiber is performed by using a movable table.

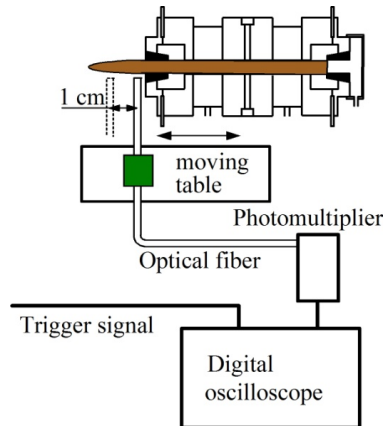


Figure 2: Optical system for velocity measurements.

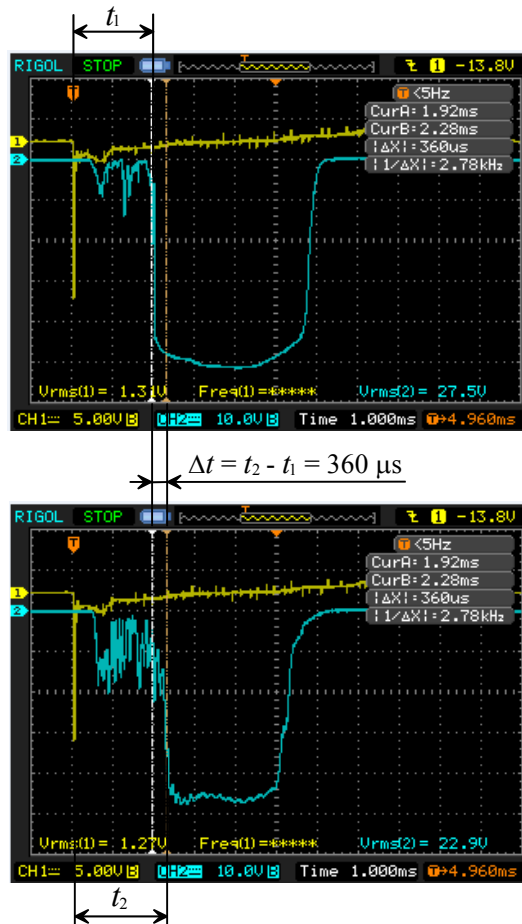


Figure 3: Optical signals from the digital oscilloscope.

Figure 3 shows the shape of the signals received from the optical fiber. The first signal is obtained when the optical fiber is positioned closer to the anode, while the second one is obtained when the optical fiber is positioned 1cm further from the anode. From the first signal it can be seen that the life time of the plasma jet outside of the plasma channel is about 4 ms.

The time difference between the beginning of the rise of the signal in the first and the second position of the optical fiber, $\Delta t = t_2 - t_1 = 360 \mu\text{s}$, is the time for which the front of the plasma jet passes the distance $\Delta s = 1\text{cm}$. The times t_1 and t_2 are measured relative to the trigger signal. The trigger signal is obtained by the Rogowski coil which is positioned in the high pulsed current circuit (Fig. 1a). This signal gives the information on the start of the high current pulse. Based on these data, the calculated velocity of plasma jet propagation is $v = \Delta s/\Delta t = 27.78 \text{ m/s} = 100 \text{ km/h}$. The estimated experimental error is around 10%.

Acknowledgement

The authors thank the Ministry of Science, Technological Development and Innovation of Republic Serbia for support under Grants No. 451-03-66/2024-03/200125 & 451-03-65/2024-03/200125

References

- Belevtsev A. A., Chinnov V. F., Isakaev E. Kh., 2006, *Plasma Sources Sci. Technol.*, **15**, 450-457.
- Ćirišan M., Djurović S., Mijatović Z., Vujičić B., Kobilarov R., 2006, *J. Res. Phys.*, **30**, 95-102.
- Djurović S., Mijatović Z., Kobilarov R., Konjević N., 1997, *J. Quant. Spectrosc. Radiat. Transfer*, **57**, 695-701.
- Djurović S., Nikolić D., Mijatović Z., Kobilarov R., Konjević N., 2002, *Plasma Sources Sci. Technol.*, **11**, 95-99.
- Hahn J., Han J. H., Yoo J-E., Jung H.Y., Suh J.S., 2004, *Carbon*, **42**, 877-883.
- Kim K. S., Kim T. H., 2019, *J. Appl. Phys.*, **125**, 070901 p. 1-26.
- Nikolić D., Djurović S., Mijatović Z., Kobilarov R., Vujičić B., Ćirišan M., 2004, *J. Quant. Spectrosc. Radiat. Transfer*, **86**, 285-298.
- Spores R., Pfender E., 1989, *Surf. Coat. Technol.*, **37**, 251-270.

THE MEASUREMENT OF PULSED GAS DISCHARGE PARAMETERS BY MEANS OF Fe I LINES IN ARGON AND ARGON-HYDROGEN MIXTURE

JOVICA JOVOVIĆ 

*Faculty of Physics, University of Belgrade – Studentski trg 12-16, 11000 Belgrade,
Serbia*

E-mail jjovica@ff.bg.ac.rs

Abstract. In this study, the optical emission spectroscopy (OES) is used to measure the pulsed atmospheric pressure gas discharge parameters in argon and argon-hydrogen mixture. The discharge source has a needle-to-cylinder configuration (NTC). When the stainless steel cathode (SS) is employed, a numerous metallic lines are identified in the discharge spectra (Cu, Zn, Fe, Cr, V, W) in the 260-800 nm spectral range. The thorough study of electron temperature T_e by means of Fe I lines intensity distribution is done. The addition of hydrogen (3% by Vol.) changed the yield of metallic lines. The results showed that $T_e=7000$ K-9000 K, which was also confirmed using an independent line ratio method. Several, multicomponent, broad Fe I lines are recorded in the scope of this study. The Stark shift of the broadest Fe I line component is used to estimate electron number density N_e in NTC discharge. The N_e results will be compared with Fe I line deconvolution results.

1. INTRODUCTION

The versatile continuous, pulsed and RF gas discharges, in which the excitation/ionization of metal atoms occurs, are used as analytical plasma sources and the environment for plasma-surface interaction. The metallic spectral lines are present also in OES spectra as a result of liquid samples treatment in case of solution-cathode-glow-discharge (SCGD) and in case of low pressure GD source (e.g. Grimm-type cell) for the depth profiling of conductive thin layered surfaces, see reference list in (Jovović 2023).

An atmospheric pressure needle-to-cylinder (NTC) discharge source driven by μ s-pulsed generator unit has been studied by means of OES in our Lab, see e.g. (Jovović and Majstorović 2022, 2024). The NTC discharge structure comprises near-cathode region, negative glow (plasma column) and anode region. Decreasing the gap between metallic cathode and graphite anode results in formation of intensive ionizing near-cathode zone, serving as a stable, reproducible source of excited and ionized metallic particles. In that case, one may use the single-frame-spectra approach on numerous Fe I lines to measure T_e applying the atomic state distribution function (ASDF) which reflects the dependence of the population of atoms and ions on their perspective internal states energy. This means that for each fixed position of the diffraction grating, the spectrum is taken by CCD camera covering 18 nm range in the first diffraction order. In addition, the Fe I lines

recorded at 538.3 nm, 539.3 nm and 542.4 nm, recorded in the second diffraction order, has asymmetric line shape indicating the existence of low- N_e and high- N_e NTC discharge regions. From the shift of broadest Fe I line component, the highest N_e is estimated.

2. EXPERIMENTAL

The schematic drawing of NTC source and experimental setup is shown elsewhere, see e.g. (Jovović and Majstorović 2024). The source consists of needle-type cathode (diameter 4 mm) and a cylindrical graphite anode (diameter 25 mm). In the present study, the cathode is made of stainless steel (2.07 % V, 3.97 % Cr, 14.84 % Mo, 13.84 % W and Fe balance). The pure argon gas (Ar 99.999 %) and argon-hydrogen gas mixture (Ar +3 % H₂ by vol.) are employed. The discharge is driven by pulsed voltage power supply that consist of DC power supply (Kepco, 0-2 kV, 0-100 mA), the bank of capacitors, HV switching unit (MOSFET technology) and rectangular pulses generator (2-999 μ s pulse width, 0.1-100 % duty cycle). During the pulse, the voltage jumps in the range 900-1300 V for 16.7 % duty cycle. The radiation from NTC source was recorded by means of 2 m Ebert type spectrometer (Carl Zeiss, O.P. f/28, an inverse linear dispersion of 0.74 nm/mm) equipped with a thermoelectrically cooled, back-thinned Hamamatsu CCD camera ($T=-10$ °C, 2048 \times 512 pixels, 12 μ m pixel size).

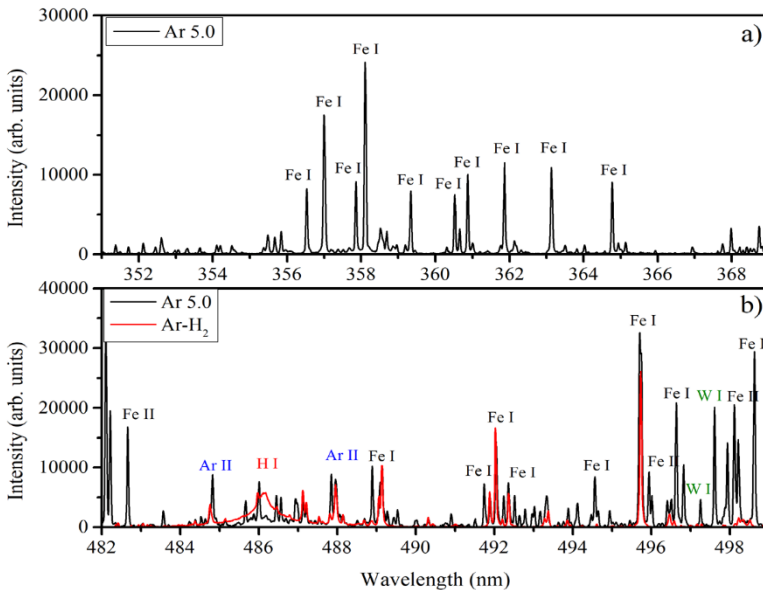


Figure 1: a) The spectrum of Fe I lines in the range 351-368 nm emitted from argon NTC discharge and b) the comparison between NTC spectra in argon and argon-hydrogen mixture in the range 482-499 nm. Experimental conditions: pulse width of 50 μ s, duty cycle of 16.7 %.

3. RESULTS AND DISCUSSION

The example of SS NTC discharge spectrum in the range 351-368 nm is given in Fig. 1a while the comparison between NTC spectra in argon and argon-hydrogen mixture in the range 482-499 nm is shown in Figure 1b. The hydrogen admixture selectively affects the absolute and relative intensities of Fe I lines, which has the impact on the accuracy of analytical results. The results of T_e measurement in both working gases versus the central wavelength of studied CCD spectral range are given in Figure 2. The advantage of single-frame-spectrum approach for T_e measurements is that there is no need for the spectral sensitivity curve. One may notice the influence of hydrogen admixture on distribution and density of points in Figure 2. The T_e values shown in Figure 2 are in agreement with T_e obtained using line ratio method (Jovović 2023).

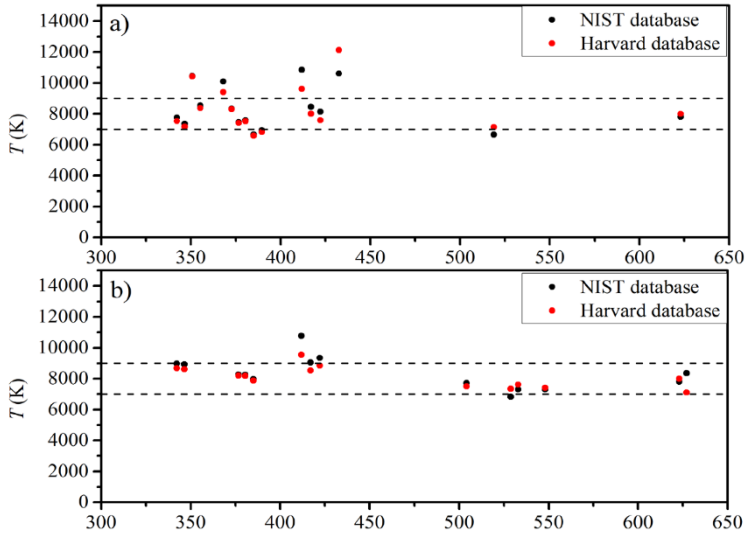


Figure 2: The T_e (K) measured from a single-frame spectrum versus the central wavelength of the studied spectral range in a) Ar and b) Ar+3% H_2 for two A_{ik} databases.

The blue-shifted wing of Fe I 538.3 nm and Fe I 542.4 nm line and the red-shifted wing of Fe I 539.3 nm line, see Fig. 3, indicate the presence of high density plasma (the shifted broadest fit component). Since we work at atmospheric pressure one needs to take into account Van der Waals shift as well. The comparison between experimental shifts measured in (Konjević et al 2002) ($N_e \approx 1 \times 10^{16} \text{ cm}^{-3}$; $T_e = 6000 \text{ K}$) for the studied Fe I lines and Stark shifts determined in our work, is given in Table 1. From Table 1, one may notice that d_e values are one order of magnitude higher than d_m which gives $N_e \approx 1.2 \times 10^{17} \text{ cm}^{-3}$ (Fe I 538.3 nm), $N_e \approx 5 \times 10^{16} \text{ cm}^{-3}$ (Fe I 539.3 nm) and $N_e \approx 8.9 \times 10^{16} \text{ cm}^{-3}$ (Fe I 542.4 nm). Although a rough estimate, these values show a reasonable agreement with the fitting results of Fe I lines in Figure 3, which will be shown during Poster session.

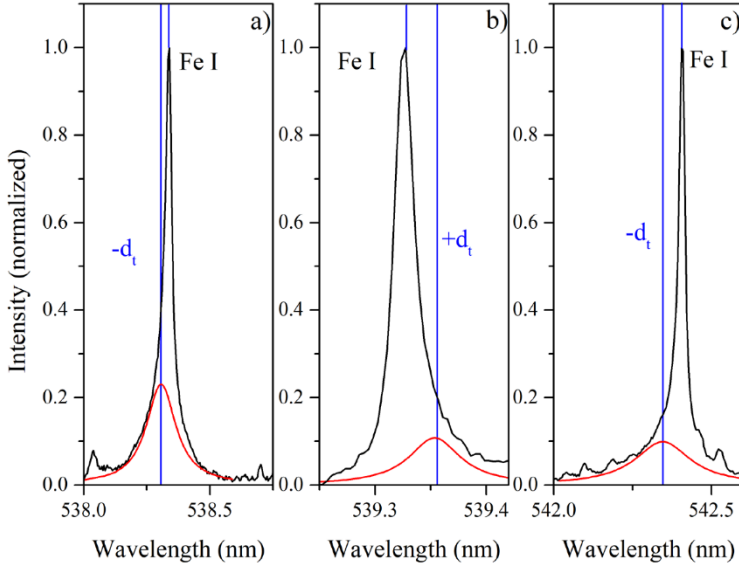


Figure 3: The normalized spectra and a broad fit component of a) Fe I 538.3 nm line, b) Fe I 539.3 nm line and c) Fe I 542.4 nm line recorded from argon and argon-hydrogen NTC discharge.

Line	Transition	d_m (nm)	d_e (nm)
Fe I 538.3 nm	$3d^7 4p - 3d^7 4d$ $z^5G^o - e^5H$	-0.003	-0.0352
Fe I 539.3 nm	$3d^6 4s 4p - 3d^6 4s 5s$ $z^5D^o - e^5D$	0.005	0.0254
Fe I 542.4 nm	$3d^7 4p - 3d^7 4d$ $z^5G^o - e^5H$	-0.007	-0.062

Table 1: The values of Stark shift d_e determined from the broadest Fe I component in Figure 3 and d_m taken from (Konjević et al 2002).

Acknowledgement

This work is supported by the Ministry of Education, Science and Technological Development of the Republic of Serbia.

References

- Jovović, J. : 2023, *J. Anal. At. Spectrom.* **38**, 865.
 Jovović, J., Majstorović, G. Lj. : 2022, *Contrib. Plasma Phys.*, **63**, e202200058.
 Jovović, J., Majstorović, G. Lj. : 2024, *Spectrochim. Acta Part B At. Spectrosc.*, **211**, 106836.
 Konjević, N., Lesage A., Fuhr, J.R. and Wiese, W.L. : 2022, *J. Phys. Chem. Ref. Data*, **31**, 819

LOW-TEMPERATURE PLASMA AND PLASMA-ACTIVATED LIQUIDS IN SOLVING AGRICULTURAL PROBLEMS: EXPERIMENTAL TECHNIQUE

E.M. KONCHEKOV^{1,2}, N.G. GUSEIN-ZADE¹, D.V. YANYKIN¹, L.V. KOLIK¹,
YU.K. DANILEIKO¹, V.I. LUKANIN¹, K.F. SERGEICHEV¹,
I.V. MORYAKOV¹, V.D. BORZOSEKOV^{1,2}, V.V. GUDKOVA^{1,2},
M.E. ASTASHEV¹ and S.V. GUDKOV¹

¹*Prokhorov General Physics Institute of the Russian Academy of Sciences, Russia,
Moscow*

E-mail konchekov@fpl.gpi.ru

²*Peoples Friendship University of Russia (RUDN University), Russia, Moscow*

Abstract. An emerging area of global research focuses on discovering new non-chemical methods to accelerate seed germination, enhance plant growth and development, and increase resistance to various stress factors. Recently, low-temperature plasma (LTP) has shown significant potential in this domain, as evidenced by numerous scientific studies (see Gudkov et al. 2024; Konchekov et al. 2023). Despite its promise, scaling LTP sources and ensuring consistent and reproducible results pose significant challenges. These challenges make it difficult to implement LTP generators directly on plants (see Konchekov et al. 2022) and seeds in practical agriculture, necessitating interdisciplinary efforts across physics, chemistry, and biology. A more scalable alternative to direct LTP application is the use of plasma-activated water (PAW) or plasma-treated solutions (PTS). PAW and PTS are produced by treating water or other solutions with LTP, thereby imparting reactive species into the liquid (Gudkova et al. 2024). This method allows for easier and more uniform application in agricultural practices compared to direct LTP treatment. This report reviews the scientific and technological advancements made at the Prokhorov General Physics Institute of the Russian Academy of Sciences. The Institute has developed innovative LTP generators and methods, conducting extensive studies on both direct LTP treatment of biological objects and indirect treatment using PAW and PTS. These studies have demonstrated improvements in seed germination, plant growth, and resistance to stress factors, showcasing the potential of LTP-based methods to enhance agricultural practices.

This publication has been supported by the RUDN University Scientific Projects Grant System, project №025323-2-000.

References

- Gudkov S.V. et al. : 2024, *Phys. Usp.*, **67**, 194.
Konchekov E.M. et al. : 2023, *IJMS*, **24**, 15093.
Konchekov E.M. et al. : 2022, *Plants*, **11**, 1373.
Gudkova V.V. et al. : 2024, *Plasma Chem. Plasma Process.*, **44**, 305.

MODELLING OF AN ICP DISCHARGE IN OXYGEN WITH FULL KINETICS SCHEME WITH NEWLY CALCULATED VV/VT RATE CONSTANTS

A. KROPOTKIN¹, A. CHUKALOVSKY¹, A. KURNOSOV², T. RAKHIMOVA¹
and A. PALOV¹

¹*Skobeltsyn Institute of Nuclear Physics (SINP MSU), Moscow, Russian Federation
E-mail kropotkin.an14@physics.msu.ru*

²*Troitsk Institute for Innovation and Fusion Research, Troitsk, Russian Federation*

Abstract. In this work, 2D model of inductively coupled plasma discharge in oxygen were developed. The complete scheme of the vibrational kinetics of O₂ molecules was included in the model. The rate constants of the excitation and de-excitation processes for vibrationally excited levels of the O₂ molecule in reactions with O atoms were calculated based on obtained inelastic cross-sections of the O₂ + O system in the ground state for a set of initial vibrational and rotational states of O₂ molecule. These rate constants as well as calculated vibrational electron scattering cross-sections of O₂ were included in model and the results were compared with literature data. The vibrational distribution function was calculated in low-pressure inductively coupled discharge. Spatial distributions of plasma parameters were also obtained.

1. INTRODUCTION

Non-equilibrium low-temperature oxygen plasma has a wide range of applications. The use of such plasma has literally revolutionized many industrial processes such as plasma etching, surface treatment, plasma sterilization and medicine. The study of vibrational excitation and relaxation in oxygen plasma is actively studied area (see, for example, Andrienko 2020) and the experimental methods for detecting the vibrational distribution function in oxygen are rather complex. New experimental data on the distribution of vibrational excitation in stationary and nonstationary discharges in oxygen was recently obtained, see Annušová et al. 2018, and this indicates the need to develop more accurate models to describe the relaxation

kinetics of vibrational excitation under conditions of significant gas dissociation and to adapt these processes into complete self-consistent models.

2. CALCULATION OF VV/VT CONSTANTS

The rate constants of the excitation and de-excitation processes for vibrationally excited levels of the O_2 molecule in reactions with O atoms were calculated based on obtained inelastic cross-sections of the $O_2 + O$ system in the ground state for a set of 8 initial vibrational and 256 rotational states of O_2 molecule, see Palov *et al.* 2024. Calculations of the vibrational energy exchange rate constants between two O_2 molecules were performed as well. The semi-classical coupled state method (see for example Hong *et al.*, 2021, Kurnosov *et al.*, 2023) was used in these calculations. The potential energy surface for the pair O_2 - O_2 was set using an improved Lennard-Jones potential model formulated in Hong *et al.*, 2021. Normalized cross-sections of vibrational excitation of O_2 molecule by electron impact were also obtained and included in our kinetic scheme. Overall, there were included 8 newly calculated first vibrational levels in addition to 25 highest ones taken from Annušová *et al.* 2018 of O_2 molecule for O_2+O collisional system with corresponding electron excitation cross-sections and VV/VT reactions in the ICP discharge kinetic scheme.

3. ICP MODEL

The two-dimensional model used in this work has been described in detail elsewhere, see Kropotkin *et al.* 2019. Briefly, the model includes hydrodynamic equations in drift-diffusion approximation for describing the kinetics of charged (electrons and ions) and neutral plasma particles, Maxwell's equations for electromagnetic fields, and equations for the temperature and neutral gas flow as well as a detailed scheme of plasma-chemical reactions. The full scheme is available in Kropotkin *et al.* 2023. Before calculations for obtaining vibrational distribution function (VDF) in oxygen, the model was tested against theoretical and experimental data in a simple cylindrical chamber. The electron density and temperature distributions were obtained over a wide range of powers deposited in the plasma (100 – 500 W) and compared with literature data, see Kiehlbauch *et al.* 2003. The cylindrical discharge chamber was 16.2 cm in radius and 10.4 cm in height. The antenna was a flat four-turn coil separated from the discharge by a 1.5 cm thick quartz glass. The inductive discharge was simulated under the following conditions: the frequency was 13.56 MHz, the gas pressure was 10 mTorr, the power applied to the coils was from 100 to 500 W, and the gas flow was 33.5 sccm. Part of the calculation results is shown in Fig. 1.

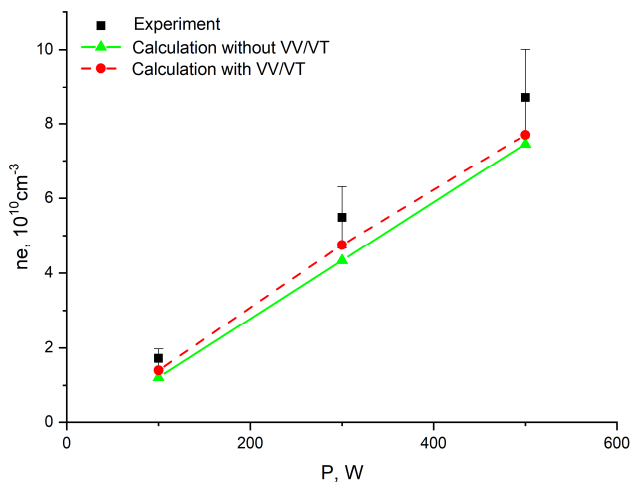


Figure 1: Electron concentration depending on the discharge power, calculated according to a simplified kinetic scheme and taking into account vibrational kinetics, in comparison with the experiment.

After verification of the model on experimental data the next goal was to compare VV/VT rate constants calculated during this work and available in literature, see Coletti et al. 2002, Esposito et al. 2008, Laporta et al. 2013, Lino da Silva et al. 2012. Calculations were carried out with an updated set of rate constants for VV/VT processes with O₂-O₂ molecules, and VT relaxation on O atoms. As can be seen from Fig. 1, the electron concentration remained practically unchanged (red dotted line), the change in values does not exceed 10%. Thus, the addition of a full set of vibrational kinetics did not affect the description of the main plasma characteristics by the model. The main focus of this work was on VDF in ICP discharge conditions. Carrying out such calculations taking into account a new set of excitation and relaxation rate constants will make it possible to clarify the form of the VDF in low pressure ICP plasma and DC glow discharge conditions (future work), and may also raise new questions about new resonant processes involving electronically excited states to explain the peculiarities of the VDF behavior observed in the experiments.

Acknowledgments

This work was supported by the Russian Science Foundation, project no. 23-22-00196.

References

- Andrienko, D. A.: 2020, *J. Chem. Phys.*, **152**, 044305.
 Annušová, A., Marinov, D., Booth, J.-P., Sirse, N., da Silva, M. L., Lopez, B., Guerra, V.: 2018, *Plasma Sources Sci. Technol.*, **27**, 045006.

- Coletti, C., Billing, G. D.: 2002, *Chem. Phys. Lett.*, **356**,14-22.
- Esposito, F., Armenise, I., Capitta, G., Capitelli, M.: 2008, *Chem. Phys.*, **351**, 91-98.
- Hong, Q., Sun, Q., Pirani, F., Valentín-Rodríguez, M. A., Hernández-Lamoneda, R., Coletti, C., Hernández, M. I., Bartolomei, M.: 2021, *J. Chem. Phys.*, **154**, 064304.
- Kiehlbauch, M. W., Graves, D. B.: 2003, *J. Vac. Sci. Technol. A*, **21**, 660–670.
- Kropotkin, A. N., Chukalovsky, A. A., Kurnosov, A. K., Rakhimova, T. V., & Palov, A. P.: 2023, *Materials. Technologies. Design.*, **12**, 177–184.
- Kropotkin, A. N., Voloshin, D. G.: 2019, *Plasma Phys. Rep.*, **45**, 786–797.
- Laporta, V., Celiberto, R., Tennyson, J.: 2013, *Plasma Sources Sci. Technol.*, **22**, 025001.
- Lino da Silva, M., Loureiro, J., Guerra, V.: 2012, *Chem. Phys. Lett.*, **531**, 28-33.
- Palov, A. P., Kropotkin, A. N., Chukalovsky, A. A., Rakhimova, T. V.: 2024, *Tech. Phys. Lett.*, **50**, 43.
- Kurnosov, A., Cacciatore, M., Pirani, F.: 2023, *Chem. Phys. Lett.*, **833**, 140901.

THE FORMATION OF MICRONEEDLES STRUCTURES FROM SILICON USING PLASMA ETCHING IN SF₆/O₂ MIXTURE IN INDUCTIVELY COUPLED PLASMA

VITALY KUZMENKO, ANDREY MIAKONKIKH and
KONSTANTIN RUDENKO

*Valiev Institute of Physics and Technology of Russian Academy of Sciences,
Nakhimovsky av. 34, 117218, Moscow, Russia
E-mail kuzmenko@ftian.ru*

Abstract. The study investigates a method for forming high aspect ratio microneedles structures from silicon using plasma etching at a sample temperature range from -20°C to +20°C in a SF₆/O₂ mixture. The resulting structures are an example of the self-formation of nanostructures due to anisotropic etching in a gas discharge plasma. The high aspect ratio microneedles structures from silicon, called black silicon, has high mechanical, chemical and thermal stability and can be used in wide range of applications, such as an anti-reflective coating: see Ayvazyan et al. 2021, photovoltaics: see Kroll et al. 2012, catalysts: see Fan et al. 2020. In this work surface morphology of the resulting structures, the autocorrelation function of surface features, and reflectivity were studied depending on the process parameters - the composition of the plasma mixture, temperature and other discharge parameters (radical concentrations). The change in the O/F concentration ratio of radicals explains the mechanism of needle formation. A novel approach has been studied to reduce the reflectance using conformal bilayer dielectric coatings deposited by atomic layer deposition. The reflectivity of the resulting black silicon was studied in a wide spectral range from 400-900 nm. As a result of the research, technologies for creating black silicon on silicon wafers with a diameter of 200 mm have been proposed, and the structure formation process takes no more than 5 minutes. Mean reflectance coefficient calculated in range 350-800 nm reaches <1%.

References

- Ayvazyan G.Y., Katkov M.V., Lebedev M.S., et al : 2021, *J. Contemp. Phys.*, **56**, 240.
Fan Z., Cui D., Zhang Z., et al : 2020, *Nanomaterials*, **11**, 41.
Kroll M., Otto M., Käsebier T., et al : 2012, *SPIE*, **8438**, 843817.

INVESTIGATING THE THERMAL PROFILE OF AN ATMOSPHERIC PRESSURE ARGON PLASMA JET ON A CONDUCTIVE AND INSULATING MESH SURFACE

JAMES LALOR¹ and VLADIMIR MILOSAVLJEVIĆ^{1,2} 

¹*School of Physics, Clinical and Optometric Sciences, Technical University of Dublin, Dublin, Ireland*
E-mail james.lalor@tudublin.ie

²*Faculty of Physics, University of Belgrade, Serbia*
E-mail vladimir@ff.bg.ac.rs

Abstract. Atmospheric pressure nonthermal plasmas hold great promise for applications in environmental control, energy conversion, and material processing. This study examines the interaction between an Argon atmospheric pressure plasma jet (APPJ) and both insulating and conducting mesh surfaces. The dielectric barrier discharge APPJ operated at a voltage range of 8 kV and a frequency of 21 kHz. Multiple studies have investigated the interaction between an atmospheric pressure plasma jet directed perpendicularly onto both dielectric and conductive flat surfaces. These studies reported that the jet exhibits a laminar flow which spreads radially from the point of impact. The highest temperature is observed at the central impact zone, with a radial temperature gradient decreasing outward due to the jet expanding along the planar surface and the associated heat dissipation. This study employs a novel technique by treating a mesh substrate with 0.8 mm x 0.8 mm openings so the gas plume can partially pass through the surface. This allows for mapping the thermal interaction between the APPJ and the substrate, enabling a thermal crosssection of the jet plume to be studied. A series of experiments were performed to investigate how different materials, such as metals and polymers, respond to thermal energy from the APPJ in terms of temperature rise, heat distribution, and cooling rates. The distance between the APPJ nozzle outlet and the mesh surface (standoff distance) was varied between 0 to 70 mm, and the corresponding thermal profile was recorded to determine an optimal standoff distance for the APPJ to prevent surface damage due to overheating. A second variable, treatment duration, was also examined. By fixing the standoff distance and varying the treatment duration from 0 to 240 seconds, the thermal data for various contact times were studied. For this research, an FLIR i7 thermal camera with a thermal resolution of 140 x 140 pixels was used.

The research demonstrated that closer standoff distances increased the energy deposition with the material properties significantly influencing temperature dynamics.

STARK WIDTH ESTIMATES FOR THE MOST PROMINENT Ce II SPECTRAL LINES IMPORTANT FOR ASTROPHYSICAL INVESTIGATIONS

ZLATKO MAJLINGER^{1,2,3} 

¹*Astronomical Observatory, Volgina 7, 11060 Belgrade 38, Serbia*

²*ES "I.G. Kovačić", Kralja Tomislava 18, 51326 Vrbovsko, Croatia*

³*ES "Vladimir Gortan", Prilaz Vladimira Gortana 2, 51000 Rijeka, Croatia*

E-mail zlatko.majlinger@gmail.com

Abstract. Stark widths for the most intensive Ce II lines were estimated using the property of regularity and systematic trends found to exist among the Stark width parameters. Estimating formulae and temperature function were taken from nonlinear regression and cluster analysis confirmed by machine learning method (Majlinger and Traparić, 2023), which proved to be more promising in this area of investigations than previously used similar formulae (for example, Cowley, 1971). Predicted accuracy of this approach, according to comparison with experimental data, is in a range between $\pm 30\%$ and $\pm 50\%$, although predicted accuracy for using random forest algorithm with equivalent results is found to be around $\pm 20\%$ (Majlinger and Traparić, 2023). Ce II lines can be important in spectral investigation of Ap type of stars, where rare-earth elements are mostly overabundant.

References

Cowley, C. R. (1971). *The Observatory*, Vol. **91**, p. 139-140

Majlinger, Z., & Traparić, I. (2023). *Contrib. Astron. Obs. Skalnaté Pleso*, **53**(3), 58-71.

STARK WIDTHS OF SEVERAL Te II SPECTRAL LINES FOR INVESTIGATION OF ASTROPHYSICAL SPECTRA

ZLATKO MAJLINGER^{1,2,3} , MILAN S. DIMITRIJEVIĆ¹  and
VLADIMIR A. SREĆKOVIĆ⁴ 

¹*Astronomical Observatory, Volgina 7, 11060 Belgrade 38, Serbia*

²*ES "I.G. Kovačić", Kralja Tomislava 18, 51326 Vrbovsko, Croatia*

³*ES "Vladimir Gortan", Prilaz Vladimira Gortana 2, 51000 Rijeka, Croatia*
E-mail zlatko.majlinger@gmail.com

⁴*Institute of Physics Belgrade, UB, P.O. Box 57 11001, Belgrade, Serbia*

Abstract. Electron-impact widths for eight Te II spectral lines with energy levels which can be found in NIST database (Kramida et al, 2023) were calculated using modified semiempirical method (Dimitrijević and Konjević, 1980), with a purpose to be useful in investigation of astrophysical spectra. Line and multiplet factors were taken from Shore and Menzel (1965), wherever it was necessary, while matrix elements were obtained using Bates-Damgaard approximation (Bates i Damgaard, 1949), as it is usual in modified semiempirical approach. In astrophysical domain, tellurium is important for study of nucleosynthesis processes of creation heavy elements in star interior.

References

- Bates, D. R., & Damgaard, A. 1949. Philosophical Transactions of the Royal Society of London. Series A, Mathematical and Physical Sciences, **242** (842), 101-122.
- Dimitrijević, M. S., & Konjević, N. 1980., **24**, 451-459.
- Kramida, A., Ralchenko, Y., & Reader, J. 2023. NIST atomic spectra database (ver. 5.11). National Institute of Standards and Technology.
- Shore, B. W., & Menzel, D. H. 1965., **12**, p. 187

RF BREAKDOWN IN ARGON AT LOW-PRESSURES: EXPERIMENT AND MODELLING

JELENA MARJANOVIĆ¹ , DRAGANA MARIĆ¹ , MARIJA PUAC¹ ,
ANTONIJE ĐORĐEVIĆ²  and ZORAN LJ. PETROVIĆ² 

¹*Institute of Physics, University of Belgrade, Pregrevica 118, 11080 Belgrade, Serbia*

E-mail sivosj@ipb.ac.rs

²*Serbian Academy of Sciences and Arts, Kneza Mihaila 35, 11001 Belgrade, Serbia*

Abstract. We present results for RF breakdown in argon discharge at low pressures, obtained experimentally and using Monte Carlo code for a frequency of 13.56 MHz. Experimental measurements are conducted at an interelectrode distance (d) of 0.7 cm for pressures (p) ranging from 0.9 to 29 Torr. In our experiment, we employ a technique that eliminates issues related to displacement current. This technique is based on the use of a balanced capacitive bridge, enabling precise breakdown detection and time-domain tracking.

1. INTRODUCTION

Low-temperature plasmas generated using RF power in the frequency range of 1 to 100 MHz find widespread applications in various industrial processes. These applications, such as plasma etching and deposition in the integrated circuit industry, electric propulsion in aerospace, materials processing, surface cleaning, and thin-film deposition, are closely tied to the breakdown itself and the underlying processes. However, when it comes to the breakdown in RF fields, there have been limited attempts to correlate experimentally measured parameters with elementary processes, as is commonly done in the case of direct current (DC) breakdown and discharge. Despite attracting considerable attention from researchers in the past period, the study of RF breakdown faces challenges due to the need to isolate minute breakdown currents from the displacement current. In this study, we present results from RF breakdown measurements at 13.56 MHz in argon and compare them with results from the Monte Carlo simulation, aiming to provide insights that can enhance the efficiency and reliability of these industrial processes.

2. EXPERIMENTAL SET-UP

Breakdown is achieved between two plane-parallel copper electrodes placed inside a tightly fitting borosilicate glass cylinder. This arrangement prevents

long-path electric discharges towards the metal parts of the housing while allowing the recording of the emission intensity distribution along the axis of the chamber. The electrodes' diameter is 3.5 cm, and their gap is adjustable. For this work, it was set at 0.7 cm. One electrode is excited, while the other remains at zero potential. The discharge chamber is housed in a special metal box to eliminate interference with the extremely sensitive balance of the capacitive bridge. The box has only openings for recording the emission distribution using an ICCD camera (Figure 1a). The chamber is first evacuated to low pressure ($<10^{-6}$ Torr), and argon is introduced into the system and kept at a slow flow rate to maintain the required gas purity during measurements. Electrodes were treated and stabilized using an argon discharge at 1 Torr for approximately 60 minutes. The treatment is done at a pressure corresponding to conditions in the left-hand branch of the breakdown curve, where ions receive enough energy from the electric field to reach electrodes and remove impurities and oxides from electrode surfaces through bombardment. Throughout the electrode treatment, we monitored changes in the discharge voltage. The process is terminated when further treatment no longer results in a change in the discharge voltage.

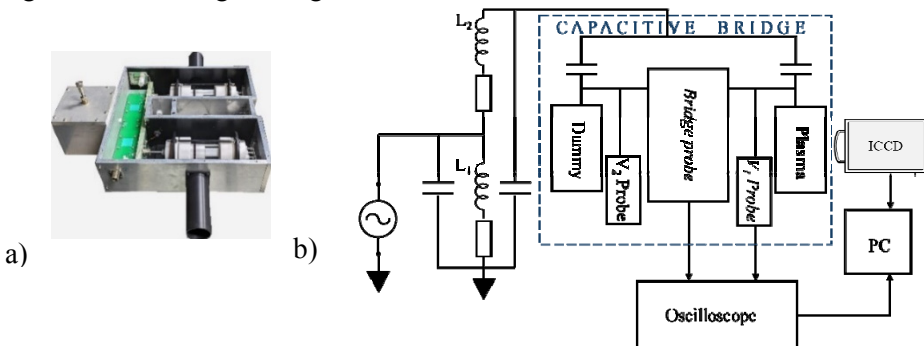


Figure 1: a) Photo of the capacitive bridge, b) schematic of the experimental set-up.

The schematic of the experimental set-up is shown in Figure 1b. The entire electrical circuit is housed in an aluminum box to protect against interference and losses. We utilized a Rigol DG5102 RF signal generator for the power source, which provides a sine signal set to a frequency of 13.56 MHz. This signal is then amplified by a linear amplifier, specifically the Barthel RFA-0.1/50-100 BOO. Coils L_1 and L_2 are part of an inductive coupling and represent a resonant transformer that operates exclusively at 13.56 MHz. This resonant transformer raises the generator voltage to the kilovolt range. The capacitive bridge comprises four capacitors, two of which are physically identical discharge chambers. While the 'Dummy' remains inactive and functions solely as a capacitor, the 'Plasma' acts as the active chamber where the discharge is observed. We monitor the voltage signal from the bridge diagonal using the 'Bridge probe'. Before taking measurements, we calibrated probe V_1 , which we use to measure the voltage on the discharge chamber. When the bridge is in balance, the signal from the diagonal is

minimal. We detect the moment of breakdown in the gas using an oscilloscope (Keysight Infiniium DSO9104A). The amplitude of the voltage signal from the diagonal of the bridge increases sharply. In other words, the bridge suddenly goes out of balance due to a change in impedance when the breakdown occurs.

3. RESULTS AND DISCUSSION

Figure 2 compares radio frequency (RF) breakdown curves for argon discharge obtained at 13.56 MHz. The curves are derived from measurements (represented by full circles) and Monte Carlo simulations (represented by open circles). The breakdown curve, obtained at the electrode distance of 0.7 cm, covers a range from 0.65 Torr cm to 20 Torr cm. Monte Carlo (MC) code was described and explained elsewhere (Raspopović et al., 1999). These simulations were carried out with only electrons, and their movement is determined by the external electric field (Puač, et al., 2018). The set of cross-sections consists of momentum transfer, two excitations and an ionization cross-section and has been tested for argon swarms in our group (Petrović et al., 2007). Physical processes on the electrodes and the effects of the heavy particles were modelled by factors of reflection $R = 0.4$ and $\gamma = 0.07$. These values were chosen to modify the breakdown voltage curve to better correspond to the measured curve. Breakdown points were determined in two ways. For the right-hand branch, pressure was fixed, and voltage was slowly increased until the number of electrons in time didn't get a positive slope (Savić et al., 2011). Similarly, points in the left-hand branch were determined by fixing the voltage and increasing the pressure until the breakdown occurred. The RF breakdown curves are expected to have the characteristic 'S' shape. However, for small interelectrode distances the curves are distorted (Lisovskiyy, Yegorenkov, 1998), in such a way that the left-hand branch is somewhat flattened, which is also observed in both of our curves (experiment and MC).

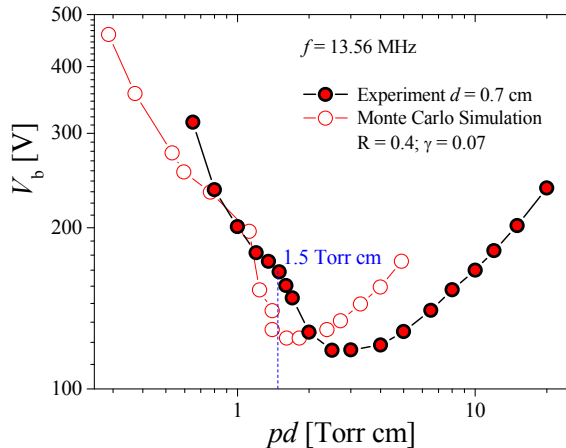


Figure 2: RF breakdown curves for Ar discharge at $f = 13.56$ MHz. Comparison of experimental results for electrode gap of 0.7 cm (full circles) and MC simulation (open circles) when the secondary electron yield is $\gamma = 0.07$, and the reflection is assumed to be $R = 0.4$.

Analyzing the breakdown behavior at high pd values, we observe that the breakdown voltage decreases with decreasing pressure (p) (the electrode gap (d) is fixed). At $pd+ = 2.5$ Torr cm, the minimum breakdown voltage occurs. Beyond this point, the breakdown voltage increases as pressure decreases further. In the left-hand branch of the curve, an inflexion point appears at 1.5 Torr cm. This inflexion can be attributed to conditions where the amplitude of electron oscillations in the RF field becomes comparable to the interelectrode distance (d), leading to increased losses. From this point on, the breakdown is conditioned by a balance between losses at the surface of electrodes and the gain of energy from the increasing field and numerous electrons crossing the threshold for ionization. Thus, the secondary electron yield at the electrodes becomes significant.


Acknowledgements

This research was supported by the Science Fund of the Republic of Serbia, Grant No. 7749560, project EGWin. Zoran Lj. Petrović is grateful to the SASA project F155 and Antonije Đorđević to the project F133.

References

- Burm, K.T.A.L.: 2005, *Contrib. Plasma Phys.* **45**, 54.
Conrads H., Schmidt M. : 2000, *Plasma Sources Sci. Technol.* **9**, 441.
Mahony C. M. O., Gans T., Graham W. G., Maguire P. D., Petrović Z. Lj. :2008, *Appl. Phys. Lett.*, **93**, 011501.
Makabe, T., Petrovic, Z. Lj.: 2006, *Plasma Electronics: Applications in Microelectronic Device Fabrication (1st ed.)*, CRC Press.
Lee H.C.: 2018, *Appl. Phys. Rev.* **5**, 011108.
Lisovskiy A. V., Yegorenkov V. D.: 1998, *J. Phys. D, Appl. Phys.*, **31**, 3349.
Korolov I., Donkó Z. : 2015, *Phys. Plasmas*, **22**, 093501.
Petrović Z. Lj., Šuvakov M., Nikitović Ž., Dujko S., Šašić O., Jovanović J., Malović G., Stojanović V.: 2007, *Plasma Sources Sci. Technol.*, **16**, S1–S12.
Puač M., Marić D., Radmilović-Radjenović M., Šuvakov M., Petrović Z. Lj.: 2018, *Plasma Sources Sci. Technol.*, **27**, 075013.
Raspopović Z. M., Sakadžić S., Bzenić S. A., Petrović Z. Lj.: 1999, *IEEE Trans. Plasma Sci.* **27**, 1241.
Savić M., Radmilović-Radjenović M., Šuvakov M., Marjanović S., Marić D., Petrović Z. Lj.: 2011, *IEEE Trans. Plasma Sci.* **39**, 2556.

THE EFFECT OF ACIDS ON PIG BONE ESTIMATED BY LIBS

MILICA MARKOVIĆ , DRAGAN RANKOVIĆ  and
MIROSLAV KUZMANOVIĆ 

*Faculty of Physical Chemistry, University of Belgrade, Studentski trg 12 - 16,
11158 Belgrade, Serbia.
E-mail milica.markovic@ffh.bg.ac.rs*

Abstract. The effect of sulfuric, hydrochloric, hydrofluoric and acetic acid on pig shoulder bone was investigated by LIBS (Laser-Induced Breakdown Spectroscopy). LIBS is a valuable tool in forensic science for the analysis of pig bones, which are often used as analogs for human bones in forensic anthropological studies and can be subjected to various experimental conditions to simulate forensic scenarios. In practice, forensic scientists often encounter the destruction of evidence by mineral acids. The ratio of Ca II (364.441 nm) to Ca I (370.603 nm) lines in LIBS spectra is used to obtain information about bone hardness, which is influenced by its mineral content and density (see Fig. 1). Selected lines are much less susceptible to self-absorption than resonant lines. Acids significantly affect the hardness and structural integrity of pig shoulder bone by dissolving mineral components, especially hydroxyapatite, and degrading organic matrices such as collagen.

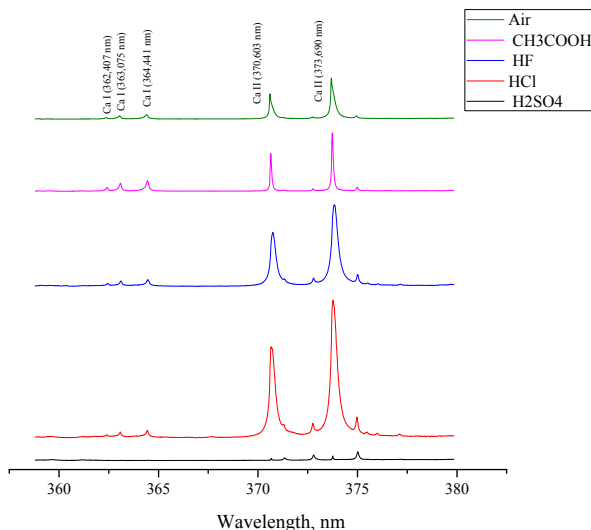


Figure 1: LIBS spectra of pig shoulder bone in 0.1 M solutions of acids

References

- Kasem, M.A., Russo, R.E. : 2011, *J. Anal. At. Spectrom.*, **26**, 1733.
Abdel-Salam, Z.A., Galmed, A.H. : 2007, *Spectrochim. Acta Part B At. Spectrosc.*, **62**, 1343.

FLUOROCARBON POLYMERIZING PLASMAS ETCHING PROCESSES FOR STRUCTURES OF MICRELECTRONICS

A. MIAKONKIKH, V. KUZMENKO and K. RUDENKO

*Valiev Institute of Physics and Technology, RAS, Nakhimovskiy av. 34, 117218,
Moscow, Russia
E-mail miakonkikh@ftian.ru*

Abstract. Precision etching of microstructures with minimal levels of introduced contaminants and electrically active defects is a key technology for creating transistor structures for ICs with process nodes below 28 nm. To ensure high accuracy in the transfer of the lithographic pattern and the verticality of the walls, it is necessary to implement an anisotropic etching mode with passivation of the walls. One of the approaches to this problem is the use of fluorocarbon plasma, which, on the one hand, provides a sufficient concentration of atomic fluorine, and on the other hand, effective passivation of the side walls due to the polymerization of fluorocarbon molecular radicals. The reactive ion etching of silicon through the mask of electron was investigated experimentally in ICP plasma with substrate biasing in the SF₆/C₄F₈ feeding mixture for different gas compositions. To understand the kinetics of film formation and etching, concentrations of neutral particles were evaluated using plasma optical emission spectroscopy. Electron temperature and electron density were measured by the Langmuir probe method, see Rudenko, 2007. A high etching selectivity equal to 8 was obtained for the etching process. As a result, the silicon nanowires with critical size of 8 nm on Silicon-On-Insulator wafer were made and investigated. The distribution of lattice displacement defects in surface layer caused by ion bombardment during plasma etching was simulated by Monte Carlo model. Also growth rates of films or etching of surfaces of functional layers from Ar/CF₄/H₂ plasma were investigated, see Kuzmenko, 2023. The polymerizing ability is determined by the CF₄/H₂ gas ratio, and Ar allows optimization of physical sputtering. At high CF₄ proportions in the plasma, the deposition rate is determined by the concentration of fluorocarbon radicals in the plasma. Understanding the kinetics of the fluorocarbon film deposition process enables optimization of the cyclic atomic layer etching process. The study was supported by the RSF grant no. 23-29-00771, <https://rscf.ru/en/project/23-29-00771/>.

References

Rudenko, K., Miakonkikh, A., Orlikovsky, A., et al: 2007, *Russ. Microel.*, 2007, 36(1), 14
Kuzmenko, V., Miakonkikh, A., Rudenko, K.: 2023, *High Energy Chem*, **57**, S100

CATHODE SHEATH DIAGNOSTICS BY INTEGRAL END-ON OPTICAL EMISSION SPECTROSCOPY IN AN ANALYTICAL GLOW DISCHARGE SOURCE IN ARGON

NIKODIN V. NEDIĆ¹ , NIKOLA V. IVANOVIĆ² , IVAN R. VIDENOVIĆ¹ ,
DJORDJE. SPASOJEVIĆ¹  and NIKOLA KONJEVIĆ^{1,3} 

¹University of Belgrade, Faculty of Physics, P.O.Box 44, 11001 Belgrade, Serbia

²University of Belgrade, Faculty of Agriculture, Nemanjina 6, 11080 Belgrade, Serbia

³Serbian Academy of Sciences and Arts, Kneza Mihaila 35, 11000 Belgrade, Serbia

E-mail ivan.videnovic@ff.bg.ac.rs

Abstract. Most conventionally used glow discharge sources for surface and bulk analysis of solid samples by optical emission and/or mass spectroscopy (OES/MS) follow the classical Grimm design, with a plane sample (cathode) adjacent to the hollow cylindrical anode. In such a design, OES is enabled from the anode end, with an integral end-on view of the entire discharge, i.e. both cathode sheath and negative glow. It has been noticed, though, that the OES of argon lines show asymmetrically broadened profiles with complex structures on the red wings. In this work, we show that these complex end-on wing broadening structures originate from the cathode sheath radiation, dominated by the quadratic Stark effect-induced splitting and shifting of argon line components in a macroscopic electric field, produced by the externally applied voltage. The cathode sheath electric field decreases from the maximum strength F_{\max} near the cathode to nearly zero at the sheath end and the beginning of the negative glow. Using the modified Grimm source that enables OES observations both from the end and from the side of the discharge axis, we compared maximum Stark component shifts $\Delta\lambda_s$ recorded side-on nearby cathode where the maximum field F_{\max} is attained, with the shifts of end-on recorded wing structures $\Delta\lambda_e$. For four neutral argon Ar I lines, 517.8 nm, 521.0 nm, 537.3 nm, and 541.0 nm, comparing the shifts $\Delta\lambda_s$ and $\Delta\lambda_e$ for different discharge conditions (pressure, voltage, current) and cathode materials, we found a stable linear correlation $\Delta\lambda_s = k \cdot \Delta\lambda_e$ for each individual spectral line, and for the whole set of four Ar I lines, with latter being $k = 1.129 \pm 0.011$. Provided that the side-on shifts $\Delta\lambda_s$ for each individual Ar I line are calibrated against the independently measured electric field and the F_{\max} is known, this correlation can be used for the estimation of F_{\max} in standard analytical glow discharge sources with end-on optical observations available only. In turn, assuming linear regression of the electric field from F_{\max} to zero towards the sheath end, its thickness d_c can be estimated also, providing important input parameters for discharge modeling and design.

THE USE OF THERMOELECTRIC RADIATION DETECTORS FOR HEAT FLUX MEASUREMENTS IN SHOCK-TUBES WITH GAS IONIZATION

S.A. PONIAEV¹, P.A. POPOV¹, N.A. MONAKHOV¹, T.A. LAPUSHKINA¹ and
M.A. KOTOV²

¹*Ioffe Institute, Polytekhnicheskaya str. 26, 194021, Saint-Petersburg, Russia*
E-mail serguei.poniaev@mail.ioffe.ru

²*Ishlinsky Institute for Problems in Mechanics of the Russian Academy of Sciences,*
Prospekt Vernadskogo, 101-1, Moscow 119526, Russia

Abstract. Investigations of the ionized gases properties and their interaction with solid surfaces in aerospace applications is a key problem of modern re-entry technology [1,2]. Experimental investigations today conducted using pulsed gas-dynamic facilities, in particular shock tubes. Shock tubes are effective tools for creation and investigation of high-speed gas flows with the high stagnation pressure and temperature. The drawback of shock tube is a short working time – maximum test time does not exceed few milliseconds. Also, it should be noted that in the stagnation region of shock-heated gas there is an ionization so the gas has a strong radiation that affects heat fluxes significantly. Serious requirements are imposed to the diagnostic tools used for studying supersonic flows in terms of minimum dimensions, mechanical and thermal strength, sensitivity and noise immunity and a short response time. In this work we present thermoelectric heat flux sensors based on the artificially anisotropic film obtained by vacuum deposition. These sensors are successfully used in laser systems for measuring the radiation power [Glebov, 1994, Kotov 2021]. The use of such sensors allows us to study heat fluxes in a very hard conditions – for example with the use of inert gas Xenon as a working gas with significant ionization the heat flux of order of 20-30 Mw/m² can be measured.

References

- Glebov V N, Manankov V M, Malyutin A M et al. 1994 Proc. SPIE 2257 225–227.
Kotov M A et al. 2021 Appl. Therm. Eng., v.195, ArtNo: #117143

DETERMINATION OF UNKNOWN ANALYTE CONCENTRATION IN GLASS SAMPLES USING THE LIBS METHOD

ALEKSANDRA ŠAJIĆ , DRAGAN RANKOVIĆ , MIROSLAV RISTIĆ  and MIROSLAV KUZMANOVIĆ 

*University of Belgrade, Faculty of Physical Chemistry, Studentski trg 12-16,
11000 Belgrade, Serbia.*

E-mail aleksandra.sajic@ffh.bg.ac.rs

E-mail dragan@ffh.bg.ac.rs

E-mail ristic@ffh.bg.ac.rs

E-mail miroslav@ffh.bg.ac.rs

Abstract. Laser induced breakdown spectroscopy, based on TEA CO₂ laser, was used for determining the unknown concentration of cadmium and copper in glass samples by calibration curve method. The intensity ratios of the analyte lines and the internal standard were used to construct the calibration curves. An internal standard in the LIBS is typically one of the major components of the sample, such is silicon in glass. The calibration curves of Cd and Cu are shown in Figure 1. Based on the obtained calibration graphs, concentrations of Cd and Cu in three glass samples were determined. Sample 1 contains 359 ppm Cd and 1925 ppm Cu, Sample 2 contains 1250 ppm Cd and 365 ppm Cu and Sample 3 contains 1700 ppm Cd and 1160 ppm Cu. XRF method was used as a control method and results obtained by LIBS showed good agreement with the concentrations determined by XRF.

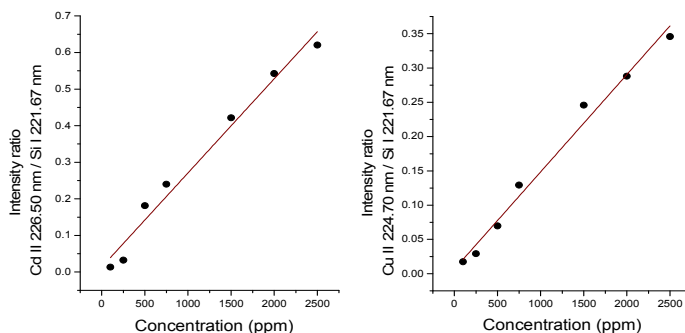


Figure 1: LIBS calibration curves of Cd and Cu

References

- Petrovic J., Savovic J., Rankovic D., Kuzmanovic M. : 2022, *Plasma Chem Plasma Process*, **42**, 519.
Tognoni, E., Cristoforetti, G. : 2015, *Optics & Laser Technology*, 79, pp. 164.

FAST PHOTOGRAPHY IN THE SERVICE OF SPATIALLY AND TEMPORALLY RESOLVED LIBS DIAGNOSTICS OF DOPED TUNGSTEN

BILJANA STANKOV¹ , MARIJANA R. GAVRILOVIĆ BOŽOVIĆ² ,
DRAGAN RANKOVIĆ³ , JELENA SAVOVIĆ⁴  and MILIVOJE IVKOVIĆ¹ 

¹*Institute of Physics, University of Belgrade, Pregrevica 118, 11080 Belgrade, Serbia*

²*Faculty of Engineering, University of Kragujevac, Sestre Janjić 6, 34000 Kragujevac, Serbia*

³*Faculty of Physical Chemistry, University of Belgrade, 11158 Belgrade, Serbia*

⁴*Vinca Institute of Nuclear Sciences, University of Belgrade, Mike Petrovića Alasa 12-16, 11000 Belgrade, Serbia.*

E-mail biljanas@ipb.ac.rs

Abstract. The spectroscopic diagnostic of laser induced plasma is challenged by its spatial inhomogeneity and dynamic evolution, which simultaneously alters plasma parameters and emission of ablated material in plasma plume (Lazic et al. 2006, A. Singh et al. 2010). Those difficulties become more pronounced when conducting spatially and temporally resolved measurements. Choosing appropriate conditions for LIBS, such as delay time, gate width, and observed plasma section is paramount. At atmospheric pressure, plasma tends to stay more localized in the vicinity of the target, with specific flattened shape. In contrast, plasma expanding into low pressure exhibits rapid and pronounced dispersion, potentially causing plasma to move out of the field of view, and/or not being captured completely. This can make determining the time of the maximum plasma emission intensity challenging. In this study influence of different additives in tungsten samples on plasma plume dynamics and expansion is investigated and possible impact on the spectroscopic diagnostics is assessed.

Acknowledgements. The research was funded by the Ministry of Science, Technological Development and Innovations of the Republic of Serbia, Contract numbers: 451-03-68/2022-14/200024 and 451-03-65/2024-03/200146, and supported by the Science Fund of the Republic Serbia, Grant no. 7753287 "NOVA2LIBS4fusion".

References

- V. Lazic and S. Jovicevic: 2006, *Spectrochimica Acta Part B: Atomic Spectroscopy*, vol. **61**, no. 7, 856
- A. Singh and P. K. Rai, "Challenges in Diagnostics of Laser-Induced Plasma," *Journal of Physics D: Applied Physics*, vol. **43**, no. 43, p. 434013, 2010.

MEASUREMENTS OF REACTIVE OXYGEN AND NITROGEN SPECIES IN PLASMA ACTIVATED WATER BY MICROWAVE DISCHARGE

DESANKA TOPALOVIĆ , NEDA BABUČIĆ , NIKOLA ŠKORO  and
NEVENA PUAČ 

*Institute of Physics, University of Belgrade, Pregrevica 118, 11080 Belgrade,
Serbia*

E-mail desketop00@gmail.com

Abstract. This study focuses on plasma activated water (PAW), which contains reactive oxygen and nitrogen species (RONS). We compared RONS concentrations in PAW produced by two microwave (MW) plasma sources - a homemade S-wave source and a commercial Sairem S-wave source. The homemade source generated higher and more consistent RONS concentrations over time. Both sources are effective, with the choice depending on whether higher reactive species concentrations are needed.

1. INTRODUCTION

Over the past 20 years, non – equilibrium cold atmospheric plasmas (CAPs) have been applied in medicine for treating medical equipment, cancer cells and dental issues. They have also been used in biology, agriculture, water treatment, and food decontamination (Puač et al. 2018). Treatments can be done directly where CAP is in contact with treated sample or indirectly by using PAW. In direct treatment both short-living and long-living RONS play a significant role in triggering desired mechanisms. When it comes to indirect treatment by PAW only long-living RONS are in contact with treated samples (Bradu et al. 2020). For both direct and indirect types of treatments, various CAP sources are used. They differ in electrode geometry, type and frequency of power/voltage supply, type working gas and gas flow etc. One of the CAPs that are not that often used, especially when it comes to direct plasma treatment of samples, are microwave plasma sources. On the other hand, due to its intense nature and high electron density resulting in increased production and concentration of reactive species, it can be used for production of larger volumes of PAW.

In this study, the concentrations of RONS were measured and their variations over time (days after the treatment) were monitored. Additionally, differences between

two microwave sources (a homemade S-wave source and a commercial Sairem S-wave source) were investigated, and the results are presented below.

2. EXPERIMENTAL SETUP

Water treatments were conducted by using two different microwave plasma sources - inductively coupled (IC) commercial Sairem S-wave source and capacitatively coupled (CC) homemade S-wave source (see Figure 1.). Argon was used as working gas, while the synthetic air was used for cooling of the system. Both gases are controlled by gas flow regulators. Sairem Solid state generator, with an adjustable output power range of 0 – 200 W, serves as a microwave power source. The coaxial cable transmits the microwave power from the generator to plasma sources (in Figure 1. 7a and 7b) very efficiently. To prevent overheating, both sources are cooled by water and air flow. The plasma jet is formed inside the quartz tube and, depending on the operating parameters, can extend outside it. During the treatments plasma plume was in contact with treated water and water was mixed homogeneously by using a magnetic stirrer to ensure even deposition of reactive species from the plasma. Treatments were performed with a power of 40 W for an argon flow of 2 slm, and 50 W for an argon flow of 1 slm and 7 slm. Treatments of 32 ml of deionized water containing 25 mg of ZnO were performed by using (a) Homemade S-Wave source and (b) Sairem S – Wave source. Zinc oxide powder was added to water samples before plasma treatments to keep the pH value of treated water in the range of 5. Treatment time was 10 min and the distance between quartz tube and water surface was 9 mm.

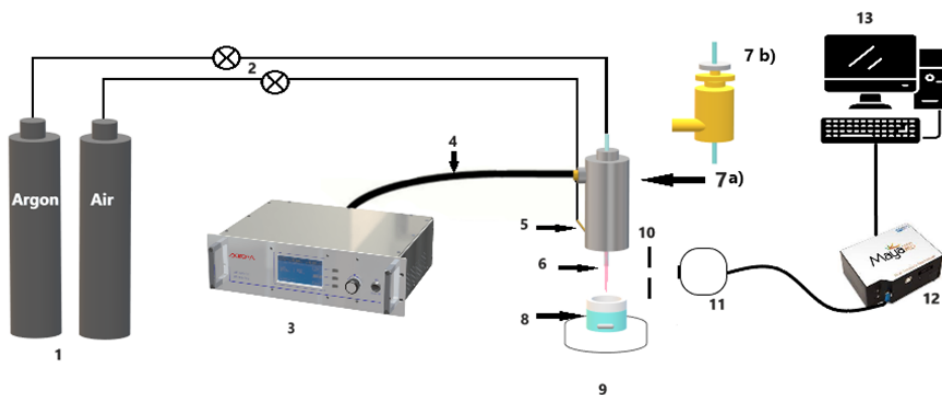


Figure 1. Experimental set up for plasma treatment: 1. Bottles with argon and air; 2. Gas flow regulators; 3. Sairem MW200 generator (0 – 200 W); 4. Coaxial cable; 5. Cooling inlets (air and water); 6. Plasma torch; 7. a) (IC) Sairem S-Wave microwave source, b) (CC) Homemade S-Wave microwave source; 8. Treated liquid; 9. Magnetic stirrer; 10. Holder for optical fiber with a slit of 0.5 mm; 11. Fiber – optic cable.

After the treatment and formation of reactive species in the water, their presence and concentration were determined by using spectrophotometry. Based on monitoring of the dependence of absorbance as a function of the wavelength of the radiation that passed through the analyzed substance, the absorption coefficients were read for all three compounds, at the appropriate wavelengths of 525 nm for nitrites, 357 nm for nitrates and 407 nm for hydrogen peroxide. After the treatment, the stability of reactive species was monitored for a certain period, starting from the day of treatment, by measuring concentration nitrites, nitrates and peroxides. Samples were stored in the refrigerator in the meantime.

3. RESULTS AND DISCUSSION

In Figure 2. we present the time dependence of RONS concentrations in the days after the plasma treatments. Although various combinations of generator power and working gas flow have been tested, the graph shows RONS concentration values for the argon flow of 1 slm and applied power of 50 W. We can see that the concentration of H_2O_2 in treated water obtained by home-made S-Wave is higher than with the commercial Sairem S-Wave. The nitrates and nitrites concentrations are quite similar for both devices. For both devices the concentrations stay almost constant in the days after the treatments.

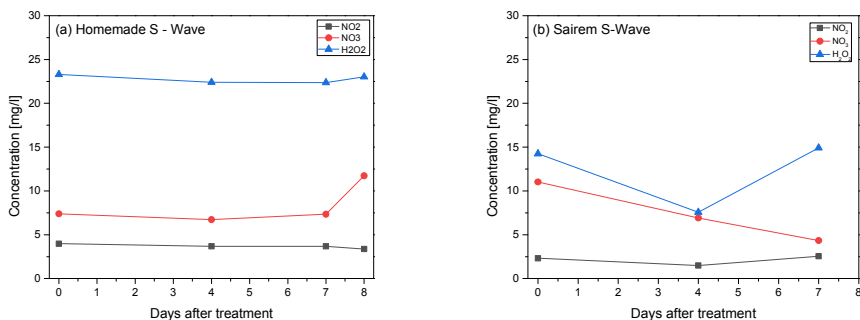


Figure 2: Stability of concentrations of long-living RONS deposited in PAW measured days after the treatment. Treatments of 32 ml of deionized water containing 25 mg of ZnO were performed by using (a) Homemade S-Wave source and (b) Sairem S – Wave source. Treatment time was 10 min; power was 50 W and argon flow was 1 slm; the distance between quartz tube and water surface was 9 mm.

4. CONCLUSION

We treated deionized water samples with different power values of Solid state generator and argon flows. When the treatment was done with homemade S – Wave microwave source, increasing the flow of argon had a greater influence on concentration change than increasing power of Solid state generator. In other hand, while using commercial Sairem S – Wave microwave source, increasing power and flow did not affect concentration of reaction species that much. They were smaller than concentration with homemade S – Wave microwave source. The addition of ZnO kept the pH in the range that does not allow destruction of NO_2^- and creation of NO_3^- .

Acknowledgements: This research was supported by the Science Fund of the Republic of Serbia, 7739780, APPerTAin-BIOM project and MSTDI- 451-03-66/2024-03/200024.

References

1. N Puač, M Gherardi, M Shiratani , (2018) Plasma agriculture: A rapidly emerging field, *Plasma processes and polymers* **15** (2), 1700174
2. Bradu, C., Kutasi, K., Magureanu, M., Puac, N., & Živković, S. (2020). *Reactive nitrogen species in plasma-activated water: generation, chemistry and application in agriculture. Journal of Physics D: Applied Physics*

DETECTION OF RHENIUM IN TUNGSTEN USING LIBS WITH ADDITIONAL FAST PULSE DISCHARGE

IVAN TRAPARIĆ , BILJANA STANKOV  and MILIVOJE IVKOVIĆ 

Institute of Physics Belgrade, Pregrevica 118, 11080, Belgrade

E-mail traparic@ipb.ac.rs

E-mail biljanas@ipb.ac.rs

Email ivke@ipb.ac.rs

Abstract. The diagnostics of the first wall of future fusion reactors represents a major source of information about the state of the machine and the expected lifetime of the first wall components. As the absorption of neutrons can cause induced radioactivity of the first wall tiles, it is of the essence to monitor the amount of absorbed neutrons. One possibility to monitor them is via nuclear transmutation reaction where tungsten absorbs neutron and create rhenium core [1]. Therefore by assessing the amount of rhenium present in the material, the number of absorbed neutrons can be deduced. In this work Laser Induced Breakdown Spectroscopy (LIBS) combined with fast pulse discharge was used to assess the concentration of rhenium. The main result is the amplification of line intensity and signal to noise ratio compared to the classical LIBS setup at reduced pressure. This results is of particular importance since only small amounts of rhenium are expected to be found, therefore making this approach suitable for this type of diagnostics. Additionally, univariate calibration method based on intensity ratio of W I 488.7 nm and Re I 488.9 nm spectral lines was proposed for determination of rhenium concentrations.

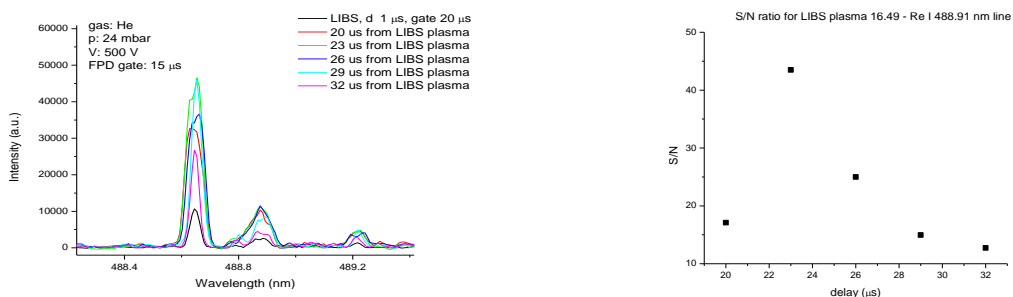


Figure 1: Amplification of Re I 488.9 nm line intensity with FPD (left) and resulting signal to noise ratio (right).

References

Ibano et al, *Journal of Nuclear Materials* **522** (2019) 324-328

INFLUENCE OF THE ABLATION ANGLE CHANGE ON SPECTRAL LINE INTENSITIES IN LIBS EXPERIMENTS

IVAN TRAPARIĆ* , BILJANA STANKOV , NIKOLA VUJADINOVIĆ ,
MILICA VINIĆ  and MILIVOJE IVKOVIĆ 

Institute of Physics Belgrade, Pregrevica 118, 11080, Belgrade

**Corresponding author: traparic@ipb.ac.rs*

Abstract. Laser Induced Breakdown Spectroscopy - LIBS is the most promising technique for the in-situ analysis of the plasma fusion reactor walls, see (Cong Li et al, 2016). The setup which is most frequently used in fusion reactors is so-called remote in-situ RIS LIBS, see (Cai et al, 2019). This configuration uses a scanning system which controls the Mo mirror to direct the laser beam to a different position inside the fusion reactor. In this study, it was investigated how changes in the ablation angles affect the intensity of the emitted spectral lines, considering that the incident beam is not always perpendicular to the PFCs. To this end, the classical LIBS setup at atmospheric pressure was employed. The angle of collection fiber with respect to the laser beam was fixed to 17 degrees. Chosen targets were tungsten-based alloys relevant to fusion research. The spectrum of the plasma was recorded with a Solar MS7504i spectrometer and a fast camera. Results show that there is a non-trivial dependence of the line intensity on the ablation angles, which was attributed to the change of laser focus and ablation surface as the angles were varied both in poloidal and toroidal directions. Additionally, the line intensity correction factor was calculated as the ratio of the intensity for the beam incident at an angle to that of the beam at normal incidence, and it exhibited a complex dependence on both angles.

Acknowledgements

The research was funded by the Ministry of Education, Science and Technological Development of the Republic of Serbia, Contract number: 451-03-68/2022-14/200024, and supported by the Science Fund of the Republic Serbia, Grant no. 7753287.

References

- Cong Li et al.: 2016, Front. Phys. **11**, 114214.
Laizhong Cai et al.: 2019, Rev. Sci. Instrum. **90**, 053503.

INFLUENCE OF INTERELECTRODE DISTANCE ON THE CHARACTERISTICS OF THREE-ELECTRODE PULSED SDBD

V.V. VOEVODIN^{1,2}, O.I. KORZHOVA¹, V.Yu. KHOMICH¹,
V.A. YAMSCHIKOV¹, N. Yu. LYSOV² and A.V. KLUBKOV²

¹ *Institute for Electrophysics and Electrical Power of the Russian Academy of Sciences, Dvortsovaya Naberezhnaya 18, Saint-Petersburg 191186, Russia*
E-mail vvvoevodin@ieeras.ru

² *Moscow Power Engineering Institute, National Research University, Krasnokazarmennaya str. 17, Moscow 111250, Russia*

Abstract. The distribution of extracted charge in the SDBD configuration with the third electrode is investigated. The amplitude of the ionic current is shown to depend on the polarity of the applied voltage and interelectrode distance

1. INTRODUCTION

In recent years, surface dielectric barrier discharge (SDBD) has attracted increased attention due to its potential for use in various technological applications. The SDBD electrode system typically consists of two electrodes: one exposed to the air and the other covered by a dielectric material. If the discharge is used as a source of ions or chemically active particles, a special electrode configuration can be used in which a third flat electrode is placed above the barrier surface to create a constant electric field. This electrode is referred to in the literature as an extraction electrode (Müller et al., 2007).

Since charge extraction occurs from the SDBD plasma, the width of the discharge region directly determines the area of ion extraction and the concentration of volume charge in the gap between the barrier and the third electrode. To increase the discharge region and the magnitude of ion current, several parallel plasma-generating electrodes located on the barrier at a certain distance L from each other are used. Studies show that as a result of the interaction of channels of the counter-developing discharge channels, the electrophysical characteristics of SDBD vary depending on L (Lazukin et al., 2022).

Using indirect measurements without time resolution, it was shown that, in the presence of a third electrode, the nature of the spatial distribution of the extracted

charge varies with L (Krivov *et al.*, 2020). However, there are no direct measurements in the existing literature of the spatial and temporal distribution of the extracted current produced by the charge carried out of the plasma during the SDBD development.

It seems relevant to carry out measurements of such a distribution using the previously created experimental setup with a sectioned third electrode when applying voltage pulses with nanosecond front duration to the electrode system (Khomich *et al.*, 2022).

2. EXPERIMENTAL

In this work, two versions of the electrode system with a plane-parallel arrangement in atmospheric air with two parallel plasma-forming electrodes (exposed electrodes (1)) made of copper with the distance between them $L=10$ mm and $L=5$ mm were used. Geometrical parameters of the electrode system are shown in Figure 1.

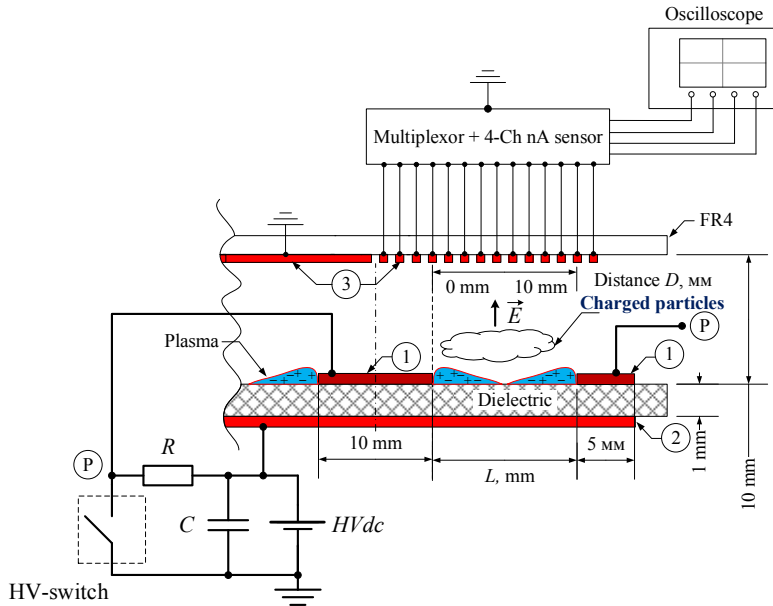


Figure 1: Scheme of the experimental setup and the electrode system: 1 – plasma generating electrodes, 2 – covered electrode, 3 – third sectioned electrode, P – pulsed voltage.

The distance from the surface of the 22XC alumina barrier (1 mm thickness) to the extraction electrode (3) consisting of 12 grounded and insulated copper strips (0.5 mm) was equal to 10 mm. A constant high potential HVdc was applied to the plasma generating electrode (exposed electrodes (1)) and the bottom electrode of the substrate (bottom electrode (2)) to create a field pushing ions towards the third electrode (3).

The voltage at the plasma-generating electrodes was created by a pulse generator by shorting them to ground for a time $\tau = 500$ ns at a frequency $f = 2$ Hz, the voltage decay and recovery times were 50 and 400 ns, and the voltage was recorded using a Tektronix P6015A high-voltage probe. An electronic nanoamperemeter developed at the IEE RAS (Khomich et al., 2022) was used to measure the spatial and temporal distribution of the extracted current.

The sections of the third electrode, located directly above the area of counter development of discharges, were grounded through the measuring channels of the nanoamperemeter. The edge of the first plasma-generating electrode was taken as the reference point for the horizontal distance D from each section. Signals from the nanoamperemeter were recorded and displayed on a LeCroy Waverunner 104Xi-A oscilloscope. The experiments were carried out in atmospheric air at a relative humidity of $30 \pm 4\%$ and a temperature of $22 \pm 3^\circ\text{C}$.

3. RESULTS AND DISCUSSION

An important characteristic of the surface dielectric barrier discharge, on which the values of the extracted current depended, was the extracted charge magnitude. Figure 2 shows the charge distribution by sections depending on the polarity and amplitude of the applied voltage $HVdc$, as well as on the distance L between the plasma-generating electrodes on the barrier surface, calculated by formula 1:

$$q_D = \int_{t_0}^{t_{end}} i(t) dt \quad (1)$$

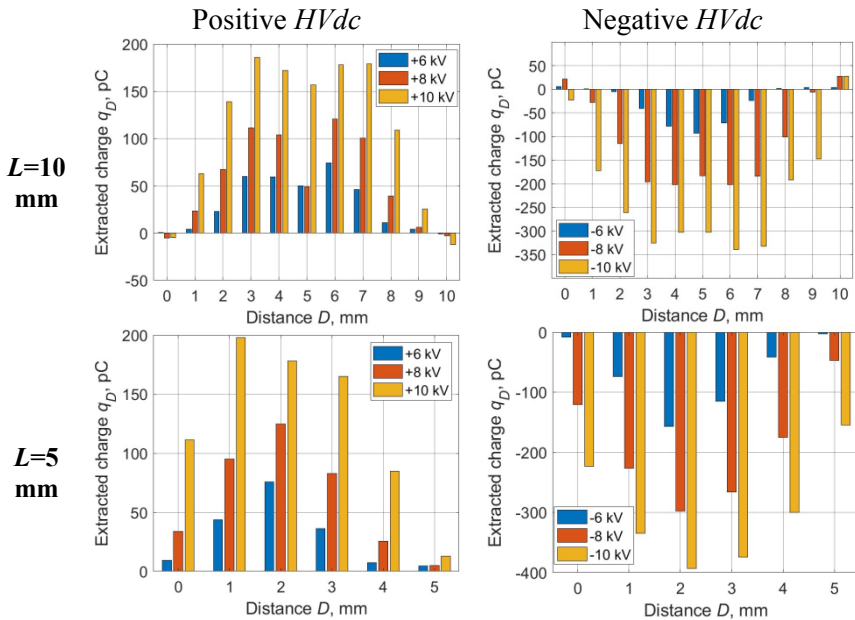


Figure 2: Distribution of the total extracted charge q_D over the measuring electrodes located at different horizontal distances D from the edge of the exposed electrode: A—positive, B—negative polarity of $HVdc$ voltage.

The total extracted charge Q_{Σ} in a three-electrode system was calculated as the sum of the charges that arrived to all measuring sections q_D according to formula 2.

$$Q_{\Sigma} = \sum_{D=0}^{11} q_D \quad (2)$$

$HVdc$, kV	E , kV cm^{-1}	Total charge Q_{Σ} , pC	
		$L=10$ mm	$L=5$ mm
+6	6	333	177
-6	6	-293	-398
+8	8	611	367
-8	8	-1142	-1133
+10	10	1180	750
-10	10	-2323	-1781

Table 1: Dependence of the total extracted charge Q_{Σ} on the $HVdc$ amplitude and polarity for different horizontal distance D from the exposed electrode.

Based on Table 1, we can conclude that the total charge extracted at negative polarity $HVdc$ was an order of magnitude higher than at positive polarity, practically at any values of amplitude and distance between plasma-generating electrodes. The charge distribution over the sections of the third electrode remains non-uniform at any voltage polarity and distance L . The obtained result may be useful for the use of discharge in plasma technologies.

This work was financially supported by the Ministry of Science and Higher Education of the Russian Federation, Agreement No. 075-15-2024-543 dated 24.04.2024.

References

- Khomich V.Yu., Rebrov I.E., Voevodin V.V., Yamshchikov V.A., Zharkov Ya.E. : 2022, *J. Phys. D. Appl. Phys.*, **55**, 275204.
- Krivov S.A., Moralev I.A., Lazukin A.V., Selivonin I.V. : 2020, *IEEE Trans. Plasma Sci.*, **48** (7), 2442.
- Lazukin A.V., Nikitin A.M., Romanov G.A. : 2022, *Technical Physics Letters*, **48**, 34.
- Müller S., Zahn R.-J., Grundmann J. : 2007, *Plasma Process. Polym.*, **4**, S1004.

A&M DATASETS FOR LTP TREATMENT OF PLANTS

VELJKO VUJČIĆ¹ , VLADIMIR A. SREČKOVIĆ² ,
OGNYAN KOUNCHEV³ and FELIX IACOB⁴

¹*Astronomical Observatory, Volgina 7, 11060 Belgrade, Serbia*

²*Institute of Physics Belgrade, Pregrevica 118, 11080 Belgrade, Serbia*

³*Institute of Mathematics and Informatics, BAS, 1113 Sofia, Bulgaria*

⁴*West University of Timișoara, Vasile Părvan Boulevard, 300233, Romania*

E-mail veljko@aob.rs, vlada@ipb.ac.rs

Abstract. Latest scientific papers related to food industry and technology indicate the potential usage of plasma in the treatment of plants without pesticides or other toxic agents, and even degradation of undesirable chemical compounds, such as allergens, toxins, and pesticide residues, often encountered on foods and food-processing equipment. Our research involves theoretical calculations of processes of LTP interest which include electrons, ions, small molecules and various excited species, and publishing datasets (Vujcic et al. 2023) both on the SerVO (Jevremovic et al. 2012) website and through VAMDC infrastructure (Dubernet et al. 2016). We cover the processes involving working LTP gases such as helium and ionization/excitation/recombination of hydrogen and alkali plasmas for conditions of interest of laboratory/technology LTPs.

Acknowledgments

The article is based upon work from COST Action CA19110 PIAgri - Plasma applications for smart and sustainable agriculture.

References

- Dubernet, M. L., Antony, B. K., Ba, Y. A., Babikov, Y. L., Bartschat, K., Boudon, V., ... & Zwolf, C. M. (2016). *J. Phys B*, **49**(7), 074003.
- Jevremović, D., et al.. (2012). Proceedings of the 13th ICCST (pp. 399-406).
- Ohta, T. (2016). Plasma in agriculture. *Cold plasma in food and agriculture*, 205-221.
- Puač, N., Gherardi, M., & Shiratani, M. (2018). *Plasma Process Polym*, **15**(2), 17001
- Priatama, R. A., et al. (2022).. *International Journal of Molecular Sciences*, **23**(9), 4609
- Vujčić, V., Marinković, B. P., Srećković, V. A., Tošić, S., Jevremović, D., ... & Mason, N. J. (2023). *Physical Chemistry Chemical Physics*, **25**(40), 26972-26985

Section 4.

GENERAL PLASMAS

HOW STARS GET THORN APART BY SUPERMASSIVE BLACK HOLES

ANDREJA GOMBOC

*Center for Astrophysics and Cosmology, University of Nova Gorica, Vipavska 13,
5000 Nova Gorica
E-mail andreja.gomboc@ung.si*

Abstract. When a star comes too close to a massive black hole (with a mass of 10^5 - 10^8 M_{Solar}), it may be shredded by the black hole's tidal forces. As the star is disrupted, its internal energy is released and the fallback of object's debris on the black hole produces a bright flare, which, according to theoretical predictions, can be seen from X-ray to UV and optical wavelengths and can last several weeks to years.

In the last decade, the study of such events, called Tidal Disruption Events (TDEs), gained momentum from advanced numerical simulations on the theoretical side and from detections of dozens of TDEs by wide-field sky surveys on the observational side.

I will briefly review the theoretical picture of TDEs, main mechanisms and parameters affecting the outcome of a stellar encounter with a black hole, and main open questions stemming from simulations and observations. I will also address the prospects of the Legacy Survey of Space and Time, expected to begin in 2025 at the Vera Rubin Observatory in Chile, in discovering TDEs and significantly enlarging their sample.

References

- Bricman, K., Gomboc, A. : 2020, *The Astrophysical Journal*, **890**, 73.
Bučar Bricman, K., van Velzen, S., Nicholl, M., Gomboc, A. : 2023, *Astrophys. J. Suppl. Series*, **268**, 13.
Jankovič, T., Gomboc, A. : 2023, *The Astrophysical Journal*, **946**, 25.
Jankovič, T., Bonnerot, C., Gomboc, A. : 2024, *MNRAS*, **529**, 1.
Petrushevska, T. et al. : 2023, *Astronomy & Astrophysics*, **669**, A140.

SUPER-EDDINGTON QUASARS: FROM ATOMIC PHYSICS TO COSMOLOGY

PAOLA MARZIANI

*National Institute for Astrophysics (INAF),
Padua Astronomical Observatory, Padua, Italy
E-mail paola.marziani@inaf.it*

Abstract. Quasars accreting matter at very high rates, known as extreme Population A (xA) or super-Eddington accreting massive black holes, represent a new class of distance indicators spanning cosmic epochs from the present-day Universe to less than 1 Gyr after the Big Bang. These quasars exhibit distinct observational properties, including a steep soft and hard X-ray continuum, strong singly-ionized iron emission, and extreme high-ionization line profile blueshifts. These characteristics not only make them easily recognizable but also indicate extreme physical properties compared to the general quasar population, such as very high metallicity and a strong high-ionization wind, likely associated with an optically thick, advection-dominated accretion flow.

In this review, we explore in detail the key optical and UV spectral properties of xA quasars, which facilitate their identification in large spectroscopic surveys from low to very high redshifts. We analyze the physical conditions responsible for the formation of their emission lines, focusing on the spectral energy distribution, ionization parameters, metallicity and density.

We address some puzzling aspects related to the formation and evolution of super-Eddington quasars. We emphasize that their importance extends beyond understanding quasar physics: their exceptionally high accretion rates enable these quasars to radiate at a stable, extreme luminosity-to-mass ratio. This stability results in consistent physical and dynamical conditions in the mildly ionized gas of the quasar low-ionization line-emitting region.

Our analysis ultimately supports the potential for identifying a virial broadening estimator based on the widths of low-ionization lines, such as the HI Balmer line $H\beta$ and $MgII\lambda 2798$. The connection between line width and quasar intrinsic luminosity super-Eddington active galactic nuclei (AGN) is a reinstatement of a law that appears universal in the form $L \propto \sigma^n$, holding from stars to clusters of galaxies. In the case of AGN, the dominance of Keplerian motions and the restriction to a very limited range of Eddington ratio for the super-Eddington sources imply a well-defined scaling between luminosity and FWHM or σ with exponent $n \approx 4$, analogous to the 21cm line broadening that is due to (mainly) Keplerian motion in galactic disks. This approach offers a promising method for deriving redshift-independent luminosity estimates grounded in the known luminosity-to-mass ratio of these quasars. By establishing a reliable virial broadening estimator, under very stable physical and dynamical conditions of the emitting regions, we lay the foundation for the exploitation of super-Eddington sources as standard candles for cosmological distance measurements.

CURRENT SITUATION AND FUTURE PROSPECTIVES OF THE EUROPEAN IFE PROGRAM, TECHNOLOGY DEVELOPMENT, SCIENCE AND RELATED APPLICATIONS

LUCA VOLPE¹

on behalf of HiPER+ consortium

¹*Polytechnique University of Madrid, Centro de Laseres Pulsados de Salamanca
E-mail l.volpe@upm.es*

Abstract. Inertial Fusion Energy production using lasers represents a key approach to nuclear fusion energy on earth. The concept of laser-driven Inertial Confinement thermonuclear Fusion (ICF) was proposed in 1972 in seminal papers by American and Russian scientists (Basov 1972, Nuckolls 1972), which initiated a worldwide effort to demonstrate inertial fusion in the laboratory. After five decades of continuous progress toward ignition. From December 2022 at the Lawrence Livermore Laboratory the laser-driven inertial fusion principle has been demonstrated several times reaching ignition and burn, with a net Energy Gain (Fusion energy Versus Laser energy) up to 3. The recent results in the US (Kritcher and Ralph 2022, Shawareb 2022, Zylstra et al. 2022, Wilson 2022) have shown clearly that laser-fusion ignition is indeed possible, predictable, and repeatable. Such breakthrough has pushed forward the interest in Laser fusion of many countries, Universities, Research Centres and private companies. The approach pursued by the Livermore scientists is based on the “Indirect drive” scheme where the incoming laser radiation is first converted in soft X-rays in a gold cylinder cavity. Then, these X-rays symmetrically uniformly irradiate a spherical capsule filled with DT fuel and positioned in the center of the cylindrical cavity. The radiation ablates the outer layers of the capsule, compresses the fuel inside more than a thousand times and heats it to a temperature of hundred million degrees. These are conditions where the fusion reactions take place and release a surplus of energy in a form of energetic neutrons, alpha-particles and radiation. The “direct drive” approach consists in the direct laser irradiation of a capsule with a DT fuel (thus bypassing the step of conversion in X-rays in the gold cylinder). It is more efficient and better suited for energy production, but implosion is less stable. Together with magnetic confinement fusion, direct drive ICF is a promising approach for construction of a fusion power plant: an abundant, clean, sustainable, and on-demand energy source for mankind.

References

- Kritcher. A. L., et al.: 2022, *Nature Physics* **18**, 251
Abu-Shawareb, H. and Indirect Drive ICF Collaboration: 2022, *Phys. Rev. Lett.* **129**, 075001
A. B. Zylstra, O. A. Hurricane, and D. A. C. et al.: 2022, *Nature* **601**, 542
T. Wilson: 2022 *Fusion energy breakthrough by US scientists...*, Financial Times, London

ASTROPHYSICAL APPLICATIONS OF STARK BROADENING OF SPECTRAL LINES

M. D. CHRISTOVA¹, MILAN S. DIMITRIJEVIĆ^{2,3}  and
S. SAHAL-BRÉCHOT³

¹*Department of Applied Physics, Technical University of Sofia, 1000 Sofia, Bulgaria*
E-mail mchristo@tu-sofia.bg

²*Astronomical Observatory, Volgina 7, 11060 Belgrade, Serbia*
E-mail mdimitrijevic@aob.rs

³*LERMA, Observatoire de Paris, Université PSL, CNRS, Sorbonne Université, F-92190 Meudon, France*
E-mail sylvie.sahal-brechot@obspm.fr

Abstract. Stark broadening data (data for spectral line broadening due to interactions of emitters with charged particles) are of interest in many research topics as astrophysical plasma, laboratory plasma diagnostics, fusion plasma, laser induced plasma and for various plasmas in technology and industry.

In this contribution will be presented an overview of our new and recently obtained calculated results for Stark width and shift of spectral lines of B I, Zn II, Si II, Ga II, Fe XXV, N II, N VI, and Sn II. Semiclassical perturbation theory in collisional approach created by Sahal-Bréchet and developed further (Sahal-Bréchet, Dimitrijević and Ben Nessib, 2014 and references therein) is applied. Plasma conditions of interest cover a wide range of temperatures and particle densities, and they are applicable for the interpretation and analysis of stellar spectra. For the chemical elements Zn III, Al IV and Lu II atomic data are missed and the modified semi-empirical method (MSE) is used where the spectral line broadening is due to electrons. A demonstration of Stark broadening influence on the spectral lines in stellar spectra is presented.

References

- Sahal-Bréchet S., Dimitrijević M. S., Ben Nessib, N.: 2014, *Atoms*, **2**, 225.
Dimitrijević, M. S., Konjević, N.: 1980, *J. Quant. Spectrosc. Radiat. Transf.*, **24**, 451.

PENNING AND PHOTO IONIZATIONS OF COLD RYDBERG ALKALI-METAL ATOMS UNDER FÖSTER RESONANCE CONDITIONS

A. CININS¹, MILAN S. DIMITRIJEVIĆ² , VLADIMIR A. SREČKOVIĆ³ ,
K. MICULIS¹, I. I. BETEROV⁴ and N. N. BEZUGLOV^{5,4}

¹*University of Latvia, Institute of Atomic Physics and Spectroscopy, Riga, Latvia
E-mail arturs.cinins@gmail.com*

²*Astronomical Observatory, Volgina 7, 11060 Belgrade 38, Serbia
E-mail mdimitrijevic@aob.rs*

³*Institute of Physics Belgrade, University of Belgrade, P.O. Box 57, 11001,
Belgrade, Serbia*

⁴*Novosibirsk State University, Department of Physics, 630090 Novosibirsk, Russia*

⁵*Saint Petersburg State University, St. Petersburg 199034, Russia*

Abstract. Cold Rydberg media under certain conditions quickly evolve into cold neutral plasma, which is accompanied by the appearance of various phenomena such as spontaneous plasma expansion, recombination of Rydberg atoms, etc. (see Lyon et al. 2017). In the physics of ultra-low-temperature plasma, in addition to traditional impact processes involving electrons and ions, one should take into account the ionization of Rydberg atoms due to thermal radiation and the Penning autoionization of Rydberg atomic pairs (see Abo et al. 2020). We report our comprehensive studies, both numerical and analytical, of various aspects of photo- and Penning ionization of Rydberg atoms, highlighting the effects of the Förster resonance. The latter is used as a controlling mechanism for varying the long-range interatomic interaction (see Dimitrijević et al. 2019) and it has numerous applications in applied problems of Rydberg media (see Paris-Mandoki et al. 2019).

References

- Abo, A., Dimitrijević, M., Srećković, V., et al. 2020, *Eur. Phys. J. D.*, **74**, 237.
Dimitrijević, M., Srećković, V., Abo, A., Bezuglov, N., Klyucharev, A. 2019, *Atoms*, **7**, 22.
Lyon, M.; Rolston, S. 2017, *Rep. Prog. Phys.*, **80**, 017001.
Paris-Mandoki, A.; Gorniaczyk, H.; Tresp, C., et al. 2016, *J. Phys. B*, **49**, 164001.

EXPLORING THE IMPORTANCE OF INTERSTELLAR IONS IN THE ENIGMA OF DIFFUSE INTERSTELLAR BANDS

UGO JACOVELLA¹

¹ *Université Paris-Saclay, CNRS, Institut
des Sciences Moléculaires d'Orsay, 91405 Orsay, France
E-mail ugo.jacovella@universite-paris-saclay.fr*

Abstract. Diffuse Interstellar Bands (DIBs), hundreds of absorption features observed in interstellar space, were discovered a century ago by Mary Lea Heger (see Heger 1922). Identifying their origins has been a persistent challenge. Although five near-infrared DIBs are attributed to the fullerene cation C_{60}^+ (see (Campbell *et al.* 2015; Walker *et al.* 2015), the carriers of over 600 visible and near-infrared DIBs remain unknown. Solving this puzzle would enhance our understanding of the carbon cycle in space, crucial for modeling stellar chemistry and the processes in planetary atmospheres and surfaces that may lead to life. There is a general consensus that DIB carriers are large gaseous carbon molecules (containing 10 to 100 carbon atoms), existing mainly in cationic forms.

Ions are typically studied using action spectroscopy, which offers greater sensitivity than conventional absorption spectroscopy by detecting photo-induced processes and counting charged particles via mass spectrometry. However, action spectroscopy struggles with obtaining undisturbed spectra, limiting its ability to determine band centers and relative intensities. Direct spectroscopy provides absolute wavelength transitions but lacks sensitivity due to low ion density. Cavity ringdown spectroscopy (CRDS) enables reaching kilometers of absorption lengths, greatly enhancing sensitivity. We propose combining action and direct spectroscopy in a single instrument, utilizing CRDS to measure spectra of trapped, cold, isomer-specific ions. This approach aims to contribute to the evaluation of the carbon budget in space, addressing the knowledge gap, through the DIBs puzzle, regarding molecules with 11 to 60 carbon atoms that remain elusive in the interstellar medium (see Fig. 1.)



INTERSTELLAR DUST AS A DYNAMIC ENVIRONMENT

G. LA MURA^{1,*}, G. MULAS¹, M. A. IATÌ², C. CECCHI-PESTELLINI³,
S. REZAEI^{2,4,5} and R. SAIJA⁴

¹ *INAF – Osservatorio Astronomico di Cagliari, Selargius, Italy*

** Speaker – e-mail: giovanni.lamura@inaf.it*

² *CNR-IPCF, Istituto per i Processi Chimico-Fisici, Messina, Italy*

³ *INAF - Osservatorio Astronomico di Palermo, Palermo, Italy*

⁴ *Dipartimento di Scienze Matematiche e Informatiche, Scienze Fisiche e Scienze della Terra, Università di Messina, Messina, Italy*

⁵ *Department of Physics, Faculty of Science, University of Kurdistan, Sanandaj, Iran*

Abstract. In spite of representing only a small fraction of the Interstellar Medium (ISM) in terms of mass, getting up to approximately 1% of ISM observed in the Milky Way, dust is a primary actor in Astrophysics. In addition to its effects of extinction in the optical/UV frequency range and to its thermal emission at IR and sub-mm wavelengths, interstellar dust collects most of the refractory elements available in the diffuse medium. Moreover, the chemical processes that occur in dust grains are crucial for the formation and evolution of complex molecular compounds. As a consequence, understanding dust is fundamental for both astro-chemistry and the physics of interaction between different phases of the ISM. Observations of silicate and carbonaceous features show that their polarisation is different. This appears to imply that dust grains reside in distinct, segregated populations, that they have complex structures, or that these effects are combined together. However, this interpretation is so far qualitative, since it does not take fully into account the detailed effects of complex structures, as particles are typically modelled under the assumption of spherical symmetry. A more accurate, and quantitative interpretation of the properties of interstellar dust thus needs to take into account realistic particle structures. Unfortunately, a full solution of the radiation scattering problem, with different materials and relaxing spherical symmetry, is extremely complicated, requiring intensive numerical calculations. In this contribution, we present the Transition Matrix (TM) approach to investigate the properties of interstellar dust particles of realistic shapes and structures. The strategy adopted by the TM method is to subdivide particles with arbitrarily complicated shapes in a collection of spherical components and then to expand the radiation fields in spherical vector harmonics. Taking advantage of the linearity of the solution of the field equations, the scattering problem of an arbitrary particle can be solved by imposing continuity conditions between the incident and the scattered field across the surface of the particle layers. The result is a linear operator, characteristic of the particle, that connects arbitrary incident fields to their corresponding scattered fields, providing a tool to obtain analytical estimates of differential and integrated quantities. We show how the implementation of this method on state of the art parallel computers leads to the ability to model radiation-particle interactions on model systems much closer to real ones, illustrating the dynamic implications of the process on the types of particles exposed to different environments.

MAGNETO-INERTIAL FUSION AND POWERFUL INSTALLATIONS

S.V. RYZHKOV

*Bauman Moscow State Technical University (BMSTU)
2-nd Baumanskaya Street, 5,1 Moscow, 105005 Russian Federation
E-mail svryzhkov@bmstu.ru*

Abstract. A review of theoretical and experimental studies in the field of compression and heating of a plasma target in an external magnetic field, which has recently been called magneto-inertial thermonuclear fusion (MIF), has been carried out. An analysis of the current state of work on the implosion of magnetized targets and the effect of an external magnetic field on the main plasma parameters and system characteristics is presented. Questions of numerical simulation of experiments on magnetic-inertial confinement of plasma are touched upon. Particular attention is paid to two promising areas of MIF - with plasma guns (plasma jets) and with a laser driver (laser beams) (Kuzenov V.V., Ryzhkov S.V. 2019, 2021, 2023, Ryzhkov S.V. 2023, Ryzhkov S.V., Chirkov A.Yu. 2018). A mathematical model has been developed for the study of nonstationary processes of heating and compression of a substance in an external magnetic field by several laser and plasma beams. The authors have created a group of models that take into account the key effects of internal thermonuclear energy release, kinetics of synthesis products and dynamics of magnetized plasma. A new model of interaction in the system "magnetized preformed plasma-high-speed plasma jets" and "magnetized target-high-power laser" is proposed. A comprehensive analysis of the retention of the plasma configuration in the seed magnetic field after uniform compression and numerical analysis based on a nonstationary two-dimensional radiation-magneto gas dynamic (RMGD) model, taking into account electronic thermal conductivity and radiation-convective, was carried out.

This research has been partially supported by the Ministry of Science and Higher Education of the Russian Federation (GosZadanie Project No. FSFN-2024-0022).

References

- Kuzenov V.V., Ryzhkov S.V. : 2019, *Physics of Plasmas* **26**, 092704.
Kuzenov V.V., Ryzhkov S.V. : 2021, *Physica Scripta* **96**, 125613.
Kuzenov V.V., Ryzhkov S.V. : 2023, *Fusion Science and Technology*, **79**, 399-406.
Ryzhkov S.V. : 2023, *Applied Sciences*. **13**, 6658.
Ryzhkov S.V., Chirkov A.Yu. : 2018, *Alternative Fusion Fuels and Systems*. CRC Press, Taylor & Francis, 200 p.

COMPREHENSIVE Z-DEPENDENCE ANALYSIS OF SOFT X-RAY SPECTRA FROM HIGHLY CHARGED HEAVY IONS USING MAGNETICALLY CONFINED HIGH-TEMPERATURE PLASMAS

C. SUZUKI^{1,2}, F. KOIKE³, N. TAMURA¹, T. OISHI⁴, Y. KAWAMOTO^{1,2},
T. KAWATE^{1,2}, M. GOTO^{1,2}, N. NAKAMURA⁵ and I. MURAKAMI^{1,2}

¹National Institute for Fusion Science, 322-6 Oroshi-cho, Toki 509-5292, Japan
E-mail csuzuki@nifs.ac.jp

²The Graduate University for Advanced Studies, SOKENDAI, 322-6 Oroshi-cho,
Toki 509-5292, Japan

³Sophia University, 7-1 Kioi-cho, Chiyoda-ku, Tokyo 102-8554, Japan

⁴Tohoku University, 6-6-01-2 Aobayama, Sendai 980-8579, Japan

⁵The University of Electro-Communications, 1-5-1 Chofugaoka, Chofu 182-8585,
Japan

Abstract. Soft X-ray spectra from highly charged heavy ions are of great interest in terms of atomic physics as well as plasma applications, e.g., nuclear fusion and industrial light sources. In the last decades, soft X-ray spectra from various heavy ions have been systematically recorded in the Large Helical Device (LHD), a magnetically confined fusion device at the National Institute for Fusion Science (see Suzuki et al. 2017, Suzuki et al. 2018). The spectral shape drastically changes between discrete and quasi-continuum features depending on the electron temperature. The LHD spectra have been compared with theoretical calculations and the other experimental data. Consequently, atomic number (Z) dependence of the discrete and/or quasi-continuum spectra for $Z=50-83$ have been investigated in more detail than ever before. In addition, we could clearly explain a peculiar Z -dependence arising from strong spin-orbit interactions specific to highly charged heavy ions (see Koike et al. 2022).

References

- Suzuki, C., Murakami, I., Koike, F., et al. : 2017, *Plasma Phys. Control. Fusion*, **59**, 014009.
Suzuki, C., Koike, F., Murakami, I., Tamura, N., Sudo, S. : 2018, *Atoms*, **6**, 24.
Koike, F., Suzuki, C., Murakami, I., Kato, D., et al. : 2022, *Phys. Rev. A*, **105**, 032802.

ON THE CONDITIONS FOR SOLITON FORMATION IN THE GALACTIC ENVIROMENT

MIROSLAVA VUKCEVIC 

Astronomical Observatory Belgrade, Volgina 7, Belgrade, Serbia
E-mail vuk.mira@gmail.com

Abstract. We discuss different astrophysical systems and establish conditions for the possible soliton creation. In the case of the galactic disk, necessary condition reads as marginal stability of the disk, for the spiral arms formation, establishing fine tuning mechanism between rotation, surface mass density distribution and thickness of the disk. As far as the accretion disk is concerned, there are several possibilities: when the self-gravity of the disk is included in the dynamics, there is certain ration of angular velocity and thickness of the disk requested for the solitary vortex formation. Similar formation occurs in the Earth's atmosphere and ionosphere. In the later one, magnetic field effects are incorporated leading for the specific balance between depth of the layer, Coriolis frequency and magnetic frequency.

INTEGRATED RADIATION-MAGNETO-HYDRODYNAMIC SIMULATIONS OF MAGNETIZED BURNING PLASMAS*

B. Z. DJORDJEVIĆ, D. J. STROZZI, C. A. WALSH, J. D. MOODY,
C. R. WEBER, S. A. MACLAREN and G. B. ZIMMERMAN

*Lawrence Livermore National Laboratory
7000 East Avenue, Livermore, CA 94550
E-mail djordjevic3@llnl.gov*

Abstract. Considering recent breakthroughs (Abu-Shawareb et al. 2022, 2024) in inertial confinement fusion (ICF), first achieving ignition conditions in National Ignition Facility (NIF) shot N210808 and then laser energy breakeven in N221204, modeling efforts have been investigating the effect of imposed magnetic fields on integrated simulations of igniting systems. Previous NIF experiments have shown fusion yield and hotspot temperature to increase in magnetized gas-filled capsules (Moody et al. 2022) in line with expected scalings (Walsh et al. 2022). We use the 2D radiation-magneto-hydrodynamics code Lasnex within the Lasnex Hohlraum Template (LHT) ICF common model (Strozzi et al. 2024). Simulations are tuned to approximate data from unmagnetized experiments: the laser power vs. time is modified to match shock velocities and nuclear bangtime, the CBET saturation clamp and cone fraction are chosen to match the P2 Legendre mode of the hotspot self-emission, and mix models for hotspot degradation to match yield.

Investigated here is the effect of imposed axial fields up to 100 Tesla on the fusion output of historically best performing ICF shots, specifically N180128 (record BigFoot shot), N210808, and N221204. The main effect is increased hotspot temperature due to magnetic insulation, as electron heat flow is constrained perpendicular to the magnetic field and alpha particle trajectories transition to gyro-orbits. Magnetic fields must be fastidiously applied however as magnetic pressure can resist the implosion and fields can decrease the propagation speed of the burn wave (Lindemuth et al. 1983, Jones et al. 1986). In conclusion it is found that magnetization can increase ion temperature by 50% and neutron yield by 5x.

* This work was conducted under the auspices of the U.S. Department of Energy by LLNL under contract DE-AC52-07NA27344 and Laboratory Directed Research and Development project 23-ERD-025. This document has been approved for distribution per Release No. LLNL-ABS-864007.

References

- Abu-Shawareb, H., et al. : 2022, *Phys. Rev. Lett.* 129, 075001
Abu-Shawareb, H., et al. : 2024, *Phys. Rev. Lett.* 132, 065102
Moody, J. D., et al. : 2022, *Phys. Rev. Lett.* 129, 195002
Walsh, C. A. et al. : 2022, *Phys. Plasmas* 29, 042301
Strozzi, D. J. et al. : 2024, *Phys. Plasmas*, submitted
Lindemuth, I. R., Kirkpatrick, R. C. : 1983, *Nuclear Fusion* 23, 263
Jones, R. D., Mead, W. C. : 1986, *Nuclear Fusion* 26, 127

PHOTOELECTRON SPECTROSCOPY OF RADICALS OF ASTROCHEMICAL INTEREST

M. DRISSI¹, G.A. GARCIA¹, L. NAHON¹, S. BOYE-PERONNE², B. GANS²,
H.R. HRODMARSSON³, H.L. Le², M.-X. JIANG² and J.-C. LOISON⁴

¹*Synchrotron SOLEIL, L'Orme des Merisiers, Saint-Aubin, Gif sur Yvette, France*
E-mail myriam.drissi@synchrotron-soleil.fr

²*ISMO, CNRS, Université Paris-Saclay, 91405 Orsay, France*

³*LISA, Campus centre de l'UPEC, 61 avenue du Général de Gaulle, 94010 Créteil*
Cedex, France, France

⁴*ISM, CNRS, Univ. Bordeaux, 351 cours de la Libération, Talence, 33400, France*

Abstract. The modelling of astrochemical media requires the characterization of thousands of physical and chemical processes. In this type of media, radicals and ions are known to be important drivers of chemistry (Smith, 2011). Their identification and characterization are therefore necessary to gain knowledge on these processes. Vacuum-ultraviolet (VUV) photoionization can be used, not only to characterize the electronic structure of molecules through photoelectron spectroscopy, but also to study their photochemistry under VUV irradiation. Additionally, in the past decade, synchrotron-based photoelectron spectroscopy has been coupled to mass spectrometry in search of a universal detection method able to probe the presence of products and intermediates in complex chemical reactions (Krüger et al., 2014), or to prepare a reactant in a given internal state prior to reaction (Ascenzi et al., 2019). Among the different types of species detected in space, sulfur bearing molecules have gained attention over the past years due to difficulties matching the detected abundances with chemical models, which highlights the importance of studying the processes in which they are involved. Here I will present the VUV photoionization of key sulfur radical molecules such as the linear sulfur carbon chains HCCS and CCS which may be precursors of polycyclic sulfur bearing molecules, or the SiS radical which is thought to play a role in the formation of sulfide grains. I will show how these highly reactive and therefore elusive species are produced within a MW discharge flowtube reactor (Garcia et al., 2015), and its coupling to the synchrotron radiation from the DESIRS VUV beamline (synchrotron SOLEIL, France), and a *i*²PEPICO (double imaging photoelectron photoion coincidence) spectrometer to measure mass-selected photoelectron spectra with vibrational resolution, which might then be used as a molecular fingerprint to detect these species in terrestrial experiments via advanced mass spectrometry, or as a starting point to record laser-based rotationally resolved photoelectron spectra that can be used to detect cationic species in space.

References

- Ascenzi, D. et al. : 2019, *Front. Chem.*, **7**, 537.
Garcia, G.A. et al. : 2015, *J. Chem. Phys.*, **142**, 164201.
Krüger, J. et al. : 2014, *Phys. Chem. Chem. Phys.*, **16**, 22791.
Smith, I.W.M. : 2011, *Annu. Rev. Astron. Astrophys.*, **49**, 29:66.

ELECTRON NS⁺ COLLISIONS IN COLD PLASMA

FELIX IACOB

West University of Timisoara,
E-mail: felix.iacob@e-uvt.ro

Abstract. The recent discovery of the NS⁺ cation in the interstellar medium¹ triggered the interest in the study of its collision with electrons. In this complex process, the electron can be captured into NS Rydberg-bound states predissociated by Feshbach resonances of this latter molecule. These both types of states have been calculated within the Born-Oppenheimer approximation using a variational ab-initio method based on the R-matrix theory². They have a large contribution to the appearance of the cross section.

The purpose of this presentation is to show how the states were determined and to provide an accurate cross-section of the collisional process.

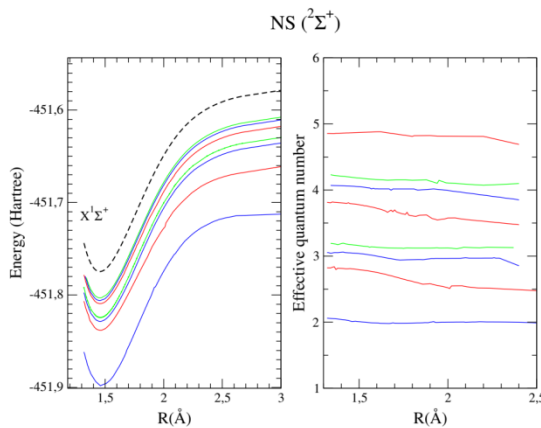


Figure 1: The bound states of the captured electron forming the NS neutral in left panel, and the quantum defects in right panel³.

References

- ¹ J. Cernicharo et al, (2018) Ap.J.L, **853** L22
- ² J. Tennyson, Phys. Rep. 491, 29 (2010)
- ³ F Iacob et al, (2022) J. Phys. B: Atomic, Molecular and Optical Physics **55** (23), 235202

PROPERTIES OF EARTH'S LOWER IONOSPHERIC PLASMA PERTURBED BY SOLAR FLARES

ALEKSANDRA KOLARSKI 

*Institute of Physics Belgrade, University of Belgrade, Pregrevica 118,
11000 Belgrade, Serbia*

E-mail aleksandra.kolarski@ipb.ac.rs

Abstract. Energetic outbursts of electromagnetic energy from solar corona, known as solar flares (SFs), are well-known agents that cause perturbations within Earth's ionospheric regions faced towards the Sun. Soft X-ray component (0.1-0.8 nm) has crucial importance related to lower ionospheric region, since this radiation penetrates deep into the Earth's atmosphere and reaches altitudes corresponding to D-region (50-90 km). Properties of Earth's lower ionospheric plasma perturbed by such energetic solar events were topic of this research, with high energy SFs' influences in special focus. For examination of lower ionospheric response to such events, remote sensing approach was utilized by the use of Very Low Frequency (VLF) radio signal (3-30 kHz) technology. Based on VLF signals' perturbations, recorded by system located at the Institute of Physics in Belgrade (Serbia), numerical simulations was conducted with the goal of obtaining electron density profile changes within this region induced by these high energy events. Main findings are presented in this research.

SUPERNOVA REMNANTS IN CLUMPY MEDIUM: HYDRODYNAMIC AND RADIO SYNCHROTRON EVOLUTION

PETAR KOSTIĆ 



Astronomical Observatory Belgrade, Volgina 7, 11070 Belgrade, Serbia
E-mail pkostic@aob.rs

Abstract. The models of radio synchrotron emission of supernova remnants (SNRs) are usually analyzed assuming uniform density environment to obtain the surface-brightness-to-diameter (Σ -D) dependence. We put other perspective at this problem, considering that non-uniform environment around the SNRs might considerably affect their Σ -D evolutionary paths. It makes the non-uniform environment an important element in investigation of this problem. We present the emission model that implies the test-particle approximation. The model is used in hydrodynamic simulations of SNRs in environments of low-density bubbles and variety of clumpy media. Based on the simulation results, we developed the semi-analytical spherically-symmetric model of hydrodynamic evolution and emission of SNRs in a clumpy medium, which we utilized to generate large SNR samples. The results show that clumpy medium initially enhances the SNR brightness, but afterward the Σ -D slope steepens proportionally to the average density jump from uniform to clumpy medium. On the contrary, the average slope of Galactic SNR sample flattens at $D \approx 14$ – 50 pc. The models of generated SNR samples with clumpy medium lead to a conclusion that the significant Σ -D flattening and scatter in Galactic sample originates in sporadic emission jumps of individual SNRs in a limited diameter interval. However, additional analyses considering the selection effects are needed.

References

- Kostić, P., Vukotić, B., Urošević, D., Arbutina, B., & Prodanović, T. 2016, *MNRAS*, **461**, 1421.
- Pavlović, M. Z., Urošević, D., Arbutina, B., et al. 2018, *ApJ*, **852**, 84. (P18), doi: 10.3847/1538-4357/aaa1e6
- Kostić, P. 2019, *Serbian Astronomical Journal*, **199**, 65, doi: 10.2298/SAJ1999065K
- Vukotić, B., Ciprijanović, A., Vučetić, M. M., Onić, D., and Urošević, D.: 2019, *Serbian Astronomical Journal*, **199**, 23, doi: 10.2298/SAJ1999023V

FLUCTUATIONS IN THE FLUX OF ENERGETIC PROTONS IN HELIOSPHERE BEFORE AND DURING SUDDEN DECREASES IN GALACTIC COSMIC RAY INTENSITY

NIKOLA VESELINOVIĆ , MIHAILO SAVIĆ , ALEKSANDAR DRAGIĆ ,
DIMITRIJE MALETIĆ , DEJAN JOKOVIĆ , RADOMIR BANJANAC ,
MILOŠ TRAVAR  and VLADIMIR UDOVIČIĆ 

Institute of Physics Belgrade, Pregrevica 118, 11090 Belgrade, Serbia
E-mail veselinovic@ipb.ac.rs

Abstract. Extreme events originated from Sun, such as solar flares and coronal mass ejections, can induce various processes in the Sun's heliosphere, like shock waves, particles acceleration (Waterfall et al. 2023). These events can increase the flux of charged particles in heliosphere, leading not only to modulation of primary cosmic rays but also affect Earth's magnetosphere and systems (see Belov et al. 2022, Kolarski et al. 2023 and references within). With the rising phase of current solar cycle 25, a better understanding and study of these transient phenomena caused by solar activity are of great importance (Savić et al.2023), primarily due to the potential negative effects those events can have on Earth's environment (Kataoka et al. 2018). In a presented work, relationship between event-integrated fluence spectra of energetic protons, various solar activity indices measured at Lagrange point L1 and parameters of cosmic rays modulations measured at Earth have been studied. The focus of the investigation is on analyzing correlation between power indices used to parameterize the differential fluence spectra, coronal mass ejection parameters and the magnitude of associated cosmic rays modulation. This parametrization uses several different proposed models to model the fluence spectra before and during extreme events, which can provide a valuable new parameters in analysis of mentioned phenomena.

References

- Waterfall, C. O. G., Dalla, S.; Raukunen, O., Heynderickx, D., Jiggins, P., Vainio, R.: 2023, *Space Weather*, **21**,
Belov, A., Shlyk, N., Abunina, M., Belova, E., Abunin, A., Papaioannou, A.: 2022, *Universe*, **8**, 403.
Kolarski, A., Veselinović, N., Srećković, V.A., Mijić, Z., Savić, M., Dragić, A. : 2023, *Remote Sens.*, **15**, 1403.
Savić, M., Veselinović, N., Dragić, A., Maletić, D., Joković, D., Udovičić, V., Banjanac, R., Knežević, D. : 2023, *Advances in Space Research*, **71**, 4, 2006-2016
Kataoka, R., Sato, T., Miyake, S., Shiota, D., Kubo, Y. : 2018, *Space Weather*, **16**, 917–923.

SLAMS-ENHANCED PARTICLE ACCELERATION AT HIGH-MACH NUMBER ASTROPHYSICAL SHOCKS: TeV IN A BLINK OF SUPERNOVA

VLADIMIR ZEKOVIĆ^{1,2} 

¹*Department of Astronomy, Faculty of Mathematics, University of Belgrade*
E-mail vladimir.zekovic@matf.bg.ac.rs

²*Department of Astrophysical Sciences, Princeton University*

Abstract. The shocks of supernova remnants are known as the nature's most efficient particle accelerators. By the mechanism of diffusive shock acceleration (DSA) particles can reach cosmic-ray (CR) energies over a life time period of the supernova remnant. The DSA is able to produce a power law particle distribution $f(p) \sim p^{-q}$ with the momentum index $q=4$. However, the radio-synchrotron emission observed at young supernovae implies steeper electron spectra with the slopes $5 < q < 6$. Since the shocks of young supernova remnants are fast, having Alfvénic Mach numbers > 100 , the CR-driven waves in the upstream evolve into short large-amplitude magnetic structures (SLAMS). The periodically amplified magnetic field inside SLAMS represents a superluminal barrier for magnetized electrons. However, the subluminal gaps in the SLAMS structure enable extremely fast electron acceleration by a recently found mechanism of quasi-periodic shock acceleration (QSA). I present the results of our particle-in-cell simulations and theory of electron acceleration at high-Mach number quasi-parallel collisionless shocks. The simulations show that electrons are able to reach TeV energies by QSA in a matter of hours. The good agreement between the slopes of simulation spectra and those observed at young supernova remnants strongly highlights QSA as the main electron acceleration mechanism up to TeV energies where we expect electrons to become unmagnetized and continue to accelerate via DSA.

VARABILITY ALONG THE MAIN SEQUENCE OF QUASARS

EDI BON¹, PAOLA MARZIANI² and NATAŠA BON¹

¹*Astronomical Observatory, Volgina 7, Belgrade, Serbia*
E-mail ebon@aob.rs

²*INAF, Padova, Italy*
E-mail paola.marziani@inaf.it

Abstract. We explore the main sequence of quasars through the variability along the Eigenvector 1 (EV1), based on relationship between the relative strength of Fe II and H β (RFe) and the full width at half maximum (FWHM) of the H β emission line. We present some examples that show variability behaviour along EV1 diagrams and discuss physical properties.

1. INTRODUCTION

Active galactic nuclei (AGN) are among the most luminous and energetic objects in the universe. Understanding their properties and behaviors is crucial for astrophysical research. The Eigenvector 1 (EV1) parametrization, introduced by Boroson & Green (1992), provides a framework for studying the diversity of quasar properties by correlating the strength of Fe II emission and the FWHM of the H β emission line (Boroson, & Green 1992).

Differences between Type 1 and Type 2 spectra of AGNs, mainly described by the different viewing angle at the nuclear region of the galaxy, are already well known. On the other hand, there is a vast number of spectral characteristics, such as shift, width of the line, line ratios, Fe II blends, and many others that create diversity between different Type 1 spectra. One could expect that diversity also depends to some extent on the viewing angle.

There have been many efforts to systematize Type 1 spectral diversity in the EV1 parameter space, which represents the linear combination of several parameters, in order to introduce some order in spectral properties. The EV1 can be seen as an equivalent to the well-known Hertzsprung-Russell diagram for stars, and therefore capable of organizing Type 1 AGN into a “main sequence” of quasars. This kind of systematization allows setting observational constraints on the dynamics and physical properties of the broad line region. The principal component analysis of Boroson and Green (1992) showed that there is a hidden single parameter responsible for the vast majority of spectral differences – R_{Fe} – the ratio of the optical Fe II blend at λ 4570 to the H β flux. This idea was further developed by Sulentic et al. (2000), and Shen and Ho (2014) among others.

EV1 is a principal component that accounts for much of the observed variance in the properties of quasars. It is primarily driven by R_{Fe} and the FWHM of the $\text{H}\beta$ emission line. This parametrization allows for a classification scheme that distinguishes between different quasar populations, often referred to as Population A and Population B (Sulentic 2000).

The relation between EV1 and some theoretically motivated parameters, such as Eddington ratio, black hole mass, chemical composition, black hole spin, orientation etc., is still not clear. The most favored parameter that drives EV1 is the Eddington ratio (Boroson & Green 1992, Sulentic et al. 2000, Marziani et al. 2001, Shen and Ho 2014). Shen and Ho (2014) argued that the viewing angle in Type 1 sources represents just a dispersion to the quasar “main sequence”, although Marziani et al. (2018) showed progression of inclination effects along the main sequence.

Sulentic et al. (2000) measured the soft X-ray photon index and a measure of CIV $\lambda 1549$ broad line profile velocity displacement at half maximum, to analyze an extended 4D Eigenvector 1 parameter space. They showed that the “main sequence” of quasars follows some physical trends involving dimensionless accretion rate and electron density, which increase down the sequence toward strong FeII emitters, while the ionization parameter decreases (Marziani et al. 2001). Pop B corresponds to high mass and low accreting quasars and is characterized by FWHM of $\text{H}\beta$ higher than 4000 km/s and higher red asymmetry, while Pop A is characterised with mainly low mass and high accreting rates (Sulentic et al 2000, Zamfir et al. 2010).

Bon et al. 2018 explored the variability of NGC 5548 along the EV1 diagram implying that the accretion rate variations may be responsible for the changes in this parameter space. These effects were later-on explored and modeled by Panda et al. 2022 using the same object and Panda & Sniegowska 2024 using a sample of extremely variable AGN (so called “changing look” AGN).

In the optical band, variability of quasars shows distinct trends along the EV1 main sequence. Quasars with broad $\text{H}\beta$ lines and low R_{Fe} values (Population B) exhibit more significant optical variability. These quasars generally have lower Eddington ratios, leading to more substantial fluctuations in both the optical continuum and broad emission lines. This pronounced variability makes them suitable for reverberation mapping studies, where time delays between variations in the continuum and line emissions are used to probe the structure of the broad-line region (see, for eg. Kaspi et al. 2000).

High Eddington ratio quasars, typically found in Population A with narrower $\text{H}\beta$ lines and higher R_{Fe} values, display less optical variability. Their relatively stable accretion rates result in smaller amplitude changes in the optical continuum, with variability timescales that are longer and less noticeable over typical monitoring periods.

With very long term monitoring campaign data, we can analyze the variability patterns in Type 1 AGN using EV1 diagrams in different variability states. We focus our analysis on the nearby and frequently observed galaxies NGC 4151 NGC 5548 and PG0026, for which data from extensive monitoring campaigns are available.

2. SOME CASE STUDIES

A detailed study of the AGN NGC 5548 provides insights into the variability along the EV1 diagram (Bon et al. 2018). They found that variability could largely

be attributed to changes in the accretion rate. Over several decades, NGC 5548 exhibited significant variability in both the optical continuum and $H\beta$ line, while remaining within the characteristics of Population B sources. This study highlights that the relationship between variability and position on the EV1 diagram can differ when considering short-term versus long-term monitoring periods (Bon et al. 2018).

NGC 4151 is also very extensively studied AGN, belonging to Pop B, similarly as NGC 5548. We can see in Figures 1a and 2, both objects significantly vary along the EV1 diagram, but nevertheless, they keep their variability patterns within the same population (Pop B), without crossing into the area of Pop A. Changes of accretion rate (assuming that their mass and inclinations are being constant) seem to be the main drivers for their variability, and we can notice that when the accretion rate significantly decreases, the observations shifts from Pop B1 (from 4000 km/s to 8000 km/s) to Pop B1+ (from 8000 km/s to 12000 km/s) bin.

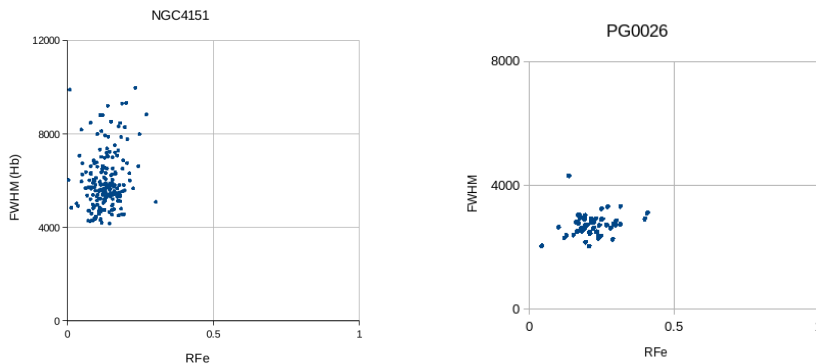


Figure 1: EV1 diagram of NGC 4151 variability (left panel) and PG0026 (right panel)

In case of PG 0026, its variability changes the position along the EV1 diagram within the population Pop A1 (see Fig. 1b), slightly increasing the RFe with the accretion rate (for a constant mass and inclination the changes of luminosity will correspond to the changes of the accretion rate).

Single epoch observations are not allowing such a complex analysis, positioning the object on one place at the EV1 diagram. With long term monitoring programs we are able to study the the complex behaviour of emission lines over the EV1 diagram, in order to analyse the accretion rate changes. For that purpose, one may needs to make a correction for the anomaly produced by the effect of lagging of the broad emission line response to the continuum variations of an analysed object. Using the reverberation mapping results which measure the lag between the broad emission lines and the continuum one can correct the response of the broad emission lines for the measured lag, and analyse variability patterns along the EV1 diagram corrected for the lag. One such example is presented on Fig. 2 for the case of NGC 5548, where the FWHM of $H\beta$ and equivalent widths of $H\beta$ and the FeII equivalent widths are recalculated using the correction for measured reverberation lags (see Fig. 2b). These variability patterns before and after delagging show slightly different behaviour.

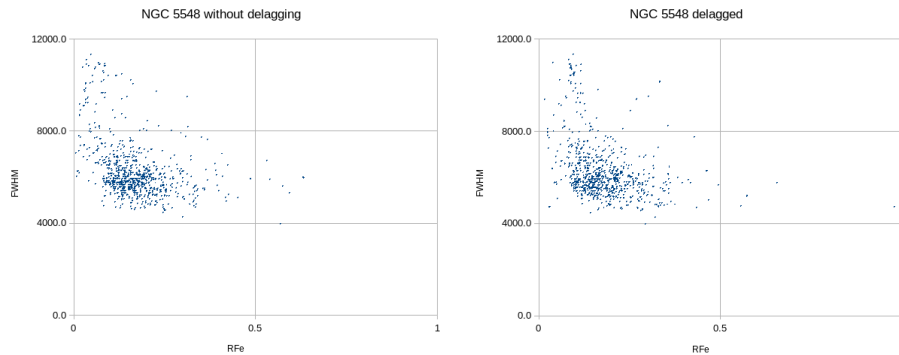


Figure 2: Variability of NGC 5548 before and after delagging correction for the reverberation lag of the $H\beta$ broad line to the optical continuum emission.

3. Implications for AGN Research

Understanding the variability of quasars along the EV1 main sequence is crucial for interpreting their physical conditions and intrinsic properties. Variability studies, particularly in the optical band provide insights into the dynamics of the broad-line region, the accretion processes, and the interplay between the black hole and its surroundings. Properly accounting for variability is essential for accurate modeling and parameter estimation (see Marziani et al. 2001).

4. Conclusion

The EV1 parametrization, based on RFe and FWHM of $H\beta$, remains a fundamental tool in the study of quasar properties. Mapping quasars onto the EV1 main sequence reveals insights into the physical conditions and processes governing these objects. Variability, while adding complexity, also provides a deeper understanding when properly considered. Continued exploration of this framework promises to enhance our comprehension of the AGN phenomenon and its role in cosmic evolution.

References

- Boroson, T. A., & Green, R. F. (1992). *Astrophysical Journal Supplement*, **80**, 109-135.
- Shen, Y., & Ho, L. C. (2014). *Nature*, **513(7518)**, 210-213.
- Sulentic, J. W., Marziani, P., & Dultzin-Hacyan, D. (2000). *Annual Review of Astronomy and Astrophysics*, **38**, 521-571.
- Marziani, P., Sulentic, J. W., Zwitter, T., Dultzin-Hacyan, D., & Calvani, M. (2001). *Astrophysical Journal*, **558(2)**, 553-560.
- Wilhite, B. C., Vanden Berk, D. E., Kron, R. G., et al. (2005). *Astrophysical Journal*, **633(2)**, 638-649.
- Kaspi, S., Smith, P. S., Netzer, H., et al. (2000) *Astrophysical Journal*, **533(2)**, 631-649.
- Marziani, P., Dultzin, D., Sulentic, et al. (2018), *Frontiers in Astronomy and Space Sciences*, **5**, 6.
- Bon, N., Bon, E., Marziani, P. (2018), *Frontiers in Astronomy and Space Sciences*, **5**, 3.
- Marziani, P., et al. (2022), *Astronomische Nachrichten*, **343**, e210091.
- Zamfir, S., Sulentic, J. W., Marziani, P., et al. (2010), *MNRAS*, **403**, 1759.

ADVANCED NONLINEAR ANALYSIS FOR DETECTING BINARY QUASARS AND TRANSIENT EVENTS IN THE LSST ERA

ANDJELKA B. KOVAČEVIĆ¹ , DRAGANA ILIĆ¹ , LUKA Č. POPOVIĆ² ,
MARINA PAVLOVIĆ³ , AMAN RAJU¹, MOMČILO TOŠIĆ¹ and
IVA ČVOROVIĆ-HAJDINJAK¹ 

¹University of Belgrade-Faculty of mathematics, Department of astronomy,
Studentski trg 16, 11158 Belgrade, Serbia
E-mail andjelka.kovacevic@matf.bg.ac.rs

²Astronomical observatory, Volgina 7, 11000 Belgrade, Serbia

³Mathematical Institute of the SASA, Kneza Mihaila 6, 11000 Belgrade, Serbia

Abstract. We present the completion of the Quasar harmonic eXplorer (QhX) and Quasar Neural Process Python (QNPY), a directable software in-kind contribution to the operations of the Vera C. Rubin Legacy Survey of Space and Time (LSST, Breivik et al 2022). QhX (Kovačević et al 2018,2019) and QNPY (Pavlović et al in prep) are designed to facilitate the nonlinear analysis of quasar emission with the aim of detecting close binary quasar (Kovačević 2024) and transient event candidates (Ilić et al 2020).

The presence of subparsec binary quasars in some galactic centers is assumed to be a key source of nHz gravitational waves, with electromagnetic radiation emitted in various forms during the inspiral phase. QhX addresses the significant challenges posed by non-sinusoidal signals, low signal-to-noise ratios, and red noise in quasar light curves, which complicate the detection of periodic signals using traditional methods. Our innovative approach employs the ‘2DHybrid’ method, an extension of two-dimensional correlation spectroscopy (Kovačević 2024), tailored for quasar emission curve analysis. QNPY complements QhX by applying deep learning model to analyze light curves with respect of presence of transient signals.

References

- Breivik, K., Connolly, A.J., Ford, K.E.S., Jurić, M., ... Ilić, D., Jankov, I., Kovačević, A., Savić, Dj, Popović, L.Č. et al. 2022, *White paper From Data to Software to Science with the Rubin Observatory LSST*, doi:10.48550/arXiv.2208.02781.
- Ilić, D., Oknyansky, V., Popović, L.Č., Tsygankov, S., et al., 2020, *A&A*, 638, id. A13
- Kovačević, A.B., 2024, *Applied Spectroscopy*, 0(0)
- Kovačević, A.B., Pérez-Hernández, E., Popović, L.Č., Shapovalova, A.I., Kollatschny, W., Ilić, D., 2018, *MNRAS*, 475, 2051
- Kovačević, A.B., Popović, L.Č., Simić, S., Ilić, D., 2019, *ApJ*, 871, article id. 32
- Pavlović, M., Kovačević, A, Raju, A., Ilić D., Čvorović Hajdinjak I., Popović, L.Č. 2024, in preparation

TWO-COMPONENT MODEL OF Fe II LINES IN SPECTRA OF ACTIVE GALACTIC NUCLEI

JELENA KOVAČEVIĆ-DOJČINOVIĆ¹, IVAN DOJČINOVIĆ² and LUKA Č. POPOVIĆ^{1,3}

¹ *Astronomical Observatory, Volgina 7, 11060 Belgrade, Serbia*
E-mail jkovacevic@aob.bg.ac.rs

² *Faculty of Physics, University of Belgrade, Studentski Trg 12, 11000 Belgrade, Serbia*

³ *Department of Astronomy, Faculty of Mathematics,*
University of Belgrade, Studentski Trg 16, 11000 Belgrade, Serbia

Abstract. The Fe II lines are among the most intriguing spectral features in the spectra of Active Galactic Nuclei (AGN). The place of their emission in AGN structure, their mechanisms of excitation, and their correlations with the other spectral parameters are still open questions. Here we represent two-component modeling of the Fe II lines, where we assume that iron lines arise from two emission regions: from the very broad line region (VBLR), the part of the BLR closer to the supermassive black hole, and from the intermediate line region (ILR), which is part of the BLR farther away from the black hole. We have constructed a large number of synthetic spectra of AGNs Type 1 using two component Fe II model and we have shown that Fe II VBLR components could form the Fe II pseudocontinuum in some special cases, and consequently affect measured spectral parameters in the optical spectra.

THE COMPLEX EMMITER INSIDE DENSE PLASMA,
CONTINUATION OF A COULOMB CUT-OFF
APPROACH, ARGON CASE

NENAD M. SAKAN¹ , ZORAN SIMIĆ² , VLADIMIR A. SREČKOVIĆ¹  and
MOMCHIL DECHEV³

¹*University of Belgrade, Institute of Physics
Belgrade, PO Box 57, 11001 Belgrade, Serbia
E-mail nsakan@ipb.ac.rs*

²*Astronomical Observatory, Volgina 7, 11060 Belgrade, Serbia*

³*Institute of Astronomy and National Astronomical Observatory, Bulgarian
Academy of Sciences, 72, Tsarigradsko chaussee Blvd. Sofia, Bulgaria*

Abstract. The work onto inclusion of the more complex emitters in plasma of moderate and high non-ideality modeling has been carried on. Since there were a good initial results in adopting a ab-initio generated pseudo-potentials as a candidates for describing of optical properties of dens plasma, this is step further where the complex argon case system is described and analyzed. The ionic core of the emitter has a strong influence onto the dipole matrix element and as so onto optical properties of analyzed plasma. Also the calculations of dense packing of emitters has been carried out, and it is expected to have more applicable pseudo-potential in near future. One of the advantages of presented calculations are complete quantum mechanical approach. The presented results are step forward towards a more detailed and more precise describing of a optical properties of dense plasma (see e.g. Srećković et al. 2018; Dimitrijević et al. 2018).

Acknowledgements

The authors acknowledge the support from the Institute of Physics Belgrade which was made possible by grants from the Ministry of Science, Technological Development., and supported by the Science Fund of the Republic Serbia, Grant No. 3108/2021—NOVA2LIBS4fusion. This article is based upon work from COST Action CA21101 Confined molecular systems: from a new generation of materials to the stars (COSY), supported by COST (European Cooperation in Science and Technology).

References

- Dimitrijević, M.S., Srećković, V.A., Sakan, N.M., Bezuglov, N.N., Klyucharev, A.N.: 2018, Free-Free Absorption in Solar Atmosphere. *Geomagn. Aeron.* **172**, 58, 1067–1072
Srećković, V.A., Sakan, N., Šulic, D., Jevremović, D., Ignjatović, L.M., Dimitrijević, M.S.: 2018, *Mon. Not. R. Astron. Soc.*, **475**, 1131–1136

INVESTIGATION OF CHEMISTRY OF HYDROGEN, HELIUM AND LITHIUM MOLECULAR IONS IN THE EARLY UNIVERSE

VLADIMIR A. SREČKOVIĆ¹ , NICOLINA POP², MILAN DIMITRIJEVIĆ³ 
and MAGDALENA CHRISTOVA⁴

¹*Institute of Physics Belgrade, UB, 11001, Belgrade, Serbia, vlada@ipb.ac.rs*

²*Politehnica University of Timisoara, Timisoara, Romania, nicolina.pop@upt.ro*

³*Astronomical Observatory, Volgina 7, Belgrade 38, Serbia, mdimitrijevic@aob.rs*

⁴*Department of Applied Physics, TU Sofia, Sofia, Bulgaria, mchristo@tu-sofia.bg*

Abstract. In the age of precision cosmology, determining the chemical composition of the early Universe necessitates a precise assessment of the reaction rates of the primary chemical processes involved. To follow the collapse of primordial clouds and afterwards examine the birth of first-generation stars, a comprehensive chemical-kinetic model for the evolution of the homogeneously expanding Universe in the post-recombination epoch is also required. Models of the early Universe stated that the chemical composition of the primordial gas includes lithium, hydrogen, and helium molecular ions e.g. LiH^+ , H_2^+ , HeH^+ . Abundances and processes (recombination, destruction, etc.) involving such species play an important role in chemistry and evolution of the early Universe, and the science community requires precise data sets for modeling. Radiation from these atomic and molecular species provides us with knowledge about the early Universe's environment. Understanding the relevant atomic and molecular processes is required to accurately interpret this radiation (Albert et al. 2020, Srećković et al. 2020, Vujčić et al. 2023). Here we calculated, recombination/ionization cross sections and rate coefficients, about such systems involving lithium, hydrogen and helium molecular ions. The result is a dataset for the chemistry of the early Universe and various astrophysical and laboratory studies.

Acknowledgements

We acknowledge the support from the Science Fund of the Republic Serbia, Grant 3108/2021—NOVA2LIBS4fusion and Action CA21136 CosmoVerse, supported by COST.

References

- Albert, D et al: 2020, *Atoms*, **8(4)**, 76.
Srećković, V. A., Ignjatović Lj. M., Dimitrijević M. S.: 2020, *Molecules* **26.1**, 151.
Vujčić, V. et al.: 2023, *Phys. Chem. Chem. Phys.*, **25(40)**, 26972.

DATASET FOR PHOTODISSOCIATION OF SMALL MOLECULAR IONS

VLADIMIR A. SREĆKOVIĆ¹ , NICOLINA POP², MILAN S. DIMITRIJEVIĆ³ ,
MAGDALENA D. CHRISTOVA⁴ and VELJKO VUJČIĆ³ 

¹*Institute of Physics Belgrade, UB, 57, 11001, Belgrade, Serbia vlada@ipb.ac.rs*

²*Politehnica University of Timisoara, Timisoara, Romania nicolina.pop@upt.ro*

³*Astronomical Observatory, Volgina 7, 11060 Belgrade 38, Serbia*

⁴*Department of Applied Physics, TU Sofia, Bulgaria; mchristo@tu-sofia.bg*

Abstract. In recent decades, new experimental techniques and computational chemistry methods have gained importance in the study of interaction and dynamics of various molecules (Albert et al. 2020, Giuliani et al. 2014). Furthermore, one can see the current importance of studying the optical properties of several small molecules, as well as the accompanying atomic and molecular data (Srećković et al. 2020, Vujčić et al. 2023). One can note that precision spectroscopy of molecular ions has applications in quantum state controlled chemical reactions, lasers, ultra-short lasers, measurements of fundamental constants, astrochemistry (Vazquez-Carson et al. 2022, Wu, Zhenlin, et al. 2024). Moreover, photodissociation of diatomic molecular ions such as CaH⁺ and N₂⁺ and ultrafast spectroscopy with trapped molecular ions are of interest. Here we present spectroscopic information, i.e., data, of such systems involving hydrogen and calcium.

Acknowledgements

We acknowledge the support from IPB and MSTD, the Science Fund of the Republic Serbia, Grant No. 3108/2021—NOVA2LIBS4fusion, COST Action CA18222—Attosecond Chemistry (AttoChem), supported by COST.

References

- Albert, et al: 2020, *Atoms*, **8(4)**, 76.
Giuliani, A., Milosavljevic, A., Canon, F., Nahon, L.: 2014, *Mass Spectrom. Rev.*, **33**, 424.
Srećković, V. A., Ignjatović Lj. M., Dimitrijević M. S.: 2020, *Molecules* **26.1**, 151.
Vazquez-Carson, S. F., Sun, Q., Dai, J., Mitra, D., Zelevinsky, T.: 2022, *New J. Phys.*, **24**, 1.
Vujčić, V., et al.: 2023, *Phys. Chem. Chem. Phys.*, **25(40)**, 26972.
Wu, Zhenlin, et al.: 2024, arXiv preprint arXiv:2401.10854."Photodissociation spectra of single trapped CaOH⁺ molecular ions."

NEW MOLECULAR DATA FOR CONFINED MOLECULAR SYSTEMS AND ASTROCHEMICAL MODELLING

VLADIMIR A. SREČKOVIĆ¹ , NICOLINA POP² and VELJKO VUJČIĆ³ 

¹*Institute of Physics Belgrade, 57, 11001, Belgrade, Serbia* vlada@ipb.ac.rs

²*Politehnica University of Timisoara, Timisoara, Romania* nicolina.pop@upt.ro

³*Astronomical Observatory, Volgina 7, 11060 Belgrade 38, Serbia* veljko@aob.rs

Abstract. Methods of computational chemistry have become increasingly important in the last decades for the investigation of interaction and dynamics of small molecules enclosed in larger structures (Albert et al. 2020, Reis et al. 2022). Despite their huge size, molecular clouds perform an important but little understood role in confined systems. Currently, there are a few hundred known molecular species in interstellar space, which include neutrals, cations, and anions ranging from diatomic to large ones. (Mandal & Roesky 2010). Due to scattering and absorption of interstellar radiation molecules that are deep inside molecular clouds can avoid photodissociation and/or photoionization (de Lara-Castells and Hauser 2020, Vujčić et al. 2023). Therefore, it is crucial to investigate not only radiative but also concurrent collisional processes.

Acknowledgements

We acknowledge the support from IPB and MSTD., the Science Fund of the Republic Serbia, Grant No. 3108/2021—NOVA2LIBS4fusion, COST Action CA21101 Confined molecular systems: from a new generation of materials to the stars (COSY), supported by COST.

References

- Albert, D., et al. : 2020, *Atoms*, **8(4)**, 76.
de Lara-Castells, M. P., and Hauser, A. W. : 2020, *Phys. Life Rev.* **32**.
Mandal, S. K., and Herbert W. Roesky: 2010, *Chemical communications*, **46.33** 6016.
Reis H., Żuchowski P., and Grubisic S.: 2022 *Frontiers in Chemistry* **10**, 941269.
Srećković, V.A., Lj. M. Ignjatović, and M. S. Dimitrijević: 2020, *Molecules* **26.1**, 151.
Vujčić, V., Marinković, B. P., Srećković, V. A., Tošić, S., Jevremović, D., Ignjatović, L. M., ... & Mason, N. J.: 2023, *Phys. Chem. Chem. Phys.*, **25(40)**, 26972.

**2nd Workshop on Swarm Physics
and Gaseous Dielectrics
(2nd SPGD)**

ANALYSIS OF CURRENT WAVEFORMS IN THE PULSED-TOWNSEND EXPERIMENT

G. J. BOYLE¹, D. L. MUCCIGNAT¹, M. J. E. CASEY¹ and R. D. WHITE¹

¹James Cook University, Townsville, Australia

E-mail gregory.boyle@jcu.edu.au

H. VEMULAPILLI², M. M. VAN RIJN², and C. M. FRANCK²

²ETH Zurich, Zurich, Switzerland

Abstract. The pulsed-Townsend (PT) experiment is the quintessential swarm experiment, wherein the spatiotemporal evolution of an electron swarm, as measured by an external circuit, allows the simultaneous determination of ionization, drift and diffusion properties (see e.g. [van Rijn *et al.* 2024]). The swarm transport properties can be used directly in the fluid modeling of plasmas [Petrović *et al.* 2009], or for the determination of the underlying scattering cross-sections [Muccignat *et al.* 2024]. Despite their importance, the interpretation of the transport properties measured in swarm experiments, including the PT, has been the subject of much historical debate and misunderstanding [Crompton 1967]. In 2021, it was shown that standard Brambring equation interpretation of the PT experiment current waveform is flawed when non-conservative processes are operative [Casey *et al.* 2021]. Specifically, the form of the continuity equation is not derivable from Boltzmann's equation, and the Townsend ionization coefficient is not consistent with either of the standard macroscopic or microscopic definitions. Casey and coworkers presented a consistent interpretation of the PT experiment and detailed how to relate the properties extracted via each description. In this work, we investigate the applicability of the analytic current waveform in extracting electron ionization, drift and diffusion properties from a simulated PT experiment. A Monte Carlo simulation was developed using simple model electron scattering cross-sections chosen to easily control the steady-state swarm properties. The accuracy of transport properties extracted from the simulated current waveform using the Casey equation form were investigated for a range of relative ionization, drift and diffusion strengths. Additionally, the effect of the electron source distribution, the relaxation to the steady-state, and Cathode re-absorption on the extracted properties are explored, and the implications to modern PT experiments is discussed.

References

- Casey, M. J. E., Stokes, P. W., Cocks, D. G., Bosnjaković, D., Simonović, I., Brunger, M. J., Dujko, S., Petrović, Z. Lj, Robson, R.E, White, R. D. : 2021, *Plasma Sources Sci. Technol.*, **30**, 035017.
- Crompton, R.W. : 1967, *J. Appl. Phys.*, **38** 4093.
- Muccignat, D. L. et al.: 2024, *Mach. Learn.: Sci. Technol.*, **5** 015047.
- van Rijn, M. M., Biagi, S., Franck, C. M. : 2024, *J. Phys. D: Appl. Phys.*, in press.

RAPIDLY EXPLORING AND DESIGNING ELECTRON TRANSPORT QUANTITIES IN DIELECTRIC GAS INSULATOR MIXTURES WITH APPROXIMATION THEORIES

N. A. GARLAND¹, D. L. MUCCIGNAT², G. J. BOYLE² and R. D. WHITE²

¹*School of Environment and Science, Griffith University, Nathan 4111, Australia*
E-mail n.garland@griffith.edu.au

²*College of Science and Engineering, James Cook University, Townsville 4810, Australia*

Abstract. Presently, most high voltage electrical infrastructure relies on SF₆, which is known as the most potent greenhouse gas with a global warming potential (GWP) approximately 23 500 times that of CO₂, and with an anticipated lifetime of up to 3200 years. To date, a number of replacements to SF₆ have been deployed in the power industry, such as dry air, N₂, CO₂, or various admixtures of natural and proprietary synthetic gases [Tian *et al.*]. Despite some adoption of replacements with lower GWP, the widespread global use of SF₆ prevails where it has not yet been bettered on an engineering basis for insulation and/or current quenching requirements. Driving the effort towards replacing SF₆ is research performing dielectric breakdown experiments or swarm experiments to characterise insulating gases. In addition to time and financial factors, there are many complexities and challenges in adequately performing and interpreting experimental measurements and so theory and simulation are vital methods to assist and complement experiments.

We discuss a semi-analytic method for approximating the density-reduced critical electric field for arbitrary mixtures of gases from swarm data of pure gases. This then enables a quick and affordable scan of very large parameter spaces of material choices or design configurations. The computational sieve approach to rapidly explore, trial, and assess potential scenarios can then inform the design of targeted experiments. We outline the theoretical basis of the approximation from electron fluid conservation equations, and validate how a mixture's critical electric field can be computed from the transport data of electrons in the pure gases. We demonstrate validity of the method in mixtures of N₂ / O₂, and SF₆ / O₂. We highlight an application of the method to approximate the critical electric field for mixtures of SF₆ and HFO1234ze(E), in which a positive synergy of an elevated critical electric field is seen in mixtures. To improve the utility of the proposed methods, we conclude with a demonstration of extending the presently published method [Garland *et al.*], which uses computed swarm coefficients, towards using only experimentally measured quantities.

References

- Garland, N. A. *et al.* : 2024, *J. Phys. D: Appl. Phys.*, **57**, 245202.
Tian S *et al.* : 2020, *AIP Adv.*, **10**, 050702

PHYSICS-INFORMED NEURAL NETWORKS FOR STUDIES ON ELECTRON SWARMS IN GASES

SATORU KAWAGUCHI¹, KAZUHIRO TAKAHASHI and KOHKI SATOH

¹*Muroran Institute of Technology*
E-mail skawaguchi@muroran-it.ac.jp

Abstract. Physics-informed neural networks (PINNs) have attracted much attention as a novel method for solving forward and inverse problems of partial differential equations (PDEs) (Raissi et al. 2019). In the PINNs, an artificial neural network (ANN) is trained to represent a solution of PDEs. The partial derivatives of the function represented by ANN can be computed analytically without generating grids. This mesh-free feature is an advantage when we tackle high-dimensional problems, such as solving electron Boltzmann equation (BE). We have developed two applications of the PINNs for studying electron swarm physics in gases. The first is solving electron BE using PINNs to calculate electron velocity distribution functions (EVDFs). So far, EVDFs in hydrodynamic equilibrium at DC electric and magnetic fields (Kawaguchi et al. 2020, 2022) and periodic equilibrium EVDFs at RF electric fields can be calculated (Kawaguchi et al. 2023a). The second is measuring electron transport coefficients by combining electron swarm experiments and PINNs (Kawaguchi et al. 2023b). The governing equation describing spatial and temporal development of measured data is discovered using PINNs. The electron continuity equation can be found from measured electron swarm maps under DC electric fields, allowing us to measure transport coefficients in the continuity equation, such as effective ionization collision frequency, bulk drift velocity, longitudinal diffusion coefficient, third-order transport coefficient and so forth.

Acknowledgements

This work is supported by JSPS KAKENHI JP22K14245 and Tokyo Electron Technology Solutions Ltd.

References

- Raissi M., Perdikaris P., Karniadakis G. E. : 2019, *J. Comput. Phys.*, **378**, 686.
Kawaguchi S., Takahashi K., Ohkama H., Satoh K. : 2020 *Plasma Sources Sci. Technol.* **29**, 025021.
Kawaguchi S. Murakami T. : 2022, *Japan. J. Appl. Phys.* **61**, 086002.
Kawaguchi S., Takahashi K., Satoh K. : 2023a *Proc. Int. Symp. Dry Process. 2023*, 103.
Kawaguchi S., Takahashi K., Satoh K. : 2023b *J. Phys. D: Appl. Phys.*, **56**, 244003.

ELECTRON SCATTERING CROSS SECTIONS OF 1,1,1,2-TETRAFLUOROETHANE (R134a)

MARNIK METTING VAN RIJN¹, STEPHEN F. BIAGI² and
CHRISTIAN M. FRANCK¹

¹*Institute for Power Systems and High Voltage Technology,
ETH Zurich, 8092 Zurich, Switzerland
E-mail corresponding author: marnikm@ethz.ch*

²*Faculty of Arts and Sciences Physics Department, Uludag University, Bursa,
Turkey*

Abstract. The standard mixtures operating in resistive plate chambers at CERN primarily consist of the refrigerant R134a (CF₃CH₂F). The presence of a high-energy particle in the detector induces an electron avalanche, which can numerically be simulated using electron-molecule scattering cross sections. In this contribution (Metting van Rijn et al. 2024), a revised set of cross sections of R134a is presented, enabling more accurate detector-performance simulations for the standard mixtures.

Electron-transport coefficients obtained in swarm experiments are crucial when deriving cross sections since they provide experimental verification in terms of absolute values. The Pulsed Townsend experiment is an established experimental technique and allows measuring the electron drift velocity, the longitudinal diffusion, and the effective ionization rate. The presented R134a cross sections were derived from swarm measurements performed in pure and argon-diluted mixtures. To ensure consistency with Monte-Carlo simulations (Biagi 1999), the electron-transport coefficients were extracted following a rigorous theoretical framework (Casey et al. 2021). Previously acquired R134a data (Urquijo et al. 2009) was translated correspondingly.

The bulk-drift-velocity measurements in pure R134a were used to fit the elastic cross section. The energy thresholds in the vibrational excitations were taken from the Computational Chemistry Comparison and Benchmark Data Base. The position of the first vibrational resonance was reduced to lower energy in comparison to the previous R134a set. The reduction led to better agreement with the bulk-drift-velocity measurements in the argon mixtures. No modifications were applied to the dipole-allowed electronic excitations and the ionization since oscillator strengths and experimental data on the ionization are not available. The triplet excitations were varied in amplitude to fit the effective ionization rate. The large experimental uncertainty on the longitudinal diffusion did not allow any constraints on the cross-section fitting.

The derived set of cross sections agrees with the experimental swarm data in certain energy regimes. At thermal and high energies, the presented R134a set reproduces the data only qualitatively. The deviations most likely stem from either underestimating the experimental uncertainties or inaccurate measurements. Especially, the high-electric-field measurements are particularly challenging, since bandwidth limitations may obscure the induced signals resulting from short electron-transit times. Investigations on the significance of boundary effects in low-pressure measurements are further required.

References

- Biagi, S.F. : 1999, *NIM-A*, **421(1-2)**, 234–240
Casey, M., et al. : 2021, *Plasma Sources Science and Technology*, **30(3)**, 035017.
Metting van Rijn, M., et al. : 2024, *Journal of Physics D: Applied Physics*, in press
Urquijo, J. et al. : 2009, *The European Physical Journal D*, **51**, 241–246.

ADVANCES IN MACHINE LEARNING METHODS
FOR THE DETERMINATION OF ELECTRON
SCATTERING CROSS-SECTION SETS

D. L. MUCCIGNAT¹, G J BOYLE¹, N. A. GARLAND² and R. D. WHITE¹

¹*College of Science and Engineering, James Cook University, Townsville 4810, Australia*
E-mail dale.muccignat@my.jcu.edu.au

²*Centre for Quantum Dynamics, Griffith University, Nathan 4111, Australia* $\&$
School of Environment and Science, Griffith University, Nathan 4111, Australia

Abstract. Accurate modelling of electron scattering from complex biological targets is critical for the development and implementation of plasma devices in fields such as medicine, nanoscale device manufacturing and agriculture [Adamovich *et al.*]. Underpinning these models are complete and self-consistent electron scattering cross-section sets that provide a microscopic description of electron scattering for a particular target molecule. While there exists a wealth of cross section set data available for select molecular targets in databases such as LXCat (see www.lxcats.net), the same can not be said for an ever growing number of molecular targets that are important for industrial and scientific applications.

A key focus of the research group at James Cook University has been to develop new, and improve existing, numerical techniques to assist in the determination of complete and self-consistent electron scattering cross-sections sets from experimental data. In particular, we focus on using deep learning methods to solve of the ill-posed ‘inverse swarm problem’, which aims to derive cross-section data from experimentally measured swarm transport coefficients.

We first present a brief history of the inverse swarm problem and outline the ill-posed nature of its solutions. We then present an overview of existing deep learning methods before highlighting the improvements made in a recent publication [Muccignat *et al.*]. We then present a preliminary investigation into the application of mixture density networks to determine the uncertainty of deep learning solutions to the inverse swarm problem. Finally, we conclude by summarising the existing limitations of deep learning methods and highlight the experimental and numerical data needed for future investigations.

References

- Adamovich, I. *et al.* : 2017, *J. Phys. D: Appl. Phys.*, **50**, 323001
Muccignat, D. L. *et al.* : 2024, *Machine Learning: Science and Technology*, **5**, 015047

THREE-BODY ELECTRON ATTACHMENT PROCESSES IN H₂O, CO₂, AND THEIR MIXTURES

L.G. PÉREZ^{1,2}, O. GONZÁLEZ¹ and J. DE URQUIJO¹

¹*Instituto de Ciencias Físicas, Universidad Nacional Autónoma de México
Av. Universidad 2001, Cuernavaca, Mor., México
jdu@icf.unam.mx*

²*IICBA, Universidad Autónoma del Estado de Morelos
lgperez@icf.unam.mx*

Abstract Three-body attachment processes have been measured and calculated in oxygen and its mixtures with nitrogen [see e.g., Chanin 1962, Grünberg 1969, de Urquijo 2024], where an electron is captured by O₂, leaving it in an excited state, O₂^{*} which, after a second collision with an O₂ molecule, is stabilised. Using a pulsed Townsend apparatus (see e.g., de Urquijo 2024 and references therein) we have explored the low E/N (electric field to gas density) region between 0.1 and 30 Td (1 Townsend=10⁻¹⁷ V cm²) and gas pressures up to 800 Torr. Over this E/N range, only electron attachment processes of the resonant type may take place since the electron energies lie below the threshold for molecular dissociation to occur. Pure H₂O and CO₂ have been studied together with the mixtures of H₂O with He, Ar and CO₂, as well as those of CO₂ with N₂. In all cases, we have found that the density-normalised attachment coefficient, η/N , depends inversely on N, contrary to the case of three-body electron attachment in oxygen, where η/N is directly proportional to N. Past this E/N regime, binary collisions occur, and dissociative attachment takes place, with η/N independent of N. To our knowledge, this three-body attachment process has hitherto not been reported. Based on a successful beam experiment (see, e.g. Allan 2011), we propose a two-step, three-body collision process in which an electron collides with the molecule, raising it to an excited state, CO₂^{*}, thereby enabling it to capture a second electron to form CO₂^{-*}. This unstable anion has a measured mean lifetime of 25 μ s, independent of pressure and E/N, which is suggestive of autodetachment. In the case of H₂O⁻, of which we only find theoretical work (see e.g. Houfek 2016), we have found that under swarm conditions this ion forms clusters readily, the mobility of which has been measured, and is pressure dependent. Together with the above, electron attachment coefficients, electron and ion drift velocities, longitudinal diffusion and effective ionisation coefficients will be presented. Regarding the latter, findings of Penning ionisation in H₂O-He mixtures will be discussed, as well as the effects of negative differential conductivity on the drift velocity and longitudinal diffusion.

Work supported by PAPIIT-UNAM IN 112223. The authors gratefully acknowledge the technical assistance of A. Bustos and G. Bustos.

Allan, A.: 2001, *Phys. Rev. Lett.* **87** 033201 Chanin L. M., Phelps A. V. Biondi M. A. 1962 *Phys. Rev.* **162** 219de Urquijo J., González-Magaña, O., Basurto, E., Juárez, A.M. 2024 *J. Phys. D: Appl. Phys.* **57** 125205
Grünberg, R. 1969 *Z. Naturforsch.* **24a** 1039
Houfek, K. Cížek, 2016, *M. Eur. Phys. J. D* **70** 107

FITTING OF ELECTRON COLLISION CROSS SECTIONS FROM SWARM DATA USING A GENETIC ALGORITHM

N. PINHÃO

*Instituto de Plasmas e Fusão Nuclear, Instituto Superior Técnico,
Universidade de Lisboa, Av. Rovisco Pais, 1049-001 Lisboa, Portugal
E-mail npinhao@ctn.tecnico.ulisboa.pt*

Abstract. The fitting of cross sections to swarm data has a central role in obtaining complete and consistent sets of cross sections (cs) needed in plasma physics modelling. While this method allows obtaining complete and consistent cs sets, the solution is not univocal and the fitting process is tedious and time-consuming. For these reasons, several authors have tested automated methods for this problem, with a particular emphasis on neural networks (Morgan 1991, Stokes 2020). In the present work, we follow a different approach, combining a *genetic algorithm* (GA) algorithm complemented with an *evolution strategy* (Beyer 2002), with the solution of the electron Boltzmann equation using a finite elements method and assuming a density gradient expansion. The validity of this method is studied for a model gas, and we find a very good agreement between the model transport coefficients and those from the optimized cs set, confirming the suitability of genetic algorithms to this problem. Additionally, the method can estimate a statistical uncertainty for the cs fitting parameters. The method is then applied to a real case: The fitting of methane cross sections considering vibrational polyad levels.

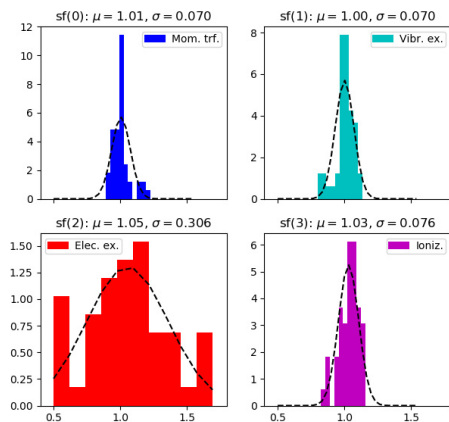


Figure 1:
Distribution of fitting parameters for the four cs obtained in several iterations.

References

- Beyer, H-G and Schwefel, H-P : 2002, *Natural Comput.* **1** 3
Morgan, W L : 1991, *IEEE Trans. Plasma Sci.* **19** 250
Stokes, P W et al. : 2020, *Plasma Sources Sci. Technol.* **29** 055009

ELECTRON INDUCED PROCESSES IN DIELECTRIC INSULATION GASES

M. RANKOVIĆ*, R. KUMAR T P, P. NAG, J. KOČIŠEK and J. FEDOR

*J. Heyrovský Institute of Physical Chemistry, Czech Academy of Sciences,
Dolejškova 3, 18223 Prague, Czech Republic
milos.rankovic@jh-inst.cas.cz

Abstract. A strong greenhouse gas SF₆ (sulfur hexafluoride) with a GWP of 23k, is still in wide global use due to its exceptionally high dielectric strength. It is mainly used in the electrical power distribution industry in various high-voltage outdoor switchgear devices. Over recent decades, a continuously increasing efforts have been invested towards reducing the emission of greenhouse gases. Therefore, a few suitable SF₆ replacement gases have been proposed, however, not much is known about their fundamental physical and chemical properties. In that regard, it is important to study electron collision processes in these gases in order to better understand their behavior under an electric discharge.

In this talk, we will give an overview of electron induced processes focusing mainly on SF₆ replacement candidate C₄F₇N (heptafluoroisobutyronitrile). Combining both experimental and theoretical approaches we explore dissociative ionization dynamics [1], transient anion states (resonances) [2], as well as electronic excitation and fragmentation processes [3]. The experiments reveal several interesting phenomena, where a number of resonances are formed in the electron scattering, leading to vibrational excitation of the molecule. Computational treatment of the ionization process indicate that a broad range of cation states is initially formed, corresponding to holes in various molecular orbitals. Moreover, modeling of the fragmentation processes using the techniques of non-adiabatic dynamics reveals the main fragments which are expected to form in an electric discharge.

References

- [1] Ranković, M., Chalabala, J., Zawadzki, M., Kočišek, J., Slavíček, P., and Fedor, J., : 2019, *Phys. Chem. Chem. Phys.*, **21**, 16451.
- [2] Ranković, M., Kumar T P, R., Nag, P., Kočišek, J., and Fedor, J., : 2020, *J. Chem. Phys.*, **152**, 244304.
- [3] Ovad T., Sapunar M., Sršeň Š., Slavíček P., Mašín Z., C. Jones N., V. Hoffmann S., Ranković M., and Fedor J., : 2023, *J. Chem. Phys.*, **158**, 014303.

MULTI-TERM BOLTZMANN MODELS: ENGINEERING TOOLS FOR THE PULSED POWER COMMUNITY

JACOB STEPHENS¹, MAX FLYNN¹ and ANDREAS NEUBER¹

¹*Center for Pulsed Power and Power Electronics, Texas Tech University, Lubbock, TX, USA*

E-mail jacob.c.stephens@ttu.edu

Abstract. Boltzmann's equation (BE) has a rich and decorated history as a powerful tool for the mathematical treatment of basic transport processes. For many decades, the BE has been employed to better understand electron transport in low temperature plasma (LTPs) and discharges. Over the years, the BE has grown from a basic science tool, to an applied science tool, and is now a powerful engineering tool in many communities (e.g. semiconductor fabrication), while still retaining strong presence in the basic and applied sciences. In spite of this history, the BE continues to have a mystical reputation among many in the engineering community. The pulsed power community is one such example.

This talk will introduce the topic of pulsed power and challenges and opportunities for BE-based modeling to advance state-of-the-art pulsed power capabilities. Some of these topics represent basic of capabilities within the BE community but have the potential to transform the future of pulsed power systems. The first topic discussed is the ability to predict the breakdown voltage of any combination of gases for which a complete set of cross-sections already exist. Secondly, the derivation of a new set of cross-section data from measured swarm parameters using a genetic algorithm is reviewed. The final topic of this talk is breakdown anomalies in pulsed power systems, which at present, are very poorly understood. This talk concludes with the question "Can the BE, an inherently deterministic transport model, be adapted or complemented to predict statistical anomalies observed in breakdown strength in gas insulated systems?".

References

G.J. Boyle, P.W. Stokes, R.E. Robson, R.D. White "Boltzmann's equation at 150: Traditional and modern solution techniques for charged particles in neutral gases" J. Chem. Phys. **159**, 024306 (2023).

PARTICLE PROPAGATION AND ELECTRON TRANSPORT IN GASES

L. VIALETTO

*Aeronautics and Astronautics, Stanford University, 496
Lomita Mall, Stanford, CA 94305, United States of America
E-mail vialetto@stanford.edu*

Abstract. Quantitative description of charged particle transport in gases is important for advancements of plasma and high voltage technology. In this talk, development of high fidelity kinetic and fluid models and their application for accurate description of charged particles swarms and discharge breakdown phenomena are presented.

First, an alternative method is presented to accelerate the convergence rate of Monte Carlo (MC) simulations of electrons (see Vialetto *et al.*). The method is based an efficient matrix-based approach called Monte Carlo Flux (MCF) and allows one to calculate electron and ion velocity distribution functions in complex gas mixtures without relying on computationally intensive MC simulations or on the two-term approximation. Advantages and disadvantages of the MCF method are discussed during the talk.

Then, a high fidelity Full-Fluid Model (FFM) is used for description of Argon DC breakdown. In FFM, the electron energy equation and inertial effects are included (see Sahu *et al.*). Results obtained with FFM are compared with the ones obtained with a Particle-In-Cell with Monte Carlo Collisions (PIC/MCC) code and ones obtained with a fluid model based on the drift-diffusion (DD) approximation for several values of pressure and electrode distance. Excellent agreement between PIC/MCC and FFM results are shown even at low values of pd (pressure times electrode distance), where discrepancies with results obtained using a conventional DD model are observed (see Mansour *et al.*).

References

- Vialetto, L., Longo, S., Diomede, P. : 2019, *Plasma Sources Sci. Technol.*, **28**, 115015.
Vialetto, L., Viegas, P., Longo, S., Diomede, P. : 2020, *Plasma Sources Sci. Technol.*, **29**, 115006.
Vialetto, L., Sugawara, H., Longo, S. : 2024, *Plasma*, **7**(1), 121–145.
Sahu, R., Mansour, A.R., Hara, K. : 2020, *Phys. Plasmas*, **27**, 113505.
Mansour, A.R., Vialetto, L., Yamashita, Y., Hara, K. : 2024, *submitted*.

DERIVING SWARM PARAMETERS FROM ION KINETICS AND DETERMINING COLLISION CROSS SECTIONS THROUGH DATA-DRIVEN METHODS FOR ECO-FRIENDLY INSULATING GASES

BOYA ZHANG, MAI HAO, PEIQIONG LIU and XINGWEN LI

*State Key Laboratory of Electrical Insulation and Power Equipment,
Xi'an Jiaotong University, Xi'an 710049, China
E-mail zhangby@xjtu.edu.cn*

Abstract. SF₆ is a favored insulating gas widely used in electric equipment, but it has a sever greenhouse effect. Recently, significant progress has been made in identifying and testing promising eco-friendly SF₆-alternative gases, such as C₄F₇N, C₅F₁₀O and HFO-1336mzz(E). This study focuses on the determination of their electron swarm parameters and electron-neutral collisional cross-sections. An efficient method is proposed to determine swarm parameters by Pulsed Townsend experiment, considering ion kinetics, including ionization, attachment, electron detachment and ion conversion. Further, a data-driven method was proposed to predict a complete and self-consistent set of electron-neutral collision cross sections of C₄F₇N and C₅F₁₀O. All the swarm parameters and cross sections data obtained in this work are available in our LXCat database www.lxcat.net/XJTUAETLab.

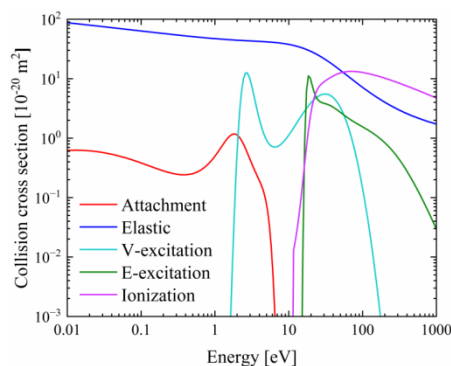


Figure 1: The refined collision cross-section set of C₅F₁₀O.

References

- Hao, M., Zhang, B., Li X., et al.: 2024, *Plasma Sources Sci. Technol.* **33**, 035005
Zhang, B., Hao, M., Yao Y., et al.: 2023, *J. Phys. D: Appl. Phys.* **56**, 134001.
Zhang, B., Liu P., Hao, M., Li X.: 2024, *J. Phys. D: Appl. Phys.* **57**, 375206.

AUTHORS' INDEX

- Astashev M.E. 129
Asvany O. 21
Atić Jasmina 29, 39
Aumayr F. 36
Avaldi Lorenzo 48
Babić Jovana 86
Babucić Neda 108, 148
Bakshaev A.S. 118
Banjanac Radomir 176
Bari Sadia 35
Becker M. M. 109, 111
Beterov I. I. 165
Bezuglov N. N. 165
Biagi Stephen F. 194
Blanco Francisco 46, 66
Bocharnikova E.N. 114
Boer Daan 30, 100
Bogachev N.N. 118, 119
Bogdankevich I.L. 119
Bon Edi 178
Bon Nataša 178
Borzosekov V.D. 129
Bošnjaković Danko 37, 39, 40, 62
Boye-Peronne S. 172
Boyle G. J. 38, 53, 191, 192, 195
Božanić Dušan K. 31
Bröcker L. 111
Casey M. J. E. 191
Cecchi-Pestellini C. 167
Chakraborty Himadri 22
Chaykovsky S.A. 114
Christova M. D. 164
Christova Magdalena D. 185, 186
Chukalovsky A. 130
Ciganovic Jovan 92
Cinins A. 165
Čolić Miodrag 108
Ćosić M. 76
Cruz Rodriguez L. 61
Cvetanović Nikola 120
Čvorović-Hajdinjak Iva 182
Danileiko Yu.K. 129
Danilović Danijela 31
De Urquijo J. 40, 196
Dechev Momchil 184
Delibašić Danilo 49
Delibašić-Marković Hristina 73
Despoja V. 74
Dimitrijević Milan S. 137, 164, 165, 185, 186
Djoković Vladimir 31
Djordjević B. Z. 171
Djurović Stevica 121
Dobnik D. 107
Dojčilović Radovan 31
Dojčinović Ivan 183
Domaracka Alicija 23
Đorđević Antonije 138
Dragić Aleksandar 176
Drissi M. 172
Dujko Saša 29, 37, 39, 40, 62
Dupuy R. 32
Ehresmann Arno 34
Esletzbichler L. 36
Fedor J. 198
Figueira de Morisson Faria C. 61
Figueira de Morisson Faria Carla 24
Filipić A. 107
Flynn Max 199
Fournier M. 32
Franck C. M. 191
Franck Christian M. 194
Gans B. 172
Garcia G.A. 172
Garcia Gustavo 46, 66
Garland N. A. 38, 41, 53, 192, 195
Gascooke J. R. 53
Gavanski Lazar 121
Gavrilović Božović Marijana R. 147
Gazeli K. 104
Gerling T. 109
Gomboc Andreja 161

González O. 196
 Gorjanc Marija 71
 Goto M. 169
 Grushko Oleg 112
 Gudkov S.V. 129
 Gudkova V.V. 129
 Gusein-Zade N.G. 119, 129
 Habibović D. 33
 Hadžijojić M. 76
 Hagelaar Gerjan 45
 Haidegger P. 36
 Hamaguchi Satoshi 99
 Hans Andreas 34
 Hao Mai 45, 201
 Hartmann Peter 101
 Heikura Emilia 34
 Hendaway N. 105
 Hildebrandt M. 41
 Höft H. 109
 Hrodmarsson H.R. 172
 Iacob Felix 158, 173
 Iati M. A. 167
 Ilić Dragana 182
 Ivanović Nikola V. 144
 Ivanović Stefan Đ. 47
 Ivković Milivoje 85, 147, 152, 153
 Ivković Saša S. 120
 Jacovella Ugo 166
 Jacquemin M. 104
 Jiang M.-X. 172
 Joković Dejan 176
 Jones D. B. 53
 Jovanović A. P. 109
 Jovanović Olivera 108
 Jovović Jovica 125
 Jureta Jozo J. 48
 Kabbara H. 104
 Kalinić Ana 74, 80
 Karbunar Lazar 74, 80
 Karfidov D.M. 119
 Kargin Denis 34
 Kasri S. 104
 Kawaguchi Satoru 193
 Kawamoto Y. 169
 Kawate T. 169
 Khomich V.Yu. 154
 Klages C.-P. 111
 Klubkov A.V. 154
 Kočišek J. 198
 Koike F. 169
 Kolarski Aleksandra 174
 Kolik L.V. 118, 129
 Koller T. 36
 Komarov F. 81
 Konchekov E.M. 118, 129
 Kon'kova A.S. 118
 Konjević N. 144
 Kornev V. 92
 Korzhova O.I. 154
 Kostic Mirjana 102
 Kostić Petar 175
 Kotov M.A. 145
 Kounchev Ognyan 158
 Kovačević Andjelka B. 182
 Kovačević-Dojčinović Jelena 183
 Kovár Samuel Peter 106
 Kramar Ana 102
 Kropotkin A. 130
 Kumar R. T P 198
 Kuraica Milorad 102
 Kursov A. 130
 Kuzmanović Miroslav 85, 86, 142,
 146
 Kuzmenko V. 143
 Kuzmenko Vitaly 134
 La Mura G. 167
 Lalor James 135
 Lapushkina T.A. 145
 Lazic Violeta 103
 Lazzaroni C. 104
 Le H.L. 172
 Leroux Juliette 35
 Li Xingwen 45, 67, 201
 Liu Peiqiong 201
 Loffhagen D. 109, 111
 Loison J.-C. 172
 Lombardi G. 104
 Lukanin V.I. 129
 Lysov N. Yu. 154
 Maclaren S. A. 171
 Maguire P. 105
 Majlinger Zlatko 136, 137
 Makarova A.S. 114
 Maletić Dimitrije 176
 Maljković Jelena B. 46, 66
 Malović Gordana 108
 Mančev Ivan 49
 Marić Dragana 138

Marinković Bratislav P. 46, 47, 48,
 66
 Mariotti D. 105
 Marjanović Jelena 138
 Marković Andjelija 108
 Marković Milica 142
 Marziani Paola 162, 178
 Matejčík Štefan 63, 106
 Mceachran R. P. 38
 Mcquaid H. 105
 Meißner Robert 35
 Menacer B. 104
 Miakonkikh A. 143
 Miakonkikh Andrey 134
 Miculis K. 165
 Milchanin O. 81
 Milenković Miloš 49
 Mille V. 104
 Milojević Nenad 49
 Milosavljević Aleksandar R. 31, 34
 Milosavljević Vladimir 135
 Milošević D. B. 33
 Mišković Z. L. 74, 80
 Momcilovic Miloš 92
 Monakhov N.A. 145
 Moody J. D. 171
 Moravský Ladislav 106
 Morina A. 108
 Moryakov I.V. 129
 Mozetič M. 107
 Muceignat D. L. 53, 191, 192, 195
 Mulas G. 167
 Murakami I. 169
 Nag P. 198
 Nahon L. 172
 Nakamura N. 169
 Nedelko M. 92
 Nedić Nikodin V. 144
 Neuber Andreas 199
 Nicolas C. 32
 Niggas A. 36
 Nikitović Ž. 57
 Obradović Bratislav M. 102, 120
 Oishi T. 169
 Oostenrijk Bart 35
 Országh Juraj 63
 Ortiz Mahecha Carlos 35
 Palaudoux J. 32
 Palov A. 130
 Papp Peter 106
 Paulus G. G. 25
 Pavlović Marina 182
 Pavlovic Sanja 110
 Penent F. 32
 Pérez L.G. 196
 Petrović Srdjan 88
 Petrović Zoran Lj. 39, 40, 108, 138
 Pietschnig Rudolf 34
 Pille Laura 35
 Pinchuk Mikhail 112
 Pinhão N. 27, 197
 Poniaev S.A. 145
 Pop Nicolina 185, 186, 187
 Poparić Goran B. 65, 75, 87, 110
 Popov P.A. 145
 Popović Luka Č. 182, 183
 Prime G. 107
 Puač Marija 138
 Puač Nevena 108, 148
 Puzyrev M.V. 81
 Radomtsev A. 92
 Radović Ivan 74, 80
 Radović Milan 72
 Rafn Hrodmarsson Helgi 28
 Rahavaya I.S. 81
 Raju Aman 182
 Rakhimova T. 130
 Ranković Dragan 85, 142, 146, 147
 Ranković M. 198
 Raspopović Z. 57
 Remigy A. 104
 Rezaei S. 167
 Ristić Miroslav 65, 86, 146
 Robson R. E. 41
 Rook T. 61
 Ruchkin Ilya 112
 Rudenko K. 143
 Rudenko Konstantin 134
 Ryzhkov S.V. 168
 Sahal-Bréchet S. 164
 Saija R. 167
 Šajić Aleksandra 86, 146
 Sakan Nenad M. 184
 Satoh Kohki 193
 Savić Mihailo 176
 Savović Jelena 147
 Schlemmer S. 21
 Schmid P.C. 21

Schwob Lucas 35
 Scuderi Debora 35
 Sergeichev K.F. 129
 Simić Nataša 121
 Simić Zoran 184
 Simonović Ilija 37, 39, 40, 62
 Škoro Nikola 108, 148
 Snetov Vadim 112
 Sokolova I.V. 114
 Solomonov V.I. 114
 Spasojević Djordje 144
 Srećković Vladimir A. 64, 137,
 158, 165, 184, 185, 186, 187
 Stachová Barbora 63
 Stankov Biljana 85, 147, 152, 153
 Stankov M. 111
 Stanković Mališ Violeta V. 65, 75,
 87
 Starčević Nikola 88
 Stepanova Olga 112
 Stephens Jacob 199
 Stepin V.P. 119
 Strozzi D. J. 171
 Subbotin Dmitry 112
 Suzuki C. 169
 Takahashi Kazuhiro 193
 Tamura N. 169
 Tarasenska N. 92
 Tarasenko N. 92
 Tchaikovskaya O.N. 114
 Thorwirth S. 21
 Tőkési K. 36
 Tomić Sergej 108
 Tong Xiao-Min 26
 Topalović Desanka 148
 Tošić Momčilo 182
 Tošić Sanja 64
 Traparić Ivan 85, 113, 152, 153
 Travar Miloš 176
 Udovičić Vladimir 176
 van Dijk Jan 30, 100
 van Rijn M. M. 191
 van Rijn Marnik Metting 194
 Vemulapilli H. 191
 Veselinović Nikola 176
 Vialetto L. 200
 Videnović Ivan R. 144
 Vinić Milica 153
 Voevodin V.V. 154
 Vojnović Mirjana M. 65
 Volpe Luca 163
 Vujadinović Nikola 153
 Vujčić Veljko 64, 158, 186, 187
 Vukalović Jelena 46, 66
 Vukcevic Miroslava 170
 Walsh C. A. 171
 Wang Guanyu 67
 Weber C. R. 171
 Werl M. 36
 White R. D. 38, 41, 53, 191, 192,
 195
 Wilhelm R.A. 36
 Wrathall S. 36
 Yamschikov V.A. 154
 Yanykin D.V. 129
 Zaplotnik R. 107
 Zeković Vladimir 177
 Zhang Boya 45, 67, 201
 Zhukov V.I. 119
 Zimmerman G. B. 171
 Zindell Christina 34
 Zivkovic Sanja 92
 Zver M. 107

SPIG 2024 PROGRAMME

Belgrade, Serbia, August 26 – 30, 2024

All indicated times are given in the Central European Summer Time (CEST) zone.

Monday 26 th August 2024		
Workshops		
	<i>2nd SPGD Workshop</i>	<i>LIBS4fusion Workshop</i>
09:20-09:30	Opening and Introduction: Saša Dujko	Opening: Milivoje Ivković
	<i>Session 1, Hall A</i>	<i>Session 1, Hall B</i>
09:30-10:00	Miloš Ranković (Czech Republic) Electron-induced processes in dielectric insulation gases	Volker Naulin (Denmark) Fusion: from science fiction to science fact
10:00-10:30	Jaime de Urquijo (Mexico) Three-body electron attachment processes in H ₂ O, CO ₂ , and their mixtures	Radomir Panek (Czech Republic) EUROfusion, the consortium coordinating European fusion research
10:30-11:00	Boya Zhang (China) Deriving Swarm Parameters from Ion Kinetics and Determining Collision Cross Sections through Data-Driven Methods for Eco-friendly Insulating Gase	Miloš Škorić (Serbia) to be confirmed Fusion related research at the University of Belgrade
<i>11:00-11:30</i>	<i>Coffee break</i>	
	<i>Session 2, Hall A</i>	<i>Session 2, Hall B</i>
11:30-12:00	Jacob Stephens (USA) Multi term Boltzmann models: Engineering Tools for the Pulsed Power Community	Corneliu Porosnicu (Romania) Plasma-wall interaction studies within the EUROfusion Consortium
12:00-12:30	Luca Vialetto (USA) Particle propagation and electron transport in gases and plasmas	V. Alimov (Russia) to be confirmed Diagnostics of the fusion reactor wall
12:30-13:00	Satoru Kawaguchi (Japan) Physics-informed neural networks for studies on electron swarms in gases	Violeta Lazić (Italy) Deployments of Laser Induced Breakdown Spectroscopy
<i>13:00-15:00</i>	<i>Lunch break</i>	
	<i>Session 3, Hall A</i>	<i>Session 3, Hall B</i>
15:00-15:30	Dale Muccignat (Australia) Advances in machine learning methods for the determination of electron scattering cross-section sets	Milivoje Ivković (Serbia) NOVA2LIBS4fusion
15:30-16:00	Greg Boyle (Australia) Analysis of current waveforms in the pulsed-Townsend Experiment	Dragan Ranković (Serbia) TEA CO ₂ laser LIBS
16:00-16:30	Nuno Pinhão (Portugal) Fitting of Electron Collision Cross Sections from Swarm Data using a Genetic Algorithm	15:50 Biljana Stankov (Serbia) Stark parameters of beryllium spectral lines 16:10 Miroslav Kuzmanović (Serbia) Problem of LIBS surface and depth elemental analysis of PFC materials
<i>16:30-17:00</i>	<i>Coffee break</i>	
	<i>Session 4, Hall A</i>	<i>Session 4, Hall B</i>
17:00-17:30	Nathan Garland (Australia) Rapidly exploring and designing electron transport quantities in dielectric gas	Ivan Traparić (Serbia) Hydrogen isotope retention diagnostics

	insulator mixtures with approximation theories	17:20 Marijana Gavrilović Božović (Serbia)
17:30-18:00	Marnik Metting Van Rijn (Switzerland) Electron scattering cross sections of 1,1,1,2-Tetrafluoroethane (R134a)	17:40 Milivoje Ivković (Serbia) In-situ LIBS for fusion reactors surface diagnostics
18:00-20:00	SPIG 2024 Welcome Cocktail (Club of SASA)	18:00-18:30 Rounding table

All indicated times are given in the Central European Summer Time (CEST) zone.

Tuesday 27th August 2024

SPIG 2024 (day 2)

PL – Plenary lecture: 35+10 min		TL – Topical lecture: 25+5 min	PR – Progress Report: 15+5 min
08:45-09:00	Opening, Chairs: Bratislav Obradović, Jovan Cvetic and Miroslav Kuzmanović		
	<i>Plenary Session 1, Hall A, Chair: Dejan Milošević</i>		
09:00-09:45	Xiao-Min Tong (Japan) Theory on dynamics of atoms in strong laser field		
09:45-10:30	Gerhard G. Paulus (Germany) Extreme UV imaging with high harmonics		
10:30-11:00	Coffee Break		
	<i>Plenary Session 2, Hall A, Chair: Miloš Škorić</i>		
11:00-11:45	Luca Volpe (Spain) Current situation and future perspectives of the European IFE program, technology development, science and related applications		
11:45-12:30	Andreja Gomboc (Slovenia) How stars get thorn apart by supermassive black holes		
12:30-14:30	Lunch Break		
	Hall A - Parallel Session: <i>Chair: Bratislav Obradović</i>		Hall B - Parallel Session <i>Chair: Ivan Mančev</i>
14:30-15:00	Paul Maguire (United Kingdom) Liquid microdroplets in a microplasma: phenomena and technological applications 3	Peter Papp (Slovakia) Ion induced reactions in IMS studied by DFT 3	
15:00-15:30	Nevena Puač (Serbia) Diagnostics and applications of atmospheric pressure plasmas for triggering of cell mechanisms 3	Violeta Stanković Mališ (Serbia) Modeling the surface interaction of cellulosic materials with CO ₂ plasmas 2 (15:00-15:20)	
		Ana Kalinić (Serbia): Interaction of ions with graphene-insulator-graphene composite systems 2 (15:20-15:40)	
15:30-16:00	Claudia Lazzaroni (France) Micro hollow cathode discharges in Ar/N ₂ used for boron nitride PECVD 3	Hristina Delibašić Marković (Serbia): Characterizing Ionization and Electron Dynamics in Biological Materials: Theoretical and Numerical Insights into Pulsed Laser-Induced Breakdown Processes 2 (15:40-16:00)	
16:30-17:00	Coffee Break		
	Hall A - Parallel Session <i>Chair: Jovan Cvetic</i>		Hall B - Parallel Session <i>Chair: Ivan Radović</i>
17:00-17:30	Chihiro Suzuki (Japan) Comprehensive Z dependence analysis of soft X-ray spectra from highly charged heavy ions using magnetically confined high-temperature plasmas 4		Myriam Drissi (France) Photoelectron spectroscopy of radicals of astrochemical interest 4 (17:00-17:20)
17:30-18:00	Sergei Ryzhkov (Russia) Magneto-inertial fusion and powerful installation 4		Matthias Werl (Austria) De-excitation cascade calculation for highly excited of hollow atoms 1 (17:20-17:40)
18:00-18:20	Blagoje Djordjevic (USA): Integrated radiation-magneto-hydrodynamic simulations of magnetized burning plasmas		Jasmina Atić (Serbia) Electron transport and negative ionization fronts in strongly attaching gases 1 (17:40-18:00)

		Danijela Danilović (Serbia) Synchrotron radiation photoelectron spectroscopy study of the electronic structure of Ag-Bi-I ruderffite nanoparticles 1 (18:00-18:20)
18:30-20:00	<i>Poster session 1</i> - SASA Gallery of Science and Technology (<i>Chair: Nikola Cvetanović</i>)	

All indicated times are given in the Central European Summer Time (CEST) zone.

Wednesday 28th August		
SPIG 2024 (day 3)		
<i>PL – Plenary lecture: 35+10 min</i>	<i>TL – Topical lecture: 25+5 min</i>	<i>PR – Progress Report: 15+5 min</i>
<i>Plenary Session 3, Hall A, Chair: Igor Savić</i>		
09:00-09:45	Stephan Schlemmer (Germany) Missing ions in laboratory and space	
09:45-10:30	Alicja Domaracka (France) Ion processing of molecular systems: a way to form complex systems in space	
10:30-11:00	<i>Coffee Break</i>	
<i>Plenary Session 4, Hall A, Chair: Dragana Marić</i>		
11:00-11:45	Jan van Dijk (Netherlands) LXCat 3 and Beyond – Fostering Reproducibility in Low-Temperature Plasma Science	
	<i>Hall A - Parallel Session</i> <i>Chair: Aleksandar Milosavljević</i>	<i>Hall B - Parallel Session</i> <i>Chair: Jelena Kovačević Dojčinović</i>
11:45-12:15	Nuno Pinhão (Portugal): Description of electron swarms in an electric field: a finite elements computation including third-order transport parameters 1	Nikolai N. Bezuglov (Russia): Penning and photoionizations of cold Rydberg alkali metal atoms under Förster resonance conditions 4
12:15-12:45	Marine Fournier (France): Photoelectron spectroscopy of solvated biological interest molecule in liquid-jet configuration 1 (12:15-12:35)	Giovanni La Mura (Italy): Interstellar dust as a dynamic environment 4
12:45-14:30	<i>Lunch Break / SPIG Committee meeting</i>	
	<i>Hall A - Parallel Session</i> <i>Chair: Sanja Tošić</i>	<i>Hall B - Parallel Session</i> <i>Chair: Vladimir Srećković</i>
14:30-15:00	Helgi Hroddmarsson (France): VUV photoionization of interstellar molecules: Making sense of our beautifully mysterious Universe molecule by molecule 1	Miroslava Vukčević (Serbia): On the conditions for soliton formation in the galactic environment 4
15:00-15:20	Dino Habibović (Bosnia and Herzegovina) Strong-field processes induced by tailored laser fields 1	Nikola Veselinovic (Serbia): Fluctuations in the Flux of Energetic Protons in Heliosphere before and during Sudden Decreases in Galactic Cosmic Ray Intensity 4
15:20-15:40	Daan Boer (Netherlands) LoKI-B C++: An open-source Boltzmann solver for reproducible electron Boltzmann calculations 1	Aleksandra Kolarski (Serbia): Properties of Earth's lower ionospheric plasma perturbed by solar flares 4
15:40-16:00	Emilia Jasmiina Heikura (Germany): Towards distant dependent inner-shell photoelectron circular dichroism 1	Vladimir Zeković (Serbia): SLAMS-enhanced particle acceleration at high-Mach number astrophysical shocks: TeV in a blink of a supernova 4
16:00-16:20	Laura Pille (Germany): Exploring biomolecular properties in the gas phase by using advanced light sources 1	Petar Kostić (Serbia): Supernova remnants in clumpy medium: hydrodynamic and radio synchrotron evolution 4
16:30	<i>Mini excursion (info at registration desk): Belgrade underground tour</i>	

All indicated times are given in the Central European Summer Time (CEST) zone.

Thursday 29th August 2024		
SPIG 2024 (day 4)		
<i>PL</i> – Plenary lecture: 35+10 min	<i>TL</i> – Topical lecture: 25+5 min	<i>PR</i> – Progress Report: 15+5 min
	Plenary Session 5, Hall A, Chair: Nenad Simonović	
09:00-09:45	Carla Faria (United Kingdom) Exploring quantum effects in the attosecond domain	
09:45-10:30	Himadri Chakraborty (USA) Impact spectroscopy and chronoscopy of gas phase atoms, molecules and fullerenes	
10:30-11:00	Coffee Break	
	Plenary Session 6, Hall A, Chair: Dragana Ilić	
11:00-11:45	Paola Marziani (Italy) Super-Eddington Quasars: from Atomic Physics to Cosmology	
11:45-12:30	Satoshi Hamaguchi (Japan): Opportunities and challenges in low-temperature plasma science for atomic-layer processing	
12:30-14:00	Lunch Break	
	Hall A - Parallel Session Chair: <i>Vladimir Milosavljević</i>	Hall B - Parallel Session Chair: <i>Marko Ćosić</i>
14:00-14:30	Marija Gorjanc (Slovenia): Plasma modification of textile fibers for adhesion improvement in bio-composites 2	Magdalena D. Christova (Bulgaria): Astrophysical applications of Stark broadening of spectral lines 4
14:30-15:00	Mirjana Kostić (Serbia): Atmospheric pressure plasma in processing of cellulose fibres: from surface cleaning to tailored properties 3	Ugo Jacovella (France): Exploring the importance of interstellar ions in the enigma of diffuse interstellar bands 4
15:00-15:30	Miran Mozetič (Slovenia): Inactivation of viruses in water by plasma treatment 3	Felix Iacob (Romania) Electron NS+ collisions in cold plasma 4 (15:00-15:20)
15:30-16:00	Coffee Break	
	Hall A - Parallel Session Chair: <i>Predrag Ranitović</i>	Hall B - Parallel Session Chair: <i>Goran Poparić</i>
16:00-16:30	Milan Radović (Switzerland) Pulse Laser Deposition and Advanced Spectroscopy: Key to Revealing Emerging Properties in Transition Metal Oxides 2	Peter Hartmann (Hungary) Using dust particles as probes in low pressure gas 3
16:30-17:00	Violeta Lazić (Italy) LIBS spectroscopy: what we can measure, and how? 3	Sanja Pavlović (Serbia) Thermal and acoustic properties of cellulose fibrous materials 3 (16:30-16:50)
17:00-17:20	Ivan Traparić (Serbia) Application of Machine Learning and Artificial Intelligence in Plasma Spectroscopy 3	Marjan Stankov (Germany) Analysis of dielectric barrier discharges in Ar-monomer mixtures using a standardized fluid modelling approach 3 (16:50-17:10)
17:20-17:40	Olga Stepanova (Russia) Air-Plasma-Water Electrophysical System: prospects and problems 3	Aleksandar Jovanović (Germany) Fluid modelling of single-filament DBD and self-pulsing discharges at atmospheric pressure using FEDM 3 (17:10-17:30)
17:50-19:00	Poster session 2 - SASA Gallery of Science and Technology (Chair: <i>Miroslav Kuzmanović</i>)	
20:00-24:00	Conference dinner and closing	

Friday 30th August 2024	
SPIG 2024 (day 5)	
10:00-17:00	<i>Excursions (optional, info at registration desk): Belgrade sightseeing cruise (10 – 13:30)</i>
17:00	Departure

LIST OF POSTERS

No.	Section	Title	Authors
1	1.1.	Excitation of acetone induced by electron impact	Barbora Stachová, Juraj Országh and Štefan Matejčík
2	1.1.	Small molecules essential to astrophysics: collisional and radiative processes	S. Tošić, V. Srećković and V. Vujčić
3	1.1.	Investigation of elastic electron scattering from desflurane molecule at intermediate electron energy	J. Vukalović, J.B. Maljković, F. Blanco, G. Garcia and B.P. Marinković
4	1.1.	Ejected electron spectra of krypton studied by high and low energy electrons	B.P. Marinković, J.J. Jureta and L. Avaldi
5	1.1.	Electron scattering cross sections represented in Belgrade electron-atom/molecule database (beam)	B.P. Marinković and S.D. Ivanović
6	1.1.	Direct electron-liquid energy loss spectra measurements using a liquid micro-jet	D. L. Muccignat, D. B. Jones, J. R. Gascooke, G. J. Boyle, N. A. Garland and R. D. White
7	1.1.	Influence of catastrophes and hidden dynamical symmetries on ultrafast backscattered photoelectrons	T. Rook, L. Cruz Rodriguez and C. Figueira de Morisson Faria
8	1.1.	Dissociative electron attachment to CO ₂ in electric and magnetic fields	M. M. Vojnović, M. M. Ristić, V. V. Stanković-Mališ and G. B. Poparić
9	1.1	Investigation of Elastic Electron Scattering by Anaesthetic Molecules in Gaseous Phase	Jelena B. Maljović, Jelena Vukalović, Francisco Blanco, Gustavo Garcia and Bratislav P. Marinković
10	1.2.	Post-prior discrepancy in the CB1-4B method for single-electron capture in fast Li ³⁺ + He collisions	Nenad Milojević, Ivan Mančev, Danilo Delibašić and Miloš Milenković
11	1.3.	Diffusion coefficients of H ₂ ⁺ ions in H ₂ gas	Ž. Nikitović and Z. Raspopović
12	1.3.	Transport properties of two-temperature SF ₆ and its alternative gases	G.Wang, B. Zhang and X.Li
13	1.3.	Monte Carlo simulation of electron swarms in pulsed Townsend experiment and validation of the swarm data derived from waveform analysis	M. Hao, G. Hagelaar, B. Zhang and X. Li
14	1.3.	An aliasing method for determination of transport data for exotic charged particles in crossed electric and magnetic fields	N. A. Garland, R. D. White, R. E. Robson and M. Hildebrandt

15	1.3.	Studies on electron swarms and streamer discharges in eco-friendly RPC gases	S. Dujko, I. Simonović, D. Bošnjaković, Z.Lj. Petrović and J. De Urquijo
16	1.3.	Electron transport in radio-frequency electric and magnetic fields in ultra-low GWP gases	S. Dujko, I. Simonović, D. Bošnjaković, J. Atić and Z. Lj. Petrović
17	1.3.	Studies on streamer discharges in ultra-low GWP gases	D. Bošnjaković, I. Simonović and S. Dujko
18	1.3.	Electron transport in simple liquid mixtures	G. J. Boyle, N. A. Garland, R. P. Mceachran and R. D. White
19	1.3	Three-dimensional streamer model in the AMREX environment	I. Simonović, D. Bošnjaković and S. Dujko
20	2.1.	Interaction of ions with drift-current biased supported graphene	A. Kalinić, I. Radović, L. Karbunar and Z. L. Mišković
21	2.1.	Rainbows in transmission of protons through thin silicon carbide crystal	N. Starčević and S. Petrović
22	2.1.	Low energy heavy ion rainbow scattering by graphene	M. Hadžijojić and M. Čosić
23	2.2.	Forming nanocrystalline SnO ₂ films on silicon and silicon dioxide by laser-plasma deposition method	F. Komarov, O. Milchanin, M. V. Puzyrev and I. S. Rahavaya
24	2.3.	Equilibrium composition of plasma obtained by laser ablation of glass	M. Ristić, A. Šajić, J. Babić and M. Kuzmanović
25	2.3.	Semiquantum simulation of cellulosic materials interaction with CO ₂ plasmas	V. Stanković Mališ and Goran B. Poparić
26	2.3.	Properties of Cu/Zn oxide nanostructures formed by plasma-activated electrolysis	N. Tarasenko, V. Kornev, M. Nedelko, A. Radomtsev, N. Tarasenka, J. Ciganović, S. Živkovic and M. Momčilović
27	2.3.	Target selection for LIBS studies of hydrogen isotope retention	D. Ranković, B. Stankov, I. Traparić, M. Kuzmanović and M. Ivković
28	3.1.	Measurement of the velocity of the plasma jet appearing from a wall stabilized arc	L. Gavanski, N. Simić and S. Djurović
29	3.1.	The measurement of pulsed gas discharge parameters by means of Fe I lines in argon and argon-hydrogen mixture	J. Jovović
30	3.1.	Stark widths of several Te II spectral lines for a purpose in investigation of astrophysical spectra	Z. Majlinger, M.S. Dimitrijević and V. Srečković
31	3.1.	Stark width estimates for the most prominent Ce II spectral lines important for astrophysical investigations	Z. Majlinger
32	3.1.	Determination of unknow analyte concentration in glass samples using the LIBS method	A. Šajić, D. Ranković, M.Ristić and M. Kuzmanović
33	3.1.	Investigating the thermal profile of an atmospheric pressure argon plasma jet on a conductive and insulating mesh surface	J. Lalor and V. Milosavljević
34	3.1.	The use of thermoelectric radiation detectors for heat flux measurements in shock-tubes with gas ionization	S.A. Poniaev, P.A. Popov, N.A. Monakhov, T.A. Lapushkina and M.A. Kotov

35	3.1.	Detection of rhenium in tungsten using LIBS with additional fast pulse discharge	I. Traparić, B. Stankov and M. Ivković
36	3.1.	Estimation of nitrogen impurity level in helium atmospheric discharge via emission spectroscopy	N. Cvetanović, S.S. Ivković and B.M. Obradović
37	3.1.	The effect of acids on pig bone estimated by LIBS	M. Marković, D. Ranković and M. Kuzmanović
38	3.1.	Fast photography in the service of spatially and temporally resolved LIBS diagnostics of doped tungsten	B. Stankov, M. R. G. Božović, D. Ranković, J. Savović and M. Ivković
39	3.1.	Influence of the ablation angle change on spectral line intensities in LIBS experiments	I. Traparić, B. Stankov, N. Vujadinović, M. Vinić and M. Ivković
40	3.2.	Modelling of an icp discharge in oxygen with full kinetics scheme with newly calculated VV/VT rate constants	A. Kropotkin, A. Chukalovsky, A. Kurnosov, T. Rakhimova and A. Palov
41	3.2.	Influence of interelectrode distance on the characteristics of three-electrode pulsed sdbd	V. V. Voevodin, O. I. Korzhova, V. Yu. Khomich, V. A. Yamschikov, N. Yu. Lysov and A. V. Klubkov
42	3.2.	RF breakdown in argon at low-pressures: experiment and modelling	J. Marjanović, D. Marić, M. Puač, A. Đorđević and Z. Lj. Petrović
43	3.2.	Cathode sheath diagnostics by integral end-on optical emission spectroscopy in an analytical glow discharge source in argon	N. V. Nedić, N. V. Ivanović, I. R. Videnović, Dj. Spasojević and N. Konjević
44	3.3.	Luminescent analysis of e-beam induced transformation of phenol in the presence of humic substances	E. N. Bochamnikova, O. N. Tchaikovskaya, S. A. Chaykovsky, V. I. Solomonov, A. S. Makarova and I. V. Sokolova
45	3.3.	The formation of microneedles structures from silicon using plasma etching in SF ₆ /O ₂ mixture in inductively coupled plasma	V. Kuzmenko, A. Miakonkikh and K. Rudenko
46	3.3.	Fluorocarbon polymerizing plasmas etching processes for structures of microelectronics	A. Miakonkikh, V. Kuzmenko and K. Rudenko
47	3.3.	A&M datasets for LTP treatment of plants	V. Vujčić, V.A. Srečković, O. Kounchev and F. Iacob
48	3.3.	Low-temperature plasma and plasma-activated liquids in solving agricultural problems: experimental technique	E.M. Konchekov, N.G. Gusein-Zade, D.V. Yanykin, L.V. Kolik, Yu.K. Danileiko, V.I. Lukanin, K.F. Sergeichev, I.V. Moryakov, V.D. Borzosekov, V.V. Gudkova, M.E. Astashev and S.V. Gudkov
49	3.3.	Compact piezotransformer source of the cold atmospheric plasma with three types of discharges	N. N. Bogachev, A. S. Bakshaev, L. V. Kolik, E. M. Konchekov and A. S. Kon'kova
50	3.3.	Measurements of reactive oxygen and nitrogen species in plasma activated water by microwave discharge	D. Topalović, N. Babučić, N. Škoro and N. Puač
51	3.3.	Ionization of a plasma antenna channel in a dielectric gas-discharge tube	N. N. Bogachev, I. L. Bogdankevich, V. I. Zhukov, D. M. Karfidov, V. P. Stepin and N. G. Gusein-Zade

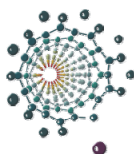
52	4.2.	Dataset for photodissociation of small molecular ions	V.A. Srečković, N. Pop, M.S. Dimitrijević, M.D. Christova and V. Vujčić
53	4.2.	Investigation of chemistry of hydrogen, helium and lithium molecular ions in the early Universe	V.A. Srečković, N. Pop, M.S. Dimitrijević and M.D. Christova
54	4.2.	New molecular data for confined molecular systems and astrochemical modelling	V.A. Srečković, N. Pop, and V. Vujčić
55	4.2.	The complex emitter inside dense plasma, continuation of a Coulomb cut-off approach, argon case	N.M. Sakan, Z. Simić, V.A. Srečković and M. Dechev
56	4.2.	Variability along the main sequence of quasars	E. Bon, P. Marziani and N. Bon
57	4.2.	Advanced nonlinear analysis for detecting binary quasars and transient events in the LSST era	A.B. Kovačević, D. Ilić, L.Č. Popović, M. Pavlović, A. Raju, M. Tošić and Iva Čvorović-Hajdinjak
58	4.2.	Two-Component Model of Fe II Lines in Spectra of Active Galactic Nuclei	Jelena Kovačević-Dojčinović, Ivan Dojčinović and Luka Č. Popović

ACKNOWLEDGEMENT

32nd SUMMER SCHOOL AND INTERNATIONAL
SYMPOSIUM ON THE PHYSICS OF IONIZED GASES

is organized by

**University of Belgrade – Faculty of Physical Chemistry
Serbian Academy of Sciences and Arts**



**Faculty of Physical Chemistry
University of Belgrade**



**Serbian Academy
of Sciences and Arts**

and

with the support of the

**Ministry of Science, Technological Development and Innovation
Republic of Serbia**



Republic of Serbia
MINISTRY OF SCIENCE,
TECHNOLOGICAL DEVELOPMENT
AND INNOVATION

sponsored by



Telekom Srbija

technical organizer

PANACOMP - Zemlja čuda d.o.o.

FLUID MODEL OF STREAMERS IN THE AMREX ENVIRONMENT

ILIJA SIMONOVIĆ^{id}, DANKO BOŠNJAKOVIĆ^{id} and SAŠA DUJKO^{id}

Institute of Physics Belgrade, Pregrevica 118, 11080 Belgrade, Serbia

Abstract. Streamers are thin filaments of weakly ionized non-stationary plasma, which appear in nature as precursors of lightning and as sprite discharges in the upper-planetary atmospheres, see Teunissen and Ebert 2017. Streamers are used for the ignition of high-intensity discharge lamps and for the purification of gases and liquids from harmful organic pollutants, and they are the main mechanism of breakdown in the high-voltage insulation technology.

We have developed a fluid model of streamer discharges in the AMReX library. Our model is implemented in both axisymmetric and 3D cases. AMReX is an open-source C++ library that is designed for massively parallel block structured adaptive mesh refinement applications, see Zhang et al. 2019. AMReX allows a straightforward use of both MPI and OpenMP parallelization on CPUs as well as parallelization on GPUs. This library also has inbuilt geometric multigrid solvers for solving elliptic differential equations, such as the Poisson equation and the Helmholtz equation.

Our code is based on the first-order fluid model with local field approximation. The time integration in our code is performed explicitly by employing the Heun's method. We employ the finite volume method for spatial discretization. The non-local source term due to photoionization is represented by employing the Zhelenznyak's model using the Helmholtz approximation, and the photon absorption function is represented by applying the Bourdon three term parametrization, see Bourdon et al. 2007. We have verified our code by comparing its results to the results of the Afivo-streamer open-source code, see Teunissen and Ebert 2017.

Acknowledgments: This work is supported by the Science Fund of the Republic of Serbia, Grant No. 7749560, Exploring ultra-low global warming potential gases for insulation in high-voltage technology: Experiments and modelling EGWin.

References

- Bourdon A., Pasko V. P., Liu N. Y., Célestin S., Ségur P. and Marode E.: 2007, *Plasma Sources Sci. Technol.* **16**, 656
- Teunissen, J. and Ebert, U.: 2017, *Journal of Physics D: Applied Physics* **50**, 474001
- Zhang, W. et al.: 2019, *Journal of Open Source Software*, **4**, 1370

